ANALYSIS OF THE ROLE OF Cdc14/Flp1 IN CHECKPOINT RESPONSE TO GENOTOXIC STRESS IN *Schizosaccharomyces pombe*

ANÁLISIS DE LA FUNCIÓN DE Cdc14/Flp1 EN LA RESPUESTA A ESTRÉS GENOTÓXICO EN *Schizosaccharomyces pombe*

Helena Díaz-Cuervo · 2008

Supervisor: Avelino Bueno

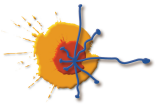

University of Salamanca

Department of Microbiology and Genetics

Institute for Cancer Research

AGRADECIMIENTOS / ACKNOWLEDGEMENTS

AGRADECIMIENTOS

Todo esto empezó gracias a un cúmulo de circunstancias (que no de casualidades) y a una llamada telefónica que decidí hacer allá por finales del 2003 desde Alemania. Empezaré por agradecer a aquellos que contribuyeron a que se diesen las circunstancias para que esta tesis fuera posible.

Tengo que agradecerles a mis padres, que ante la eterna duda entre Ciencias y Letras, ya con los impresos de preinscripción para la Universidad en la mano, me aconsejaran decantarme por la opción teóricamente más versátil de las que me rondaban la cabeza. Y ¡voilà!, ahora puedo decir que la Ingeniería Química no me cerró ninguna de las puertas a las que me decidí a llamar. En mi trayectoria ingenieril *especial* agradecerle a Luis Arsenio sus valiosos consejos. El salto de la Ingeniería a la Biología (o mejor el puente entre ambas) se lo debo a Julio Sáez. Gracias Julio por todo lo que pasamos juntos; por haber sido el pionero en Stuttgart, por introducirme a la Biología de Sistemas. Por toda tu ayuda y tu apoyo.

I want to thank Dr. Reuss and Dirk Mueller for making of my first contact with science an exciting experience, and for their support (thanks specially for the FEBS meeting!) even long after I had left their group. Gracias también, Luciano, por toda tu ayuda con el proyecto y por hacer mis últimos meses en Stuttgart más agradables.

Este primer contacto con la Biología de Sistemas (y con la biología pura y dura: todavía recuerdo mi confusión cuando intenté leer los primeros papers. Genes y proteínas, ¡para mí solo eran combinaciones extrañas de números y letras!) fue decisivo para mi decisión posterior de dejar el Project Management y empezar esta tesis. Después de casi dos años ocupada principalmente en planificar y coordinar proyectos que llevaban a cabo otros, echaba en falta generar resultados con mis propias manos. Justo en el momento adecuado apareció Sira en la oficina con un listado de las FPI… y de allí a aquí hay sólo un paso...

…La llamada. Gracias Avelino por confiar en mí y darme esta oportunidad. Por apostar por una Ingeniera que solo había visto levadura en los bizcochos y a través de fórmulas en el ordenador. Gracias por tenerme paciencia con mi visión *diferente* y mi obsesión por los números. Y por tu reacción en el crítico momento. A ti te debemos también el “casting” de Buen@s, que hace del L5 un grupo que transciende de lo profesional.

Cuando llegué al laboratorio todavía andaba algo liada con los genes y desde luego no manejaba una pipeta en condiciones. Tengo mucho que agradecer a todo el grupo (de entonces y de ahora) por su acogida y su ayuda. Por el cajón, las celebraciones, las salidas, las risas, los cafés… ¡En definitiva, por estos cuatro años! Gracias a los más veteranos, María, Arturo, Vero, Sandra, por estar siempre dispuestos a explicar, discutir y echar una mano. Gracias Vero, por llevarme de la mano en mis primeros pasos con Flp1p y *pombe*. Por tus

ACKNOLEDGEMENTS

¡¿EHs?! Por tus invitaciones a comer para desestresar. Arturo, eres el paciente entre los pacientes ¡y el incordiante por excelencia! (desde el cariño). Gracias por encontrar siempre un rato para aconsejar, dentro y fuera. ¡Y por el girasol en naranja! A Sonix le debemos que el laboratorio funcione tan bien. Gracias por apaciguarnos con tu buen humor y por estar siempre tan dispuesta a ayudar, por los cruces, por las minis, por los miles de favores varios. A mi generación. A Violetilla, llena de energía positiva y a sus canciones. A Juanjín por el mérito múltiple de aguantarme en el laboratorio y en casa; por las risas, por nuestras noches de triple M, por obligarme a usar cremas y tacones, jeje. Lolilla, sin nuestras charlas trascendentales, la risa silenciosa y las bañeritas, la tesis no hubiera sido la misma. Y por supuesto a la *next generation.* Pilarilla, te dejo ahora para ti sola el título de la más grande del laboratorio. ¡Me debes un diccionario! Alfonso, ¡cómo amenizas los experimentos tardíos! Y qué bien se te dan los collages con *pombes* y todo tipo de fricadas. Laurilla, una pena no haber coincidido más tiempo, y en mejores condiciones (mentales, temporales… mías por supuesto), creo que conectamos bien. ¡Espero que las dos *pomberas* me dejéis el pabellón bien alto!

Considero una suerte también haber trabajado en este centro. ¡Las noches de karaoke serán difíciles de olvidar! Gracias Celso por la organización de eventos sociales. Quiero agradecerle a Ángel su trabajo como FACSeador oficial, tan majete, y que tanta faena nos ahorra. A Antonio y Fernando su ayuda en domesticar al Leica. A Sonia (Almacén) su efectividad en gestionar radiactivos. A Pablo todo el consejo informático. A Carlos sus apaños varios siempre con una sonrisa. Gracias a l@s Moren@s por ser los mejores vecinos de enfrente imaginables, con sus préstamos y sus consejos. Tengo que hacer una mención especial a Livia por aguantar mi histeria pre-tesis. Al sector Deutsch del 18, Martina, Aarne, Kathrin, a David Herrero, por pinchos, comidas en farmacia, conversaciones varias, que amenizan el día a día. Y a mi Soni Flower Metal: los tiempos de Los Perdones fueron de lo mejor de estos cuatro años.

I am really grateful to all the Computational Systems Biology Group of the Molecular Genetics-MPI, my host group in Berlin, for making me feel at home, with such a nice atmosphere in the *Gartnerei*. Thanks Edda for giving me the opportunity to work in your great team and for all your support. I also want to especially thank my *co-workers* Matteo and Christian, the experimentalist and the bioinformatician, for their help and patience, and for taking me out of home! Matteo, grazie per fare la nonna!

Aunque estos agradecimientos ya están siendo bastante largos, no puedo dejar de lado que la tesis marca un período largo e intenso, en el que pasan muchas cosas y se mezcla lo personal y lo profesional.

Fran y el micri, con todo su kilometraje fueron imprescindibles para esta tesis. Gracias Fran por ayudarme tanto, por entenderme, tenerme paciencia, estabilizarme. Por hacer de los fines de semana fechas de guardar. Por tu empeño en las cosas bien hechas, sin el cual probablemente no estaría ahora escribiendo esto.

Gracias a toda mi familia por estar siempre ahí. A mis abuelos. A Anto, Mari Paz, Lola, Isa. A mis padres por estar siempre tan pendientes y hacer de Salamanca parada fija en sus rutas. A los hermanurrios. A Bus porque sin los playmobil no hubiera llegado hasta aquí. Al Ñuín por recordarme siempre las cosas importantes de la vida. A Cali por sus visitas y por ejercer de primo mayor, bueno, de él mismo.

A mis amigos de siempre, Sara, Izaskun y Jose, por ser de los buenos. Por hacerme sentir siempre que estais ahí. Por visitas, llamadas, organización de fiestas, maquetaciones… Por aceptarme como soy, culo inquieto y todo. A las IQs por nuestras cenas de chicas y alguna que otra juerga loca. Gracias a todo el clan de Stuttgartianos ¡se que en el fondo disfrutáis con nuestros regalos personalizados! En especial a Laurita (Anadón) por nuestras charlas sobre ciencia, futuro, idas y venidas. Y a otra gran familia, la de los Bremerhavianos, de la que me siento muy orgullosa. Gracias por adoptarme y por guiarme en esa escuela de la vida. Por las fiestas temáticas, los “Y sin embargo”, el *afelmús* y todos nuestros encuentros en marco incomparable. Por todo lo que vivimos juntos. Gracias Sonia (Rodriguez) por animarme a dar el salto y hacer la tesis.

CONTENTS

CONTENTS

CONTENTS

CONTENTS

INTRODUCTION

1. *Schizosaccharomyces pombe*

The studies included in this thesis, aiming to achieve a better understanding of checkpoint response to unreplicated or damaged DNA in eukaryotes, have been performed using the yeast *Schizosaccharomyces pombe* as a model organism.

S. pombe was first isolated in 1893 by Lindner from East African millet beer. In fact, the species name is derived form the Swahili word for beer (Pombe). It is a rod-shaped unicellular eukaryote of 3-4 μm in diameter and 7-14 μm in length. *S. pombe* cells maintain their shape by growing exclusively through their cell tips. They divide by means of a septum formed in their medial part to give rise to two identical daughter cells. Therefore *S. pombe* is also called fission yeast.

S. pombe genome is divided into three relatively large chromosomes. These present features typical of higher eukaryotes, including large diffuse DNA replication origins (~1 kb) and large heterochromatic centromeres (~40-100 kb). *S. pombe* origins display a wide range of efficiencies, and lack defined consensus sequences just like in metazoans and differing from *Saccharomyces cerevisiae*.

S. pombe is the sixth model eukaryotic organism whose genome was fully sequenced, in 2002 (Wood *et al.*, 2002). Characteristic of the fission yeast genome are its low number of genes compared to other eukaryotes and the presence of introns in 43% of its genes. Fifty genes were found that had significant similarity with human disease genes and half of these are cancer related.

From gene-sequence comparisons, *S. pombe* and *S. cerevisiae* are estimated to have diverged from each other in evolution around 400 million years ago, and their sequences are as divergent from each other as either yeast is from higher eukaryotes. Thus there are around 145 genes in *S. pombe* that have metazoan homologues but are not found in *S. cerevisiae* and a similar number viceversa. These similarities and divergences among the both yeasts and larger eukaryotes turned *S. pombe* and *S. cerevisiae* into two complementary model organisms for the study of the organization and behaviour of mammalian cells.

Fission yeast was first developed as an experimental model for cell cycle research by Murdoch Mitchison in the 1950s. The fission yeast researcher Paul Nurse together with Lee Hartwell and Tim Hunt received the Nobel Prize in Physiology or Medicine in 2001 for their work on cell cycle regulation. *S. pombe* has proven to be a valuable

model organism for research of many other biological relevant aspects like sexual differentiation, chromosome dynamics and polarized cell growth and for the study of cellular responses to DNA damage and replication stress.

2. CELL CYCLE

Cell cycle in eukaryotes consists of a number of coordinated cellular events that must guarantee correct duplication and subsequent segregation of all cellular components necessary for survival and functionality of daughter cells.

Due to the complexity of this process, yeasts as unicellular eukaryotes have proven to be valuable model organisms to study the regulatory and control mechanisms of cell cycle. *S. cerevisiae* and *S. pombe* have thus provided important contributions to the

Figure I1. Cell cycle in Fission yeast

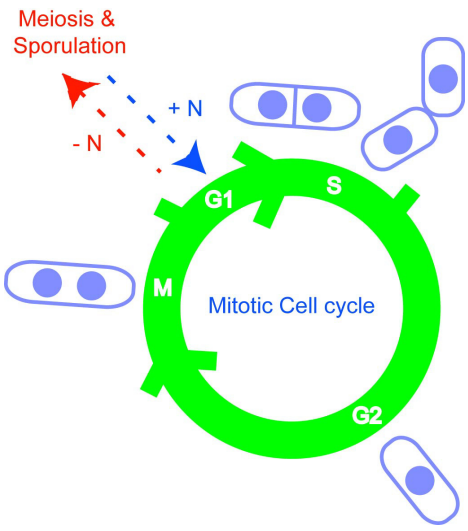

S. pombe mitotic cell cycle is characterized by an extremely long G2 phase, accounting for the 70% of the doubling time. In addition, in exponentially growing *S. pombe* cells, cytokinesis occurs when cells have nearly completed S-phase. Since the *S. pombe* genome is haploid this mechanism ensures the availability of a reference copy to allow for repair in case of DNA-damage, being the time during which cells have only one copy of their genome very brief. *S. pombe* divides by means of constriction of the medial ring to give two identical daughter cells. On the contrary *S. cerevisiae*, diploid in the wild, presents a prolonged G1-phase that allows small daughter cells resulting from asymmetric division to grow before initiation of replication.

If nutrients are insufficient to allow for mitotic growth, *S. pombe* cells can enter stationary phase or initiate a meiotic cell cycle. In the latter, cells of different mating type can mate during G1. They fuse, mixing their genetic material to form a diploid zygote. The zygote immediately undergoes a meiotic cell cycle to give rise to four haploid spores. If favourable nutritional conditions are restored, spores germinate to form cells which can re-entry into mitotic cell cycle.

discovery of basic mechanisms of cell proliferation.

As in higher eukaryotes, cell cycle of yeasts can be divided into four periods: G1 (Gap phase 1), S-phase (DNA Synthesis phase), G2 (Gap phase 2) and M-phase (Mitotic phase).

During **G1** the proteins necessary for later progress into cell cycle are actively synthesized and accumulated. The START or Restriction Point in G1 is a non return point after which cells are determined to progress through the entire cell cycle (Hartwell et al., 1974; Nurse, 1990). G1 is also a preparatory phase for DNA synthesis, in which pre-replication complexes (pre-RCs) are formed at replication origins in a process known as licensing for DNA replication. This process requires the sequential binding to DNA replication origins of the origin recognition complex (ORC) and the replication licensing factors Cdt1p and Cdc6p/Cdc18p which in turn allow for the loading of the hexameric minichromosome maintenance complex (MCM). Transition through START also requires de Cdc10p transcriptional activator. Forming a complex with Res1p and to a lesser extent Res2p, Cdc10p activates the transcription of several genes required for DNA replication, including *cdc22*, encoding the enzyme ribonucleotide reductase, *cdc18* and *cdt1*.

During **S-phase** the initiation of replication takes place, a process that happens simultaneously in different parts of the genome. Licensed origins are activated for replication in a process known as origin firing by phosphorylation and binding of other essential replication factors including Cdc45p, Mcm10p, RPA and DNA polymerases α and ε. In this phase, the genetic material of the cell must be completely and accurately replicated once. Thus, since replication is initiated at multiple points, the activation or firing of each replication origin must be tightly controlled in order to guarantee genomic stability. Phosphorylation of pre-RC components particularly by cyclin-dependent kinases (CDKs) inhibit re-replication processes once origins are fired either directly by the inhibitory effect of phosphorylation or by leading to degradation or nuclear export of the target.

During **G2**, after replication of genetic material, cells grow until they reach the adequate size to allow progression into the next phase.

During **M-phase**, DNA is segregated to form two new nuclei. Mitosis comprises four sub-phases. During Prophase the duplicated genetic material condenses into chromosomes, presenting two sister chromatids bound together at the centromere. The mitotic spindle assembles between the two centrosomes, which have duplicated

and moved apart. In Metaphase chromosomes align at the equator of the spindle and the kinetochore microtubules attach sister chromatids to opposite poles of the spindle. At Anaphase, sister chromatids synchronously separate to form two daughter chromosomes that are pulled apart by microtubule shortening and spindle pole movement. During Telophase the two sets of daughter chromosomes arrive at the poles of the spindle and decondense forming two independent nuclei. The division of the cytoplasm begins with the assembly of the contractile ring.

Finally cellular contents split during cytokinesis to give rise to two daughter cells.

The production of two viable daughter cells depends on the execution of DNA synthesis, mitosis and cytokinesis in a strict sequential order. In this way, mitosis is initiated only upon completion of DNA synthesis and cytokinesis is initiated only after mitosis has been completed. In addition, checkpoint mechanisms operate to ensure that DNA is not damaged and completely replicated before entry into mitosis, and that kinetochores have attached correctly to the mitotic spindle before anaphase onset.

2.1 Cell cycle and CDKs

In eukaryotes, the cell cycle is controlled by the periodic activation and inactivation of the highly conserved cyclin dependent kinases (CDKs). Timely activation and inactivation of CDKs regulate most cell-cycle transitions. For example, entry into mitosis requires CDK activation and exit from mitosis and cytokinesis requires loss of CDK activity and dephosphorylation of CDK substrates. CDK activity is regulated in part by its binding to cyclins (proteins of oscillatory expression) to form kinase-cyclin complexes specific of the cell cycle stage. There are thus different types of cyclins depending on the cell cycle phase during which they perform their role: G1-cyclins, S-phase-cyclins and Mitotic-cyclins. Activity of G1 CDKs promotes passage of cells through START. S-phase CDKs begin to accumulate at the end of G1, and are accumulated during G2 and mitosis. On reaching a critical level, they promote DNA replication. Mitotic CDKs are activated at the onset of mitosis and, among other processes, promote chromosome condensation, formation of the mitotic spindle and breakdown of the nuclear envelope. For cells to exit from mitosis, undergo cytokinesis and enter the following G1, mitotic CDK must be inactivated.

	S. pombe	*S. cerevisiae*	Higher eukaryotes
G1 CDKs	Puc1 + Cdc2	Cln1, Cln2, Cln3 + Cdc28	CycD1, CycD2, CycD3 + Cdk4, Cdk6
S-phase CDKs	Cig2 , Cig1 + Cdc2	Clb5, Clb6 + Cdc28	CycE + Cdk2 CycA + Cdk2/Cdk1
Mitotic CDKs	Cdc13 + Cdc2	Clb1, Clb2, Clb3, Clb4 + Cdc28	CycB1, CycB2, CycB3 + Cdk1 CycA + Cdk2/Cdk1

Table I1. Cell cycle dependent CDK-cyclin complexes in yeasts and higher eukaryotes

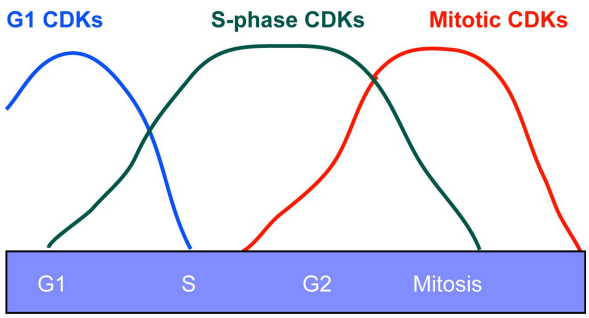

Figure I2. Schematic representation of the fluctuation in the activities of the different CDK-cyclin complexes, responsible for adequate cell cycle progression

If the CDK is not bound to a cyclin, its catalytic centre is not accessible. CDKs get an active conformation both after binding to its regulatory subunit and by subsequent phosphorylation of the CDK-cyclin complex by a CDK-activating Kinase (CAK) (Fisher and Morgan, 1994; Espinoza *et al.*, 1996; Kaldis *et al.*, 1996).

2.2 Regulation of cell cycle progression in *S. pombe*

S. pombe has proven to be a highly useful model organism to study cell cycle functioning due to its simplicity and parallelism in behaviour to mammalian cells. *S.*

pombe relies on a single CDK, Cdc2p, four cyclins (three B type cyclins Cig1p, Cig2p, and Cdc13p, and Puc1p) and one CDK inhibitor (CKI), Rum1p, to drive and control all mitotic cell-cycle events.

Cdc2p activity is regulated during the cell cycle by three different mechanisms: through its binding to different cyclins and phosphorylation by CAK in its Thr167 residue, by the phosphorylation state of some of its residues and by the action of its inhibitor.

Cdc2p protein levels remain constant throughout the cell cycle, while B type cyclins and Rum1p are strictly regulated in terms of protein amounts at the different stages by transcription and ubiquitin-mediated proteolysis.

The Cdc2p inhibitor Rum1p accumulates in mitotic anaphase and persists through G1. Before onset of S-phase it targets Cdc13p for degradation and inhibits kinase activities of Cdc2p-Cdc13p and Cdc2p-Cig2p until the cell has reached the adequate size to initiate replication (Correa-Bordes *et al.*, 1997; Benito *et al.*, 1998).

Puc1p levels do not vary during the cell cycle, although its role is restricted to G1, being implicated in transcription of genes necessary for G1/S transition and in the activation of Rum1p degradation and cyclin B stabilization (Caligiuri *et al.*, 1997; Martin-Castellanos *et al.*, 2000). Degradation of Rum1p at G1/S transition allows Cdc2p-Cig2p to induce entry into S-phase.

Cig2p is the major S-phase cyclin (Fisher and Nurse, 1996; Martin-Castellanos *et al.*, 1996; Mondesert *et al.*, 1996). It accumulates late in G1 and disappears upon exit from S-phase. Cdc2p-Cig2p complex is involved in pass through START and replication initiation. Firing of origins requires the concerted actions of Cdc2p and Dbf4-dependent kinase Hsk1p (DDK) which activate MCM at origins by phosphorylation. This allows loading of Cdc45p and the GINS complex, turning MCM into a replicative helicase that unwinds DNA to produce short regions of ssDNA (Sogo *et al.*, 2002; Feng *et al.*, 2006). Replication protein A (RPA) is loaded to protect ssDNA and moves along with the replication fork. In Δ*cig2* cells Cig1p and Cdc13p can trigger S-phase entry.

Cig1p levels reach maximum values in G2/M and decrease at the end of Metaphase. Its stability is regulated by PEST sequences (Bueno *et al.*, 1991).

Cdc13p is the only essencial cyclin in *S. pombe* (Fisher and Nurse, 1996; Martin-Castellanos et al., 1996; Mondesert et al., 1996). Cdc13p protein levels are low in G1

but increase in G2 and are maintained until the end of M-phase (Creanor and Mitchison, 1996). This periodicity is necessary to ensure adequate cell cycle progression and to inhibit unscheduled re-initiation of S-phase (Hayles *et al.*, 1994). The Cdc13p-Cdc2p complex accumulates in the nucleus during S-phase and G2 and can be detected in the nucleolus, spindle pole body and spindle (Alfa *et al.*, 1989; Alfa *et al.*, 1990).

At the end of G2, when cells reach a critical size, M-phase is induced by a large increase in Cdc2p-Cdc13p activity (Booher *et al.*, 1989; Moreno *et al.*, 1989). Cdc2p-Cdc13p complex forms early in S-phase but its activity is kept rather low by the kinases Wee1p and Mik1p through inhibitory phosphorylation of Cdc2p on Tyr15 (Russell and Nurse, 1987; Featherstone and Russell, 1991; Lundgren *et al.*, 1991; Parker *et al.*, 1992; Lee *et al.*, 1994). This phosphorylation is reversed by Cdc25p at the end of G2 to induce M-phase. Activation of Cdc2p is thus promoted both by accumulation and activation of Cdc25p and inactivation of Wee1p and Mik1p. Cdc25p is cell cycle regulated displaying maximum protein levels at the end of G2 (Ducommun *et al.*, 1990; Moreno *et al.*, 1990; Daga and Jimenez, 1999) and hyperphosphorylation and hyperactivation at the G2/M transition (Kovelman and Russell, 1996). Wee1p is inhibited by the kinase Nim1p/Cdr1p and the related kinase Cdr2p (Coleman *et al.*, 1993; Parker *et al.*, 1993; Wu and Russell, 1993; Breeding *et al.*, 1998; Kanoh and Russell, 1998). Decrease of Cdc2p activity at the end of mitosis and return to G1 and S-phase is achieved by inactivation and destabilization of Cdc25p by the phosphatase Flp1p (Esteban *et al.*, 2004; Wolfe and Gould, 2004).

3. Flp1p

3.1 Flp1p and its orthologues

The Cdc14 family of phosphatases plays an important role in the negative regulation of mitotic CDKs by specifically reversing CDK-dependent phosphorylation events (Visintin *et al.*, 1998; Kaiser *et al.*, 2002; Gray *et al.*, 2003). In *S. cerevisiae* the *CDC14* gene is essential for cell viability, and thermosensitive mutants arrest cell cycle progression in telophase with high levels of Cdc28p-Clb associated kinase activity (Wan *et al.*, 1992; Taylor *et al.*, 1997; Visintin *et al.*, 1998). On the basis of sequence similarity to the budding yeast *S. cerevisiae*, orthologues have been

identified in several eukaryotes including *S. pombe* (cdc-fourteen-like-protein named Flp1p or Clp1p)*, Caenorhabditis elegans* (CeCDC-14)*, Xenopus laevis* (XCdc14A and XCdc14B) and *Homo sapiens* (hCdc14A and hCdc14B) (Li *et al.*, 1997; Cueille *et al.*, 2001; Trautmann *et al.*, 2001; Gruneberg *et al.*, 2002; Kaiser *et al.*, 2002; Krasinska *et al.*, 2007). Cdc14 proteins are dual-specificity protein phosphatases that share a core of approximately 300 amino acids towards the amino terminus that includes a strictly conserved protein-phosphatase domain motif (Gray *et al.*, 2003).

3.2 Cdc14 phosphatases and the control of mitotic exit

In *S. cerevisiae* Cdc14p plays a role in mitotic exit by dephosphorylation and activation of substrates of mitotic CDK such as Hct1/Cdh1 protein, a component of the anaphase promoting complex/cyclosome (APC/C) responsible for ubiquitination of mitotic cyclins, or the CDK inhibitor Sic1p, in both cases to achieve down-regulation of kinase activity (Jaspersen *et al.*, 1999; Shou *et al.*, 1999; Visintin *et al.*, 1999).

In *S. pombe* Flp1p also regulates mitotic exit, but through a distinct mechanism. Flp1p does not dephosphorylate Rum1p or Ste9p, homologues of Sic1p and Hct1p of *S. cerevisiae*, respectively. Instead, it antagonizes mitotic CDK activity by dephosphorylating and targeting to degradation Cdc25p, which indirectly leads to down-regulation of Cdc2p activity by promoting its Tyr15 phosphorylated form (Esteban *et al.*, 2004; Wolfe and Gould, 2004).

CDK1 phosphorylated residues on human Cdc25A are *in vitro* substrates for hCdc14A, and this phosphatase can rescue a *Δflp1* strain in *S. pombe* by dephosphorylation of Cdc25p, suggesting a parallelism in the mechanism of mitotic exit between fission yeast and humans (Vazquez-Novelle *et al.*, 2005; Esteban *et al.*, 2006). On the other hand Hct1p has also been identified as a substrate for hCdc14A (Bembenek and Yu, 2001; Kaiser *et al.*, 2002).

3.3 Regulation of the activity of Cdc14 proteins

The activities of the Cdc14 proteins are controlled at least in part by regulated sequestration and release from the nucleolus (Shou *et al.*, 1999; Visintin *et al.*, 1999; Bembenek and Yu, 2001; Cueille *et al.*, 2001; Trautmann *et al.*, 2001; Kaiser *et al.*, 2002).

In *S. cerevisiae* Cdc14p is sequestered in the nucleolus in an inactive form from G1 until metaphase by binding the nucleolar inhibitor Net1p/Cfi1p, member of the RENT complex (Regulator of Nucleolar Silencing and Telophase) (Shou *et al.*, 1999; Straight *et al.*, 1999; Visintin *et al.*, 1999; Traverso *et al.*, 2001). In early anaphase, ScCdc14p is released from the nucleolus by the combined action of a set of proteins termed the FEAR (Cdc-fourteen early anaphase release) network (Stegmeier *et al.*, 2002; Azzam *et al.*, 2004). The FEAR promotes the phosphorylation of Net1p/Cfi1p by CDK (Azzam *et al.*, 2004) and subsequently dissociation from Cdc14p, probably by down-regulation of the protein phosphatase 2A (PP2A) (Queralt *et al.*, 2006). Nucleolar release of Cdc14p is then sustained during anaphase progression by the MEN (mitotic exit network), a GTPase signalling cascade that becomes active upon spindle elongation into the daughter bud (Jaspersen *et al.*, 1998; Bardin *et al.*, 2000). It has been recently reported that Cdc14p itself is responsible for its inactivation at the end of mitosis, by triggering degradation of the polo kinase Cdc5p (component of the FEAR network and a key regulator of the MEN) through activation of APC/C-Cdh1. Cdc14p-mediated degradation of Cdc5p leads to silencing of both the FEAR and the MEN and promotes the return of the phosphatase to the nucleolus (Visintin *et al.*, 2008).

While ScCdc14p is retained in the nucleolus until anaphase, other family members are

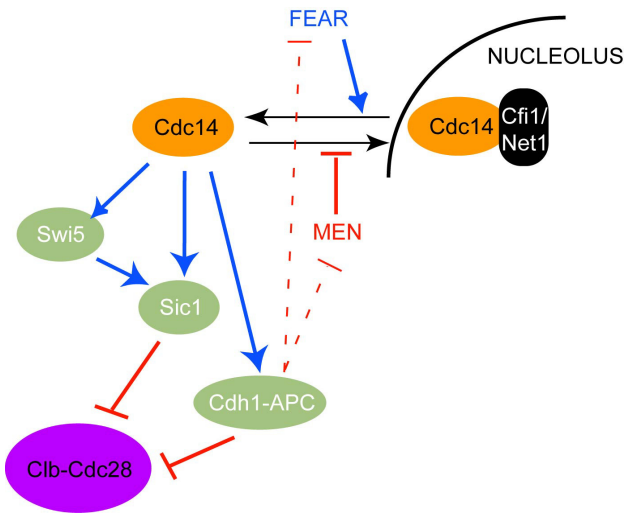

Figure I3. Regulation of ScCdc14p localization and its role during exit from mitosis

not regulated in the same manner. *S. pombe* Flp1p, human Cdc14 isoforms A and B and *Xenopus* Cdc14A change their cellular location upon entry into mitosis (Cueille *et al.*, 2001; Trautmann *et al.*, 2001; Kaiser *et al.*, 2002; Mailand *et al.*, 2002; Kaiser *et al.*, 2004).

The mechanisms by which Flp1p localization and activity are regulated are reviewed in the following section.

3.4 Flp1p: functions and localization

Serine/threonine phosphatase Flp1p, unlike its *S. cerevisiae* counterpart, is not essential and *⊿flp1* cells survive with a phenotype of advanced mitosis (Cueille *et al.*, 2001).

Flp1p has been proven to control rapid degradation of Cdc25p at the end of mitosis (Esteban *et al.*, 2004; Wolfe and Gould, 2004), which results in enhanced inhibitory Tyr15 phophorylation of Cdc2p and in the corresponding loss of kinase activity necessary for mitotic exit. Flp1p is required for the ubiquitination of Cdc25p by the APC/C at this cell cycle stage, and cells deleted for $flp1^{+}$ present higher basal levels of Cdc25p. As mentioned above, this role may be conserved in higher eukaryotes. In fission yeast, *∆flp1* cells enter mitosis at a reduced cell size, presenting a wee-phenotype (Cueille *et al.*, 2001; Trautmann *et al.*, 2001). Over-expression of Flp1p arrests cells in G2 with dephosphorylated Cdc25p, in a process dependent on active Wee1p (Cueille *et al.*, 2001; Esteban *et al.*, 2004). Beside its role in cell cycle progression, Flp1p is required for an efficient cytokinesis checkpoint (Cueille *et al.*, 2001; Trautmann *et al.*, 2001; Trautmann and McCollum, 2005) and for faithful chromosome segregation (Trautmann *et al.*, 2004).

In order to carry out its distinct functions, Flp1p must be correctly localized within the cell. In the course of a normal cell cycle Flp1p localizes in the nucleolus and to the SPB (spindle pole body) throughout interphase, and to the nucleus, spindle and medial ring during mitosis (Figure I4).

How Flp1p is inhibited in the nucleolus during interphase is not known. Recently a nucleolar protein that presents sequence similarity to ScNet1/Cfi1 has been identified. However, this protein, Dnt1p, is not responsible for anchoring or inhibition of Flp1p (Jin *et al.*, 2007).

Similarly to mammalian Cdc14Bp (Cho *et al.*, 2005), and unlike ScCdc14p, Flp1p is released from the nucleolus upon mitotic entry. Thus, in prophase it is released from the nucleolus to occupy the nucleus, medial ring and mitotic spindle (Cueille *et al.*, 2001; Trautmann *et al.*, 2001). Localization of Flp1p in the kinetochores and mitotic spindle during mitosis is necessary to prevent defects in chromosome segregation (Trautmann *et al.*, 2004).

The mechanism of Flp1p release to the nucleus remains unknown. Although the *S. cerevisiae* FEAR pathway components (separase-Esp1p, polo kinase–Cdc5p, Slk19p and Spo12p) are conserved in *S. pombe*, these do not play a role in the release of Flp1p to the nucleolus (Chen *et al.*, 2006). In anaphase, much like the MEN in budding yeast, the SIN (Septation Initiation Network) acts to keep Flp1p out of the nucleolus until cytokinesis is complete. The SIN is an SPB-based regulatory network required to initiate cytokinesis in late anaphase (reviewed in Simanis, 2003). Although the release of Flp1p from the nucleolus does not depend on the SIN, its SIN dependent maintenance in the cytoplasmatic locations is necessary for the cytokinesis checkpoint (Cueille *et al.*, 2001; Mishra *et al.*, 2005). In fact it has been shown that Flp1p binds to the 14-3-3 protein Rad24p to be retained in the cytoplasm in response to cytokinesis defects (Mishra *et al.*, 2005; Trautmann and McCollum, 2005). Attenuation of the SIN is needed for the proper relocalization of Flp1p to the nucleolus at the end of mitosis

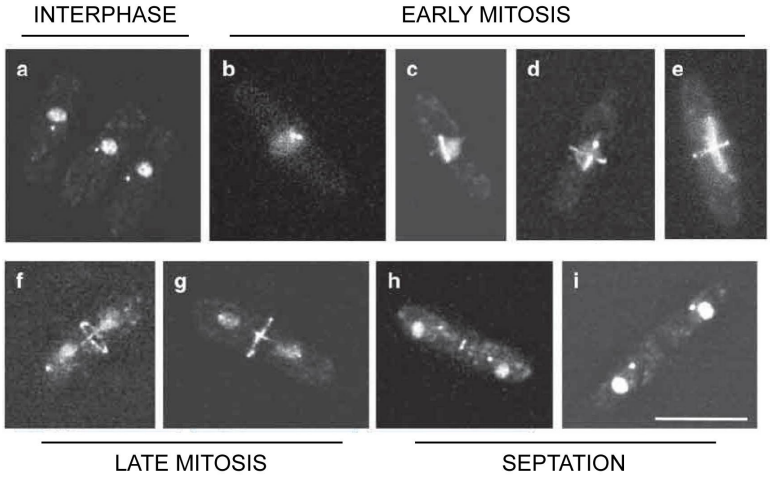

Figure I4. **Flp1-GFP subcellular localization at the different stages of the cell cycle**
Image modified from Cueille *et al.*, 2001.

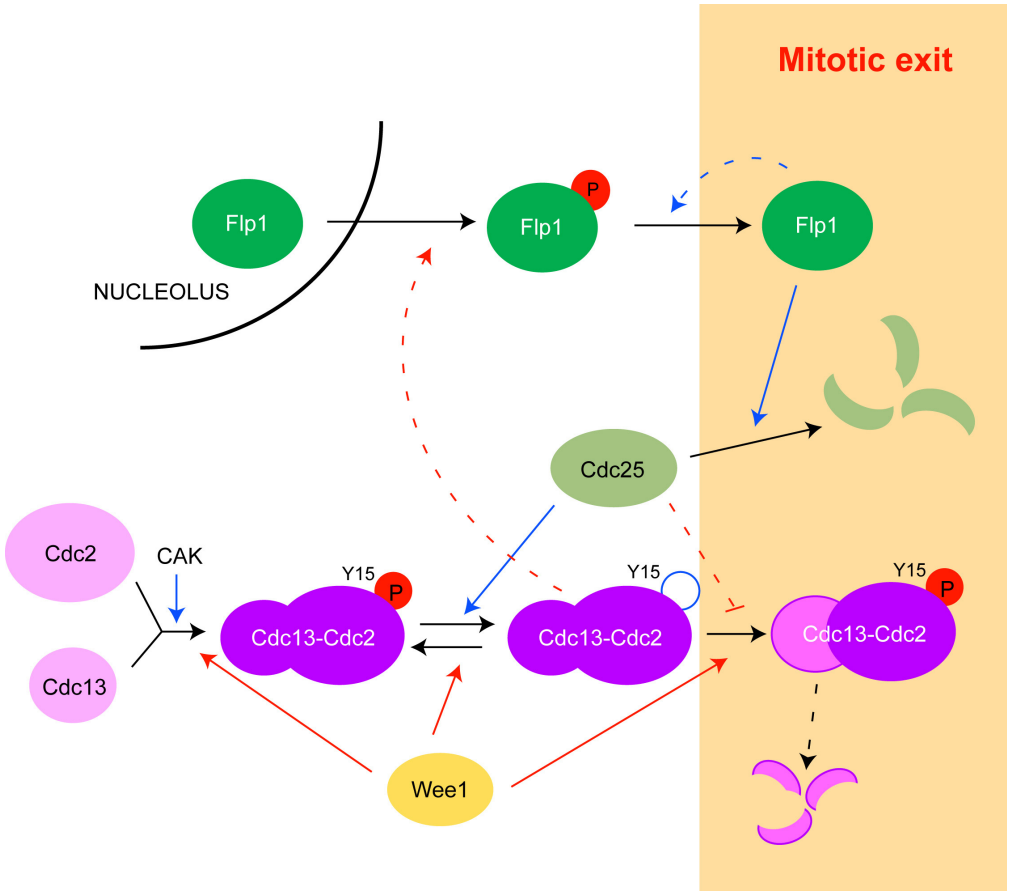

Figure I5. Regulation of Flp1p localization and its role during exit from mitosis

(Cueille *et al.*, 2001).

Flp1p activity is inhibited at the early stages of mitosis by CDK hyperphosphorylation. XCdc14p is similarly hyperphosphorylated during early mitosis (Kaiser *et al.*, 2002; Kaiser *et al.*, 2004). During anaphase the phosphatase undergoes autocatalytic reversal of Cdk1-mediated inhibitory phosphorylation events, and its catalytic activity is enhanced. During this phase, Flp1p is able to dephosphorylate Cdc25p, targeting it to degradation, to disrupt the Cdk1 autoamplification loop, and potentiate SIN signaling (Esteban *et al.*, 2004; Wolfe and Gould, 2004).

4. GENERAL OUTLINE OF DNA CHECKPOINT RESPONSES IN *S. pombe*

The DNA checkpoint response pathways are signalling cascades, by means of which in the course of cell cycle progression the presence of unreplicated DNA or DNA-damage is detected by sensor proteins to subsequently activate cellular responses in order to guarantee genomic stability. These responses include cell cycle retardation or block, replication fork stabilization, DNA-repair processes, alteration of the transcriptional program, chromatin remodelling and apoptosis. In the same way, there are mechanisms to allow for resumption cell cycle progression when the source of stress is removed or when the threat persists for a long time. These are known as checkpoint recovery and adaptation.

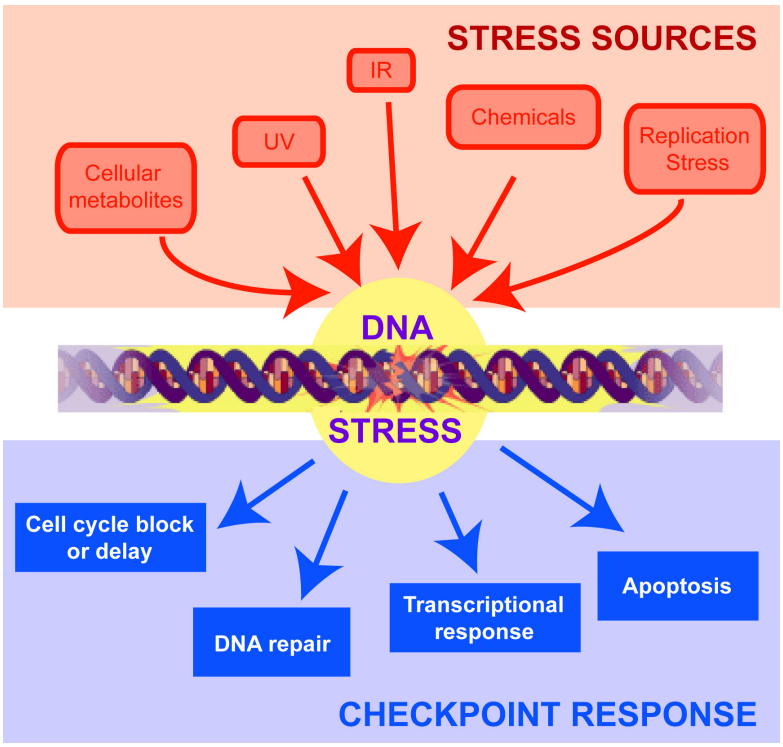

Figure I6. **Checkpoint responses to DNA stress through endogenous and exogenous agents**

Checkpoint responses work in this way to provide the organisms with time to cope with endogenous or exogenous threats and to coordinate the corresponding mechanisms to solve or to override their cellular consequences. Failure to enforce the adequate checkpoint responses can lead to aneuploidy, accumulation of mutations and chromosomal rearrangements, commonly associated to cell death and cancer.

DNA checkpoints respond to a general scheme in which the triggering stress is sensed by a set of sensor proteins and the signal is transmitted to the effector proteins with mediation of adaptors or scaffold proteins. In this way stress signals are traduced to the specific checkpoint response leading to adequate cellular behaviour to preserve genomic integrity.

		S. pombe	*S. cerevisiae*	Mammals
SENSORS	**RFC**	Rad17	Rad24	Rad17
		RFC_{2-5}	RFC_{2-5}	RFC_{2-5}
	PCNA-like	Rad9	Ddc1	Rad9
		Rad1	Rad17	Rad1
		Hus1	Mec3	Hus1
	DSB recognition	Rad32	Mre11	Mre11
		Rad50	Rad50	Rad50
		Nbs1	Xrs2	Nbs1
	PIKK	Rad3	Mec1	ATR
		Tel1	Tel1	ATM
		Rad26	Ddc2	ATRIP
ADAPTORS		Crb2	Rad9	BRCA1
		Mrc1	Mrc1	Claspin
		Rad4/Cut5	Dbp11	TopBP1
		Rad24-25	BMH1-2	14-3-3
EFFECTORS		Cds1	Rad53	Chk2
		Chk1	Chk1	Chk1

Table I2. Major sensors, mediators and effectors of DNA-checkpoint response in yeasts and mammals

S. pombe has proven to be a valuable model organism to study the functioning of checkpoints, due to its relative simplicity and parallelisms to human cells. DNA checkpoints in *S. pombe* include the replication checkpoint in response to unreplicated DNA during S-phase and the DNA-damage checkpoint in response to lesions in DNA during G2. In addition the intra-S-phase checkpoint has been defined as the pathway responsible for slowing-down of S-phase progression in response to DNA-damage during S-phase.

The components of the general scheme of DNA checkpoint response in *S. pombe* are reviewed in the next sections.

4.1 Checkpoint sensors

Studies in fission yeast and humans have shown that Rad9p, Rad1p, Hus1p, Rad17p together with SpRad26p/hATRIP and phosphoinositol phosphate 3-kinase-related kinases (hATM, hATR, SpRad3p) play central roles in checkpoint sensing and activation.

Rad9p, Hus1p and Rad1p form a heterotrimeric complex (the 9-1-1 complex) which exhibits structural similarity with the proliferating cell nuclear antigen (PCNA), sliding clamp implicated in replication processivity. The 9-1-1 complex loads to DNA upon genotoxic stress in a Rad17p-RFC_{2-5} dependent manner. Rad17p-RFC_{2-5} binds to single-to-double strand transitions (Venclovas and Thelen, 2000)

Rad17p protein is a paralogue of the largest subunit of RFC (replication factor C), and it forms the alterative clamp loader with RFC_{2-5}. In this way 9-1-1 complex and Rad17p-RFC_{2-5} function as a clamp/clamp–loader pair, alternative to PCNA and RF-C.

In fission yeast of the two phosphatidylinositol 3-kinase-related proteins Rad3p (hATR homolog) and Tel1p (hATM homolog), Rad3p plays a major role in both the DNA damage checkpoint and the DNA replication checkpoint. Rad3p constitutively forms a complex with the regulatory subunit Rad26p (hATRIP homologue). The Rad3p-Rad26p complex is recruited to DNA upon genotoxic stress (Wolkow and Enoch, 2002). A recent report has shown that Cdc18p gets stabilized during replication stress to ensure Rad3p association to chromatin by direct Cdc18p-Rad26p interaction (Hermand and Nurse, 2007).

Recruitment of Rad3p-Rad26p homologues and the 9-1-1 complex occur independently (Kondo *et al.*, 2001; Melo *et al.*, 2001).

Although the checkpoint signals generated by replication stress and DNA-damage clearly differ one from another, this mechanism of sensor recruitment to DNA seems to be common to all DNA checkpoint responses.

It has been suggested that these sensor checkpoint proteins may detect a common intermediate, such as single-stranded DNA coated by RPA (replication protein A), which is processed by various DNA repair pathways (Zou and Elledge, 2003). RPA has been shown to directly interact with the 9-1-1 complex (Wu *et al.*, 2005).

However, some events involving these sensor proteins are stress-specific. In this way, Rad3p phosphorylates Rad26p specifically after DNA-damage sensing (Edwards *et al.*, 1999).

Rad9p phosphorylation seems to be a key event in differentiation of checkpoint signals depending on the type of stress. Several Rad3-dependent phosphorylation events have been identified on fission yeast Rad9p. Phosphorylation of Thr412 and Ser423 (carboxy-terminal tail residues) is required to activate Chk1p in response to DNA-damage. Thr225 (within the PCNA-like domain) is required for Rad9p phosphorylation on replication-fork collapse (Furuya *et al.*, 2004). Rad9p Thr225 phosphorylation has been shown to be crucial to regulate the choice of repair pathways after genotoxic stress sensing (Kai *et al.*, 2007).

In addition, checkpoint sensor proteins have been shown to interact with a number of repair proteins, sometimes considered as adaptors since their interaction with checkpoint proteins seems to be required for damage sensing. For instance Nbs1p, member of the MRN (Mre11, Rad50, Nbs1) is required to recruit ATM to damage sites (You *et al.*, 2005). Such adaptor proteins may be DNA damage recognition proteins involved in mismatch repair, nucleotide excision repair and double-strand break repair. In *S. pombe* the 9-1-1 complex has been shown to interact with base excision repair (BER) member MYHp (Chang and Lu, 2005).

4.2 Adaptor proteins and scaffolds

Checkpoint adaptor or mediator proteins are required to transmit the checkpoint signal from the sensor phosphatidylinositol 3-kinase-like kinases to the

effector kinases Cds1p and Chk1p. In fission yeast, Crb2p, is the adaptor that connects the Rad3p-Rad26p complex to Chk1p (Saka *et al.*, 1997), whereas Mrc1p mediates signal transduction from Rad3p-Rad26p to Cds1p (Tanaka and Russell, 2001).

Rad4p/Cut5p is thought to function as a scaffold in a large protein complex containing both checkpoint proteins and replication proteins to selectively enforce the adequate checkpoint effector according to the triggering stress (Taricani and Wang, 2006).

Crb2p

The most conserved structural feature of Crb2p is a C-terminal BRCT tandem repeat (protein-protein interaction domain), which resembles similar domains in budding yeast ScRad9p and mammalian 53BP1, BRCA1, and MDC1/NFBD1. These BRCT proteins are each required for the phosphorylation of certain substrates of checkpoint sensor kinases, and collectively have been referred to as adaptors or mediators of the DNA damage checkpoint (Melo and Toczyski, 2002; Wang and Elledge, 2002; Canman, 2003). Crb2p and its homologues also present two tandem Tudor folds, which are protein-protein and protein-DNA interaction domains.

The BRCT domain of Crb2p mediates the homo-oligomerization of the protein, necessary for Chk1p activation by Rad3p-Rad26p phosphorylation (Du *et al.*, 2004). Crb2p itself is phosphorylated in a Rad3p-dependent but Chk1p-independent manner upon DNA damage (Saka *et al.*, 1997).

Crb2p is recruited to repair foci upon histone H2A phosphorylation by the Rad3p or Tel1p kinases and histone H4-K20 residue methylation (Nakamura *et al.*, 2004; Sanders *et al.*, 2004)

This mediator protein also plays a role in regulation of homologous recombination in G2 by modulating the activity of the Rqh1p helicase (Caspari *et al.*, 2002).

Mrc1p

Mrc1p (mediator of replication checkpoint) plays an essential role in checkpoint activation of Cds1p. Mrc1p is expressed predominantly during S phase and is phosphorylated by Rad3p and Tel1p on HU treatment (Tanaka and Russell, 2001;

Zhao *et al.*, 2003), being Rad3p phosphorylation sufficient for its interaction with Cds1p (Xu *et al.*, 2006).

Tel2p, member of the Tel2/Rad5/Clk2 protein family has also recently been implicated in Mcr1p phosphorylation and Cds1p activation (Shikata *et al.*, 2007).

Mcr1p N-terminal region presents a typical DNA-binding helix-loop-helix motif, also present in its human homologue Claspin. This domain interacts preferentially with branched DNA structures *in vitro* and is essential for its checkpoint function (Zhao and Russell, 2004).

Rad4p

Fission yeast Rad4p/Cut5p, a BRCT domain protein, orthologue of mammalian TopBP1, is also required for Chk1p phosphorylation and Cds1p activity (Harris *et al.*, 2003). It has been shown to associate with the replicative DNA polymerases, checkpoint sensor proteins Rad3p-Rad26p, Hus1p, Rad9p and Rad17p and with Crb2p and the WD-repeat protein Crb3p (Saka *et al.*, 1997; Garcia *et al.*, 2005; Taricani and Wang, 2006).

Phosphorylation of Rad9 on Thr412 and Ser423 in response to DNA-damage promotes its association to Rad4p via its two C-terminal BRCT domains. This association is necessary for activation of the Chk1p branch of the checkpoint but not Cds1p replication checkpoint (Furuya *et al.*, 2004).

14-3-3 proteins

The 14-3-3 proteins constitute a family of conserved multifunctional adapter proteins involved in a multitude of cellular functions, such as cell growth, cell signaling and cell death (van Hemert *et al.*, 2001). Of the two fission yeast 14-3-3 proteins, Rad24p and Rad25p, Rad24p appears to play the more important role in the checkpoint response and is involved in the proper execution of cell cycle arrest in response to DNA damage. However, multicopy expression of Rad25p can rescue *Δrad24* defects (Ford *et al.*, 1994). Simultaneous disruption of both 14-3-3 proteins is lethal.

14-3-3 proteins mediate the checkpoint response by affecting the localization of signaling proteins and checkpoint-targets.

Thus in *S. pombe* both 14-3-3 proteins, Rad24p and Rad25p have been shown to interact with Chk1p and the association between these proteins is stimulated by DNA damage (Chen *et al.*, 1999a). Rad24p is required for nuclear accumulation of Chk1p after replication fork collapse (Dunaway *et al.*, 2005). Rad24p also binds to Cdc25p and is required for the DNA damage-induced relocation of Cdc25p to the cytoplasm, necessary for cell cycle arrest (Chen *et al.*, 1999a; Lopez-Girona *et al.*, 1999; Zeng and Piwnica-Worms, 1999).

4.3 Effectors

In response to genotoxic stress the main checkpoint event is the phosphorylation of the effector protein kinases Chk1p and Cds1p by Rad3p (Lopez-Girona *et al.*, 2001b; Tanaka *et al.*, 2001; Capasso *et al.*, 2002).

Replication stress and DNA-damage inflicted during S phase leads to activation of the checkpoint kinase Cds1p (Murakami and Okayama, 1995; Lindsay *et al.*, 1998; Brondello *et al.*, 1999), whereas DNA-damage activates the checkpoint kinase Chk1p during G2 phase (Walworth *et al.*, 1993; Brondello *et al.*, 1999). Rad3p is necessary for both Chk1p and Cds1p activation but is only essential for maintenance of the replication checkpoint signal (Martinho *et al.*, 1998).

Replication stress and DNA-damage trigger by activation of either kinase a cell cycle block in S-phase or G2 in order to prevent progression into mitosis with damaged or unreplicated genetic material. Thus, activation of Cds1p and/or Chk1p leads to inhibition of Cdc25p and activation of Mik1p (Furnari *et al.*, 1997; Rhind *et al.*, 1997; Furnari *et al.*, 1999; Rhind and Russell, 2001). This results in enhanced inhibitory phosphorylation of Tyr15 of Cdc2p and the corresponding down-regulation of kinase activity necessary to prevent entry into mitosis.

Cell cycle block is not the only cellular response triggered by effector proteins upon checkpoint activation. As mentioned before, effector proteins also play key roles in coordination of cellular processes ensuring stability, repair and recovery from checkpoint arrest. Further information about Cds1p, Chk1p and their pathways can be found in sections 5 and 6.

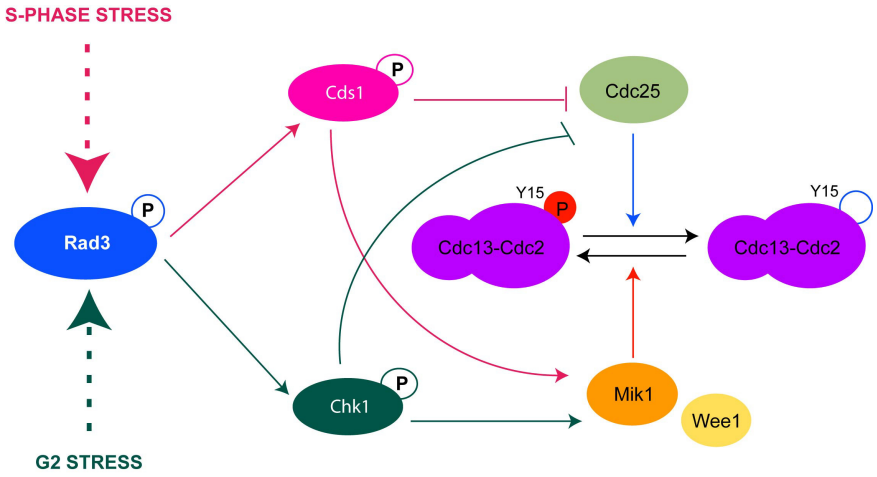

Figure I7. **Down-regulation of Cdc2p activity in response to DNA damage or replication stress**

Simplified scheme showing how upon DNA-stress, activated sensor protein Rad3p phosphorylates effector proteins Cds1p or Chk1p which in turn act over Mik1p and Cdc25p to inhibit Cdc2p activity and avoid cell cycle progression into mitosis.

5. DNA REPLICATION CHECKPOINT IN *S. pombe*

The replication checkpoint is a complex signal transduction pathway that is activated when nucleotide pools become limiting for DNA synthesis or replication forks encounter lesions in template DNA (Nyberg *et al.*, 2002; Osborn *et al.*, 2002). Under these circumstances, checkpoint activation is crucial for maintenance of genomic integrity and cell survival. Stalled forks represent serious threats to genomic integrity because they are prone to collapse or rearrangement (McGlynn and Lloyd, 2002c, b, a).

If replication forks are stalled, for instance as a consequence of ribonucleotide shortage, ssDNA accumulates as a consequence of uncoupling of DNA synthesis and MCM-driven DNA unwinding (Sogo *et al.*, 2002; Byun *et al.*, 2005; Nedelcheva *et al.*, 2005; Feng *et al.*, 2006). These ssDNA regions recruit RPA, which activates the checkpoint signal (You *et al.*, 2002; Zou and Elledge, 2003). The checkpoint triggers downstream pathways that prevent futile initiation events, stimulate the repair or

bypass of DNA damage, delay mitosis, and stabilize the replisome, allowing replication to resume when normal conditions are restored.

Cell cycle progression strongly delays at S-phase as a consequence of activation of the replication checkpoint. However, emerging evidence indicates that the most important effect of the replication checkpoint is to stabilize replication forks by maintaining proper assembly of replisome components and DNA structures in replication competent states when forks stall (Lopes *et al.*, 2001; Tercero and Diffley, 2001; Sogo *et al.*, 2002; Noguchi *et al.*, 2003; Tercero *et al.*, 2003; Noguchi *et al.*, 2004; Meister *et al.*, 2005; Ansbach *et al.*, 2007).

In addition, late replication origin firing is actively repressed under these conditions (Paulovich and Hartwell, 1995; Santocanale and Diffley, 1998; Kim and Huberman, 2001).

5.1 Cds1p: general features

In *S. pombe* Cds1p is the main effector of the checkpoint response to replication stress. According to the described roles of this checkpoint, Cds1p plays central roles in fork protection and stabilization, regulation of transcriptional response and coordination of processes involved in delay of S-phase progression and recovery. As mentioned when reviewing the checkpoint effectors, Cds1p plays a role in regulating Cdc2p activity and mediating cell cycle block in response to replication stress. However, the fact that Δ*cds1* cells can experience checkpoint block because of Chk1p activation but rapidly loose viability after HU treatment (Boddy *et al.*, 1998; Lindsay *et al.*, 1998), underscores the importance of Cds1p role in stabilizing replication forks rather than in mediating cell cycle arrest.

The *cds1* gene (checking DNA synthesis) was isolated as a multicopy suppressor of a temperature sensitive *pol*α mutant (Murakami and Okayama, 1995).

Cds1p is a 460 aminoacid serine-threonine kinase. It belongs to the Chk2 family of checkpoint kinases, which includes *S. cerevisiae* Dun1p, Rad53p and Mek1p and human Chk2p. Like all members of this family it presents a forkhead-associated (FHA) domain in its N-terminal region and a protein kinase domain. Its budding yeast counterpart is unique within the family in presenting an additional C-terminal FHA domain. The FHA domain mediates protein-protein interactions, being its optimal

binding sequence TXXD (Sun *et al.*, 1998; Durocher *et al.*, 1999; Durocher *et al.*, 2000).

Cds1p presents pancellular localization, being more highly concentrated in the nucleus during S-phase (Brondello *et al.*, 1999; Matsuyama *et al.*, 2006). Constitutive nuclear localization of the protein does not enhance its activation, indicating that its checkpoint role does not depend exclusively on this localization (Brondello *et al.*, 1999).

5.2 Cds1p activation

Cds1p is activated by replication stress in a two-step mechanism (Figure I8). In the first step, Cds1p interacts with active Rad3p-phosphorylated Mrc1p by means of its FHA domain. This is necessary to take Cds1p into the proximity of active Rad3p-Rad26p complex at stalled replication forks. Rad3p then phosphorylates Cds1p in its

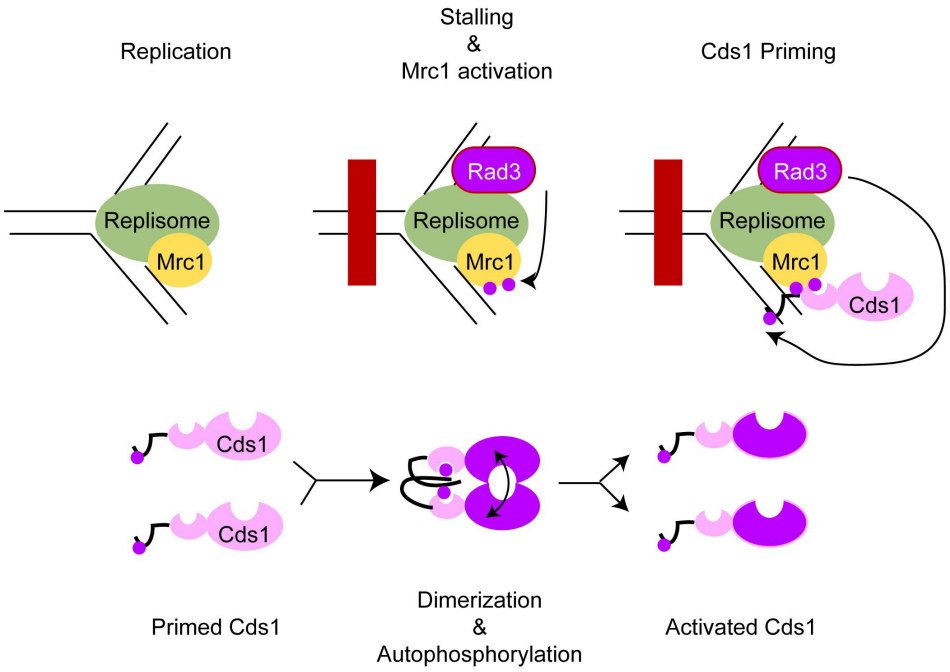

Figure I8. **Two-stage activation of Cds1p**
Adapted from Xu *et al.*, 2006.

Thr11 residue, completing the priming step (Tanaka and Russell, 2004; Xu *et al.*, 2006). In a second step, two primed Thr11-phosphorylated Cds1p molecules interact in a FHA-dependent manner to form a homodimer that is activated by autophosphorylation. Two sites in its activation loop, Thr328 and Thr332, seem to be responsible for this auto-induced activation (Xu *et al.*, 2006).

This mechanism is similar to that leading to human Chk2p activation, which is also mediated by oligomerization and autophosphorylation of two activation loop residues (Lee and Chung, 2001; Ahn and Prives, 2002; Ahn *et al.*, 2002; Xu *et al.*, 2002).

Other proteins implicated in Cds1p activation and fork stabilization

Other fork associated proteins like the Swi1p-Swi3p complex, also called FPC (Fork Protection Complex), and Sap1p are required for full activation of Cds1p (Noguchi *et al.*, 2003; Noguchi *et al.*, 2004; Noguchi and Noguchi, 2007).

All three proteins are involved in fork pausing at mating type switching and at ribosomal DNA repeats (Arcangioli *et al.*, 1994; Dalgaard and Klar, 2000; Mejia-Ramirez *et al.*, 2005). The Swi1p-Swi3p complex is evolutionary conserved. It is homologous to the Tof1p-Csm3p complex in *S. cerevisiae* and to the Timeless-Tipin complex in humans (Gotter, 2003; Mayer *et al.*, 2004; Noguchi *et al.*, 2004). Both human and budding yeast complexes have been implicated in checkpoint signalling (Foss, 2001; Katou *et al.*, 2003; Unsal-Kacmaz *et al.*, 2005). Sap1p has been shown to bind to at least one origin of replication and is required to recruit Swi1p-Swi3p to chromatin (Noguchi and Noguchi, 2007). The FPC is thus chromatin-bound during S-phase and travels along with the replication machinery. In this way the FPC is involved in the stabilization of stalled replication forks in a configuration that enables full checkpoint recognition and signalling.

A putative helicase, Chl1p, has been recently proposed to work in the same pathway as Swi1p acting cooperatively in its fork stabilization and checkpoint functions (Ansbach *et al.*, 2007).

A replication competent state seems, thus, to be necessary to guarantee proficient Cds1p activation. Further supporting this, proteins implicated in replication initiation and progression such as Hsk1p, Ctf18p, Orc1p and Cdc45p have shown to be

required for full activation of the checkpoint kinase (Snaith *et al.*, 2000; Takeda *et al.*, 2001; Nitani *et al.*, 2006; Ansbach *et al.*, 2007).

5.3 Cds1p and co-workers: linking fork stabilization to recovery from checkpoint arrest

The mechanisms of fork stabilization during replication stress, of which Cds1p is the main effector, are complex and further linked to a number of related processes essential for genomic integrity such as sister chromatid cohesion, regulation of recombination, and recovery from replication block.

Thus, for instance, the minichromosome maintenance (MCM) complex, a helicase essential for replication initiation and elongation, has been shown to play roles in fork stability and recovery. To achieve this, its subunit Mcm4p is bound to and phosphorylated by Cds1p during HU treatment, and further interacts with the homologous recombination protein Rph51p (Bailis *et al.*, 2008). The regulation of the MCM complex by the checkpoint has been proposed to be necessary to avoid the de-attachement of the replisome from stalled replication forks and thus to be an essential mechanism in the maintenance of fork stability (Forsburg, 2008).

Hsk1p also plays multiple roles during and after replication stress. Hsk1p is a serine/threonine kinase homologous to Cdc7p in *S. cerevisiae* necessary for origin activation by regulation of targets such as the MCM (Lee *et al.*, 2003). In addition to its mentioned role in Cds1p activation, Hsk1p in its turn gets phosphorylated by the checkpoint kinase during early S-phase arrest (Snaith *et al.*, 2000; Takeda *et al.*, 2001). Depletion of Hsk1p at the recovery stage allows bulk replication but leads to aberrant mitosis and loss of nuclear integrity (Snaith *et al.*, 2000).

In addition Hsk1p, its regulatory subunit Dfp1p/Him1p, and Swi1p-Swi3p have been implicated in slowing S-phase in response to DNA-alkylation in a checkpoint independent manner (Sommariva *et al.*, 2005).

Ctf18p, an RFC1-like subunit of the alternative replication factor C complex, and Swi1p-Swi3p in addition to their role in Cds1p activation are required for sister chromatid association and Ctf18p is also involved in timely replication resumption during recovery (Ansbach *et al.*, 2007).

Sap1 is also necessary for replication restart after block of replication forks (Noguchi and Noguchi, 2007).

Cds1p is, as presented, the key regulator coordinating fork stability, recovery and stress bypass upon replication stress. Further illustrating this, Cds1p kinase activity is responsible for the prevention of unwanted recombinational events at stalled replication forks through regulation of Mus81p-Eme1p endonuclease complex, Rqh1p helicase and Rad60p. The extent of Cds1p activation determines the degree in which cells tolerate replication stress. When the activation of the checkpoint kinase is low, fork protection is not completely ensured and recombinational processes may occur to cope with aberrant DNA structures and to tolerate replication stress (Kai *et al.*, 2005; Froget *et al.*, 2007). Rad60p and other proteins involved in homologous recombination are necessary for recovery from replication arrest (Miyabe *et al.*, 2006) further underscoring the importance of proficient regulation of recombination by the checkpoint. Further analysis of Cds1p implication in the regulation of recombinational events can be found in section 7.2.

6. DNA-DAMAGE CHECKPOINT IN *S. pombe*

The DNA-damage checkpoint coordinates cell cycle block in G2 with repair mechanisms in order to preserve genomic integrity when DNA damage is detected.

In fission yeast, mitotic entry is inhibited by the activation of the conserved Chk1p kinase in response to damaged DNA in late S and G2 phases of the cell cycle (Walworth and Bernards, 1996; Martinho *et al.*, 1998). Furthermore, the Chk1p pathway is activated in response to damaged or collapsed replication forks, a situation that can occur after processing of certain structures during S-phase or as a result of a defective response of the replication checkpoint (Boddy *et al.*, 1998; Lindsay *et al.*, 1998; Wan *et al.*, 1999).

Cross-talk between the DNA-damage checkpoint and the spindle checkpoint via Mad2p occurs to provide adequate cell cycle delay when DNA checkpoints efficiency is compromised (Sugimoto *et al.*, 2004; Collura *et al.*, 2005).

6.1 Chk1p

Chk1p is a 496 aminoacid Serine/Threonine protein kinase, consistent of a highly conserved N-terminal kinase domain and a C-terminal non-catalytic domain.

Chk1p is essential for survival in response to DNA damage, as fission yeast cells lacking the *chk1* gene do not delay cell cycle progression, resulting in hypersensitivity to DNA damaging agents (Walworth *et al.*, 1993; al-Khodairy *et al.*, 1994).

Chk1p presents a basal level of kinase activity that is elevated at least two-fold in response to DNA-damage (Capasso *et al.*, 2002). The precise mechanism by which Chk1p is activated in response to various DNA lesions has yet to be elucidated.

Rad1p, Rad3p, Rad9p, Rad17p, Rad26p, Hus1p, Rad4p/Cut5p, and Crb2p are essential for Chk1p activation (al-Khodairy and Carr, 1992; Enoch *et al.*, 1992; al-Khodairy *et al.*, 1994; Walworth and Bernards, 1996; Saka *et al.*, 1997). Rad24p is also critical for Chk1p function as it binds to phosphorylated Chk1p and facilitates its nuclear localization following DNA damage (Ford *et al.*, 1994; Dunaway *et al.*, 2005).

Ser345 in fission yeast Chk1p is phosphorylated *in vivo* by Rad3p and this phosphorylation is required to activate Chk1p kinase activity in the presence of DNA damage (Ford *et al.*, 1994; Lopez-Girona *et al.*, 2001b; Capasso *et al.*, 2002; Dunaway *et al.*, 2005). Human Chk1p is also phosphorylated at S345, emphasizing the evolutionary importance of Chk1p in the checkpoint pathway (Liu *et al.*, 2000; Zhao and Piwnica-Worms, 2001).

Recently a conserved aspartic acid at position 469 of fission yeast Chk1p has been involved in checkpoint specificity to certain DNA lesions (Palermo *et al.*, 2008).

Chk1p is also implicated in regulating dNTP production necessary for repair processes. Activation of Chk1p in G2 induces Spd1p degradation, necessary for the exclusion of the small subunit of ribonucleotide reductase (RNR), Suc22p, from the nucleus. In the cytoplasm Suc22p interacts with Cdc22p to form the RNR active complex, leading to dNTP production. Chk1p-independent degradation of Spd1p and subsequent processes are also necessary for dNTP production during unperturbed S-phase (Liu *et al.*, 2003).

Once repair of damaged DNA has been completed Chk1p activity is down-regulated through dephosphorylation by Type 1 protein phosphatase to allow for cell cycle re-entry (den Elzen and O'Connell, 2004).

7. DNA DAMAGE AND REPAIR MECHANISMS

DNA damage is an extremely common event in a cell's lifetime. Cells are exposed to both exogenous and endogenous sources of stress and DNA damage, ranging from reactive oxygen species resulting from cellular metabolic processes and the inacuracy of DNA replication itself to environmental factors such as ultraviolet radiation from the sun and chemical mutagenic compounds.

Different sources of stress lead to different kinds of DNA damage: DNA base modifications (oxidation, alkylation, hydrolysis and mismatches), breaks in the DNA backbone (single strand breaks, SSBs, and double strand breaks, DSBs) and crosslinking of the DNA (on the same DNA strand, intrastrand, or on the opposite strand, interstrand).

Damaged or inappropiate bases can be repaired either by direct chemical reversal of the damage by specific enzymes, or by Excision Repair, in which the damaged base or bases are removed and then replaced with the correct ones through localized DNA synthesis. There are three types of excision repair (Base Excision Repair, BER, Nucleotide Excision Repair, NER, and Mismatch Repair, MMR) differing in the way and extent to which bases are removed and the enzymes involved.

Single-strand breaks are repaired using the same enzyme systems used in BER. Double-strand breaks are normally either repaired by direct joining of the broken ends in a process known as Nonhomologous End-Joining (NHEJ) or Homologous Recombination (HR) by means of which the broken ends are repaired using the information of an intact homologous strand.

7.1 Double-strand Break repair

Double strand breaks appear both due to endogenous cellular processes, such as nucleotide excision repair or meiotic recombination, and to exposure to exogenous sources of DNA-damage or replication stress.

It is assumed that human cells suffer approximately 10 spontaneous DSBs per cell cycle. Spontaneous DSBs are supposed to appear when the replication machinery encounters single strand breaks, and also as a result of inadequate action of topoisomerase II (reviewed in Haber, 1999). Ionizing radiation is an important external source of DSBs. Other DNA-damaging agents, directly or indirectly, lead to DSB formation.

Among the forms of DNA-damage, DSBs are especially deleterious, since they can lead to loss of large chromosomal fragments resulting in loss of heterozygosity and cell death. Therefore, eukaryotic organisms have evolved different pathways for DSB repair: the previously cited NHEJ and HR, together with single strand annealing (SSA). Since DSBs normally involve base pair loss, mechanisms which act through ligation of the strand ends (NHEJ and SSA) are error-prone. During HR a homologous strand from the sister chromatid or the homologous chromosome is used as a template to copy the intact sequence missing in the damaged strands, thus normally achieving an error-free repair.

CDK activity may positively regulate HR and thus the choice between NHEJ and HR seems to be cell cycle regulated (Ferreira and Cooper, 2001; Caspari *et al.*, 2002). In *S. pombe*, G1 is very short, DNA is replicated before cytokinesis, being G2 the longest cell-cycle phase. Thus a sister chromatid is available as a repair template during most cell cycle. Therefore HR is the dominant DSB repair pathway in fission yeast, being NHEJ the active repair pathway in G1.

Homologous recombination

Homologous recombination includes different pathways that apply a common mechanism of DSB repair which consists on invasion and copy of a homologous strand to replace the sequence missing as a consequence of the break.

Recognition of DSBs is performed by the MRN complex (Mre11p^{SpRad32p}–Rad50p–Nbs1p), which is highly conserved and further implicated in NHEJ, HR, telomere maintenance and activation of the DNA damage checkpoint. The MRN promotes resection of the DSBs to form single stranded DNA overhangs which are subsequently coated by RPA. These overhangs serve as primers for invasion and copy of the homologous strand which serves as a template.

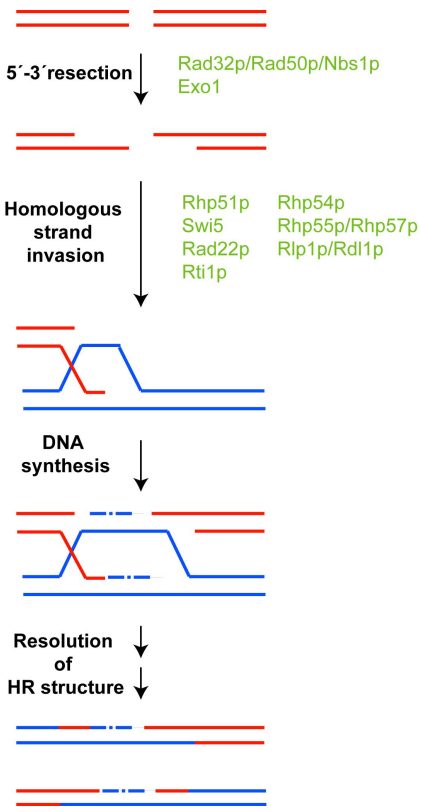

Figure I9. HR in Fission yeast

Schematic representation of DSB repair by HR in *S. pombe* including the main proteins involved. Damaged strands are coloured in red and the intact template in blue.

The main event in HR is the strand exchange reaction catalysed by Rad51p^{SpRhp51p}, homologue of the bacterial RecA protein. *S. pombe* Rhp51p binds ssDNA forming a nucleoprotein filament and promotes exchange reactions with homologous duplex DNA (Sauvageau *et al.*, 2005). Rad51p^{SpRhp51p} binding to ssDNA requires mediator proteins to overcome the inhibitory effect of the competitor protein RPA, which presents high affinity to ssDNA. Recombination mediators in *S. pombe* include ScRad52p homologues, Rad22p and Rti1p, Rhp54p (ScRad54p homologue), Rhp55p (ScRad55p homologue), Rhp57p (ScRad57p homologue), and Rad51-like proteins, like Rlp1p and Rdl1p. Rlp1p has been suggested to function in the recombinational pathway of DSB repair together with Rhp51p, Rhp55p and Rad22p and may be required for proficient DNA recombination and cell survival when replication forks collapse (Khasanov *et al.*, 2004).

The resulting nucleoprotein filament finds its homologous sequence by single-end invasion, a process aided by Rad54p^{SpRhp54p}. The 3' end of the invading strand is extended by a DNA polymerase.

During resolution of HR structures, crossovers between homologous DNA sequences can occur, which can lead to abnormal chromosomal rearrangements and other deleterious events during mitotic cell cycle. Mitotic crossovers arise primarly through the action of Mus81-Eme1 acting downstream of Swi5 (Hope *et al.*, 2007), a small protein implicated in an HR process alternative to the action of Rhp55/57p (Akamatsu *et al.*, 2003). HR, however, occurs mainly through an Rhp57p dependent pathway where Rqh1p-Top3p acts to block crossing over (Hope *et al.*, 2007). Adaptor protein Crb2p, regulated by CDK activity and Rad3p phosphorylation, controls the function of Rqh1p and Top3 at the late stages of the recombination repair process.

Rad22p

In *S. pombe* two ScRad52p homologues, Rad22p and Rti1p/Rad22Bp have been identified. Both Rad22p and Rti1p have been shown to interact with each other and with Rhp51p and RPA (Kim *et al.*, 2000; Tsutsui *et al.*, 2001; van den Bosch *et al.*, 2001; van den Bosch *et al.*, 2002) and they are able to bind to ssDNA and form multimeric structures like Rad52p (de Vries *et al.*, 2007). Rad22p seems to play a predominant role during HR in mitosis, being Δ*rad22* cells sensitive to ionizing radiation (IR) (Muris *et al.*, 1997). Rad22p recruitment to DSBs seems to be independent of checkpoint signaling and of other HR proteins (Meister *et al.*, 2003). Rti1p is expressed to low levels during vegetative growth and is not induced upon DNA-damage. Cells deleted for *rti1* are only slightly sensitive to DNA-damage but over-expression of *rti1* is able to partially recue Δ*rad22* sensitivity to DSB formation. Rti1p seems to be involved in HR during meiosis (van den Bosch *et al.*, 2001; van den Bosch *et al.*, 2002).

Rad22p seems to be central to most HR events in *S. pombe.* This protein has been associated to two Rhp51p-independent recombinational pathways, one associated to repair of collapsed forks together with Mus81p, and in the replication of tandem repeats of rDNA locus together with Slx1p-Slx4p (Doe *et al.*, 2004; Coulon *et al.*, 2006). In fact, approximately 50% of the spontaneous Rad22p repair foci that occur in cycling cells depend on Slx1p and localize to the nucleolus, which contains the rDNA repeats (Coulon *et al.*, 2006). Futhermore Rad22p is involved in other mechanisms of DSB repair, such as single strand annealing (van den Bosch *et al.*, 2002).

7.2 DNA repair and HR during S-phase and replication stress

Work in bacterial systems indicate that Holliday Junctions can form at stalled replication forks by fork reversal, which are subsequently cleaved to form DSBs (Cox, 2001). HR has been implicated in the bypass of replication fork barriers and replication restart at stalled forks (McGlynn and Lloyd, 2002a).

In addition to its role in DNA-damage repair, HR machinery is recruited to DNA during a perturbed S-phase probably to deal efficiently with structures that may arise from replication fork stalling. The regulation of recombinational activity at this stage is determinant for cell viability. The presence of recombination machinery can result in appearance of non-functional structures if replication forks are not adequately stabilized, resulting in toxicity. Thus the double mutant ∆*rhp51* ∆*cds1* has been proven to recover from replication fork stalling whereas ∆*cds1* cells rapidly loose viability (Meister *et al.*, 2005).

A direct regulation of the recombination machinery by the Cds1p-branch of checkpoint response to preserve genomic integrity has been proposed. Cds1p interacts by means of its forkhead-associated domain whith recombination proteins Mus81p, Rad60p and Rqh1p (Boddy *et al.*, 2000; Boddy *et al.*, 2003). Endonuclease Mus81p is implicated in the maturation or recombination intermediates and in processing of abnormal replication structures (Boddy *et al.*, 2000; Doe *et al.*, 2002). The complex Mus81p-Eme1p has been proposed to be responsible for deleterious deletion mutations in cells undergoing replication stress (Boddy *et al.*, 2000). Rad60p is required for DSB repair during replication (Morishita *et al.*, 2002). Rqh1p prevents regression of stalled replication forks (Doe *et al.*, 2002). Thus, ∆*rqh1* cells are unable to recover from HU induced S-phase arrest and show strongly increased levels of recombination after HU treatment (Stewart *et al.*, 1997). Checkpoint activated Cds1p triggers Mus81p-Eme1p dissociation from chromatin (Boddy *et al.*, 2000; Kai *et al.*, 2005), promotes nuclear delocalization of Rad60p (Boddy *et al.*, 2003) and enhances Rqh1p activity. These events result in prevention of inadequate recombinational repair and stabilization and recovery of stalled replication forks. They further prove a direct link between Cds1p and regulation of recombinational repair processes. Consistent with this, Rad22p foci appear during S-phase in cells presenting an S-phase deficient checkpoint.

8. TRANSCRIPTIONAL RESPONSE OF *S. pombe* TO DIFFERENT SOURCES OF STRESS

Checkpoint response in endogenously or exogenously harassed cells involves changes in gene expression which account for consecution of the adequate cell environment to prevent genomic instability. Although the way in which cell signaling and protection occurs is in most cases specific for each type of stress, there is a common set of genes whose expression is altered in response to most stresses. This core environmental stress response (CESR) was initially defined in a study involving oxidative stress (H_2O_2), osmotic stress (Sorbitol), heat shock, heavy metal stress (Cd) and DNA damage (MMS), and involves 140 induced genes and 11 repressed genes common to at least four of the five stresses (Chen *et al.*, 2003). Other studies have shown a considerable overlap between the CESR and the genes regulated in checkpoint response to Cisplatin (48), Ionizing radiation (108) and HU (50) (Gatti *et al.*, 2004; Watson *et al.*, 2004; Chu *et al.*, 2007). The induced genes code mainly for antioxidants, regulatory proteins and proteins involved in carbohydrate metabolism. Surprisingly, the CESR contains only two heat shock proteins, and two genes predicted to be involved in DNA repair. The repressed genes (106 in a less restrictive cut off for 3 out of the 5 stresses) are involved in protein synthesis and transport, transcription, signaling and cytoskeleton organization. This core response is largely dependent on the stress-activated mitogen-activated protein kinase Sty1p, partially by means of the transcription factor Atf1p (Chen *et al.*, 2003). Rad3p has also been shown to play a minor role in CESR regulation (Watson *et al.*, 2004). The CESR overlaps significantly with the CER/ESR of *S. cerevisiae*, pointing to an evolutionary conserved response to environmental stress (Chen *et al.*, 2003).

In addition to this core transcriptional response there are subsets of genes that are specifically regulated depending on the stress source. Sty1p is only important for the specific response to oxidative and osmotic stresses (Chen *et al.*, 2003).

DNA damage caused by H_2O_2, IR and MMS, alters a common set of 12 genes including genes involved in initiation of replication (*cdc18* and *cdt2*) and stress response (*trr1*) (Watson *et al.*, 2004). Homologous recombination genes *rhp51* and *rhp54*, as well as translesion DNA synthesis repair gene *dinB* are induced in IR treatment in a Rad3p dependent and Cds1p or Chk1p independent manner (Watson *et al.*, 2004). Surprisingly few genes involved in DNA repair are induced by these

stresses and genes encoding checkpoint proteins are largely unaffected, indicative of a predominant posttranslational modulation.

Transcriptional response to S-phase block induced by HU involves 49 CESR genes, 18 of which are Rad3p dependent and 39 Cds1p dependent (Chu *et al.*, 2007). Replication stress specific response includes expression of Mlu1-like cell cycle box (MCB) motif-containing genes and histone cluster genes as well as repression of FKH and ACE2 clusters (Chu *et al.*, 2007). MCB genes (such as *cdc22, cdc12, cdt1, cig2* and *mik1*) are cell-cycle regulated by MBF-DSC1 (Cdc10p, Res1p, Res2p and Rep2p) and peak at G1. Most of them are involved in DNA replication and required for G1/S transition (Rustici *et al.*, 2004; Oliva *et al.*, 2005; Peng *et al.*, 2005). Zinc finger transcription factor Ace2p regulates ACE2 motif-containing genes which code for proteins involved in cytokinesis (Martin-Cuadrado *et al.*, 2003). *ace2* expression, in its turn, is controlled by forkhead transcription factor Sep1p and Fkh2p members of the FKH cluster (Zilahi *et al.*, 2000; Buck *et al.*, 2004). Expression of MCB genes during HU block depends on the checkpoint branch Rad3p-Cds1p and should guarantee the adequate cellular conditions for re-start of replication at the recovery stage, whereas FKH and ACE2 repression, only bypassed in Δ*rad3* cells since it can be triggered either by the Cds1p or the Chk1p checkpoint pathways, is important for replication checkpoint block (Chu *et al.*, 2007).

9. MATHEMATICAL MODELLING OF BIOLOGICAL NETWORKS

Many human diseases, such as cancer, diabetes, and neural disorders are caused by defective or abnormal intra- or inter-cellular signalling. Studying the behaviour and mechanism of action of the respective signalling pathways under different situations is thus the key to understand the reasons that lead to pathology and to identify possible targets of therapy. Biological research in its different aspects generates by means of high-throughput methods and specific low-throughput studies an enormous amount of information on the signalling cascades subject to study relating their components, the interactions among them and their coordination. However, the complexity of biological systems precludes untangling these networks with the human mind alone. Due to the complex mechanisms involved, such as feedback loops and crosstalk between paths, the resulting behaviour is non-linear and often non-intuitive. Therefore, abstraction of complex biological systems such as signalling pathways into mathematical models proves to be a useful tool to understand

the mechanisms that underlie their observed behaviour. Computational modelling of cellular processes has proved to represent experimental knowledge in a mathematically testable form, to elucidate design principles, and to describe the dynamics of biological pathways under different experimental conditions.

9.1 Some notions on mathematical modelling of biological networks

Different types of models and simulation techniques can be used for mathematical modeling of biological networks. Continuous deterministic models based on ordinary differential equations (ODEs) are often used for the modeling and simulation of dynamic processes. Continuous models are used to dynamically simulate the profile of the network over time, in opposition to discrete models in which only certain time points are considered. In deterministic simulation present model states influence future ones, in opposition to stochastic simulation that is based in the probability of successive states.

Continuous deterministic models are based on a scheme of the hypothesised interactions among the main components involved. This scheme should be built using state of the art information derived from the experimental characterisation of the network. The resulting diagram is then converted into a set of differential equations that describe how the concentration of each component changes over time and eventually space. These equations are based on the law of mass conservation after which, if diffusion and dilution terms are neglected, a species is accumulated depending on the net rate of its production. Such differential equations are expressed in the form:

$$\frac{dc_i}{dt} = \sum_{j=1}^{r} n_{ij} v_j$$

where *r* is the number of reactions in the network, *vj* the rate of the *j* reaction and *nij* the stoichiometric coefficient of c_i in reaction *j* (see MATERIALS AND METHODS). Taking into account that a considered species is produced and/or consumed in a number of reactions, these equations represent the summation term of the reaction rates in which a species is produced minus the reaction rates in which it is consumed.

In its turn, each reaction rate is mathematically expressed as a function of the abundances of the substrate and modifiers or enzymes involved, and includes reaction constants or parameters whose values are often not known. If the concentrations of some species at determined time points are known, that is, if experimental data points are available, these unknown parameters can be estimated to obtain an accurate mathematical description of the system.

Parameter estimation or fit consists on an automated process by means of which the parameter set that better fits the experimental data points is searched. It basically consists on a refinement loop: an initial set of parameter values is assigned and the dynamic equations are solved to give simulated values of the species concentrations at each time point. The simulations are compared quantitatively with the available data points. If the match between simulation and experimental data is unsatisfactory, then the parameter assignments are adjusted to achieve a better fit. There are many strategies for searching the optimum parameter set.

Parameter estimation can be considered as step for model validation itself. Often no set of parameters can be found that adequately fits the experimental data points. That means that the model is not able to describe the behaviour of the system and the initial scheme of the network and/or the kinetic equations for the reactions should be written in another way.

Fitted models should then be validated using experimental data not previously used for the parameter fit (for instance, behaviour of different mutants) in order to obtain reliable models that can be used to make predictions about the behaviour of the system under conditions not tested.

9.2 Mathematical modelling as a useful tool for biological investigation

Validated models are a valuable tool for biological investigation. First of all, they present a mechanistic scheme for the networks usually globalising and connecting huge amounts of isolated experimental data and bridging the gaps where experimental evidences are missing. The state of the art knowledge based in unconnected experiments normally allows for the writing of network interactions in different ways, which *a priori* can be equally valid. Thus, in the process of building and validating the model, initial working schemes have frequently to be discarded to favour

others that prove to better reproduce the observed behaviour of the pathway. In this way, mathematical modelling can be regarded as an iterative process involving a close interplay of mathematical and biological inputs and outputs. Modelling itself is useful as a process, even if the resulting model is not satisfactory. It forces abstract thinking and the extraction of essential features of a process. It highlights aspects where our understanding of a matter is wrong or insufficient and it facilitates a unique description of our current knowledge and of the gaps therein.

On the other hand, mathematical analysis of validated models provides us with information that is difficult to achieve by undirected biological experiments. For instance, by means of sensitivity analyses of the network, one can predict which reactions/species play the most important role in maintaining the stability or reproducing the output of the system. Validated models are furthermore a valuable tool to predict the behaviour of the pathway under different experimental conditions. For example, in a given network one can knock-out or increase the concentration of a specific component to study the local or global effects of these changes.

Mathematical modelling of biological networks should be regarded as an emerging and highly useful tool for biological investigation that is intimately linked to experimental work. Accurate models can only be built upon reliable experimental data, necessary for model construction, parameter fit and validation. Models in its turn provide investigators with valuable information and a global and local vision of the network that can be difficultly obtained without computational power. Once again, relevant model predictions should be validated by experiments. In this way, close work between experimentalists and modellers often give rise to unexpected and exciting discoveries.

9.3 Mathematical modelling of the cell cycle and checkpoint responses

Understanding the mechanisms underlying cell cycle progression and control is a key biological and medical question that greatly helps the advances in treatment and prevention of related disorders like cancer.

Cell cycle progression has been subject to a number of dynamic modelling approaches. Early modelling attempts tried to understand the oscillatory nature of the cell cycle (Tyson, 1979; Goldbeter, 1991).

Comprehensive models for cell cycle progression have been historically developed by the Tyson and Novak groups, who paved the way to include more and more molecular details and to understand the contribution of individual components of the cell cycle machinery. They built models for different aspects of the cell cycle engine in *Xenopus* oocytes (Novak and Tyson, 1993; Marlovits *et al.*, 1998; Ciliberto *et al.*, 2003; Ciliberto *et al.*, 2005), fission yeast (Novak and Tyson, 1997; Novak *et al.*, 1998; Sveiczer *et al.*, 2000; Novak *et al.*, 2001; Sveiczer *et al.*, 2001, 2004; Csikasz-Nagy *et al.*, 2007; Csikasz-Nagy *et al.*, 2008), budding yeast (Chen *et al.*, 2000; Chen *et al.*, 2004; Toth *et al.*, 2007) and mammalian cells (Novak and Tyson, 2003, 2004). These models are based on a huge amount of experimental evidence in the literature and the major test for their validity is to reproduce the phenotypes of a large series of mutants correctly. While qualitative predictions of these models for wild-type cells agree with available data, they do not include time-course data to prove the correctness of the simulated dynamics.

Different approaches to mathematical modelling and analysis of cell cycle related events in eukaryotes have been undertaken by numerous groups. The scope of these models is diverse, ranging form detailed descriptions of specific cell cycle transitions, to the inclusion of transcriptional events and checkpoint modules or even to the study of cell cycle in tumour cells (Aguda, 1999b, a; Aguda and Algar, 2003; Qu *et al.*, 2003a; Qu *et al.*, 2003b; Cokus *et al.*, 2006; Faure *et al.*, 2006; Srividhya and Gopinathan, 2006; Alarcon and Tindall, 2007; Barberis *et al.*, 2007; Tindall and Please, 2007, among others).

The relevance of mathematical modelling of cell cycle related events has also led to the creation of cell cycle specific databases like the Cell Cycle Database (Alfieri *et al.*, 2007, 2008) for yeast and mammals (that integrates information about genes and proteins involved in the cell cycle process, stores complete models of the interaction networks and allows direct simulations), and the Cyclonet database on cell cycle regulation in mammals in normal and pathological states (Kolpakov *et al.*, 2007).

OBJECTIVES

1. To elucidate if *Schizosaccharomyces pombe* phosphatase Flp1p is involved in checkpoint response to genotoxic stress.

2. To study the role of the phosphatase in checkpoint response to genotoxic stress: analysis of the phenotypes associated to mutation of *flp1* in checkpoint response to unreplicated or damaged DNA.

3. To study the mechanism of action of Flp1p in checkpoint response to genotoxic stress: analysis of the functional relationship between the phosphatase and different proteins involved in the cellular response to unreplicated or damaged DNA.

MATERIALS AND METHODS

1. MEDIA AND CULTURE MANIPULATION

1.1 *Schizosaccharomyces pombe*

The standard culture media and conditions used in this work have been previously described by Moreno *et alter* (Moreno *et al.,* 1991).

Standard rich medium yeast extract plus supplements (YES) or minimal medium (MM) adequately supplemented with aminoacids (leucine, histidine) and/or nitrogenated bases (adenine, uracil) depending on the auxotrophies of the strain at 225 mg/L final concentration in liquid or solid form were used for growth (Moreno *et al.*, 1991).

Experiments in liquid medium were performed, unless otherwise specified, at 30ºC, adjusting exponential growing cultures to an initial optical density of 0.4-0.5 measured at 595 nm (4-5·10^6 cells/ml). For growth in solid medium plates were incubated at 30ºC unless otherwise specified.

Over-expression of genes

Strains containing repressible *nmt1*-plasmids were grown in minimal medium (MM) appropriately supplemented and containing 5mg/ml thiamine. Induction was triggered by washing exponentially growing cultures and resuspending in medium without thiamine as described previously (Cueille *et al.*, 2001). The standard induction time used was 16 hours.

Repression of genes and synchronization in temperature sensitive alleles

Temperature sensitive alleles were grown to exponential rate at 25ºC.

Strains containing *cdc10-129* or *cdc10-M17* alleles were synchronised by temperature shift to 36ºC for 4 hours. Release was performed at 25ºC.

mts1-1/*rpn9*-1, *mts2*-1/*rpt2*-1 and *mts3*-1/*rpn12*-1 were incubated in YES to exponential growth at 25ºC. Repression of the genes was performed at 36ºC.

Drug treatment

In asynchronous cultures drug was added to exponentially growing (4-5·10^6 cells/ml) cultures.

In synchronized or temperature sensitive alleles the drug was added at the release/temperature shift time point.

Standard drug concentrations used in liquid medium: 12mM HU, 0.033% MMS or 7.5 mU BL. Use of other concentrations is specified.

1.2 *Escherichia coli*

E. coli was incubated at 37ºC using the culture media and conditions described in Sambrook et al., 1989.

2. STRAINS USED

The different *S. pombe* strains used in the experiments described in RESULTS, and the parental strains of the strains specifically generated for this study, as well as their genetic characteristics and procedure, are shown in Table M1.

E. coli DH5α was used in experiments involving plasmid production in bacteria.

3. GENERATION OF STRAINS AND TRANSFORMATION TECHNIQUES

3.1 Strain crossing

S. pombe strains generated for this study were normally obtained by genetic cross. Spores were selected using random analysis or tetrad selection as described in Moreno et al., 1991.

GENOTYPE	STRAIN	SOURCE
h- ade6-704 leu1-32 ura4-d18	S88	Dr. Moreno
h+ ade6-704 leu1-32 ura4-d18	S89	Dr. Moreno
h+ cdc10-129 leu1-32 ura4-d18	4.75	Dr. Bueno
h- cdc10-129 flp1::KanMX6	31.1	Dr. Bueno
h+ cdc10-129 flp1::flp1-GFP-KanMX6 ura4-d18	41.60	This study
cdc10-129 flp1::flp1-9a-EGP-leu2-KanMX6	51.11	This study
cdc10-129 rad3::ura4+ flp1::flp1-GFP-KanMX6	54.06	This study
cdc10-M17 ade6-704 leu1-32 ura4-d18	53.29	Dr. O'connell
cdc10-M17 rad3::ura4+	54.07	This study
cdc10-M17 flp1::KanMX6	54.08	This study
h+ cdc17-K12 ura4-d18	263	Dr. Moreno
cdc17-K12 flp1::flp1-GFP-KanMX6	52.17	This study
h+ cds1:2HA6his leu1-32 ura4-d18		Dr. Russell
cds1:2HA6his flp1::KanMX6	42.05	This study
h- cds1::ura4+ leu1-32 ura4-d18		Dr. Russell
h- cds1::ura4+ flp1::flp1-3HA-KanMX6 ade6-704 leu1-32 ura4-d18	42.43	This study
h- cds1::ura4+ flp1::flp1-GFP-KanMX6 ura4-d18	41.70	This study
cds1::ura4+ flp1::KanMX6 ade6-704 leu1-32	42.11	This study
h+ chk1:9myc2HA6his leu1-32 ura4-d18		Dr. Russell
chk1:9myc2HA6his flp1::KanMX6	42.23	Dr. Bueno
h+ chk1:HA ade6-704 leu1-32	S1012	Dr. Moreno
chk1:HA flp1::KanMX6	51.13	This study
h- dis2::ura4+ leu1-32 ura4-d18		Dr. Simanis
h- dis2::ura4+ flp1::KanMX6 ura4-d18		Dr. Simanis
h- chk1::ura4+ ade6-704 leu1-32 ura4-d18		Dr. Russell
h- chk1::ura4+ flp1::flp1-3HA-KanMX6 ade6-704 leu1-32 ura4-d18	42.46	This study
h- chk1::ura4+ flp1::flp1-GFP-KanMX6 ade6-704 leu1-32 ura4-d18	41.72	This study
chk1::ura4+ flp1::KanMX6 ade6-704 leu1-32	42.17	This study
h- flp1::flp1-3HA-KanMX6 ade6-704 leu1-32 ura4-d18	44.32	Dr. Bueno
h- flp1::flp1-GFP-KanMX6 ade6-704 leu1-32 ura4-d18		Dr. Simanis
h- flp1::flp1-9a-EGP-leu2-KanMX6	50.69-71	This study
h- flp1::KanMX6 ade6-704 leu1-32 ura4-d18	43.56	Dr. Bueno
h+ flp1::KanMX6	30.20	Dr. Bueno
h+ flp1::KanMX6 ade6-704 leu1-32 ura4-d18	30.21	Dr. Bueno
h+ flp1::flp1-3HA-KanMX6 ade6-704 leu1-32 ura4-d18	30.50	Dr. Bueno
h+ flp1::flp1-GFP-KanMX6 ade6-704 leu1-32 ura4-d18	43.23	Dr. Bueno

Table M1. Strains used (continues)

GENOTYPE	STRAIN	SOURCE
H90 gar2-RFP-KanMX leu1ad6-M210	FY13580	YGRC
gar2-RFP-KanMX flp1::flp1-GFP-KanMX6	52.10	This study
gar2-RFP-KanMX - flp1::flp1-9a-EGP-leu2-KanMX6	52.15	This study
h- mts1-46 leu1-32	S443	Dr. Moreno
h- mts2 leu1-32	S444	Dr. Moreno
h- mts3 leu1-32	S445	Dr. Moreno
mts1-46 flp1::flp1-3HA-KanMX6 leu1-32	42.76	This study
mts2 flp1::flp1-3HA-KanMX6 leu1-32	42.77	This study
mts3 flp1::flp1-3HA-KanMX6 leu1-32	42.78	This study
h+ rad3::ura4+ ade6-704 leu1-32 ura4-d18	S1017	Dr. Moreno
h+ rad3::ura4+ flp1::flp1-GFP-KanMX6 ura4-d18	44.14	This study
h+ rad22::rad22-YFP-KanMX leu1-32 ura4-d18 his3-d1	TMN3333	Dr. Russell
rad22::rad22-YFP-KanMX cds1::ura4+	48.65	This study
rad22::rad22-YFP-KanMX flp1-9A-leu2	49.70	This study
rad22::rad22-YFP-KanMX flp1::KanMX6	48.64	This study
h- rad24::ura4+ ade6-704 leu1-32 ura4-d18		Dr. Russell
h- rad24::ura4+ flp1::flp1-GFP-KanMX6 ade6-704 leu1-32	44.21	Dr. Bueno
h- rad24::ura4+ flp1::KanMX6 ade6-704 leu1-32 ura4-d18	42.73	This study

Table M1. Strains used (continued)

3.2 Construction of the strain *flp1-9A-EGFP*

Mutation of the 9 RXXS putative phosphorylation sites on Flp1p was performed sequentially by PCR (Quick change site-directed mutagenesis protocol, see 4.3) using pREP-KZ-*flp1* as a template and complementary primers of 30 bases containing the desired mutation (S160A AGC->GCC, S396A TCT->GCT, S408A TCA->GCA, S467A TCA->GCA, S468A AGT->GCT, S493A AGT->GCT, S499A AGT->GCT, S513A AGC->GCC, S537A TCT->GCT). Each mutation was verified by DNA sequencing analysis. Oligos used for mutagenesis and sequencing are listed in Table M2.

The *flp1-9A* gene was obtained by PCR of pREP-KZ-*flp1-9A* with flanking BglII-XmaI sites and cloned into the pREP41^{flp1promoter} -EGFP (pREP41-EGFP vector in which the *nmt1* promoter had been previously substituted by the 1.2 Kb endogenous promoter region of *flp1*, see 4.6). The resulting construction was then integrated in a *flp1::kanMX* strain using the unique restriction site SpeI located in the promoter region of *flp1* by the transformation technique described by Keeney and Broeke (Keeney and

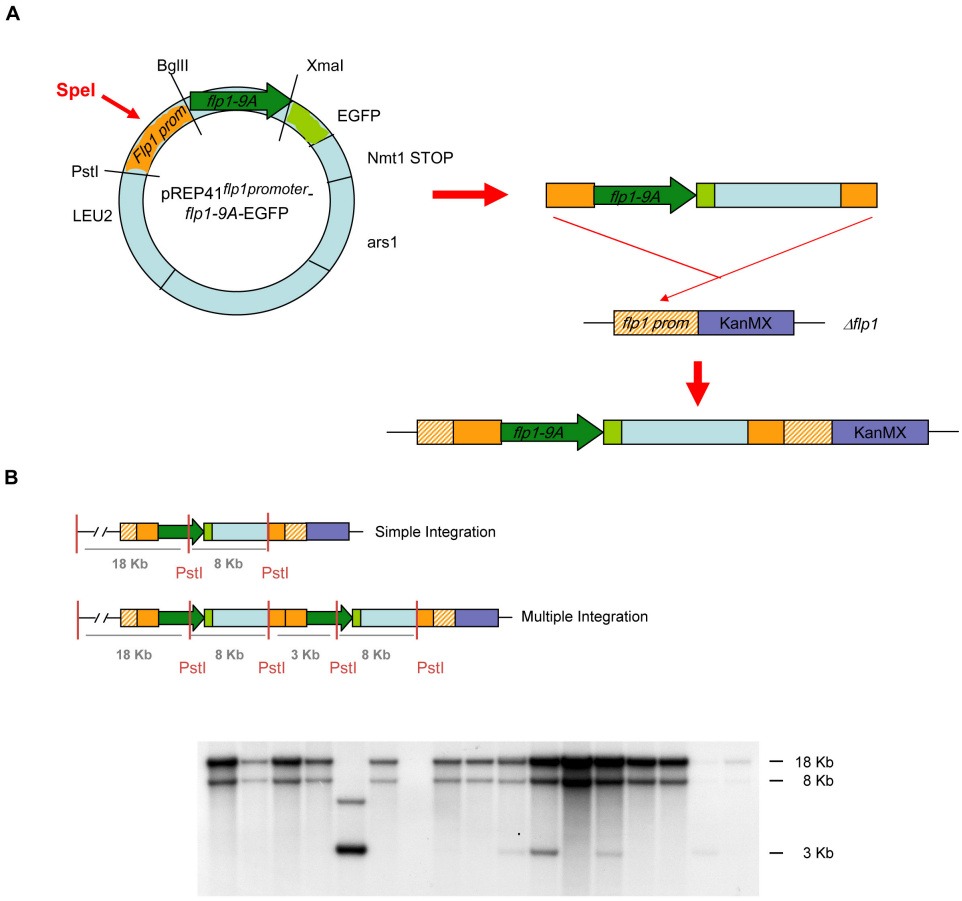

Figure M1. Integration of *flp1-9A-EGFP* in a *Δflp1* strain

(A) Schematic representation of the integration of flp1-9A-EGFP into a *Δflp1* strain. The plasmid pREP41flp1^{promoter}-*flp1*-9A-EGFP was cut with SpeI that produces a single cut in the promoter region. A *Δflp1* strain was transformed with the linear form which should be integrated through recombination into the promoter region of the receptor. (B) Southern blot analysis to detect the clones that had correctly integrated *flp1-9A-EGFP*. If the fragment was correctly integrated a 18 Kb and a 8 Kb band should be detected by digestion with Pst1 using a probe for flp1. If multiple integrations occurred an additional 3 Kb band should appear. Schematic representation for single and multiple integrations are shown.

Broeke, 1994). The correct and unique integration in the genome was corroborated by Southern blot analysis (Figure M1). Genomic DNA was obtained from the different clones and cut using Pst1 as restriction enzyme. The probe (*flp1* ORF lacking the first 120 bases) was constructed by PCR using primers 1.84 and 1.85 (see Table M2).

3.3 *S. pombe* transformation

S. pombe cells were normally transformed using competent cells using Lithium Acetate (Norbury and Moreno, 1997).

3.4 *E. coli* transformation

For *E. coli* transformation with PCR products we followed the procedure described by Kushner (Kushner et al., 1998). For transformation with plasmids we followed the fast procedure described by Golub (Golub, 1988).

4. DNA AND RNA MANIPULATION AND ANALYSIS TECHNIQUES

4.1 DNA isolation

Plasmid isolation from *E. coli*

For small scale isolation of plasmidic DNA from bacteria the boiling lysis miniprep method was used. In this way a single colony of *E. coli* was grown overnight at 37ºC in 2 ml of LB supplemented with Ampicillin. 1.5 ml of the culture was processed. Bacteria were collected by centrifugation at 8000 r.p.m for 1 minute and resuspended in 200 µl Miniprep Lysis Buffer (8% Saccharose, 0.5% Triton x-100, 50 mM EDTA and 10 mM Tris-HCl pH 8.0) containing 0.7 mg/ml Lysozyme. Samples were boiled for 1 minute and subsequently centrifuged for 10 minutes at room temperature. Snot pellet was pulled out with a sterile toothpick. 20 µl of Natrium Acetate 3M and 200 µl Isopropanol were added for DNA precipitation. After centrifugation pellet was washed with 70% Ethanol. Pellet was dried and resuspended in 50 µl miliQ water containing 20 µg/ml RNase.

The Plasmid Maxi-Kit (Quiagen) was used for large scale plasmidic DNA isolation.

Isolation of genomic DNA of *S. pombe*

S. pombe genomic DNA extraction was performed following the protocol described in Moreno et al. 1991.

4.2 RNA extraction

RNA was extracted from $3 \cdot 10^8$ cells collected by centrifugation at 4ºC from exponentially growing cultures. 20 µl of extraction solution (0.1 M EDTA pH 8.0, 0.1 M NaCl, 0.05 M Tris pH 8.0), 20 µl phenol/chloroform/isoamilic alcohol at -20ºC, 5 µl SDS 10% and 400 µl glass beads were added. Cells were disrupted using a Bio 101 Fast-Prep® Instrument (2 cycles of 15 s at 5.5 m/s). Lysates were extracted with 200 µl extraction solution and 200 µl phenol/chloroform. RNA was extracted in five subsequent extractions, once using phenol, three times with phenol/chloroform, and once with chloroform/isoamilic alcohol. RNA was precipitated with 3M Natrium acetate and 2.5 volumes of 100% EtOH at 4ºC, washed with 70% EtOH and resuspended in 30 µl DEPC water. Concentration was measured at 260 nm.

4.3 Polymerase chain reaction (PCR)

DNA amplification and mutagenesis were performed in an Eppendorf Mastercycler Personal® instrument. Reaction conditions depended on the characteristics of the fragment to be amplified. PCR mix contained template DNA (100-200 ng of genomic DNA, 15-20 ng of plasmidic DNA), 100 pM from each oligonucleotide, 20 pM of each dNTP and 1 unit of the corresponding polymerase.

Quick change site-directed mutagenesis

For site-directed mutagenesis of a gene in a plasmidic construction, the quick change site-directed mutagenesis was used. The PCR mix (50 µl) contained 5-20 ng of template DNA, 125 ng of each specific primer, 2.5 mM of each dNTP, 5 µl of 10x Pfu Buffer and 1 µl of Pfu DNA polymerase (PFU Turbo®, Stratagene). Reaction was performed in 12 cycles of denaturing at 95ºC for 1 minute, annealing at the

corresponding temperature for 1 minute, and extension at 68ºC for 2 minutes/Kb. 10 µl of PCR products were digested in 20 µl with Dpn1 at 37ºC for 2-3 hours to degrade template DNA. DH5α *E. coli* cells were transformed with 10 µl of digestion. DNA was extracted using the boiling lysis miniprep methods, and mutations were verified by sequencing.

4.4 Oligonucleotides used

The oligonucleotides used in this study were synthetized by ISOGEN Bioscience BV or THERMO Electron GmbH. In Table M2 the complete sequence of the oligos, as well as their use in this study is specified.

4.5 Processing of DNA fragments

Purification of DNA fragments

Resuspended DNA was purified using the Jet Quick PCR Product Purification Spin Kit of Genomed®.

DNA fragments contained in agarose plugs were purified using the Jet Quick Gel Extraction Spin Kit of Genomed®.

Alkaline Phosphatase treatment

To avoid plasmid religation phosphate groups of 5' end of linearized plasmids were removed by incubation with 1 U/mg DNA calf intestine alkaline phosphatase (Roche Diagnostics) in the provided buffer for 30 minutes at 37ºC.

Ligation of DNA fragments

Ligation of a DNA fragment and a receptor plasmidic vector was performed using DNA ligase T4 (Fermentas) either at 16ºC overnight or at room temperature for 4 hours.

OLIGO	SEQUENCE 5'-3'	NR	USE
3'S14Sp	TACCCGGTTAAGAAATAAGCCGGCTTT	1.84	Obtention of Southern probe
3'INT14	GATACCATGACTATCACTG	2.27	Sequencing of *flp1*
5'INT 14	ATGGATTACCAAAGATGATGG	2.28	Sequencing of *flp1*
5'BN14Sp	TAGGATCCATATGCATTTTTTTACTATCGA	1.85	Sequencing of *flp1* Obtention of Southern probe
5'MID1782	ATCATGCGAGCACACGTCCA	2.13	Sequencing of *flp1*
5'TAP01	CAGTGGTTCGCTTGCGTCGCTC		Sequencing of *flp1*
Flp1-pREP41 forward	GAAGATCTTCATGGATTACCAAGATGATGG	379	Cloning of *flp1* in pREP41 (BglII site)
Flp1-pREP41 reverse	TCCCCCCGGGCCAGAAATTAGCCGGCTTTT	380	Cloning of *flp1* in pREP41 (XmaI site) Sequencing of *flp1*
Forward Flp1 promoter	AAAACTGCAGCCAAAGAGTTGCTTGGTGAA	381	Construction of pREP41$^{flp1\text{promoter}}$
Reverse Flp1 promoter	GAAGATCTCAGACAAGTAATTGCGAATCTC	383	Construction of pREP41$^{flp1\text{promoter}}$
S160A forward	GAGCACGAGAGAGCGCCATACTAAATATACG		Mutation of RXXS sites
S160A reverse	CGTATATTTAGTATGGCGCTCTCTCGTGCT		Mutation of RXXS sites
S408A forward	GCGAGACGTCTCCCTGAGCGTCCTCTGTC		Mutation of RXXS sites
S408A reverse	GCGAGACGTCTCCCTGCAGCGTCCTCTGTC		Mutation of RXXS sites
S513A forward	GCTCAGCGAAGTGTTGCCATGTCATCACTTAAC		Mutation of RXXS sites
S513A reverse	GTTAAGTGATGACATGGCAACACTTCGCTGAGC		Mutation of RXXS sites
S467A forward	GCTTGCGTCGCTCAGCAGCTCAAAGCAATTATC	375	Mutation of RXXS sites

Table M2. Oligonucleotides used (continues)

S467A reverse	GATATTGCTTTGAGCTGCTGAGCGACGCAAGC	376	Mutation of RXXS sites
S468A forward	CTTGCGTCGCTCATCAGCTCAAAGCAATATCGAAC	384	Mutation of RXXS sites
S468A reverse	GTTCGATATTGCTTTGAGCTGATGAGCGACGCAAG	385	Mutation of RXXS sites
S396A forward	CAACCGAGAAAAGTTGCTGGACATAATCCACCG	386	Mutation of RXXS sites
S396A reverse	CGGTGGATTATGTCCAGCAACTTTTCTCGGTTG	387	Mutation of RXXS sites
S493A forward	CAATTCGACGTCAGCTGGAAATAGGTGGT	388	Mutation of RXXS sites
S493A reverse	GACCACCTATTTCCAGCTGTACGTCGAATTG	389	Mutation of RXXS sites
S499A forward	GGAAATAGGTGGTCTGCTGGGTCTAGTCATTC	390	Mutation of RXXS sites
S499A reverse	GAATGACTAGACCCAGCAGACCACCTATTTCC	391	Mutation of RXXS sites
S537A forward	CTAAAAGCCGGCTAATTGCTTAATAAACCTG	392	Mutation of RXXS sites
S537A reverse	CAGGTTTATTAAGCAATTAGCCGGCTTTTAG	393	Mutation of RXXS sites

Table M2. Oligonucleotides used (continued)

4.6 Plasmids used

The plasmids used in this study are listed in Table M3.

Construction of pREP41 ^{flp1promoter}-*flp1*- EGFP

In order to obtain expression of *flp1* under its own promoter in the tagged EGFP plasmidic form, the nmt1 promoter of pREP41-*flp1*-EGFP was replaced by the endogenous promoter region of *flp1*. A 1.2 Kb fragment of the promoter region of *flp1* was amplified by PCR using USB FideliTaq^{TM} polymerase and primers 381 and 383 (see Table M2). *nmt1* promoter was removed from the plasmid by digestion with BglII and Pst1 and gel purification of the vector. The insert was also digested with BglII and Pst1, purified and ligated to the vector. *E. coli* was transformed with the ligation

PLASMID	Source
pREP-KZ-GST	Dr. Bueno
pREP-KZ-GST-*flp1+*	Dr. Bueno
pREP-KZ-GST-$flp1^{CS}$	Dr. Bueno
pREP-KZ-GST-$flp1^{468}$	This study
pREP-KZ-GST-$flp1^{396\ 468\ 493\ 499\ \ 537}$	This study
pREP-KZ-GST-$flp1^{160\ 396\ 408\ 467\ \ 468\ 493\ 499\ 513\ 537}$	This study
pREP-KZ-GST-*rad24+*	Dr. Bueno
pREP-KZ-GST-*rad25+*	Dr. Bueno
pREP41-EGFP	Dr. Moreno
pREP41-*flp1*-EGFP	This study
pREP41^{flp1promoter}-*flp1*-EGFP	Dr. Russell
pREP41^{flp1promoter}- $flp1^{160\ 396\ 408\ 467\ \ 468\ 493\ 499\ 513\ 537}$ -EGFP	This study

Table M3. Plasmids used

product and correct constructions were selected by digestion with HincII and sequencing of the Minipreps.

4.7 Southern blot analysis

Southern probes were constructed by PCR using genomic DNA as a template and using DFS-Taq polymerase (Bioron). In order to dilute the concentration of genomic DNA in the probe, a second PCR was performed (300µl) using 1 µl of the first PCR as a template. PCR products were purified using Jet Quick PCR Product Purification Spin Kit of Genomed®, and eluted in 30µl miliQ water. DNA concentration was quantified in gel.

Genomic DNA of the strains to study was cut with the chosen restriction enzymes. Salt transfer to GeneScreen Plus membranes (NEN), UV crosslinking to fix DNA and hybridization were performed following the indications of the manufacturer.

4.8 Analysis of gene expression

For the analysis of gene expression using microarray technology, exponential growing cultures of *wt* and Δ*flp1* ($5 \cdot 10^6$ cells/ml) were treated for 90 minutes with 20 mM HU. RNA was extracted for the samples (see 4.2). RNA quality and quantity was tested using an Agilent Technologies 2100 BioAnalyzer. Gene expression profiles were obtained using a Yeast 2.0 array™ of Affymetrix™. Data processing was performed using Affymetrix™ GeneChip Operating Software and Data Mining Tool.

5. PROTEIN MANIPULATION TECHNIQUES

5.1 Preparation of protein extracts

To avoid protein degradation the whole process was performed on ice or using cooled instruments.

Protein extracts for Western Blot analysis (denaturing conditions)

Approximately $3 \cdot 10^8$ cells were collected by centrifugation, washed with 1mL of STOP solution (NaCl 0,9%, NaN3 1 mM, EDTA 10 mM, NaF 50 mM, pH 8,0) and 30 µl of RIPA (Na_3PO_4 10 mM, Triton X-100 1%, SDS 0,1%, EDTA 10 mM, NaCl 150 mM, pH 7,0) supplemented with protease inhibitors [leupeptin 10 µg/ml, aprotinin 10 µg/ml, soy bean 10 µg/ml, TLCK 100 µM (N-a-Tosyl-L-Lysine Chloromethyl Ketone Hydrochloride), pepstatin 10 µg/ml] were added. Samples were boiled for 5 minutes and immediately frozen in carbonic dry ice and stored at -80ºC until their processing. To obtain cell lysates, approximately 750 mg of glass beads and 40 µl of supplemented RIPA were added to the samples. Subsequently cells were disrupted using a Bio 101 Fast-Prep® Instrument (3 cycles of 15 s at 4m/s). Lysates were them extracted using 400 µl of supplemented RIPA. Protein concentration was determined in a colorimetric assay using the BCA kit (Pierce). The final set of samples was

prepared diluting the individual samples to a standard concentration using supplemented RIPA and adding Sample Buffer (Tris-HCl pH 6,8 80 mM, DTT 5 mM, SDS 2%, glycerol 7,5%, EDTA 5 mM, bromophenol blue 0,002%). Samples were finally boiled for 5 minutes and clarified.

Protein extracts for Immunoprecipitation (native conditions)

Approximately $3 \cdot 10^8$ cells were collected by centrifugation and washed with 1 mL of STOP buffer (NaCl 0,9%, NaN3 1 mM, EDTA 10 mM, NaF 50 mM, pH 8,0). For immunoprecipitation protein extracts were prepared directly after cell collection using immunoprecipitation lysis buffer [50 mM Tris (pH 7.5), 80 mM β-glycerophosphate, 250 mM NaCl, 15 mM nitrophenylphosphate, 50 mM NaF, 5 mM EDTA, 1 mM DTT, and 0.1% NP-40] supplemented with aprotinin, and leupeptin both at 10 µg/ml final concentration, vanadate and PMSF (phenylmetylsulfonyl fluoride) both 1mM final concentration. The procedure of cell lysis is identical to that specified for denaturing conditions. Lysates were extracted in 400 µl of supplemented lysis buffer, and clarified by centrifugation (twice, 7 minutes at 12000 rpm and 4ºC). Protein concentration was determined in a colorimetric assay using the BCA kit (Pierce).

5.2 Western blot analysis

Sodium dodecyl sulfate (SDS) polyacrylamide gel electrophoresis (PAGE)

Depending on the characteristics of the protein to detect 50 to 100 mg of estimated total protein contained in denaturalized protein extracts were separated in an 8% to 16% SDS-polyacrylamide gel. As molecular mass markers we used Invitrogene Benchmark™ pre-stained markers. Electrophoresis was performed in a Mini-PROTEAN® II Cell (Bio-Rad) at constant voltage (120-150V), using Running Buffer (Tris-HCl 25 mM, glycine 192 mM, SDS 0,1% pH 8,3).

Immunodetection in nitrocellulose membranes

The polyacrilamide gel was transferred for two hours at 100 V in a Mini Transblot® Cell (Bio-Rad) to a nitrocellulose membrane (Hybond ECL, Amershan) using transfer buffer [10mM CAPS (3-cyclohexylamino-1-propane sulfonic acid), 10% methanol pH 11]. Then the membrane was blocked in 50mL PBS (NaCl 137 mM, KCl 2.7 mM, Na2HPO4 8 mM, KH2PO4 1,5 mM, pH 7,2) containing 5% dried milk (Sveltesse, Nestle) and 0.1% Tween-20, for 1 hour at room temperature. The membrane was incubated (2 hours at room temperature or overnight at 4ºC) with the corresponding primary antibody in the same block solution. Then the membrane was washed four times for 5 minutes with 50 ml PBS-Tween (0.1% Tween-20), incubated with the secondary antibody (anti-mouse 1:2000 or anti-rabbit 1:3500 in block solution) for 1 hour at room temperature and washed again twice in PBS-Tween for ten minutes and once in PBS for at least 10 minutes. In order to detect the antibody signal the enhanced chemiluminiscence kit (ECL, Amersham) or the Super Signal kit (Pierce).

Membranes were re-hybridized with mouse TAT1 anti-tubulin monoclonal antibody (1:500) as a loading control, if possible.

Immunoprecipitation

For immunoprecipitation of strains tagged with haemagglutinin (HA) a mix of antibody [2µg of α-HA (12CA5, Roche) for immunoprecipitation of 1 mg of extract] and 10 µl protein A (Protein A Sepharose, Amersham Biosciences) was incubated in supplemented lysis buffer (see preparation of extracts for Immunoprecipitation) for 1 hour at 4ºC. Then the mix was incubated with 1mg extract in 300µl of supplemented lysis buffer for 2 hours at 4ºC and washed 4-6 times with the same buffer.

5.3 Kinase and phosphatase assays

GST-Flp1p phosphorylation by Cds1p-Ha

Exponentially growing cultures of *cds1-Ha* cells were treated either with 20 mM HU or 0.033% MMS for 2 hours. Protein extracts were obtaining in native conditions and Cds1p-Ha was immunoprecipitated from the different samples following the protocol

specified before. Cds1p activity was assayed using MBP as a substrate as reported in (Lindsay *et al.*, 1998).

Kinase assays were performed over GST purified Flp1p (obtained from a Δ*cds1* strain) and controls. GST purification has been described previously (Shiozaki and Russell, 1997). 2.5 µg of the corresponding substrate and protein A-bound kinase were incubated with 10 µl of kinase buffer (10 mM Hepes pH 7.5, 75 mM MgCls, 0.5 mM EDTA, 1 mM DTT) containing 2.5 µCi of γ32P-ATP and ATP 0.2 mM final concentration, at 30ºC for 15 minutes. Reaction was stopped by the addition of 20 µl of 2X Sample Buffer.

Assay of phosphatase activity of GST-Flp1p phosphorylated by Cds1p-Ha

Cds1p was inmunoprecipitated after 2 hours of 12mM HU treatment as explained above. Phosphorylation assays over GST-Flp1p were performed as mentioned above using non hydrolysable ATP (0.2 mM final concentration in buffer) to avoid possible auto-dephosphorylation. GST-Flp1p was treated with the immunoprecipitation mix without antibody as a control. Samples were washed three times with phosphatase buffer pH 6.6 (50 mM Imidazol, 1 mM DTT, and 1 mM EDTA). A dephosphorylation assay (30 minutes at 30ºC) of treated and control-treated GST-Flp1p using 250 µM DiFMUP as a substrate in 200 µL phosphatase buffer was performed. The activity of the immunoprecipitated kinase was assayed as a further control. Samples were analyzed in a TECAN ULTRA EVOLUTION instrument, using 360 nm and 465 nm excitation and emission wavelengths respectively. Readings were normalized taking intro account the quantity of GST-Flp1p contained in each sample, determined by gel-electrophoresis and subsequently staining and quantification of the gel.

5.4 Protein interaction assays

Analysis of potential protein interactions was performed by GST purification or immunoprecipitation of one target protein and Western blot of the resulting sample for the detection of the other antibody-tagged target as above mentioned.

ANTIBODY	M/P	ORGANISM	USE	SOURCE
α-HA 12CA5	Monoclonal	Mouse	1:500	Roche
α–TAT1	Monoclonal	Mouse	1:300	Dr. Gull
α-Cdc2 C2	Polyclonal	Rabbit	1:250	Dr. Moreno
α-Cdc25	Polyclonal	Rabbit	1:250	Dr. Moreno
α-Cdc2^{Y15P}	Polyclonal	Rabbit	1:1000	Cell Signaling
α-GFP	Monoclonal	Mouse	1:5000	BD Biosciences
α-IgG Rabbit-HRP	Polyclonal	Sheep	1:3500	Amersham
α-IgG Mouse-HRP	Polyclonal	Sheep	1:2000	Amersham

Table M4. Antibodies used

5.5 Mass spectrometry (identification of phosphorylation sites on Flp1p)

Characterization of phosphorylation sites on Flp1p by checkpoint activated Cds1p was performed essentially as described previously (Esteban *et al*., 2006), by real time ionization and precursor ion scanning analysis on a 4000 Q-Trap LC-MS/MS hybrid system (Applied biosystems, MDS, Sciex) mass spectrometer.

5.6 Antibodies

The antibodies used in this study and their conditions of use are listed in Table M4.

6. SENSITIVITY, RECOVERY AND ADAPTATION ASSAYS

6.1 Sensitivity assays to chronic drug exposure

The strains object of study were cultured in fresh YES or adequately supplemented MM plates at 25ºC. We took different colonies of each strain and resuspended them in 500 µl of MiliQ water in order to determine cell number in each dilution, cells were counted in a Thoma Chamber. A dilution containing 10^7 cells/ml was prepared for each strain, and then three serial dilutions were performed (10^7-10^4). A drop of 10 µl of each strain and dilution was inoculated on control YES or adequately supplemented MM plates as a control and plates containing different concentrations of the drugs considered in the experiments. The experiment was normally performed in duplicates in order to test the growth and sensitivity at 25ºC and 30ºC.

6.2 Recovery assays

Strains were cultured in liquid rich medium to exponential growth. Then each culture was divided into four sub-cultures of 10ml each that were treated either with 12mM HU, 0.033% MMS or 7.5mU BL for four hours (and an untreated culture to monitor the growth of the culture during the treatment time). At the 1h, 2h, 3h and 4h time points of the treatment a 10 µl drop of each culture was inoculated on a fresh drug-free YES plate.

6.3 Study of checkpoint response and adaptation to long term drug exposure

Kinetics of checkpoint block and adaptation of the checkpoint to long term 12mM HU exposure of different strains were determined. Strains were grown in rich liquid medium to exponential growth and then treated with HU for 10 hours. The number of cells presenting septa (for septation index analysis) or binucleated cells (for mitotic index) was checked at each hour of treatment. The experiment was performed twice and at least 400 cells were counted at each time point and strain (see 7.1).

7. CELL MANIPULATION AND ANALYSIS TECHNIQUES

7.1 Microscopy and cell staining

Cell and protein imaging was performed in a Leica DM 600B microscope (63x objective, 1,32 Oil Plan-APO) equipped with a Hamamatsu ORCA-ER c4742-95 digital camera and Improvision software Openlab 4.0.3.

In vivo nuclear staining was performed with Hoechst (Bisbenzimide H 33342, Sigma). Cells were collected by centrifugation at 3000 rpm and incubated in Hoechst for 15 minutes minimizing exposure to light.

For *in vivo* imaging of Rad22p-YFP foci strains were grown in YES at 30ºC or 25ºC to minimize background fluorescence. At least 400 nuclei from two separate experiments were examined for each strain and each time point.

In order to quantify the mitotic index, cells were fixed in 70% EtOH, then washed and resuspended in PBS 1X previously mixed with DAPI to a 1X concentration of the staining agent. At least 400 cells were classified into uni- or binucleated in each count.

Septation index was determined by counting the number of septated cells using dark field microscopy in a population of at least 400 cells for each time point in, at least two independent experiments.

7.2 Flow Cytometry Analysis (FACS)

DNA content in individual cells was determined by flow cytometry using a FACScalibur Benton Dickinson instrument. Cell culture (300 µl) was fixed in ethanol to a 70% final concentration. Aliquots of normally 200 µl of fixed cells were washed in Sodium Citrate 50 mM and resuspended in 500 µl of Sodium Citrate 50 mM containing 0.1 mg/ml RNase. Samples were incubated for at least 2 hours (usually overnight) at 37ºC. For staining samples were transferred to a 5 ml FACS tube and 500 µl of Sodium Citrate 50 mM containing 8 µg/ml Propidium Iodine (4 µg/ml final concentration PI) were added (exposure to light should be minimized from this point). Samples were sonicated using a Sonic Dismembrator 550 instrument (Fisher Scientific). Cell Quest 3.2.1f1 software was used for data acquisition and analysis.

8. CHEMICAL AGENTS USED IN THIS STUDY AS DNA-DAMAGE AND REPLICATION-STRESS TRIGGERS

Hydroxyurea (HU)

HU is a ribonucleotide reductase inhibitor, which arrests replisome progression by depleting the cellular pool of dNTPS, causing stalling of replication forks.

Methyl methanesulfonate (MMS)

MMS is an SN2-type alkylating agent that predominantly methylates nitrogen atoms in purines, but will also methylate proteins. The consequences of the produced DNA methylation are, either degradation of the modified base, giving rise to an abasic site, or base mispairing. MMS has been proven to cause fork-associated DNA-damage.

Bleomycin (BL)

BL is a glycosylated linear nonribosomal peptide antibiotic produced by the bacterium *Streptomyces verticillus* that acts by induction of DNA strand breaks.

9. MATHEMATICAL MODELLING

9.1 Mathematical description of the system

The model is mathematically described by the set of differential equations gathered in APPENDIX 2. The temporal evolution of each species is written in the form:

$$\frac{dc_i}{dt} = \sum_{j=1}^{r} n_{ij} v_j$$

for $i = 1,..,m$, where *m* is the number of biochemical species with the concentrations c_i, *r* is the number of biochemical reactions with the rates v_j, and n_{ij} denote the stoichiometric coefficients of the compounds in the corresponding reactions.

Individual rates v_j have been written responding to three types of kinetics:

Mass Action Kinetics

$$v_j = k_j \cdot \prod_x c_x$$

where k_j is the rate constant, while the index *x* runs over all substrates and modifiers of reaction *j*.

Michaelis Menten Kinetics

$$v_j = k_j \cdot \frac{c_S \cdot c_M}{K_M + c_S}$$

where k_j is the rate constant, K_M is the value of the stimulus at which the response is half-maximal, s accounts for the substrate and $_M$ for the modifier.

Saturation Kinetics

$$v_j = k_j \cdot \left(1 - \frac{c_S}{K_{C\max}}\right)$$

where k_j is the rate constant, *s* accounts for the substrate, and $K_{C\ max}$ is the maximum allowed concentration.

The set of reactions and the involved species and parameters is summarized in Table 1 in RESULTS.

9.2 Simulation tools

Model building and simulations were performed using COPASI 4.2-4.3 (Hoops *et al.*, 2006) and Cell Designer 3.5 (Funahashi *et al.,* 2003).

9.3 Parameter fit

Parameter estimation was performed using SBML-PET 1.4 (Zi and Klipp, 2006). For the cell cycle fits we used published data generated in our group (concentrations of total Cdc25p, of active Cdc25p, of total Cdc13p, and Cdc2p activity) (Esteban *et al.*, 2004), and checkpoint fits correspond to data generated in this study (concentration of total Cdc25p, of inactive Cdc2p and active Cds1p). Blots were quantified using Quantity One® Bio-Rad software and adjusted to the corresponding loading controls. Fits were performed using normalized data. In the fits of the cell cycle module we used two repetitions of the experimental time courses to favour parameter sets that could account for biological oscillations. We took G_2 as a starting point for cell cycle simulations, thus based on analysis and comparison of the available data, data points corresponding to *nda3* synchronization were shifted forward 15 minutes with respect to *cdc25-22* blocks.

RESULTS

1. ANALYSIS OF Flp1p LOCALIZATION DURING GENOTOXIC STRESS

In the course of a normal cell cycle Flp1p changes its subcellular location to carry out its different functions. Flp1p localizes to the nucleolus and spindle pole body in interphase. In prophase it is released from the nucleolus by an unknown mechanism to the nucleus, medial ring and mitotic spindle (Cueille *et al.*, 2001; Trautmann *et al.*, 2001).

During vegetative cell cycle Flp1p plays a role in regulation of mitotic exit by triggering rapid degradation of Cdc25p and thus indirectly promoting a reduction of Cdc2p activity, necessary for mitotic exit. Cdc2p activity must be also kept low in part by Cdc25p action to exert the required cell cycle block during checkpoint response to genotoxic stress.

The similarity of the regulatory targets of the mitotic exit cascade and the checkpoint response to genotoxic stress lead us to investigate the potential role of the phosphatase Flp1p in the cellular response to replication stress and/or DNA damage.

1.1 Flp1p-GFP changes its subcellular localization in cells undergoing replication stress or suffering DNA-damage

As a first approach it was assumed that if the phosphatase was involved in the mentioned checkpoints it would probably leave its nucleolar location during checkpoint-mediated cell cycle blocks in order to interact with its potential targets. Therefore a study of the localization of the protein in asynchronous populations of a *flp1-GFP* strain was performed under the effect of three different drugs: the ribonucleotide reductase inhibitory drug hydroxyurea (HU), the DNA-alkylating agent methyl methanesulfonate (MMS) and DNA-breaks inducing drug bleomycin (BL).

After two hours of 12mM HU treatment most population was unseptated, uninucleated and partially elongated as a result of the checkpoint induced block in early S-phase. If compared to the nucleolar staining of untreated interphase cells, Flp1p-GFP signal in HU treated cells covered a larger, round area, which we considered to be the nucleus. In 0.033% MMS and 7.5 mU BL treated cells Flp1p-GFP localization also seemed to be nuclear but still presenting predominant nucleolar staining (Figure 1).

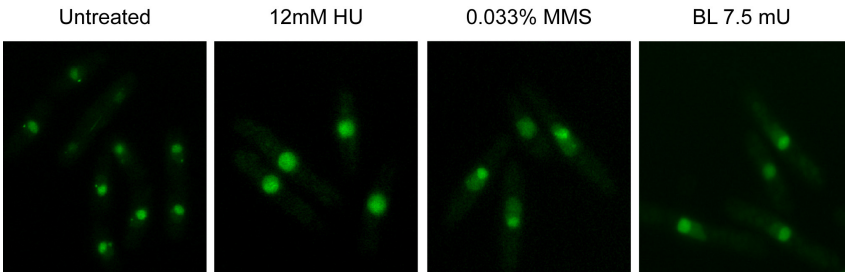

Figure 1. **Flp1p-GFP changes its subcellular localization as a consequence of treatment with genotoxic agents**
Asynchronous cultures of exponential growing *flp1GFP* cells were treated with either 12mM HU, 0.033% MMS or 7.5mU BL. *In vivo* Flp1p-GFP staining after two hours of treatment revealed a change of localization of the phosphatase from its nucleolar and SPB localization in untreated interphase cells to the nucleus in treated cells. Staining in HU is almost uniform throughout the nucleus, whereas in MMS and BL predominant nucleolar staining is still observed.

To check that the observed localization was indeed nuclear and that the expansion of the signal was not due to drug-induced nucleolar reorganization, we studied the localization of the nucleolar marker Gar2p-RFP in HU treated cells in combination with Hoechst, a stain that binds to DNA and thus marks the no-nucleolar region of the nucleus. We observed that Gar2p-RFP remained nucleolar after HU treatment, and thus Gar2p-RFP and Hoechst proved to be valid markers for Flp1p-GFP localization (Figure 2A). In HU treated cells, Flp1p-GFP signal indeed co-localized with Hoechst, and was also present in the Gar2p-RFP stained region (Figures 2B and 2C). Gar2p-RFP staining in treated cells allowed us to state that no observable remodelling of the nucleolus took place under exposure to 12mM HU (Figures 2A and 2C) , and that the change of localization we observed for Flp1p was not general for nucleolar proteins.

We could thus conclude that Flp1p was specifically released from the nucleolus to occupy the whole nucleus upon HU-induced replication stress.

To confirm that Flp1p remained nucleolar during unperturbed DNA synthesis we monitored the localization of the phosphatase after release from a *cdc10-129* G1 block throughout S-phase (Figure 3A). *cdc10-129 flp1-GFP* presented normal Flp1p-GFP localization in asynchronous cells. After 4 hours of incubation at the restrictive temperature, cells were blocked in G1 with 1C content (Figure 3B). Flp1p-GFP presented localization in the nucleolus and SPB at this stage as previously reported

(Trautmann *et al.*, 2001). This localization remained unaltered during release at the permissive temperature, until S-phase was completed after 150 minutes, and mitotic staining appeared in most population (Figures 3B and 3C).

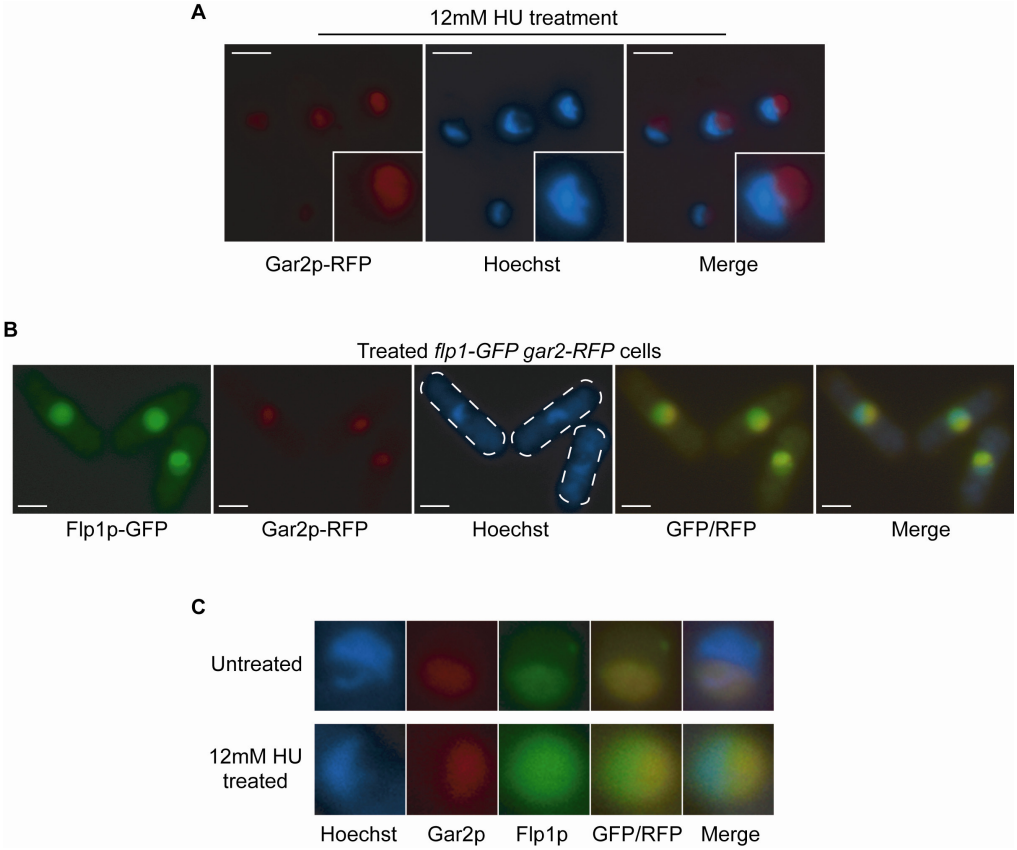

Figure 2. **Flp1p-GFP localization during HU treatment**

(A) Characterization of Gar2p as a nucleolar marker during replication stress. Gar2p localization remains unaltered as a result of treatment with 12mM HU. Gar2p and Hoechst staining cover complementary regions of the nucleus. 3.5x magnified nuclei are shown. Bar 4 μm. (B) *In vivo* Flp1p-GFP staining at two hours of 12mM HU treatment co-localized both with Hoechst and Gar2p, indicative of pan-nuclear localization of the phosphatase under these conditions. (C) 3.5x nuclei magnification of untreated interphase (upper panels) and 12mM HU treated cells (lower panels). Note that no physical nucleolar reorganization can be observed as a result of HU treatment. Bar 4 μm.

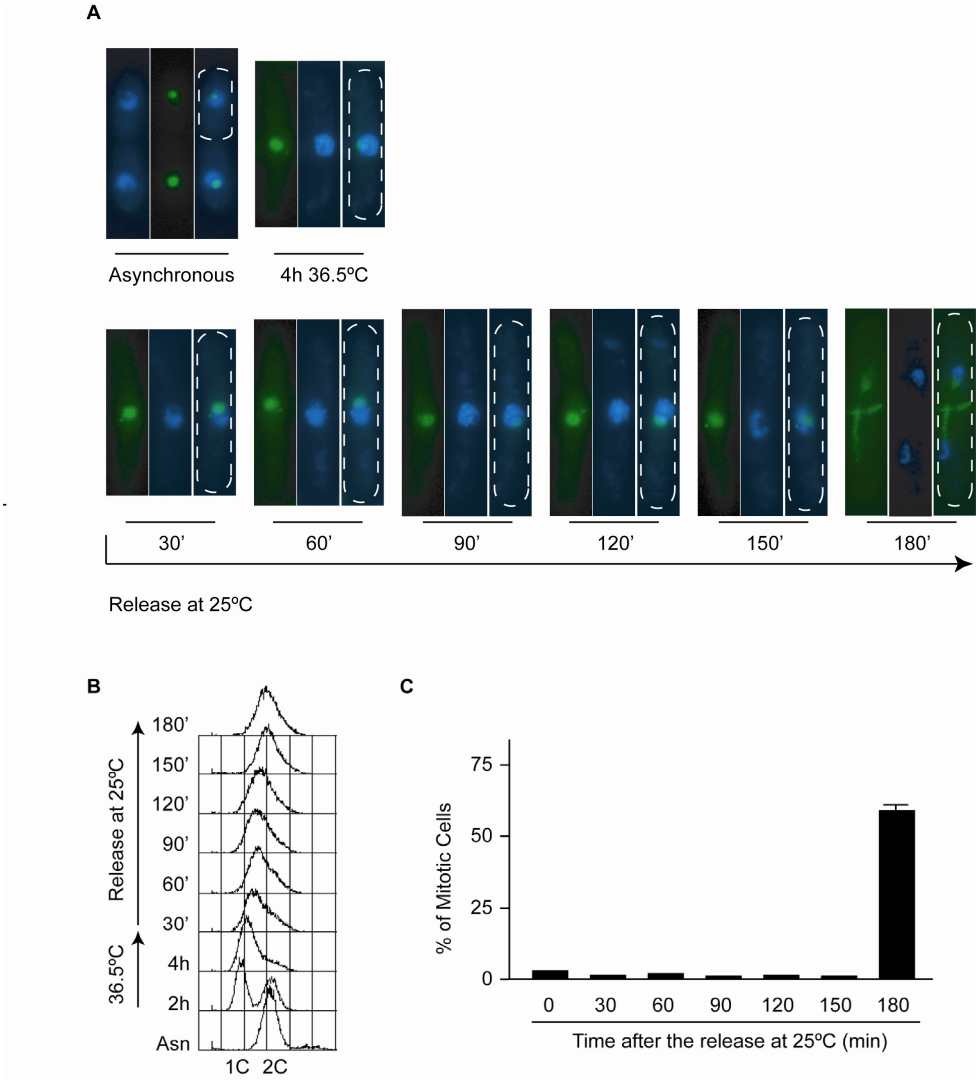

Figure 3. **Flp1p-GFP localizes to the nucleolus throughout S-phase**

(A) Flp1p-GFP localization during release from a G1 block in a *cdc10-129 flp1GFP* strain. Note that Flp1p-GFP localization is *wt* in asynchronous interphase *cdc10-129 flp1GFP* cells. The culture was incubated for 4h at the restrictive temperature (36.5ºC) and then released at the permissive temperature (25ºC). Flp1p-GFP staining was monitored during progression through S-phase. (B) FACS analysis showing a G1 block of *cdc10-129 flp1GFP* and S-phase progression kinetics after release at 25ºC. S-phase is very slow under these block and release conditions (Segurado *et al*., 2002) and is completed after 150 minutes of incubation at the permissive temperature. (C) Mitotic index of a *cdc10-129 flp1GFP* strain after release from the G1 block. Count of mitotic cells corresponds to cells in which Flp1p-GFP is located at the nucleus, mitotic spindle and medial ring.

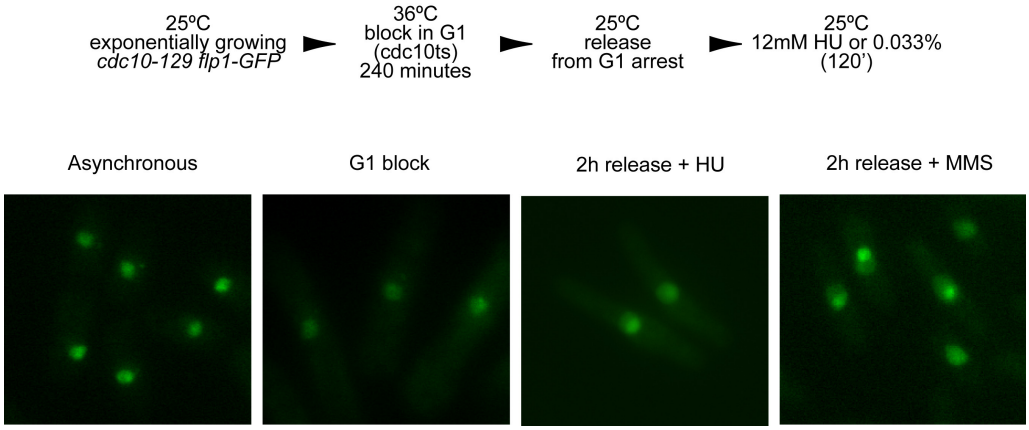

Figure 4. **Change of localization of Flp1p can be specifically triggered by replication stress or DNA damage inflicted in S-phase**

cdc10-129 flp1GFP cells were synchronized by incubation at the restrictive temperature and then released to permissive conditions in medium containing either 12mM HU or 0.033% MMS. Localization to the nucleus was observed after two hours, to the same extent as in asynchronously growing populations after treatment.

Since Flp1p remained at the nucleolus during S-phase in cycling cells, the change of subcellular localization observed in HU seems to be specifically triggered by the action of the drug and not to be a result of the cell cycle stage at which cells blocked.

To check if Flp1p-GFP change of localization could be specifically triggered by replication stress and/or DNA damage inflicted in S-phase, a localization experiment was performed in *cdc10-129 flp1-GFP* synchronised cultures. After 4h of block at 36ºC, the cultures were released at 25ºC and simultaneously treated with either 12mM HU or 0.033% MMS (Figure 4). After two hours of treatment cells were checkpoint blocked. At this time point Flp1p change of localization to the nucleus was indeed observed in both HU and MMS treated cultures. In MMS the staining was still predominantly nucleolar as previously described for treatment in asynchronous cultures.

1.2 Flp1p change of localization depends on the checkpoint machinery

We next wanted to prove that Flp1p change localization was dependent on the checkpoint and not just an effect of the drugs themselves.

Δrad3 mutants are unable to block cell division since they lack the main sensor to

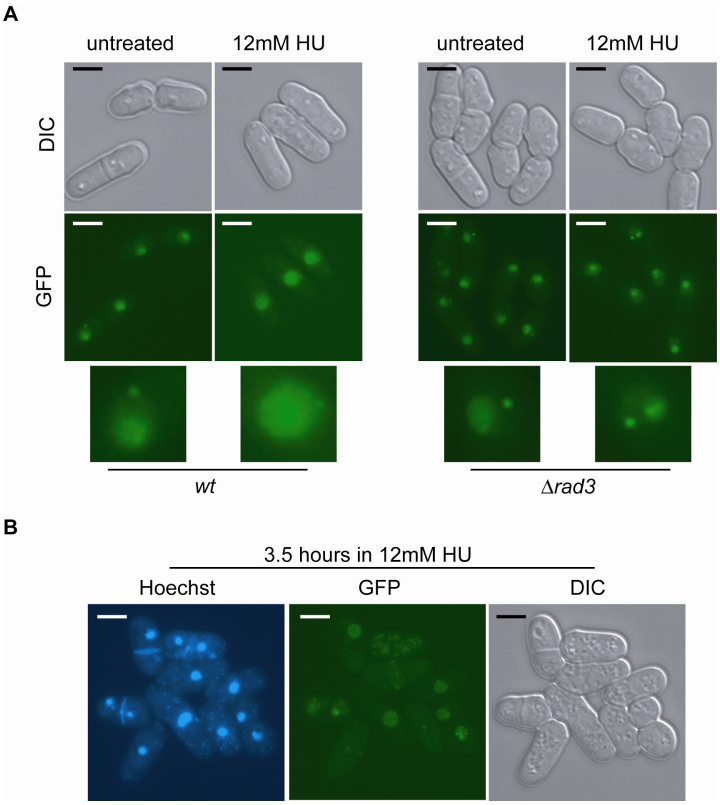

Figure 5. **Nuclear accumulation of Flp1p depends on checkpoint response**
(A) Flp1p-GFP does not delocalize in checkpoint deficient Δ*rad3* cells after 12mM HU treatment. 3.5x magnified nuclei are shown in the bottom panels. (B) HU treated Δ*rad3* cells present cut phenotype as a result of their checkpoint deficiency after 3.5 hours of treatment. Flp1pGFP staining corresponding to the different cell cycle stages as well as partially defective localization of the phosphatase can be observed in these cells. Bars, 4 μm.

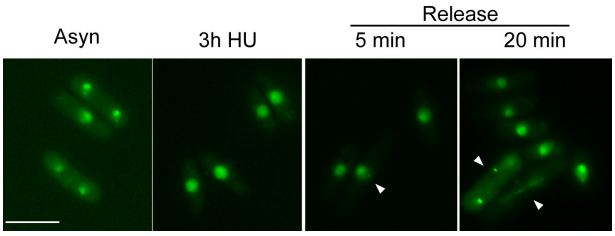

Figure 6. Flp1p returns to the nucleolus as soon as the source of replication stress is removed

flp1-GFP cells were treated with 12mM HU for three hours. Then, the culture was washed three times with drug-free medium in order to release the cells from the checkpoint block. After 5 minutes of release, Flp1p-GFP was observed to localize back in the nucleolus and spindle pole body and further monitoring revealed that the protein localizes normally as cells re-enter cell cycle.

genotoxic stress (Boddy *et al.*, 1998; Brondello *et al.*, 1999). In untreated cells, Flp1p-GFP localization in this strain was indistinguishable from that of wild-type cells (Figure 5A). After 2 hours of 12mM treatment Δ*rad3* cells continued their progression through cell cycle and Flp1p-GFP localization was identical to that of untreated cells, proving that Flp1p localization to the nucleolus after drug treatment depends on an active checkpoint. As a consequence of lack of checkpoint block anucleated cells and fragmented nuclei, characteristic of the cut phenotype of strains which perform unscheduled mitosis, could be observed in *Δrad3 flp1-GFP* after 3.5 hours of HU treatment, presenting also altered Flp1p-GFP staining in some cells (Figure 5B).

If the change of localization of Flp1p was dependent on the checkpoint, it would be further expected that the phosphatase re-localized to its interphase and cell cycle positions once the source of genotoxic stress was removed. To test this, a block and release experiment was performed (Figure 6). After three hours of 12mM HU treatment cells were perfectly blocked and Flp1p-GFP was nuclear, as described earlier. Then the culture was washed and the cells were allowed to grow in drug-free rich medium. After 5 minutes Flp1p-GFP started to localize back to the nucleolus as expected for cells re-entering cell cycle. At 20 minutes of release cells entering mitosis and the corresponding nuclear, medial ring and spindle localizations of Flp1p could be observed.

1.3 Flp1p change of localization in *cds1* and *chk1* checkpoint mutants

Given the dependency of Flp1p change of localization on an active checkpoint, we next wanted to check if this event could be more concretely associated to one of the two branches of the checkpoint response. With this aim, we studied Flp1p-GFP localization in strains deleted for either *cds1* or *chk1* during genotoxic treatment, being Cds1p and Chk1p the main effectors of checkpoint signalling in response to replication stress and DNA-damage, respectively.

In untreated cells, Flp1p-GFP localization in these strains was indistinguishable from that of wild-type cells (Figures 7 and 8A). In cells treated either with 0.033% MMS or 7.5mU BL Flp1p is released to a lower or higher extent in both mutant strains. However, when treated with 12mM HU for 2h the *cds1* mutant presented nucleolar

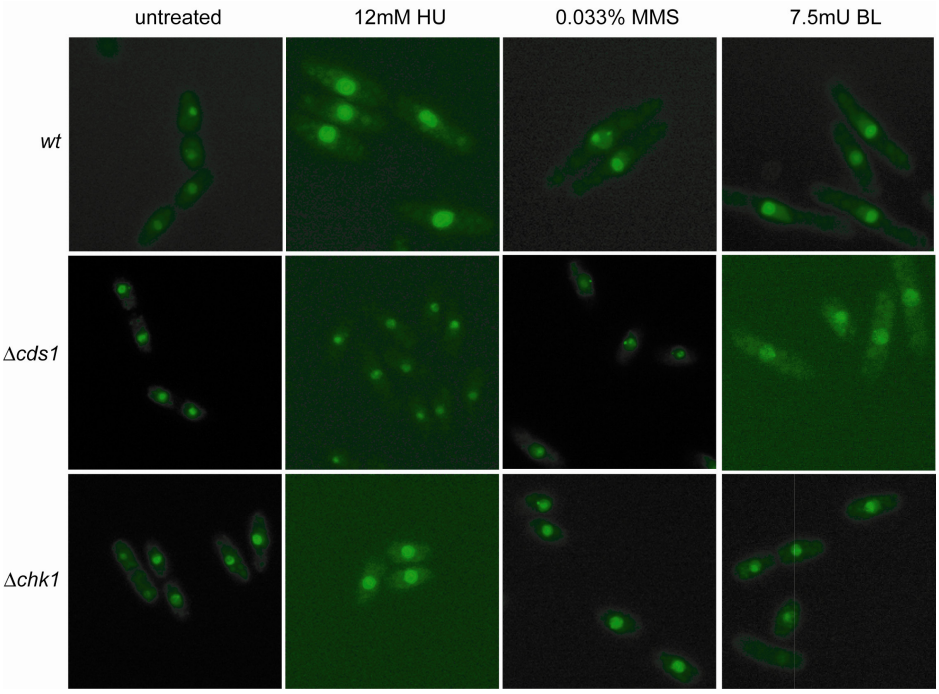

Figure 7. **Flp1p-GFP localization in Δ*cds1* and Δ*chk1* mutants during genotoxic stress**
Asynchronous cultures of exponential growing *flp1GFP,* Δ*cds1 flp1GFP* and Δ*chk1 flp1GFP* cells were treated with either HU 12mM, 0.033% MMS or 7.5 mU BL. Flp1p localization was observed after 2 hours of treatment.

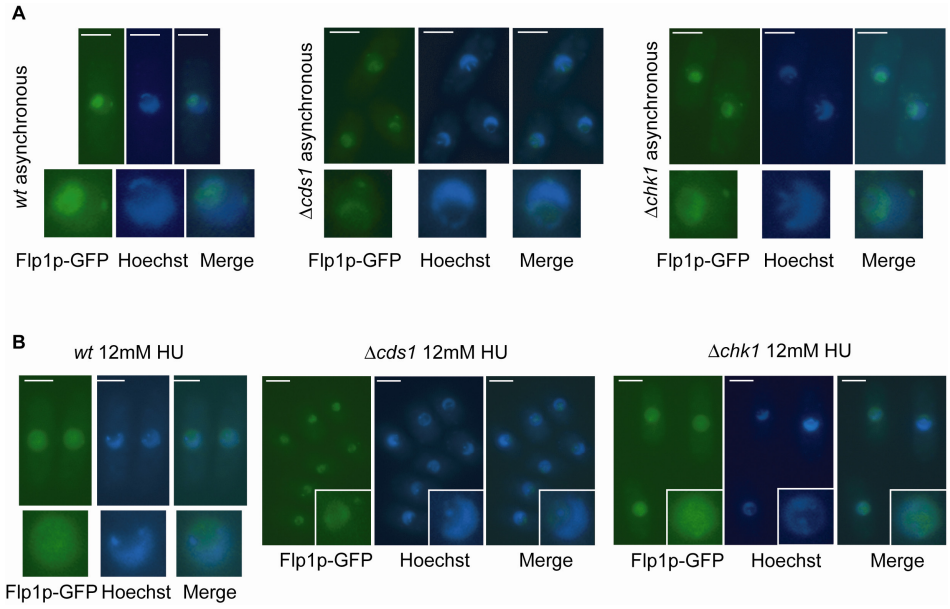

Figure 8. **Nuclear localization of Flp1p during replication stress depends on checkpoint kinase Cds1p**

(A) Flp1p-GFP localizes normally in both Δ*cds1* of Δ*chk1* untreated cells. (B) Flp1p-GFP localization in 12mM HU treated cells lacking either Δ*cds1* or Δ*chk1*. Whereas Δ*chk1* cells localize Flp1p-GFP to the nucleus in response to replication stress like wild-type cells, the phosphatase remains nucleolar in cells deleted for *cds1*. 3x magnified nuclei are shown. Bar 4 μm.

and SPB staining resembling that of untreated cells, and clearly differing from Δ*chk1 flp1-GFP*, which still presented nuclear staining as *flp1-GFP* cells (Figures 7 and 8B). This result indicates that Flp1p localization during replication stress depends directly or indirectly on Cds1p.

To further prove the dependency of Flp1p change of localization on Cds1p, we wanted to check if replication stress forms that do not activate Cds1p are still able to trigger release of Flp1p to the nucleus. For that we used the DNA ligase temperature sensitive mutant *cdc17-K12*, which at restrictive temperature delays S-phase progression leading to cell elongation but it does not present significant activation of Cds1p (Barker *et al.*, 1987; Lindsay *et al.*, 1998). Consistently with the observation that Cds1p action is necessary to trigger Flp1p release to the nucleus upon replication stress, Flp1p remained at its interphase localization in a *cdc17-K12* background during incubation at the restrictive temperature (Figure 9).

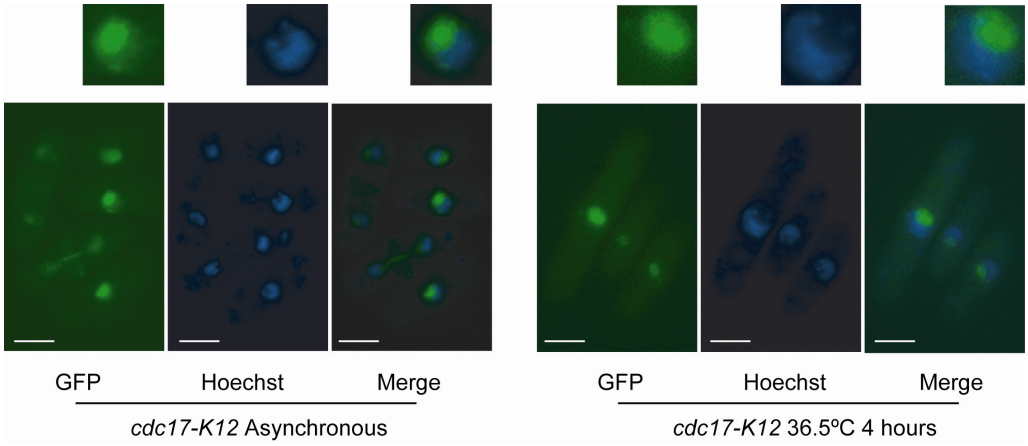

Figure 9. **Flp1p-GFP localizes to the nucleolus in a *cdc17-K12* mutant at restrictive temperature**

Flp1p-GFP localization in temperature sensitive *cdc17-K12* DNA ligase mutants at permissive temperature and during incubation at restrictive temperature. Incubation at restrictive temperature delays S-phase progression leading to cell elongation but not to significant activation of Cds1p (Barker *et al.*, 1987; Lindsay *et al.*, 1998). Bar 4 μm.

2. ANALYSIS OF THE STABILITY OF Flp1p DURING GENOTOXIC STRESS

2.1 Stability of Flp1p during HU, MMS and BL treatment

Levels of Flp1p remain constant during a normal cell cycle (Cueille *et al.*, 2001; Esteban *et al.*, 2004). At sight of the protein's change of localization and given the different degree to which Flp1p seems to be released to the nucleus depending on the type of alteration inflicted, we studied if DNA-damage or replication stress altered Flp1p stability/levels. A Western blot assay was performed to analyse the levels of Ha-tagged Flp1p in asynchronous cultures during 4 hours of 12mM HU, 0.033% MMS or 7.5mU BL treatment. *flp1-Ha* has been previously shown to present a *wt* like behaviour (Cueille *et al.*, 2001; Esteban *et al.*, 2004).

Flp1p-Ha levels remained constant throughout a four hour HU treatment, whereas Flp1p-Ha levels decreased significantly during MMS treatment, and more moderately in BL (Figure 10).

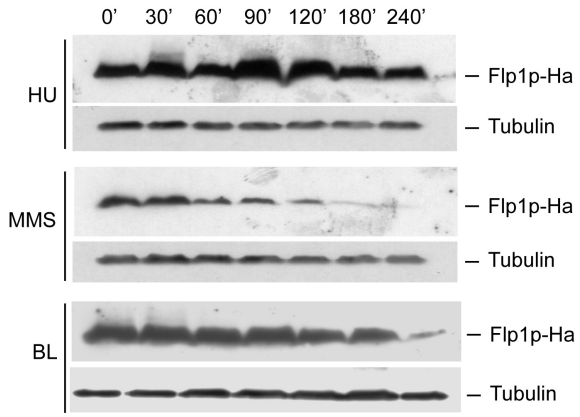

Figure 10. Treatment with MMS or BL induces Flp1p-Ha degradation

Asynchronous cultures of Flp1p-Ha tagged strains were treated either with HU 12mM, 0,033% MMS or 7.5mU BL. Flp1pHa levels remained stable in the course of a 4 hour HU treatment whereas the protein was degraded in cultures exposed to MMS and BL.

2.2 Flp1p-Ha levels during MMS treatment are stabilized in Δ*cds1*

Given the relationship between Flp1p and the signalling pathway of Cds1p, we were next interested in finding out if Cds1p could regulate the degradation of the phosphatase. Since according to the last point Flp1p seemed to be more dramatically degraded in response to MMS treatment than in BL, we compared the levels of the protein during a 4 hour 0.033% MMS treatment in *flp1-Ha*, Δ*cds1 flp1-Ha* and Δ*chk1 flp1-Ha.* Whereas in Δ*chk1 flp1-Ha* the phosphatase was degraded as in control cells, Flp1p-Ha levels were stabilized in a Δ*cds1 flp1-Ha* strain (Figure 11A).

This result points again to functional interaction between Flp1p and the Cds1p signalling cascade in response to genotoxic stress.

2.3 MMS-induced Flp1p-Ha degradation depends on the proteasome

In order to understand the mechanism underlying the degradation of Flp1p triggered by treatment with DNA-damaging agents, Flp1p levels were studied in three

proteasome mutant strains *mts1*-1/*rpn9*-1, *mts2*-1/*rpt2*-1 and *mts3*-1/*rpn12*-1 during MMS treatment. *mts* mutants (Metylbenzylcabamylate-resistant temperature sensitive) are conditional lethal mutants of different subunits of the regulatory complex (19S) of the 26S protease (Gordon *et al.*, 1993; Gordon *et al.*, 1996; Seeger *et al.*, 1996; Wilkinson *et al.*, 1998). These mutants undergo a conformational change at the restrictive temperature, which renders them defective in selectively degrading proteins targeted for destruction by the ubiquitin pathway.

mts1-1/*rpn9*-1, *mts2*-1/*rpt2*-1 and *mts3*-1/*rpn12*-1 mutants and a wild-type control were grown at the permissive temperature and shifted to 36ºC when MMS was added.

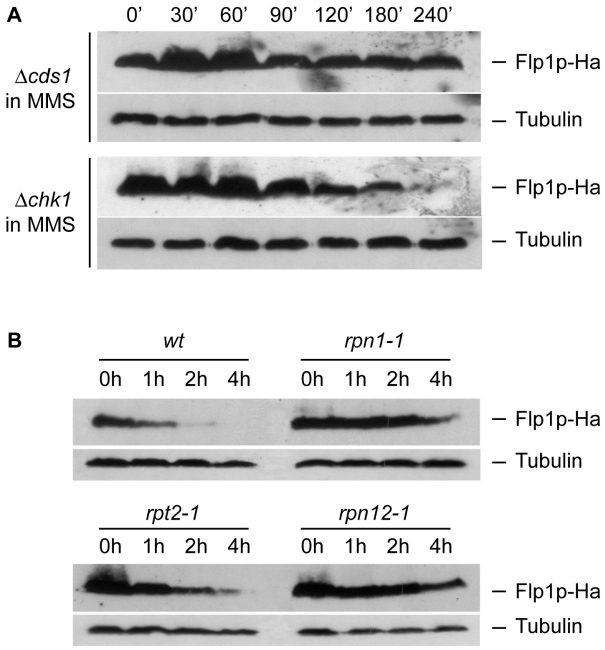

Figure 11. Degradation of Flp1p in MMS depends on Cds1p and the proteasome

(A) Flp1p-Ha levels in strains deleted for *cds1* or *chk1* during 0,033% MMS treatment. Flp1p-Ha is degraded in a Δ*chk1* strain whereas no such protein levels variation is produced in Δ*cds1*. (B) Western blot showing stabilization of Flp1pHa levels during MMS treatment in proteasome mutant strains. Three proteasome temperature sensitive mutant strains (*mts1-1/rpn9-1, mts2-1/rpt2-1* and *mts3-1/rpn12-1*) and control cells were grown at permissive temperature until exponential growth and then shifted to restrictive temperature and treated with 0,033% MMS.

Flp1p-Ha levels were strongly stabilized in the three proteasome mutants indicating that Flp1p-Ha may be a substrate of the ubiquitin pathway (Figure 11B). Differences in the degree of stabilization in these mutants seemed logical attending to the different nature of the proteins which compose the 26S regulatory complex, responsible for substrate specificity.

3. ANALYSIS OF THE RELATIONSHIP OF Flp1p AND Cds1p IN CHECKPOINT RESPONSE

3.1 Flp1p and Cds1p interact physically *in vivo*

Having related Flp1p-GFP localization to Cds1p during checkpoint response, one attractive possibility was that Flp1p interacted with Cds1p *in vivo*. Therefore we performed a pull-down assay to check for GST-Flp1p/Cds1p-Ha physical interaction. We also included in the assay the catalytic inactive form of Flp1p, since our group has shown earlier that GST-Flp1p^{CS} is more effective in interacting with Cdc25p *in vivo* than GST-Flp1p (Esteban *et al.*, 2004; Vazquez-Novelle *et al.*, 2005).

GST-Flp1p and GST-Flp1CS were induced and affinity-purified (see Methods) both from untreated and checkpoint activated cells either in 12mM HU or 0.033% MMS. Blots were incubated with α-Ha antibody in order to detect Cds1p-Ha.

Although no interaction was found in untreated cells, our assay showed interaction between Cds1p and Flp1p both in cells treated with 20mM HU or 0.033% MMS. As expected, this result was more evident in a strain expressing the catalytic inactive form of Flp1p, were physical interaction between the studied proteins can also be seen in untreated cells (Figure 12A). These results indicate that Cds1p is able to form a complex with both the catalytically inactive Flp1p^{CS} mutant and with the wild type protein *in vivo*, suggestive of a substrate/enzyme interaction. The low degree of interaction found may be explained by the transient nature of phosphatase interactions.

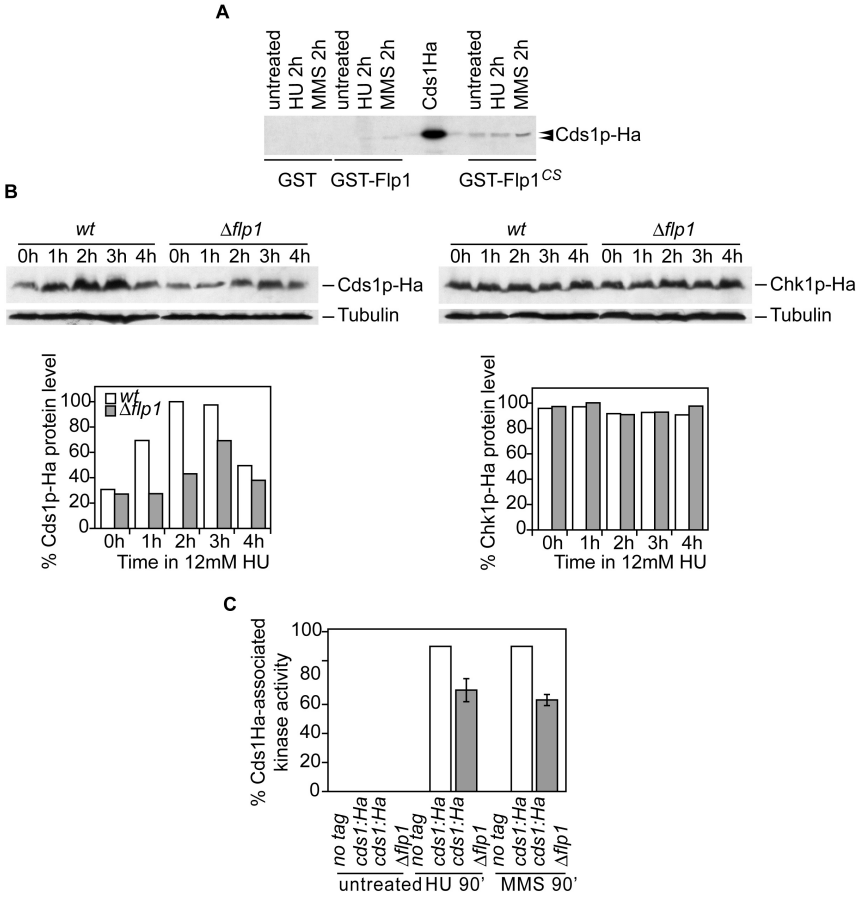

Figure 12. Cds1p and Flp1p interact physically.

***Δflp1* presents reduced Cds1p protein levels and kinase activity in response to genotoxic stress**

(A) Flp1p and Cds1p can interact physically *in vivo*. Pull-down assay showing physical interaction between Cds1p and Flp1p or catalytic inactive Flp1p ($Flp1p^{CS}$). GST-Flp1p and GST-$Flp1p^{CS}$ were purified both from untreated and checkpoint activated cells, blots were incubated with α-Ha antibody in order to detect Cds1pHa. Higher interaction is detected in catalytic inactive Flp1p samples. (B) Western blot analysis of Cds1pHa and Chk1pHa protein levels in wild-type and Δ*flp1* cells treated with 20mM HU. Samples were quantified and normalized to loading controls. Quantification is shown in bar diagrams. Whereas Δ*flp1* cells accumulate less Cds1p in checkpoint response to HU, Chk1p levels are similar in both strains. (C) Cells deleted for *flp1* present decreased *in vivo* Cds1p activity in checkpoint response. Kinase assay of Cds1p using MBP as substrate. Active Cds1pHa was immunoprecipitated from wild-type and Δ*flp1* strains, both from HU and MMS treated cells. Activity was quantified taking into account the amount of Cds1pHa immunoprecipitated in each sample and represented in a bar diagram. Cds1p-associated kinase activity in wild-type cells, both for HU and MMS treated cells, was arbitrarily normalized to 100%. Error bars are shown for three independent experiments.

3.2 Protein levels and activity of Cds1p are altered in Δ*flp1*

Flp1p, as a phosphatase, could be involved in down-regulation of the checkpoint response by removing activating phosphate residues from certain effectors of the signalling cascade to genotoxic stress. Cds1p appeared as an appealing potential target of Flp1p activity, given our previous evidences relating the Flp1p to the kinase.

As a first approach, levels of Cds1p during checkpoint response to replication stress were analysed by western blot. Cds1p protein levels significantly increased in the first two hours of HU treatment in *wt* cells, to decrease again in the last stages of the 4 hour treatment. In Δ*flp1* cells, although basal Cds1p levels are similar to those of the *wt*, the quantity of the kinase rises only moderately after three hours of drug treatment, to decrease normally at the four hours time point (Figure 12B). Levels of the other main effector or the checkpoint response in *S. pombe*, Chk1p, were examined in response to HU. Almost constant protein levels were detected for both *wt* and Δ*flp1* cells throughout the treatment.

We next studied if the activity of Cds1p in checkpoint response was altered in a Δ*flp1* strain. With this purpose Cds1p-Ha was immunoprecipitated from untreated and 12mM HU treated cells every 30 minutes during a 4 hours exposure to the drug. Cds1p-Ha activity was assayed using myelin basic protein (MBP) as a substrate. The obtained activity was then normalized taking into account the quantity of Cds1p-Ha immunoprecipitated in every sample. Interestingly the activity of the kinase in the Δ*flp1* background resulted to be lower than in *wt* cells during the whole treatment (Figure 12C). The most significant difference in activation between *wt* and Δ*flp1* was observed at 90 minutes of treatment, time of maximum activation, when Cds1p in cells depleted of Flp1p only reaches about 70% of the activity achieved in a *wt*. Interestingly, we also proved that the kinase was activated during treatment with MMS, being the difference in activation between *wt* and Δ*flp1*at 90 minutes even greater under these conditions.

Surprisingly, taken together these data indicate that rather than enhancing Cds1pHa activity, absence of Flp1p results in reduced activity and levels of Cds1p, suggesting that Flp1p may act as an activator of Cds1p either directly or by its action over some inhibitor or activator of Cds1p activity.

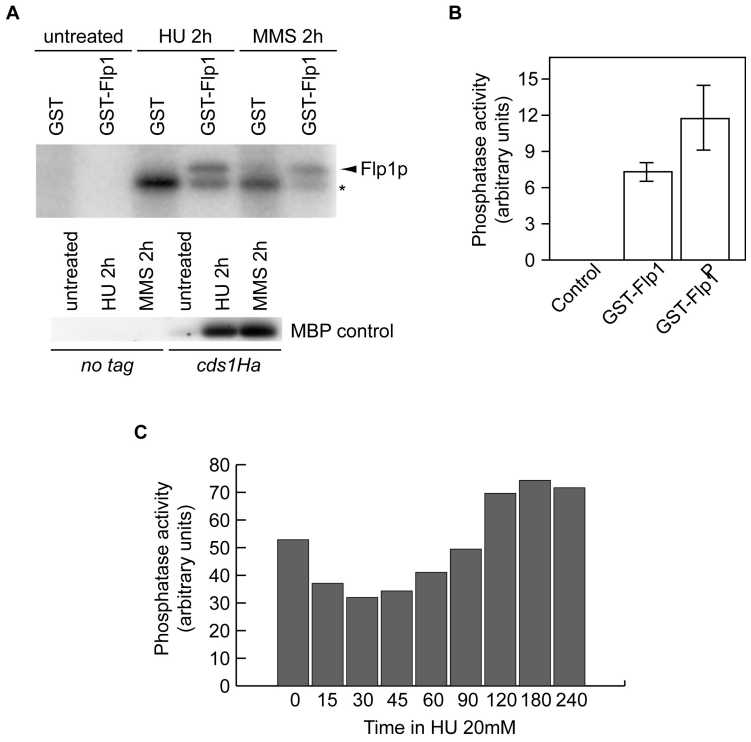

Figure 13. Cds1p phosphorylates Flp1p *in vitro* resulting in an enhancement of its phosphatase activity

(A**)** Checkpoint activated Cds1p phosphorylates Flp1p *in vitro*. Kinase assay of Cds1p using Flp1p as substrate. Cds1pHa was immunoprecipitated from untreated cells and checkpoint activated cells respectively and assayed using purified GST-Flp1p and GST (control) as substrates. Activity of checkpoint activated Cds1pHa and of an untagged strain as a control were assayed using MBP as substrate (lower panel). Flp1p is phosphorylated by the checkpoint activated kinase. Phosphorylated Flp1p is marked by an arrow. The band marked by a star corresponds to a protein which co-immunoprecipitates with active Cds1p. (B) Cds1-mediated Flp1p phosphorylation enhances the phosphatase activity of Flp1p *in vitro*. Quantification of phosphatase assay using DiFMUP as a substrate. Unphosphorylated and Cds1p phosphorylated GST-Flp1p were assayed *in vitro* for their ability to dephosphorylate the fluorescent substrate DiFMUP. Active immunoprecipitated Cds1p was used as a control. (C) Plot of the activity of Flp1p using DiFMUP as a substrate during 4 hour exposure to replication stress. Exponentially growing Flp1p-Ha cells were treated with 20 mM HU and samples were taken at the indicated time points (minutes). A phosphatase assay using Flp1p-Ha immunoprecipitated from each sample and DiFMUP as a substrate was performed, by incubation in phosphatase buffer at 30ºC for 30 minutes. Fluorescence was quantified in each sample as an output.

3.3 Cds1p phosphorylates Flp1p *in vitro*

We showed before that Flp1p-GFP change of localization during replication stress depended on Cds1p presence. This seemed indicative of an action of the kinase over the phosphatase in checkpoint response. We therefore studied if Flp1p could be phosphorylated by active Cds1p.

Activated Cds1pHa was immunoprecipitated after 2 hours of treatment with 20mM HU and 0.033% MMS. Activity of the immunoprecipitated kinase was tested using MBP as a substrate. Immunoprecipitates from untreated cells were used as controls. Cds1p was then assayed over GST-purified GST-Flp1p and over GST as a control, resulting in specific phosphorylation of Flp1p both by HU- and MMS-activated Cds1p (Figure 13A). A lower band of unspecific phosphorylation was found, which was proven to account for a protein present in the immunoprecipitates from the kinase.

3.4 Phosphorylation of Flp1p by Cds1p enhances its phosphatase activity

Our *in vitro* observations suggest that Flp1p may be an *in vivo* substrate for the Cds1p-S-phase checkpoint kinase in response to replication arrest or to replication fork-associated DNA damage. We next tested if the phosphorylation of Flp1p by Cds1p was able to alter its phosphatase activity *in vitro*. With this purpose, GST-Flp1p was purified to homogeneity from *S. pombe* Δ*cds1* cells expressing the GST-fusion protein. GST-Flp1p was phosphorylated by activated Cds1p using non-hydrolysable ATP in order to prevent possible auto-dephosphorylation events during the subsequent phosphatase assay. *In vitro* Cds1p-phosphorylated and unphosphorylated GST-Flp1p activities were assayed using DiFMUP as a substrate. Phosphorylated GST-Flp1p resulted to be more active, proving an enhancement of Flp1p phosphatase activity by the *in vitro* Cds1p-mediated phosphorylation (Figure 13B).

Interestingly, we were also able to detect alterations of Flp1p phosphatase activity during replication stress *in vivo* assaying over DiFMUP the activity of immunoprecipitated Flp1p-Ha at different times of HU treatment. The activity of Flp1p decreased immediately after addition of the drug to the culture and increased abruptly after two hours of treatment (Figure 13C). Stimulation of the phosphatase's activity correlates thus with the observed timing for Cds1p-dependent release of Flp1p to the

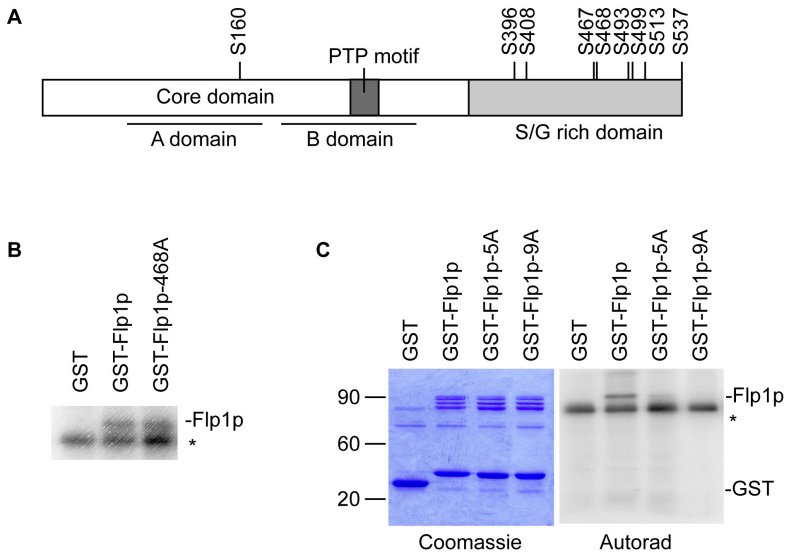

Figure 14. **Construction of a Flp1p mutant protein that can not be phosphorylated by Cds1p**
(A) Schematic representation of Flp1p showing the location of its 9 RXXS sites. (B) Kinase assay showing that mutation of Ser^{468} to Ala did not abolish phosphorylation of GST-Flp1p by activated Cds1p. Ser^{468} located at a RXXS consensus phosphorylation site for Chk2p on Cdc25A, had been identified as a residue phosphorylated with high score in a mass spectrometric assay on GST-Flp1p phosphorylated *in vitro* by Cds1p. (C) Simultaneous mutation of Ser^{468} and the 4 RXXS sites located in not analyzed regions in the spectrometric assay, practically abolished phosphorylation on Flp1p. In the mutant for all 9 RXXS sites phosphorylation could not be detected.

nucleus, indicating that Flp1p change of localization and enhancement of its phosphatase activity may be related.

3.5 Determination of Cds1p phosphorylation sites on Flp1p by mass spectrometry

Since Cds1p was able to phosphorylate Flp1p *in vitro* to enhance its phosphatase activity, we were interested in finding out the residues in the phosphatase in which this reaction occurred. Mutation of these residues to construct a non phosphorylatable form of Flp1p would then be a useful tool to check the effects of the disruption of the possible *in vivo* modification of the phosphatase by Cds1p as a result of genotoxic stress.

No consensus phosphorylation sequence has been described for SpCds1p. However analysis of the sequence of Flp1p revealed nine RXXS consensus phosphorylation sites for hChk2p in Cdc25A and an I/L/V/M X S/T X I/L/V/M Rad53p consensus phosphorylation site, putative candidate residues for Cds1p phosphorylation on the phosphatase.

Identification of phosphorylation sites on Flp1p by checkpoint activated Cds1p was performed by mass spectrometry. Samples were obtained by means of a kinase assay of immunoprecipitated Cds1pHa over GST-Flp1p as described before, using no-radioactive ATP. The analysis identified phosphorylation of serine 468 in samples incubated with both HU-activated and MMS-activated Cds1p kinase. Interestingly Ser468 lies in a RXXS consensus phosphorylation site for Chk2p mammalian kinase in Cdc25A (O'Neill *et al.*, 2002). The protein contains a total of 9 RXXS sites (Figure 14A).

3.6 Construction of a Flp1p mutant protein non phosphorylatable by Cds1p: *flp1-9A*

Following the goal of constructing a form of Flp1p which Cds1p was not able to phosphorylate, we mutated the identified aminoacid Ser468 to the non phosphorylatable residue Alanine. The mutation was performed in the Prep-KZ-*flp1+* plasmid by PCR as described in MATERIALS AND METHODS, and checked by DNA sequencing. The expressed GST-Flp1p^{S468A} mutant protein was then used as a substrate for Cds1p phosphorylation. The mutant protein could be still phosphorylated by the checkpoint kinase (Figure 14B).

As mentioned before there are 8 further RXXS sites in Flp1p located at Serines 160, 396, 408, 467, 493, 499, 513 and 537. 4 of them (Ser396, Ser493, Ser499, Ser537) lied in protein fragments that had not been analysed in the mass spectrometric assay probably due to its size or difficulty to become ionized. In order to check if any among these residues was responsible for the phosphorylation, we constructed the (S468A S396A S493A S499A S513A S537A) 5A mutant. Although the expressed GST-Flp1p^{5A} mutant could not be phosphorylated to the same extent as the native protein, some phosphorylation still took place. We therefore decided to construct the 9A mutant, mutating all nine RXXS sites of Flp1p to RXXA. The resulting GST-Flp1p^{9A} mutant was not phosphorylated in the Cds1p kinase assay (Figure 14C).

Study of Flp1p-9A-EGFP localization during replication stress

According to our previous observations Cds1p was able to determine Flp1p localization during replication stress. Moreover, Cds1p and Flp1p interacted physically and checkpoint activated Cds1p was able to *in vitro* phosphorylate Flp1p. These facts lead to the hypothesis that disruption of Flp1p phosphorylation sites by Cds1p could lead *in vivo* to an abolishment of Flp1p movement from the nucleolus to the nucleus during replication stress.

In order to check this hypothesis, we constructed an integrated form of EGFP tagged *flp1-9A* (see MATERIALS AND METHODS), and we characterized the behaviour of the resulting *flp1-9A-EGFP* strain during HU treatment.

First we checked Flp1p-9A-EGFP localization during unperturbed cell cycle. Flp1p-9A-EGFP correctly localized to the nucleolus and spindle pole body in interphase cells, to the nucleus and spindle during early mitosis and also to the medial ring in the late stages of mitosis (Figure 15A).

However, whereas treatment with 12mM HU triggered nuclear localization in control cells, the 9A mutant protein remained in its nucleolar and SPB localizations throughout the treatment (Figures 15B and 15C). This result interestingly, points to an *in vivo* phosphorylation of Flp1p by Cds1p, which disruption results in abolishment of Flp1p shuttle to the nucleus.

flp1-9A presents reduced Cds1p activity during replication stress

We showed earlier that the Δ*flp1* strain presented reduced Cds1p activity in response to replication stress induced blocks. If Flp1p plays a role in somehow regulating Cds1p activity, it would be expected that cells that can not release the phosphatase to the nucleus would present a similar phenotypes to that observed in Δ*flp1*. By means of a kinase assay using immunoprecipitated Cds1p-Ha from *flp1-9A* cells and MBP as a substrate we confirmed that *flp1-9A* cells presented indeed reduced Cds1p activity with respect to *wt* cells (Figure 15D).

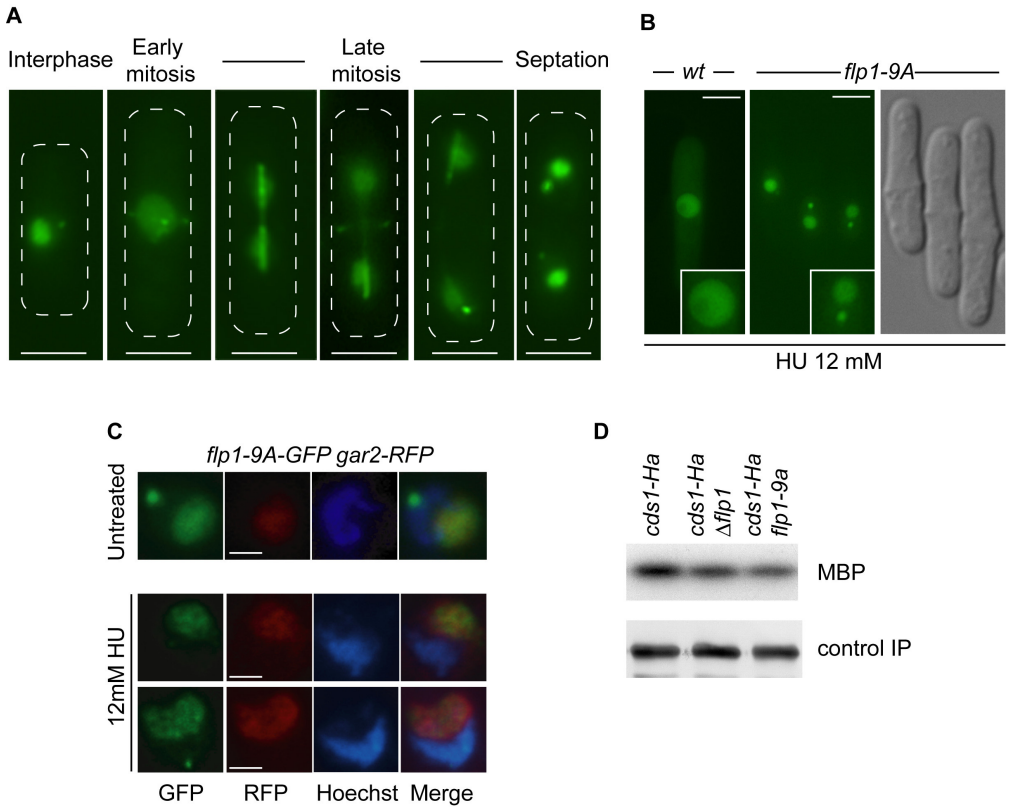

Figure 15. **Characterization of the *flp1-9A* mutant: localization of Flp1p and Cds1p activity in response to replication stress**

(A) The integrated *flp1-9A* strain presents unaltered subcellular localization of the protein during the different stages of an unperturbed cell cycle. *In vivo* Flp1p-9A-EGFP staining shows interphase and mitotic cells undergoing normal changes in the subcellular localization of Flp1p-9A as described before for wild-type Flp1p (Cueille *et al*., 2001). Dot lines represent the cells contour. Bar, 4 μm. (B) Flp1p-9A-EGFP staining in cells undergoing replication stress. Flp1p-9A-EGFP is not released to the nucleus in checkpoint response to HU treatment. Bars, 4 μm. 3x magnified nuclei are shown in the bottom right corners. Note that *flp1-9A-GFP* cells elongate indicating that they are responding to the checkpoint arrest. (C) 4x Magnified nuclei showing co-localization of Flp1p-9A-EGFP with the nucleolar marker Gar2p-RFP in both untreated and 12mM HU treated cells. (D) Kinase assay of active Cds1p-Ha over MBP. A control western blot showing the quantity of immunoprecipitated Cds1p-Ha in each sample has been included. The kinase resulted to be less active in the *flp1-9A* mutant than in a *wt* background, resembling the behaviour in Δ*flp1*.

4. ANALYSIS OF THE INFLUENCE OF Flp1p ON THE CHECKPOINT RESPONSE TO GENOTOXIC STRESS

4.1 Sensitivity to long term drug exposure

In order to analyse the possible role of Flp1p in checkpoint response, the first step we took was the study of the sensitivity associated to the deletion of *flp1* alone or combined with Δ*cds1* or Δ*chk1*, mutants for the main effectors of checkpoint signalling, in response to chronic exposure to replication stress or DNA-damaging agents. Deletion of *flp1* behaved in a *wt* fashion in terms of survival on drug containing plates and did not add any significant defect to the impeded growth of checkpoint mutants at the concentrations used (Figure 16A).

On the other hand we were able to detect long term sensitivity plating G1 synchronized Δ*flp1* cells (Figure 16B). Exponentially growing cultures (25ºC) of *cdc10-129, cdc10-129 Δflp1* and *cdc10-129 Δrad3* were incubated for 4.5 hours at the restrictive temperature to obtain G1 synchronized cultures and then assayed for their survival in HU 5mM and drug-free medium. The same experiment was performed in a *cdc10-M17* background. *cdc10-129* Δ*flp1* and *cdc10-M17* Δ*flp1* resulted to be more sensitive to long term exposure to HU than the respective *flp1+* controls, and in their turn, less sensitive than Δ*rad3* cells. It should be noted that synchronized *cdc10-M17* Δ*flp1* and *cdc10-M17* Δ*rad3* readily show a loss of viability in drug-free medium when compared to *cdc10-M17* control strain.

To assess the sensitivity of the *flp1-9A* mutant to chronic exposure to replication stress, a plate assay comparing the behaviour of this strain to that of *wt*, *flp1-GFP*, Δ*flp1* and Δ*cds1* in HU was performed. Paying attention to *flp1* mutants and tagged forms, whereas the GFP tag seemed to confer the strain a slight resistence to the drug *flp1-9A* presented a Δ*flp1*-like behaviour with smaller colonies than the *wt* (Figure 16C).

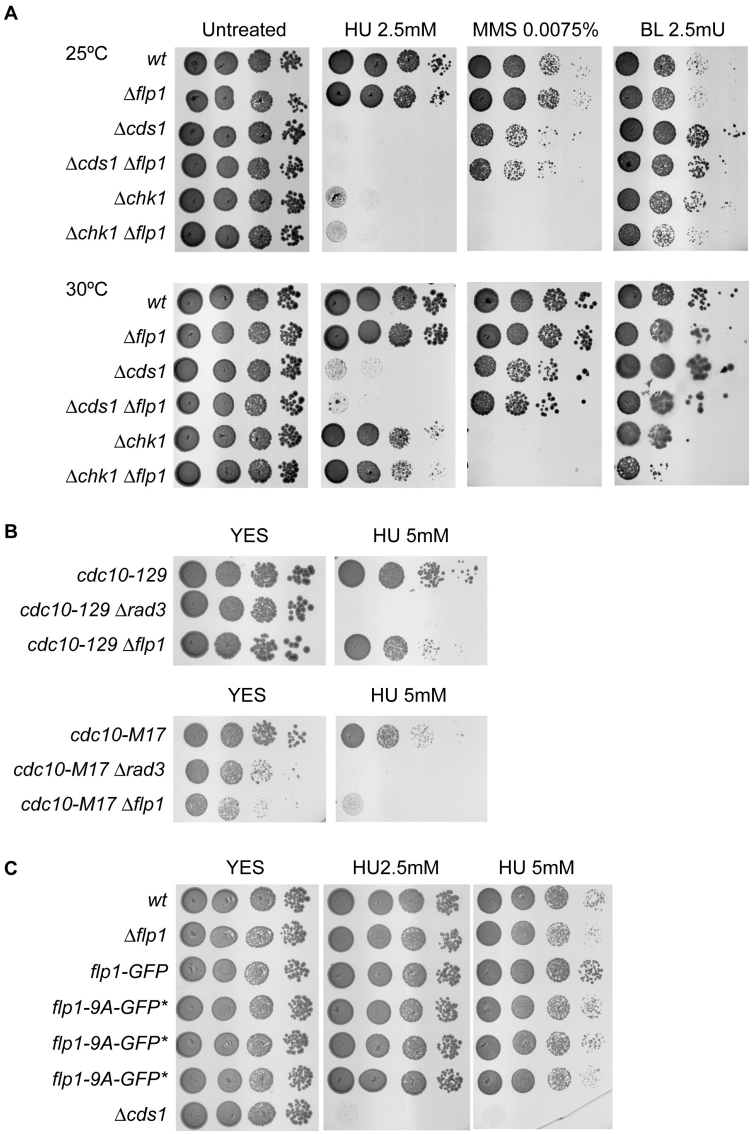

Figure 16. Sensitivity of *flp1* mutants to chronic exposure to HU

(A) 10-fold dilution plate assay of *Δflp1*, *Δcds1 Δflp1* and *Δchk1 Δflp1* sensitivity to chronic exposure to HU, MMS and BL compared to *wt* and the simple mutants. Plates were incubated for 72 hours at the indicated temperatures. (B) Plate assay showing sensitivity of Δ*flp1* to HU after G1 synchronization using *cdc10-129* and *cdc10-M17* alleles. Note that *cdc10-M17* Δ*flp1* and *cdc10-M17* Δ*rad3* show already a defect in growth in drug free medium after synchronization. (C) Plate assay showing the sensitivity of three different clones of *flp1-9A-GFP* to HU. It can be observed that the behaviour is similar to that of Δ*flp1*, presenting only a decrease on colony size when compared to wild-type cells.

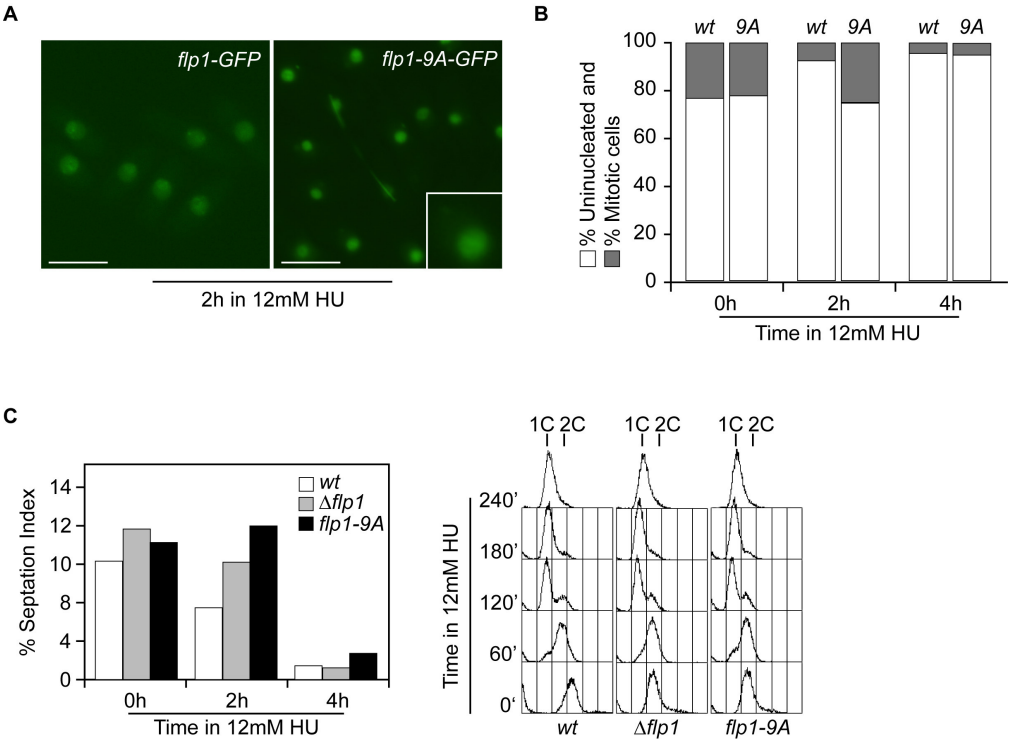

Figure 17. ***flp1* mutants present a defect on checkpoint block upon replication stress**

(A) *In vivo* fluorescence microscopy images showing the difference in behavior of *flp1-9A* and wild-type cells after 2h of 12mM HU treatment. Whereas in *flp1-GFP* cells, nuclear staining of the protein is generally observed, in *flp1-9A-GFP* the protein can be detected not only in the nucleolus but also in the mitotic spindle in some cells, indicating that a subpopulation of this strain is undergoing mitosis and not blocking in S-phase as expected. (B) Plots of uninucleated and mitotic cells observed upon 0, 2 and 4 hours treatments with HU in *flp1-9A* and wild-type strains. *In vivo* Flp1p-GFP localization was scored in both strains, note that more than 20% of *flp1-9A-GFP* cells had a mitotic pattern of Flp1p-GFP subcellular localization at the 2 hours time point. (C) Quantification of checkpoint defects in *flp1* mutants. Septation and mitotic index was measured in wild-type and *flp1* mutants by means of dark field microscopy. Whereas this parameter significantly decreases in a wild-type strain after 2h of 12mM HU treatment, correlating with an adequate checkpoint response, this change is not patent in *flp1* mutant cells. The FACS monitoring DNA content of the strains during the treatment has been included.

4.2 Short-term response of *flp1* mutants to replication stress

While *flp1-9A* did not present any significant alteration in checkpoint response in terms of end-term survival, when studying their behaviour in liquid cultures we could detect a higher rate of cells undergoing mitosis in this mutant than in *wt* after two hours of 12mM HU treatment (Figure 17A).

As a first approach to quantify this effect, we determined the percentage of cells undergoing mitosis in the presence of HU by counting duplicated SPBs, short spindle, long/extended spindles and binucleated cells (Figure 17B), by *in vivo* following the pattern of Flp1p-9A-EGFP and Flp1p-GFP as a control. While *wt* cultures were blocked to a high extent after two hours of treatment (reduction from 23% of cells undergoing mitosis in asynchronous cultures to 9% in treated cells), the 9A mutant did not reduce its mitotic rate in the first two hours of treatment (21% in untreated cultures, 24% in treated cultures). Surprisingly, after 4 hours exposure to the drug the mutant presented 95% of blocked cells, equalling *wt* behaviour.

We next checked if this transient defect in checkpoint block could be seen in *Δflp1* to uncover the potential parallelism in between *flp1-9A* and Δ*flp1* mutants in dealing with HU treatments. Septation index of wild-type, Δ*flp1* and *flp1-9A* strains were measured at 0, 2 and 4 hours time points during a 12mM HU treatment in YES-liquid media (Figure 17C). FACS analysis and cell elongation indicated that all three strains were responding to the HU-induced nucleotide depletion. However, in these experiments both *flp1* mutants presented higher numbers of septated cells than the wild-type after 2 hours of drug treatment. Consistently with the previous quantification of mitotic forms in the *flp1-9A* mutant, septation index in both mutants was similar that of *wt* after 4 hours of exposure to the drug.

We were next interested in finding out if aberrant DNA segregation could be detected as a consequence of this deficiency in checkpoint block in Δ*flp1* cells. In order to rule out a possible interference of cell cycle kinetics of Δ*flp1* mutants in our observations, we checked checkpoint proficiency of this mutant in synchronized cells. *cdc10-129*, *cdc10-129* Δ*flp1* and *cdc10-129 Δrad3* strains were synchronized in G1 by incubation at 36.5ºC for four and a half hours and then released at the permissive temperature in the presence of 12mM HU, samples were taken at regular intervals and processed for nuclear staining, DNA content and cell size analysis (Figure 18). Binucleated (normal and cut) cells were monitored at indicated intervals after release (Figure 18A). While in synchronized *cdc10-129* cells (control) the percentage of binucleated (normal and cut)

cells remained low all throughout the experiment, *cdc10-129 ∆flp1* mutants already presented a moderate percentage of cells undergoing mitosis as soon as 60 minutes after the release in HU (up to 15%) with a steady increase (in percentages) as cells were exposed longer to the replication block (reaching a maximum of 22%). As expected, we found that the checkpoint defects observable in *cdc10-129 ∆rad3* mutant cells were more severe than those found in *cdc10-129 ∆flp1* mutant cells, as the percentages of cells undergoing mitosis in the absence of DNA replication ranked from 18%, at the block point, to 62%, at the last time point in *∆rad3* mutants. Examination of cells (Figure 18B) and FACS analysis of DNA content (Figure 18C) confirmed that *cdc10-129 ∆flp1* and *cdc10-129 ∆rad3* were defective in their response to the HU arrest, as cells with less than an haploid content of DNA (1C) were detected.

To rule out a possible allele-specific interference of *cdc10-129* in our results, due to the extended time this mutant needs to complete S-phase after release, we performed the same experiment using another temperature sensitive allele, *cdc10-M17* (Figure 19). To our surprise we found that *cdc10-M17 ∆flp1* and *cdc10-M17 ∆rad3* readily presented aberrant nuclei as a consequence of incubation at the restrictive temperature (Figure 19A), indicating that *rad3+* and *flp1+* are required to preserve the G1 block and prevent unscheduled progression into mitosis in a *cdc10-M17* strain. During release at the permissive temperature in the presence of 12mM HU, *cdc10-M17 ∆flp1* cells presented a significant increase of cells undergoing aberrant mitosis 90 minutes after the release in HU. This percentage was moderate when compared to data obtained with *cdc10-M17 ∆rad3* cells (Figure 19B). However, even though the results were consistent with those in a *cdc10-129* background, we are fully aware that the observed defect during incubation at the restrictive temperature makes the interpretation of the response of these cells to replication stress difficult. In fact, as inferred from the severity of the synthetic lethality in *cdc10-M17 ∆rad3* cells and, to a lesser extent, in *cdc10-M17 ∆flp1* cells, we observed only a moderate increase in the percentage of aberrant mitosis (cut cells) after the exposure to HU compared to *cdc10-129* data.

Taken together the data obtained form treatment of asynchronous cultures and G1 pre-synchronized cells reflect a defect in checkpoint response associated to mutation of *flp1* in cells undergoing replication stress.

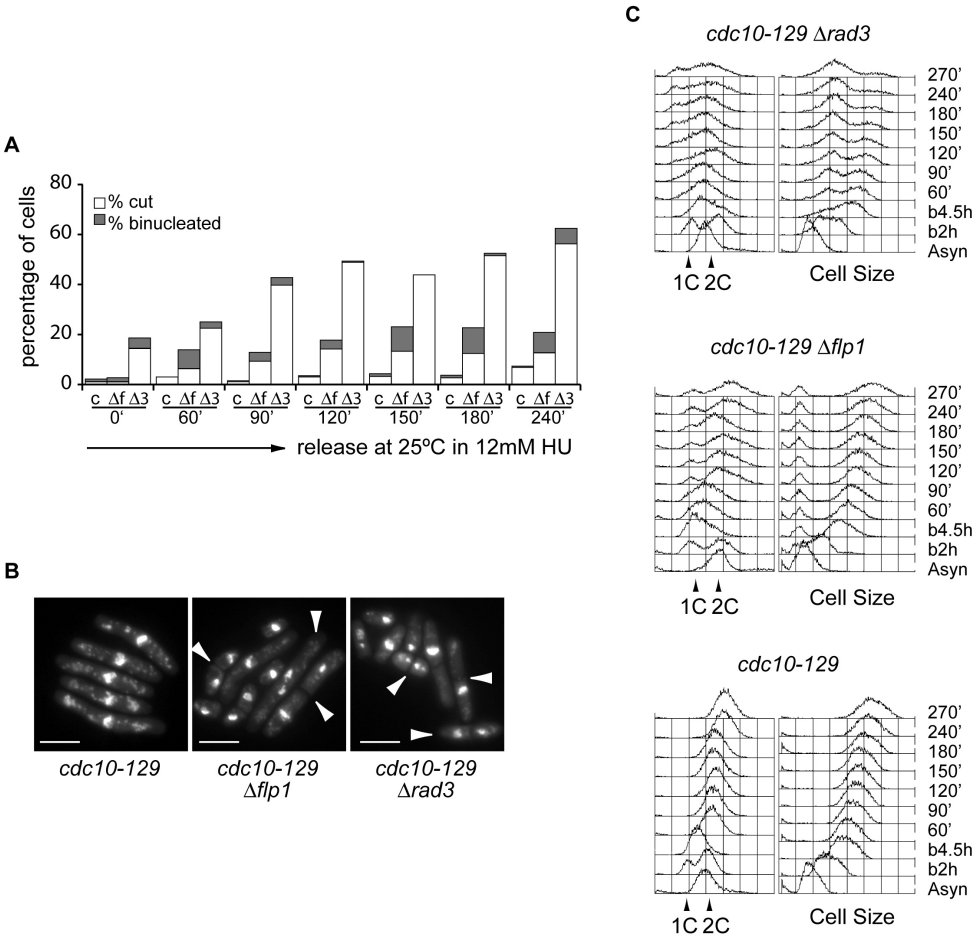

Figure 18. **Defects on checkpoint block in Δ*flp1* results in aberrant mitoses**

(A) Quantification of mitotic nuclei during HU treatment after synchronization in G1. *cdc10-129* (*c*), *cdc10-129 Δflp1* (*Δf*), *cdc10-129 Δrad3* (*Δ3*) strains were synchronized (4.5h at 36.5ºC), and then they were released from the G1 block (25ºC) in the presence of 12mM HU. Percentages of binucleated and cut cells were determined by visualization and counting of DAPI stained nuclei. At least 200 cells were counted for every strain at each time point and the experiment was repeated twice. (B) Strains deleted for *flp1* and *rad3* in a *cdc10-129* background accumulate binucleated and cut cells (marked by arrows) upon HU treatment after synchronization. Bar, 10 μm. (C) DNA content and cell size analyses by FACS during block and release in HU (experiment described in A) confirm that *cdc10-129 Δflp1* and *cdc10-129 Δrad3* are defective in their response to checkpoint mediated arrest, as cells with less than an haploid content of DNA (1C) are detected. Note that *cdc10-129 Δflp1* presents a subpopulation of small cells. As shown in B, both small and elongated cells undergo aberrant mitoses in the presence of HU.

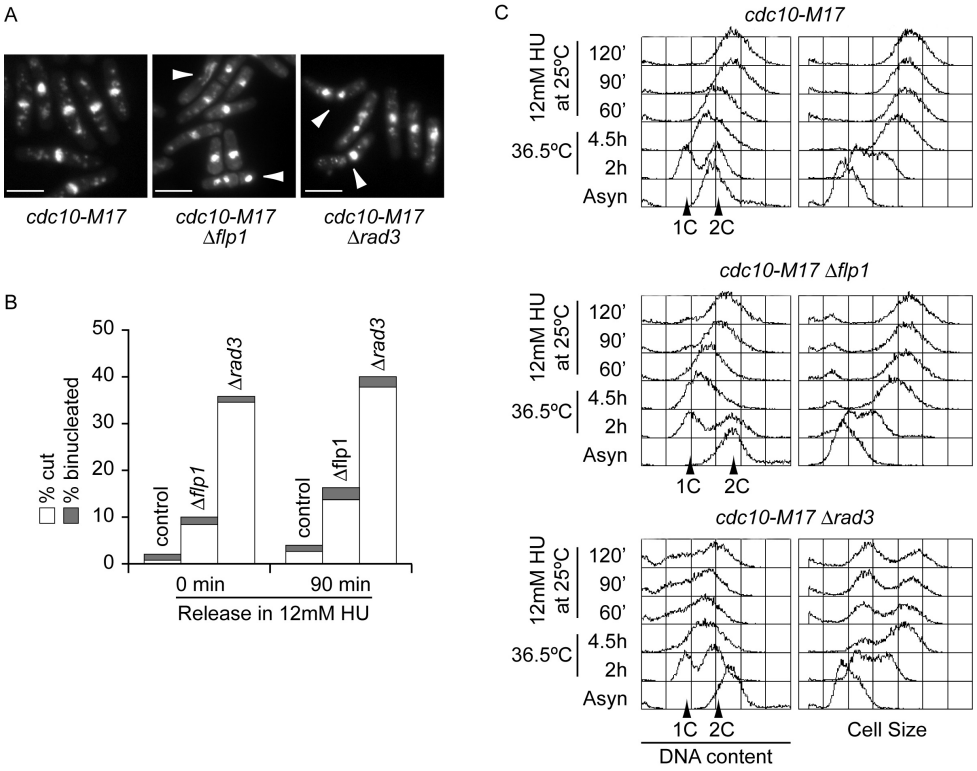

Figure 19. Analysis of Δ*flp1* in a *cdc10-M17* background

(A) Deletion of *flp1* and *rad3* in a *cdc10-M17* background results in unscheduled mitoses during incubation at the restrictive temperature. DAPI nuclear staining of *cdc10-M17* , *cdc10-M17 Δflp1* and *cdc10-M17 Δrad3* strains after 4.5 hours at 36.5ºC showing binucleated and cut cells exclusively in *flp1* and *rad3* mutants (indicated by arrows). Bar, 10 μm. (B) *cdc10-M17*, *cdc10-M17 Δflp1* and *cdc10-M17 Δrad3* strains were incubated at the restrictive temperature (36.6ºC) for 4.5 hours and then released to the permissive temperature (25ºC) in the presence of 12mM HU. Percentages of binucleated and cut cells at the release point and after 90 minutes of treatment were determined. At least 200 cells were examined for each strain and time point, and the experiment was performed three times. The corresponding standard deviations are for the time point 0 minutes: *cdc10-M17* binucleated 0.79 cut 0.29, *cdc10-M17 Δflp1* binucleated 1.1 cut 0.51 and *cdc10-M17 Δrad3* binucleated 0.75 cut 1.51. For the time point 90 minutes: *cdc10-M17* binucleated 0.23 cut 0.86, *cdc10-M17 Δflp1* binucleated 0.55 cut 1.82 and *cdc10-M17 Δrad3* binucleated 1.21 cut 1.79. (C) DNA content and cell size analysis by FACS for the experiment described in B, including additional time points. Note that FACS analysis data are consistent with the results obtained in a *cdc10-129* background.

4.3 Cdc25p accumulation and Cdc2p Tyr15 phosphorylation during checkpoint response are not significantly altered in Δ*flp1*

Checkpoint response promotes nuclear exclusion of Cdc25p (Lopez-Girona *et al.*, 1999; Lopez-Girona *et al.*, 2001b). Since Flp1p controls rapid degradation of Cdc25p to promote adequate down-regulation of Cdc2p/Cd13p-associated kinase activity at mitotic exit in the course of normal cell cycle (Esteban *et al.*, 2004; Wolfe and Gould, 2004), we were interested in studying the possible role of Flp1p in degrading Cdc25p during a HU-mediated block triggered by DNA replication inhibition or MMS-induced replication fork-associated DNA-damage.

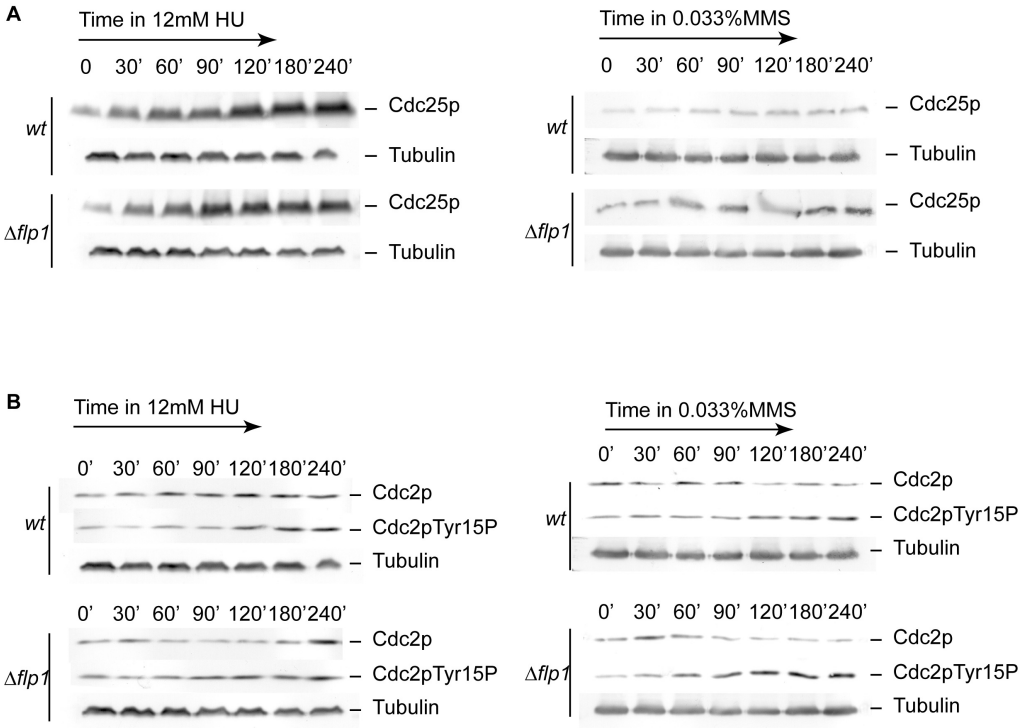

Figure 20. **Checkpoint dependent accumulation of Cdc25p and phosphorylation of Cdc2p in tyrosine 15 are not significantly altered in Δ*flp1* cells.**
(A) Western blot analysis of Cdc25 levels in asynchronous cultures of *wt* and Δ*flp1* strains during treatment with 12mM HU or 0.033% MMS. (B) Western blot analysis of Cdc2p and Tyr15 levels in the same samples. No significant difference in the dynamics of Cdc25p accumulation or Cdc2p tyr15 phosphorylation is observed for cells deleted for *flp1*.

We analysed Cdc25p protein levels in a *wt* and a Δ*flp1* strain in the course of either 12mM HU or 0.033% MMS treatment by western blot analysis (Figure 20A). The amount of cellular Cdc25p increased as a result of drug treatment both in *wt* and Δ*flp1*. Taking into account that Cdc25p basal levels are higher in Δ*flp1* than in *wt*, the kinetics of Cdc25p accumulation seemed to be similar in both strains, allowing us to conclude that Flp1p is not involved in Cdc25p degradation during checkpoint response to genotoxic stress.

Given the relationship between Flp1p and Cds1p checkpoint branch, we next wanted to check if this interaction could affect the net checkpoint response in terms of cell cycle block in response to replication stress or DNA damage. We therefore examined Tyr15 phosphorylation levels of Cdc2p in a *wt* and a Δ*flp1* strain in the course of either 12mM HU or 0.033% MMS treatment by western blot analysis.

Phosphorylation of Tyr15 increased in both strains a result of a 4 hour drug treatment (Figure 20B), indicating that Flp1p is not involved in the control of Cdc2p activity during checkpoint response.

4.4 *flp1* mutants present enhanced recombination in response to replication stress

Apart from regulating Cdc2p activity during genotoxic stress, the Cds1p kinase pathway of checkpoint response is involved in certain mechanisms of DNA protection that Chk1p is not able to perform. As detailed in the introduction, Cds1p plays a central role in stabilization of replication forks and coordination of checkpoint recovery, retaining the replisome assembled during arrest and regulating the recombination machinery. Cds1p prevents unscheduled recombination events at stalled forks by stabilizing their components, and through regulation of endonuclease Mus81p, helicase Rqh1p and Rad60p. S-phase checkpoint deficient Δ*cds1* mutants harbour multiple recombination-associated foci when exposed to HU (Meister *et al.*, 2005). Concentration of Rad22p, fission yeast Rad52p homologue into a few bright nuclear spots, or foci, is an indication of the induction of homologous recombination (Lisby *et al.*, 2001; Du *et al.*, 2003; Meister *et al.*, 2003; Noguchi *et al.*, 2003). Single foci appear with relative frequency even in *wt* cells and are assumed to be sites of post-replicative DNA repair (Meister *et al.*, 2003; Noguchi *et al.*, 2003).

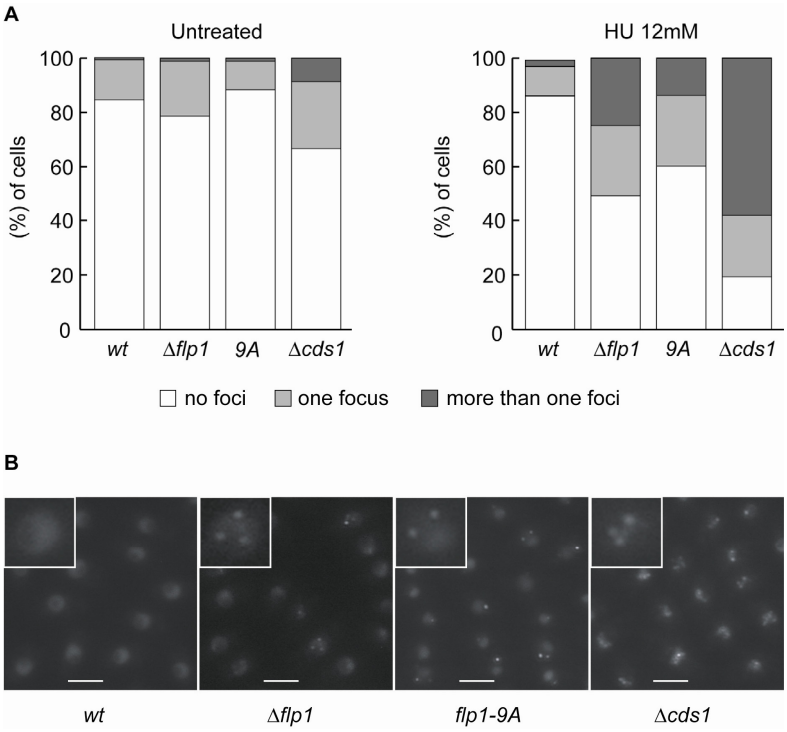

Figure 21. *flp1* mutants present Rad22p recombination foci when exposed to replication stress

(A) Quantification of nuclei containing single or multiple Rad22p-YFP foci in asynchronous exponentially growing *flp1* mutant cells (untreated) and after 2h of 12mM HU treatment. Control counts in checkpoint proficient *wt* cells and checkpoint mutant Δ*cds1* are shown. Results are representative of at least two independent experiments. Standard deviations are: untreated cells, *wt* % no foci 1.16, % one focus 1.64, % multi foci 0.48, Δ*flp1* % no foci 1.05, % one focus 0.80, % multi foci 0.24, *flp1-9A* % no foci 3.02, % one focus 3.40, % multi foci 0.37 and Δ*cds1* % no foci 3.51, % one focus 1.09, % multi foci 2.41; HU treated cells, *wt* % no foci 1.74, % one focus 1.47, % multi foci 0.27, Δ*flp1* % no foci 6.32, % one focus 5.16, % multi foci 1.15, *flp1-9A* % no foci 0.75, % one focus 1.25, % multi foci 0.5 and Δ*cds1* % no foci 0.36, % one focus 1.34, % multi foci 0.97. (B) Live imaging of Rad22p-YFP foci (bright spots) in *flp1* mutants and control strains after 2h of 12mM HU treatment. Bar 4 μm. While recombination foci are rarely seen in *wt*, single and multiple Rad22p-YFP foci are detected in *flp1* mutants. This effect is however weaker than in checkpoint mutant Δ*cds1*.

Since no clear implication of Flp1p could be found in regulating checkpoint block by influencing Cdc2p Tyr15 phosphorylation, we were interested in testing whether the

putative interaction of the phosphatase with the Cds1p pathway could affect the functions of the kinase in inhibiting recombination during checkpoint response.

With this aim, Rad22p-associated recombination foci were visualized *in vivo* in either untreated or HU-treated wild-type, Δ*cds1,* Δ*flp1* and *flp1-9A* cells harbouring a single *rad22*-YFP allele (Figure 21). Over 400 nuclei were classified (for each strain in three independent experiments) depending on the number of foci they born (no foci, single focus, multi foci). The counts for the *wt* and Δ*cds1* correlated with those found in the literature (Meister *et al.*, 2005). Δ*cds1* presented an enhanced number of recombination foci readily in untreated cells, giving account of the importance of surveillance mechanisms and their collateral functions even in exogenously unaltered cell cycles. Importantly, the percentage of Δ*flp1* and *flp1-9A* mutant cells with multiple nuclear Rad22p-YFP spots showed a marked increase when exposed to HU for two hours (from 1% to 25% in Δ*flp1*, from 1% to 15% in *flp1-9A*), whereas the number of foci in wild-type cells remained almost constant (from 1% to 2.5%), probably indicating a defect in checkpoint response associated to depletion or mislocalization of Flp1p. It should be noted that the number of recombination foci present in *flp1* mutants upon HU treatment is moderate when compared to that of Δ*cds1* (up to 57%), which again points to a partial loss of checkpoint activity in the *flp1* mutant strains.

4.5 Analysis of the effect of the moderate over-expression of Flp1p

Over-expression of Flp1p is lethal since it leads to G2 arrest due to constitutive dephosphorylation Cdc25p, in a process dependent on active Wee1p (Cueille *et al.*, 2001; Esteban *et al.*, 2004).

However, by substitution in a pREP41-*flp1*-EGFP plasmid of the nmt1 promoter by *flp1* endogenous promoter region and transformation of a Δ*flp1* strain we were able to constitutively over-express Flp1p to moderate levels without altering the viability of the strain under normal growth conditions. This transformed strain is hereafter referred to as *opflp1.* The over-expressed protein was stable during HU treatment (Figure 22A).

Flp1p-EGFP expressed by this plasmid localized normally during mitotic cell cycle, but showed a slight accumulation of fluorescence in the spindle pole bodies. FACS analysis during HU treatment showed a retard in the establishment of the 1C peak, and a broader distribution of DNA content in *opflp1.* When we examined the behaviour

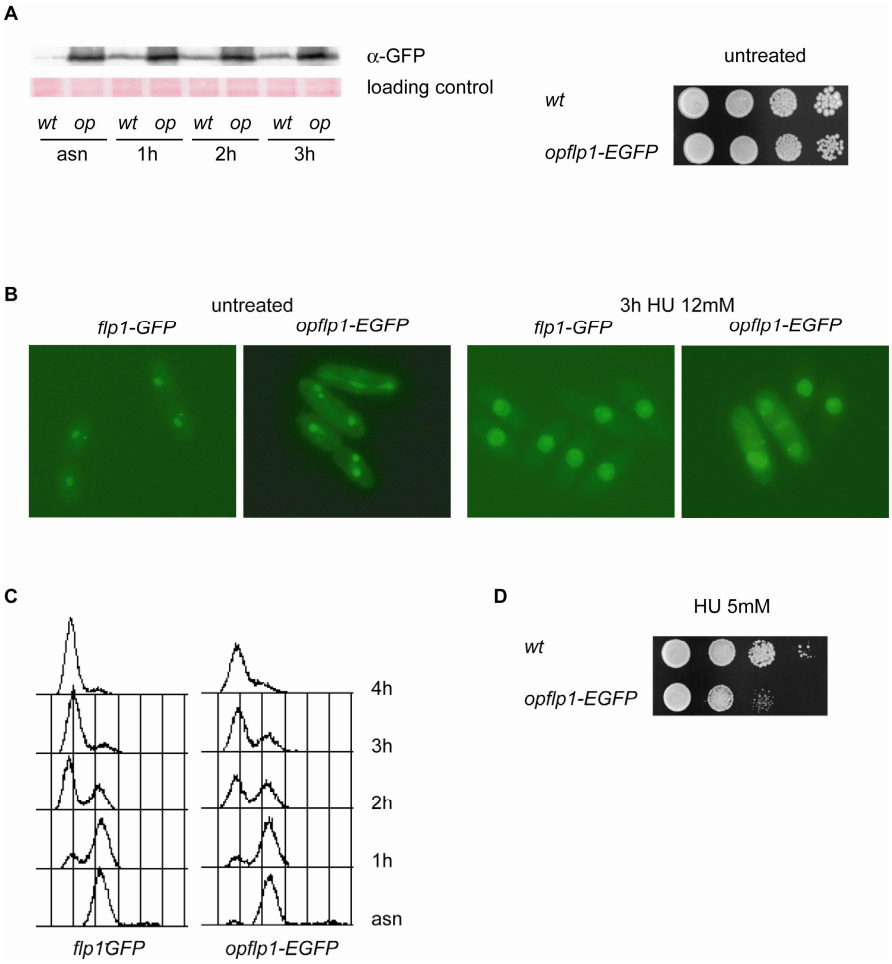

Figure 22. **Effect of the moderate over-expression of *flp1***

(A) A moderate increase in Flp1p protein levels was achieved by expression of *flp1* under its own promoter in a *Δflp1* strain transformed with a pREP41 plasmid in which 1200bp of the intergenic region ahead *flp1* substituted for the *nmt1* promoter (*opflp1*). This increase in protein levels does not imply loss of viability in rich medium. (B) *opflp1* presented normal interphase and mitotic localizations of Flp1p in cyclin cells, although the protein seemed to accumulate differentially to a low extent in the cytoplasm and more importantly in the SPB. Upon replication stress release of Flp1p form the nucleolus occurred in *opflp1* but cycling cells and aberrant mitosis could be detected. (C) FACS analysis revealed retardation in checkpoint block in *opflp1* cells as well as incremented population between 1C and 2C when compared to the non over-expressing *flp1GFP* strain. (D) *opflp1GFP* is sensitive to chronic exposure to HU.

of the tagged protein in response to HU treatment, we found that it was released to the nucleus like endogenously produced Flp1p. However, we observed an abnormal number of cycling cells after three hours of treatment, and the nuclei we detected by Flp1p-EGFP staining pointed to the existence of aberrant mitoses (Figure 22B-C).

We therefore checked the sensitivity of the strain to chronic HU exposure. In a plate assay (in MM to avoid loss of the plasmid) we found that according to the qualitatively observed partial loss of checkpoint block, *opflp1* was more sensitive to different concentrations of HU than the control strain (Figure 22D).

4.6 Adaptation to the checkpoint in *flp1* mutants

In response to replication stress, cells block their progression through cell cycle as a result of checkpoint activation. However, if the source of stress is not

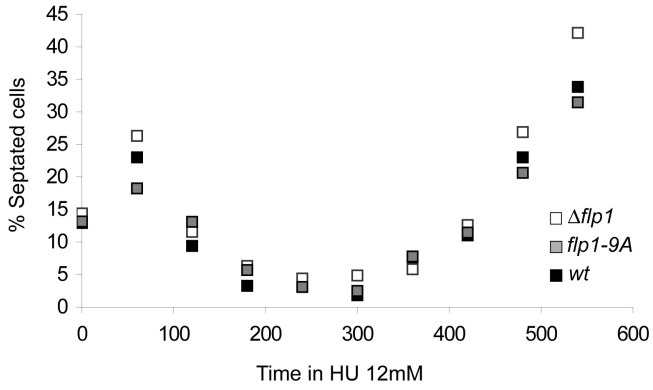

Figure 23. Dynamics of adaptation to HU in *flp1* mutants

Representation of the variation of septation index in *wt* and *flp1* mutants during extended exposure to HU (time in minutes)**.** Asynchronous cultures of *wt*, Δ*flp1* and *flp1-9A* strains were treated with HU 12mM and septation index was determined each hour after treatment for 9 hours. 400 cells were analyzed in each count using dark field microscopy. According to the graphic two regions can be distinguished: before 6 hours of treatment cells are responding to checkpoint signal and septation index sinks, whereas after 6 hours of treatment cells start to adapt to the presence of the drug and override checkpoint block, indicated by an increase in septation index.

removed, in the course of the treatment an adaptation to the new conditions occurs. The checkpoint is progressively deactivated and cells finally enter mitosis. Thus cells undergoing replication stress caused by HU treatment have been reported to re-enter the cell cycle after six hour of exposure to the drug (Sazer and Sherwood, 1990). In order to check if Flp1p could somehow play a role in the processes that regulate checkpoint adaptation, we treated exponential growing cultures of Δ*flp1* and *flp1-9A* and *wt* cells with 12mM HU and monitored the behaviour of the strains in terms of checkpoint block and cell cycle re-entry for 10 hours (Figure 23). During the first hour of treatment the three strains presented an increase in their septation index, most likely due to the asynchrony of the cultures at the initial conditions. As described before, at two hours of treatment the septation index of *flp1* mutants was higher than that of *wt* cells, and was reduced almost to *wt* levels at the four hours time point. After 6 hours of treatment the septation index increased, indicating that cells started to adapt to the new environmental conditions and overrode the checkpoint block. From this point to the 10 hours of treatment the septation index increased in the three strains, indicating that cells accumulated in this stage and did not undergo cytokinesis to progress into a new cell cycle. No remarkable difference could be observed between the kinetics of the *wt* strain and those of *flp1* mutans at this stage, indicating that Flp1p does not play an important role in the regulation of adaptation.

5. STUDY OF THE RELATIONSHIP BETWEEN Flp1p AND OTHER PROTEINS IMPLICATED IN CHECKPOINT RESPONSE TO GENOTOXIC STRESS

5.1 14-3-3 proteins: Rad24p and Rad25p

Release of Flp1p to the nucleus during replication stress depends on Rad24p

14-3-3 *S. pombe* proteins Rad24p and Rad25p are required for proper localization and function of proteins implicated in checkpoint response, like Chk1p and Cdc25p (Chen *et al.*, 1999b; Lopez-Girona *et al.*, 1999; Lopez-Girona *et al.*, 2001b; Dunaway *et al.*, 2005). Furthermore Rad24p and Flp1p have been shown to interact in response to cytokinetic stress (Mishra *et al.*, 2005; Trautmann and McCollum, 2005).

We were therefore interested in finding out if Rad24 was involved in the nuclear accumulation of Flp1p upon DNA stress. With this aim we examined Flp1p-GFP localization in a Δ*rad24* strain (Figure 24A). Nuclear dispersion of Flp1p-GFP relied on a functional *rad24+* wild-type allele, indicating that Rad24p is required for release of the Flp1p phosphatase from the nucleolus in response to replication stress.

Flp1p interacts with 14-3-3 proteins during replication stress

To check if the dependence of Flp1p localization on Rad24p availability could rely on a direct interaction between the phosphatase and 14-3-3 proteins, we performed a pull-down assay for GST-tagged Rad24p in cultures treated with 12mM HU and detected Flp1p-Ha in the samples (Figure 24B). No interaction between Flp1p and Rad24p could be detected in untreated cells, whereas interaction was clearly detected after 1 hour of HU treatment. In a similar experiment we detected that Flp1p and Rad25p also interacted physically.

Flp1p and Rad24p interact genetically

As mentioned before, 14-3-3 protein homologues Rad24p and Rad25p are required for adequate checkpoint response in fission yeast (Ford *et al.*, 1994). In particular, it has been published that Δ*rad24* mutants are defective in the checkpoint response to the DNA replication inhibitor HU at 37ºC but proficient at lower temperatures (Forbes *et al.*, 1998). We combined Δ*rad24* and Δ*flp1* mutations and found that the double mutant was more sensitive to HU than single Δ*rad24* mutants even at 25ºC (Figure 24C). This genetic interaction indicates that deletion of *flp1* enhances the replication stress defect of Δ*rad24* cells and suggests that Flp1p and Rad24p may play certain roles implicated in different branches of the checkpoint response.

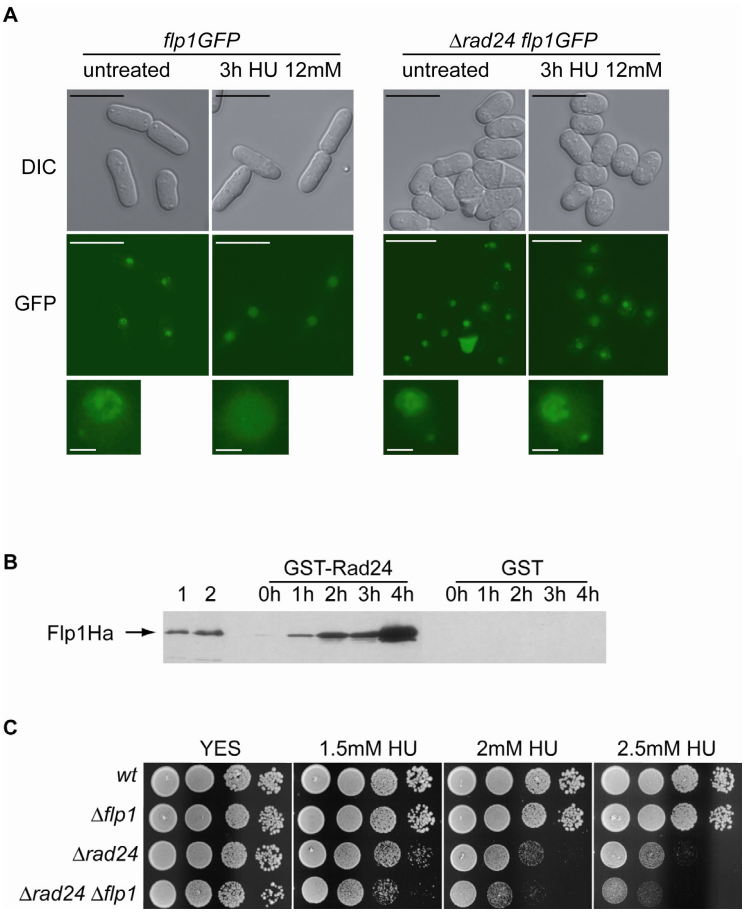

Figure 24. **Interaction of Flp1p with 14-3-3 proteins**

(A) Flp1p is not released to the nucleolus in a Δ*rad24* background. Live imaging of Flp1p-GFP in a strain deleted for *rad24* after 3 hours of 12mM HU treatment. Flp1p remains nucleolar whereas in control cells the staining is nuclear, as previously described. Bars, 10 μm. 3x magnified nuclei are shown in the lower panel. Bars, 1 μm. (B) Rad24p can interact physically with Flp1p *in vivo* during checkpoint response to HU. GST-Rad24p was purified from untreated cells and at different times of 12mM HU treatment. The membrane was incubated with α-Ha antibody in order to detect Flp1pHa. Purified GST was used as a control. In lanes 1 and 2, 10 μg and 20 μg respectively of whole cell protein extracts were included as references. (C) Sensitivity assay of Δ*rad24* and Δ*rad24* Δ*flp1* cells to chronic HU exposure at 25ºC. Δ*rad24* is partially sensitive to HU treatment. Δ*rad24* Δ*flp1* presents a more sensitive phenotype than each simple mutant.

5.2 Dis2p

Dis2p is the phosphatase responsible for Chk1p dephosphorylation to inactivate checkpoint control over cell cycle once DNA-damage has been repaired (den Elzen and O'Connell, 2004). We were interested in checking if Flp1p could in some way interact with Dis2p during genotoxic stress, to uncover a possible role for Flp1p in checkpoint recovery.

Flp1p and Dis2p interact genetically

Due to the role of Dis2p in regulating Chk1p activity, Δ*dis2* strains are hypersensitive to certain concentrations of MMS (den Elzen and O'Connell, 2004). This fact has been interpreted to be a result of an over-activation of Chk1p in cells which lack Dis2p. In a plate assay we compared Δ*dis2,* Δ*flp1* and the double mutant's sensitivities to 0.005% MMS (Figure 25A). At this concentration Δ*dis2* resulted to be starkly sensitive and Δ*flp1* presented a w*t* behaviour. Interestingly, deletion of *flp1* partially rescued Δ*dis2* sensitivity.

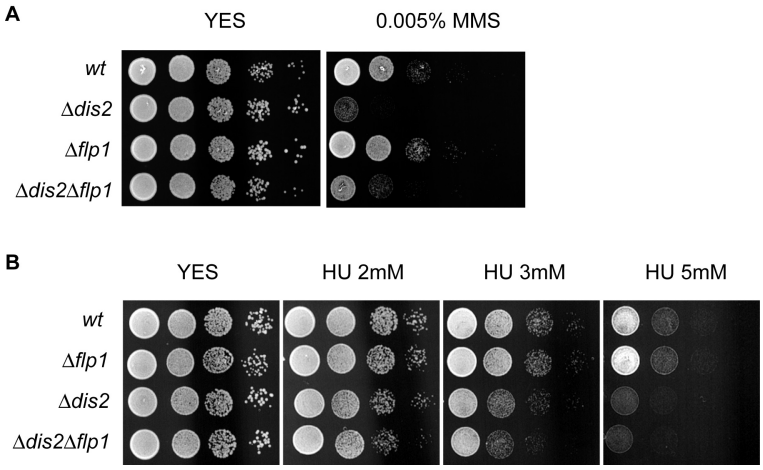

Figure 25. Genetic interaction between *dis2* and *flp1*
(A) Plate assay showing sensitivity of Δ*dis2* and the double mutant Δ*dis2*Δ*flp1* to MMS. Δ*dis2* is markedly sensitive to the concentration of MMS used whereas deletion of *flp1* in this background partially suppresses the loss of viability. (B) Plate assay showing sensitivity of Δ*dis2* and the double mutant Δ*dis2*Δ*flp1* to HU. Δ*dis2* is sensitive to high concentrations of HU. The double mutant displays a similar behaviour.

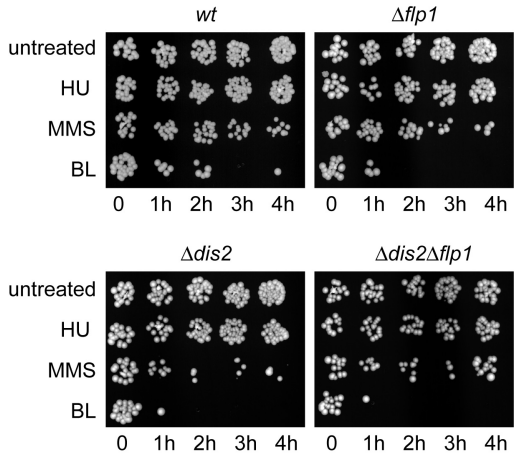

Figure 26. Recovery assay of cells deleted for *dis2* and/or *flp1*
Δ*flp1,* Δ*dis2* and the double mutant Δ*dis2*Δ*flp1* were assayed for their ability to recover from treatment with genotoxic agents. Asynchronously growing cultures of these strains were treated with 12mM HU, 0.033% MMS or 7.5mU BL. Samples were taken after every hour of treatment and 10μm of 1:1000 dilutions were plated on drug-free medium. Plates were incubated at 30ºC for 72h.

Intriguingly, we found that deletion of *dis2* also resulted in sensitivity to HU at certain concentrations (Figure 25B), pointing to a possible role of the phosphatase in the Cds1p branch of the checkpoint response. Under these conditions the double mutant Δ*dis2*Δ*flp1* behaved as the simple Δ*dis2* mutant.

Recovery studies

At sight of the interaction of both genes in the response to chronic drug exposure, we next studied the behaviour of the strains at the recovery stage from drug treatment. *wt*, Δ*dis2,* Δ*flp1* and Δ*dis2*Δ*flp1* cultures were treated with 12mM HU, 0.033% MMS or 7.5mU BL and a fixed number of cells were plated after each hour of treatment on drug-free rich medium plates (Figure 26). Δ*flp1* presented *wt*-like recovery after treatment with HU and seemed to recover slightly worse from BL and from long term exposure to MMS. Δ*dis2*, as expected, clearly showed defective recovery from 2h and longer MMS treatments. Coherently with the results obtained for long-term drug exposure Δ*dis2*Δ*flp1* double mutant recovered better from exposure to MMS than the

single Δ*dis2* mutant especially from an extended 4 hour treatment. Recovery from BL was also impeded in Δ*dis2* and Δ*dis2*Δ*flp1* to a similar extent.

6. ANALYSIS OF THE TRANSCRIPTIONAL RESPONSE TO REPLICATION STRESS IN Δ*flp1*

Gene expression after 90 minutes of 20 mM HU treatment in asynchronous cells deleted for *flp1* was studied using a Yeast 2.0 array from Affimetrix™ and results were generated using as a reference *wt* expression profile (see MATERIALS AND METHODS). We chose this early point of checkpoint block in order to get the first transcriptional wave of checkpoint response minimizing the effects of cell cycle dependent transcription.

APPENDIX 1 contains a classification of the most relevant genes whose expression was repressed or induced at least twofold in Δ*flp1* with respect to the expression profile for the *wt* at this point of treatment. 688 genes were repressed and 466 were induced in Δ*flp1* applying this criterion, from which 230 and 221, respectively, were found to be implicated in protein synthesis and degradation, DNA replication and repair, stress response or meiosis and mitotic cell cycle. Expression profile of genes involved in stress response and DNA repair seems to be specially altered in Δ*flp1*. Among the 30 repressed genes which belong to these categories, 13 genes involved in response to oxidative stress were found, including transcription factors *pap1* and *prr1*, the gene encoding their target *trr1*, 5 genes encoding heat shock proteins and two encoding proteins involved in checkpoint response to genotoxic stress, *rad25* and *cdc18*, whose product in addiction to its role in DNA replication initiation is also implicated in Cds1p activation (Murakami *et al.*, 2002). Among the 43 induced genes, 4 are involved in spindle checkpoint response, 6 in nucleotide excision repair, 2 in ssDNA repair and 9 in recombination including *rad22*, whose product appears in repair loci under replication inhibition when intra S-checkpoint is not active (Meister *et al.*, 2005), *top3* and *eme1* encoding for a endonuclease which together with Mus81p may be implicated in processing collapsed replication fork intermediates (Kai *et al.*, 2005). Regarding genotoxic stress related genes, *chk1*, *wee1* encoding for kinases directly implicated in Cdc2p Tyr15 phospho-regulation and *cid11*, *cid12* and *cid13* were found to be induced. Cid13p, a poly(A) polymerase, targets genes involved in dNTP metabolism, and its over-expression suppresses loss of viability in defective S-M checkpoint under DNA replication inhibition (Read *et al.*, 2002).

Attending to the CESR (Core Environmental Stress Response, see INTRODUCTION), of the 88 induced genes with known function, 16 were found to be down-regulated (*gdp1, ctt1, gpx1* and *rds1*, among others) and 8 were up-regulated (*mpr1/spy1*, among others) in Δ*flp1* with respect to *wt* behaviour. Of the accepted 106 CESR repressed genes, 27 were found to be over-repressed in Δ*flp1.*

Importantly, three components of the MBC known to be induced as a result of the specific stress response to HU (Chu *et al.*, 2007), *cig2*, *cdc22* and *cdc18* resulted to be down-regulated in cells deleted for *flp1* with respect to *wt*.

7. A SYSTEMS BIOLOGY APPROACH TO THE STUDY OF CELL CYCLE AND REPLICATION STRESS AND THE IMPLICATION OF Flp1p IN THE CORRESPONDING SIGNALLING PATHWAYS IN *S. pombe*

In the framework of our investigation, we are currently building a mathematical model for the checkpoint response to replication stress in *S. pombe*. Our goal is to achieve a fitted and validated model, by means of which we intend to better understand the complex interplay among the different components involved in control of cell cycle progression both in unperturbed and stress conditions.

It should be noted that the data here presented are preliminary results of an ongoing project in collaboration with the Computational Systems Biology group of the Max Planck Institute for Molecular genetics (Bsc. Christian Diener, PhD. Matteo Barberis and PhD. Edda Klipp).

7.1 Model development

Our model for the cellular response to replication stress is formed by two different modules. The first module accounts for a model for cell cycle progression in *S. pombe*, and the second supplementary module accounts for checkpoint response to replication stress (Figure 27). This organisation responds to the need for an adequate representation of the cell cycle in unaltered conditions in order to accurately simulate checkpoint block under stress conditions. The two modules can be put together and the whole model can still account for unperturbed cell cycle if the input for checkpoint response, the variable “Replication_stress” is given the value 0.

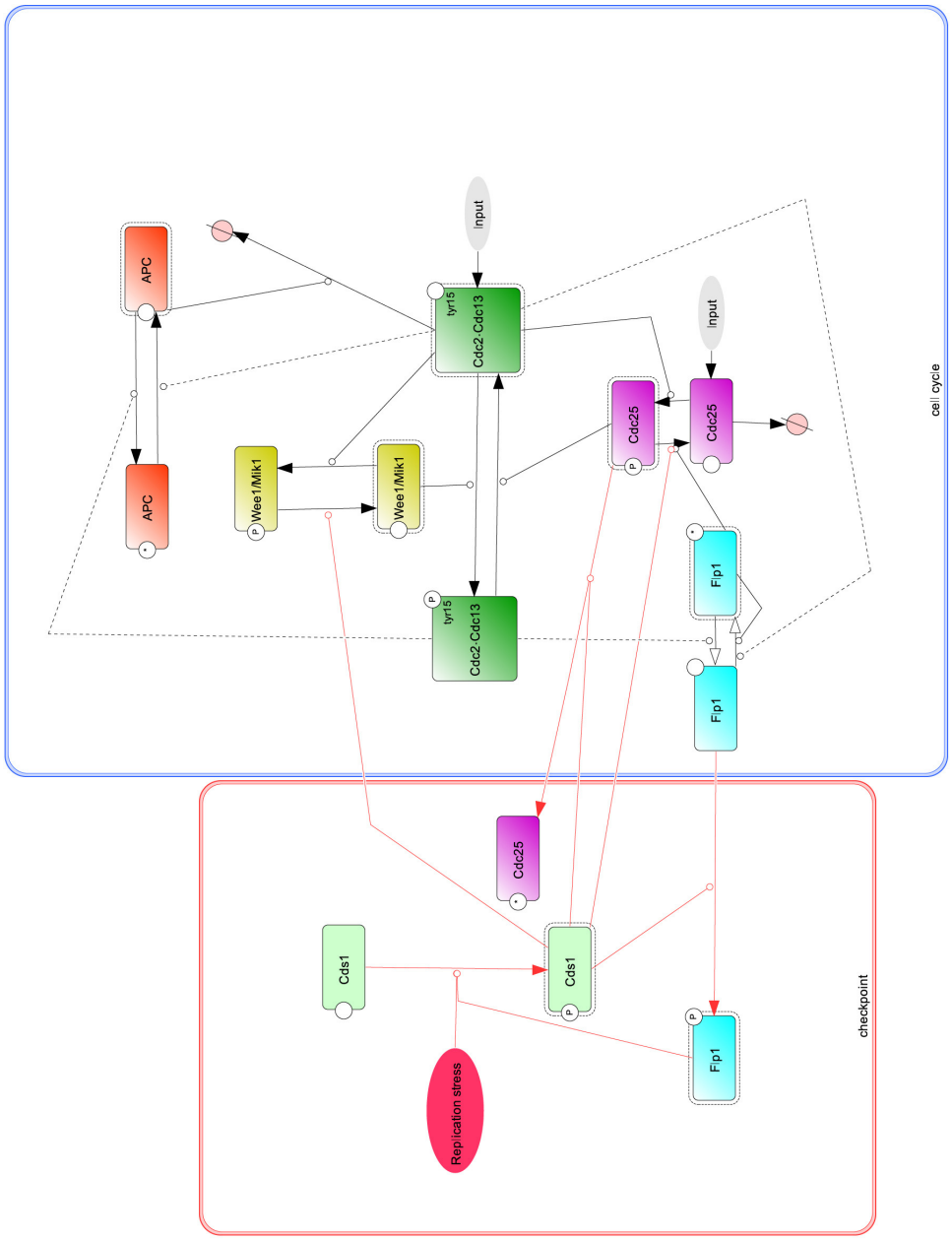
cell cycle
checkpoint
APC
APC
Input
tyr15
Cdc2-Cdc13
Input
Cdc25
Cdc25
Wee1/Mik1
Wee1/Mik1
tyr15
Cdc2-Cdc13
Fip1
Fip1
Cdc25
Cds1
Cds1
Fip1
Replication stress

Figure 27. Global scheme of the mathematical model for checkpoint response to replication stress in *S. pombe*

This diagram shows the species and interactions considered for the mathematical modelling of checkpoint response to replication stress. For a detailed description of model assumptions see text.

The model is composed of two modules: an independent model for cell cycle progression (blue box) and a sub-module for the checkpoint response (red box). Active species are highlighted by an additional dot box. Reactions specific of checkpoint response are marked by red lines. Dot lines indicate the action of the complex Cdc13p-Cdc2p in reactions that are not directly driven by the kinase but are specific of the cell cycle stage. Arrows indicate conversion of one species into another, and circular heads indicate the action of a modifier. Ø indicates degradation. Regarding protein modifications P stands for phosphorylation and a point stands for an undefined modification.

In the model, cell cycle progression is driven by the kinase activity of the Cdc13p-Cdc2p complex. Kinase activity is inhibited by Wee1p/Mik1p and by timely degradation of Cdc13p from the active complex Cdc13p-Cdc2p by APC. Kinase activity is enhanced by the phosphatase Cdc25p and by the synthesis of the cyclin Cdc13p. Active Cdc13p-Cdc2p complex promotes its own activation by inactivating Wee1p/Mik1p and activating Cdc25p. Cdc25p is in its turn inactivated by activated Flp1p. The inactive form of Cdc25p is thus targeted for degradation. Flp1p is activated dependently on the cell cycle stage and its own phosphatase activity. APC activation is also cell cycle driven. Synthesis of degraded species is considered.

In the checkpoint module only active if the species “Replication_stress” > 0, replication stress triggers Cds1p activation. Cds1p acts activating Wee1p/Mik1p and turning Cdc25p into an inactive, non-degradable form. It also triggers accumulation of the checkpoint active form of Flp1p that in turn drives further activation of Cds1p.

Model assumptions for the cell cycle

As stated before, in order to correctly simulate checkpoint response and therefore cell cycle block in response to replication stress we needed a model for the cell cycle that could autonomously drive progression through all cycle stages. Self-regulation of the system is of special importance for our approach since external orders to drive cell cycle progression would interfere with any attempt of stopping cell cycle by means of checkpoint response. Since all published cell cycle models for *S. pombe* include switches in model parameters to regulate cell cycle progression (Novak *et al.*, 1998; Sveiczer *et al.*, 2000), the construction of an improved cell cycle model was required.

Our main goal when modelling the cell cycle was thus to achieve a self-regulated system capable of accurately reproducing the oscillations of Cdc2p kinase activity and of all other model components.

Figure 27 shows the scheme of all species and interactions included in our cell cycle model. This scheme was built on the basis of the state of the art knowledge about regulation of cell cycle progression in fission yeast, specified in INTRODUCTION. The model scheme contains the main cell cycle regulators and definitively those implied in Cdc2p activity regulation also during checkpoint response. On the other hand, the model has been kept as simple as possible so that the mathematical description of the system does not require too many parameters to favour an adequate posterior fit to experimental data. The following assumptions were made to achieve a simple but still functional model:

The trigger of cell cycle progression is the activity of the Cdc2p-Cdc13p complex over time. Cdc2p-Cdc13p is thus the only CDK-cyclin complex considered. This assumption has been made on the basis that Cdc13p is the only essential cyclin in *S. pombe*. On the other hand checkpoint effects have been shown to play a major role in regulation of the mitotic CDK complexes.

The effect of the CKI Rum1p on Cdc13p-Cdc2p inactivation has been lumped in the APC mediated degradation of Cdc13p.

Cdc13p is considered to be the limiting species for the formation of the Cdc2p-Cdc13p complex. This is logical considering that the cyclin is regulated by periodic expression and degradation. According to this, in the cell cycle fits the concentration of the Cdc2p-Cdc13p is considered to be equal to that of the detected Cdc13p.

A single species accounts for both Cdc2p kinase inhibitors Wee1p and Mik1p.

Synthesis is considered for the two species that get degraded as a consequence of cell cycle progression, that is, the active form of the Cdc2p-Cdc13p complex (because of Cdc13p degradation) and the inactive form of Cdc25p. Synthesis has been assumed to follow saturation kinetics, that is, a maximal concentration of the species can not be trespassed, even under checkpoint block.

Species that are cell cycle regulated but whose regulators are unknown or not part of the scheme (APC and Flp1p) achieve their balances through the action of the cell cycle trigger itself.

Flp1p is activated during mitosis (when Cdc13p-Cdc2p activity is high) dependently on its own phosphatase activity.

Model assumptions for the checkpoint

The checkpoint module is also shown and explained in Figure 27. Checkpoint response to replication stress is modelled primarily as the action of the checkpoint kinase Cds1p on cell cycle block. However, we also intend to obtain some information about the role of the kinase in fork stabilization (see DISCUSSION). The following assumptions were made when modelling the checkpoint module:

The model accounts only for the stages of checkpoint activation. Since the mechanisms of adaptation and recovery are poorly understood, no reactions for checkpoint inactivation are included in this first approach. Therefore, for parameter fit only points up to 180 minutes of HU treatment are used. Consequently, simulations should not be run in time courses longer than 180 minutes.

Cds1p is activated by checkpoint response. No synthesis or degradation of Cds1p is considered as a first approach.

Cds1p drives inactivation of Cdc25p turning it into an inactive, non-degradable form.

A module for the action of Flp1p in the checkpoint has been included, based on our interpretation of the experimental results for the role of the phosphatase in response to replication stress (see section 2. and Figure D1 in DISCUSSION).

7.2 Mathematical structure of the model

The mathematical construction of the model was based in the biological structure depicted in Figure 27 and on the above mentioned model assumptions. The complete model for cell cycle and checkpoint response consists of 15 species, 17 reactions and 23 parameters, as specified in Table 1. The set of differential equations accounting for all kinetics and for the complete mathematical description of the system can be found in APPENDIX 2.

Name	Reaction	Kinetics	Modifiers	Parameters
				Kinput
				Kconc_max
rCdc2_input	-> Cdc2_on	S		Cdc2_tot
rCdc2_deg	Cdc2_on ->	MA	APC_on	Kcdc2_deg
rCdc2_on	Cdc2_off -> Cdc2_on	MA	Cdc25_on	Kcdc2_on
rCdc2_off	Cdc2_on -> Cdc2_off	MA	Wee1_on	Kcdc2_off
				Kinput
				Kconc_max
rCdc25_input	-> Cdc25_off	S		Cdc25_tot
rCdc25_deg	Cdc25_off ->	MA		Kcdc25_deg
				Kcdc25_on
rCdc25_on	Cdc25_off -> Cdc25_on	MM	Cdc2_on	Jcdc25_on
				Kcdc25_off
rCdc25_off	Cdc25_on -> Cdc25_off	MM	Flp1_on	Jcdc25_off
rCdc25_check	Cdc25_on -> Cdc25_checkpoint	MA	Cds1_on	Kcds1_cdc25
				Kwee1_on
				Jwee1_on
rWee1_on	Wee1_off -> Wee1_on	MM	Cds1_on	Kcds1_wee1
				Kwee1_off
rWee_off	Wee1_on -> Wee1_off	MM	Cdc2_on	Jwee1_off
rAPC_on	APC_off -> APC_on	MA	Cdc2_on	Kapc
rAPC_off	APC_on -> APC_off	MA	Cdc2_off	Kapc
			Cdc2_on	
rFlp1_on	Flp1_off -> Flp1_on	MA	Flp1_on	Kflp1
rFlp1_off	Flp1_on -> Flp1_off	MA	Cdc2_off	Kflp1
rFlp1_check	Flp1_off -> Flp1_checkpoint	MA	Cds1_on	Kcds1_flp1
			Replication_stress	Krs
rCds1_on	Cds1_off -> Cds1_on	MA	Flp1_checkpoint	Kflp1_cds1

Table 1. **Model reactions**

Set of reactions describing the model. Reactions where no substrate has been specified represent synthesis and reactions with no product represent degradation. The column Kinetics stands for the type of kinetic written for each reaction: MM = Michaelis Menten, MA = Mass Action, S = Saturation. A list of the species that catalyze each process (modifiers) and the parameters involved in each reaction has been included.

Species	Concentration (μM)		Parameter	Value
Cdc25_off	0.4810	0.4114	Kcdc2_on	10.4652
Cdc25_on	0.3020	0.8063	Kcdc2_off	36.0696
Cdc2_on	0.3128	0.4210	Kcdc2_deg	0.1571
Cdc2_off	2.0709	1.5500	Kinput	0.0287
Wee1_on	0.5812	0.8593	Kcdc25_on	456.8510
Wee1_off	0.0652	0.1407	Kcdc25_off	4331.51
APC_on	0.0695	0.1070	Kcdc25_deg	0.0502
APC_off	0.4602	0.3930	Kwee1_on	0.1070
Cds1_off	7.463	7.463	Kwee1_off	0.2269
Cds1_on	0	0	Kapc	187.4180
Flp1_off	3.8531	0	Kflp1	0.5560
Flp1_on	1.3409	0	Krs	0.0134
Flp1_check	0	0	Jcdc25_on	103.7280
Cdc25_check	0	0	Jcdc25_off	4661.9000
Replication_stress	0 / 0.5	0 / 0.5	Jwee1_on	0.0383
			Jwee1_off	0.0035
			Kconc_max	10.2600
			Kflp1_cds1	4.1020
			Kcds1_wee1	0.0086
			Kcds1_cdc25	68.5300
			Kcds1_flp1	0.0090

Table 2. **Initial concentrations and parameter values of the fitted model**
Concentrations are expressed in μM. Parameters have different units depending on the order of the reaction in which they are involved (concentration unit μM, time unit min). Values in green are parameters fitted using cell cycle data for Δ*flp1*, values in blue are parameters fitted using cell cycle data for *wt*, and values in red were fitted using checkpoint data of *wt*.

Parameter Fit

Three sequential fits of parameters were performed, in order to maximize the experimental input for the election of parameters and initial concentrations: fit of ∆*flp1* in cell cycle progression, fit of *wt* in cell cycle progression and fit of *wt* in checkpoint response. For the cell cycle fits, we used published data generated in our group (concentrations of total Cdc25p, of active Cdc25p, of total Cdc13p, and Cdc2p activity) (Esteban *et al.*, 2004), and checkpoint fits correspond to data generated in this study (concentration of total Cdc25p, of inactive Cdc2p and active Cds1p). An explanation about the proceeding for experimental data processing and fit can be found in MATERIALS AND METHODS. The set of fitted parameters and initial concentrations that account for the fitted model can be seen in Table 2. Figure 28 shows the correlation between experimental data and the corresponding simulated behaviour of the system using the chosen parameter set. This set accounted for reasonably accurate profiles for all fitted variables but for Cdc25p total amount during cell cycle progression. We were not able to find a parameter set that could better reproduce this variation in Cdc25p levels, indicating that the biological/mathematical description used for Cdc25p accumulation and degradation in this model structure is inaccurate (see DISCUSSION).

7.3 Simulation of cell cycle and checkpoint response to replication stress

Simulations were run to check the behaviour of the non-fitted species. As shown in Figure 29, the curves for Wee1p/Mik1p and APC during cell cycle progression account for the documented experimental behaviour both for *wt* and ∆*flp1*. The model is also able to reproduce Flp1p dynamics of nuclear sequestration and release (note however that we are considering the active and inactive species of Flp1p and that the simulated activation of Flp1p is slightly advanced in mitosis).

Another not trivial output of the cell cycle model is the achievement of periodic, stable oscillations of the involved species accounting for the ability of the system to reproduce cell proliferation (progression through numerous cell cycles).

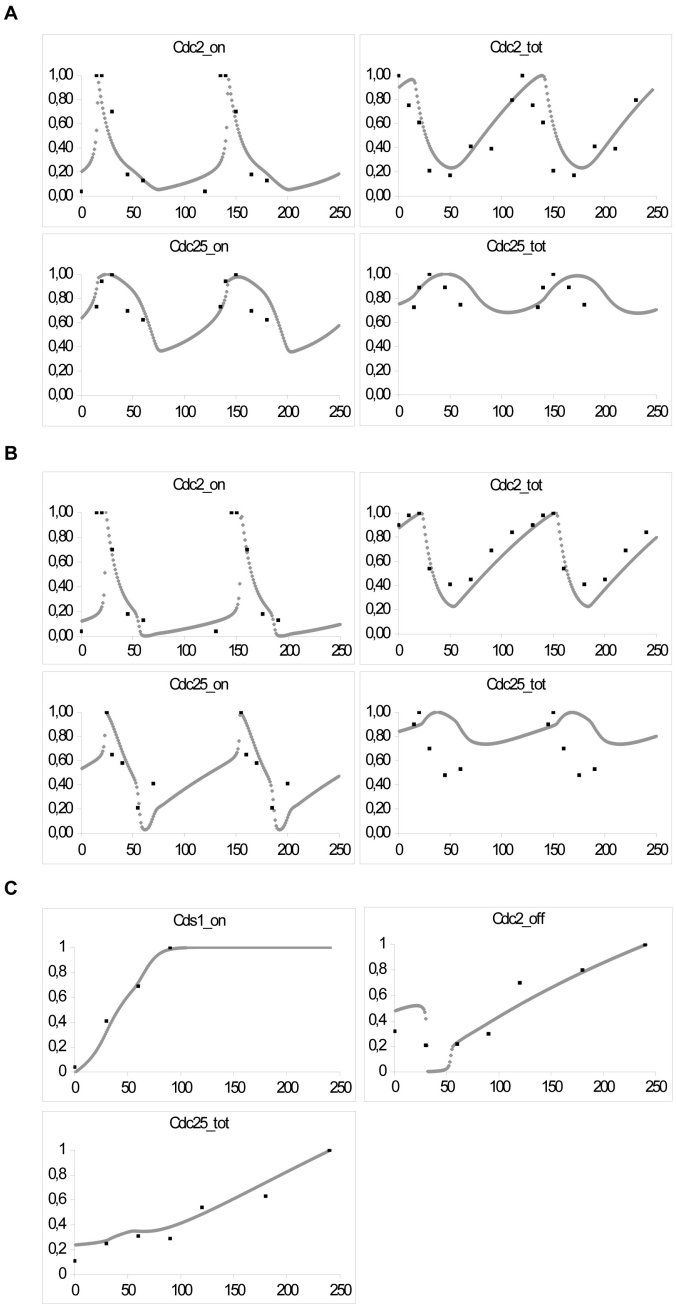

Figure 28. **Simulated results for the fitted model *vs* experimental data points**

The dynamic behaviour of the model species (grey lines) were compared to the experimental data points to which they were fitted (black dots). (A) Plot for Δ*flp1* (Flp1p species = 0) in unaltered cell cycle (Replication stress = 0). (B) Plot for *wt* in unaltered cell cycle (Replication stress = 0). (C) Checkpoint response in *wt* (Replication stress = 0.5)

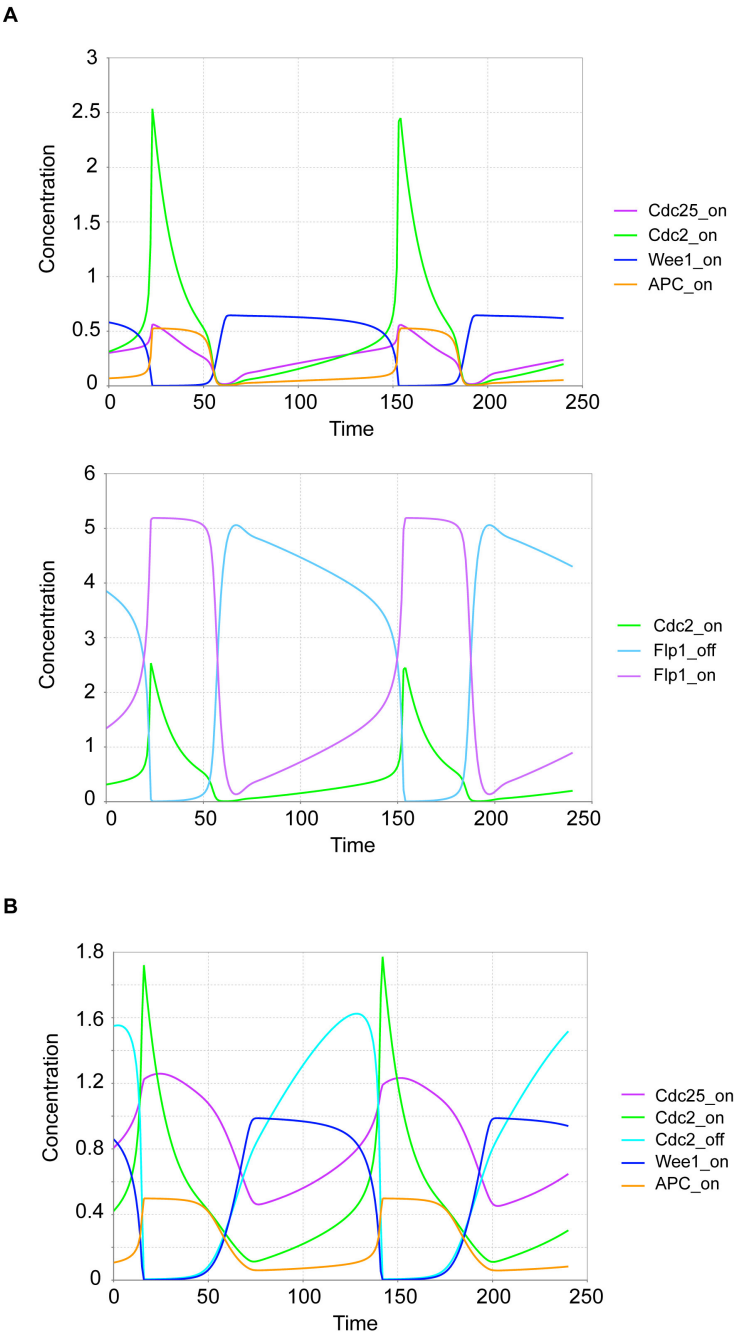

Figure 29. Simulation of cell cycle progression

Simulation of the time courses for specified species in *wt* (A) and Δ*flp1* (B)

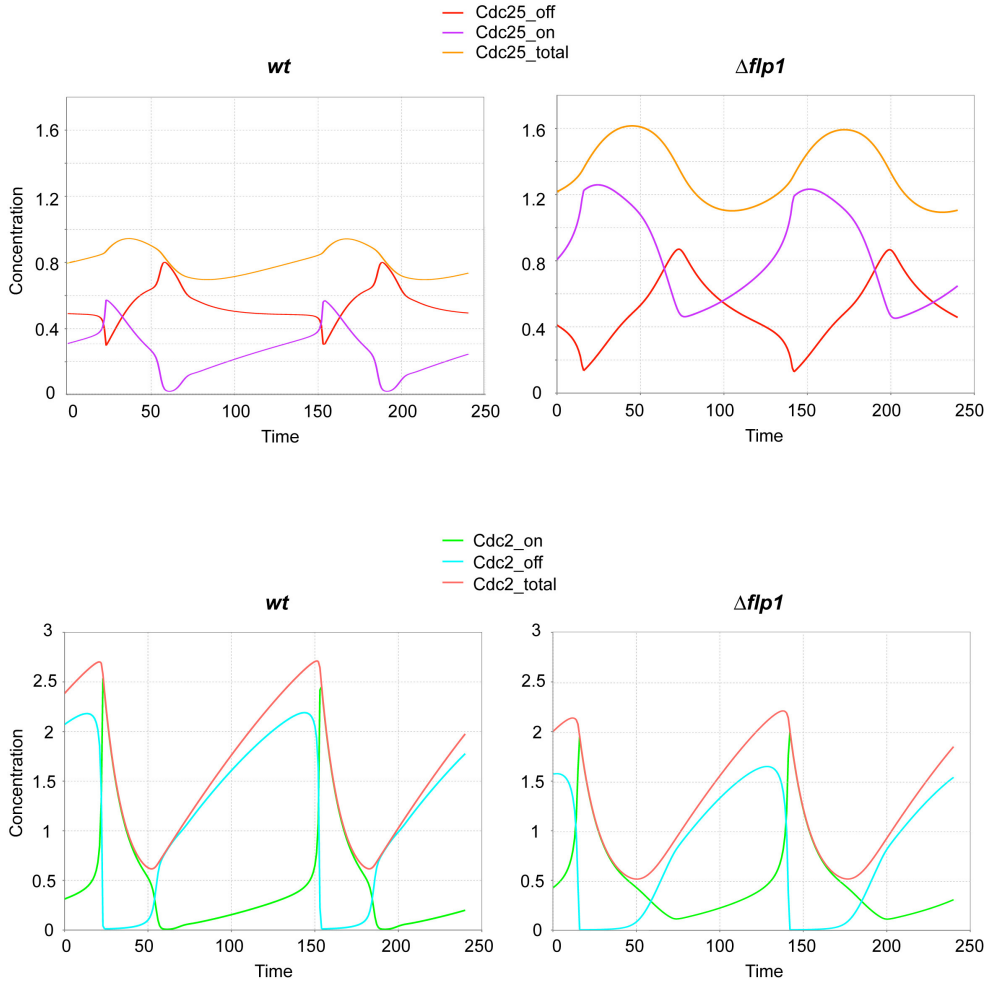

Figure 30. **Comparison of Cdc25p and Cdc2p profiles in wt and Δ*flp1***
The model in its current state is able to account for experimental observations. Cdc25p basal levels are higher in Δ*flp1* and this mutant presents altered profiles of Cdc25p activation and inactivation with respect to *wt*. On the other hand, a higher basal level of active Cdc2p (time 0 of the simulation, corresponding to G2 could be considered as the model state that could better describe the characteristics of an asynchronous population) and inefficient down-regulation of the kinase at mitotic exit are observed in Δ*flp1*.

Furthermore, comparison of *wt* and Δ*flp1* simulations (fitted independently for initial concentrations) reveals higher concentration of Cdc25p and deficient down-regulation of the active form in Δ*flp1* together with inefficient down-regulation of the Cdc13p-Cdc2p active complex in this mutant (Figure 30).

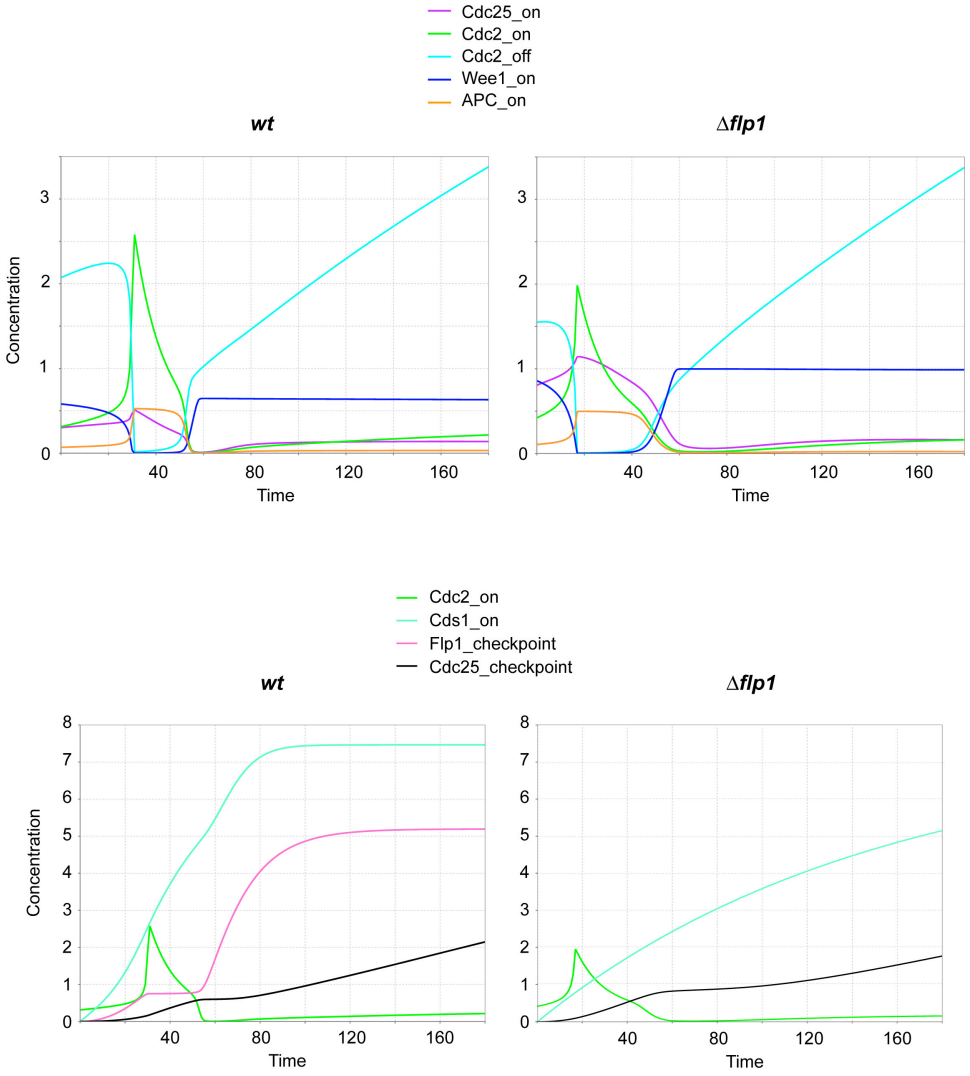

Figure 31. Simulation of checkpoint response
Simulation of the time courses for the specified species in *wt* and Δ*flp1*

On the other hand, when turning the input “Replication_stress” on, we could observe the action of the checkpoint sub-module in stopping cell cycle progression. The model accounts for the down-regulation of active Cdc2p and Cdc25p and up-regulation of the active Wee1p/Mik1p species (Figure 31). An important outcome of the model is its ability to simulate a smooth curve for Cds1p activity in the Δ*flp1* mutant in contrast to the almost switch like response observed in *wt*. Thus even with the same amount of the checkpoint kinase in the system (no input for Cds1p synthesis during checkpoint

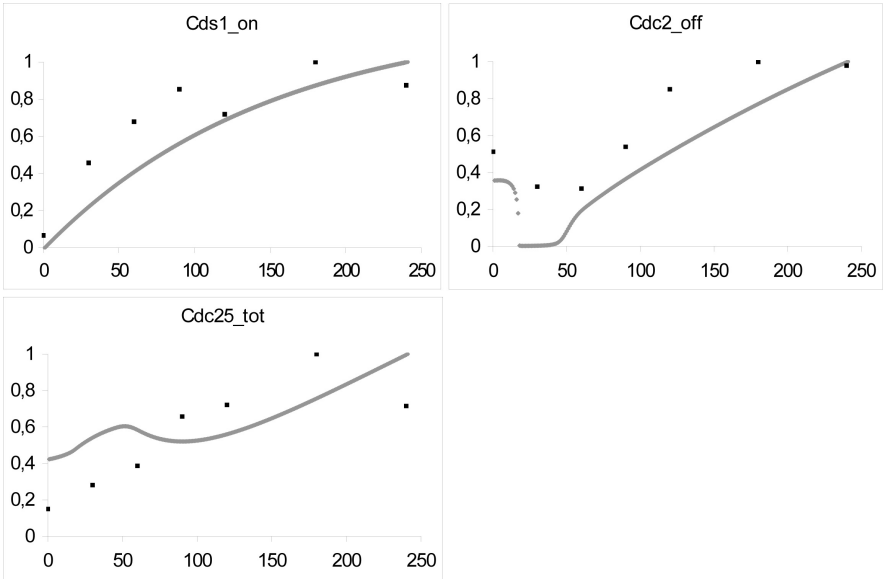

Figure 32. **Model validation for checkpoint response in *Δflp1***
We used the comparison between simulated behaviour and experimental data points for checkpoint response in Δ*flp1* (not used in parameter fit) as a validation for the fitted model. As previously stated at sight of the quality of the fits for the cell cycle, this validation points to a defect in model description for Cdc25p regulation.

response was considered in this first approach), we could observe slower and weakened activation of Cds1p in cell lacking Flp1p.

In addition to the study of the simulated qualitative behaviour of non fitted species, we used experimental data points for Δ*flp1* under replication stress for validation (Figure 32). Once again the model is able to reproduce accurately enough the behaviour of Cdc2p inactivation and Cds1p activation, but not the dynamics of Cdc25p accumulation in this mutant.

We are currently building an improved model, in order to better reproduce the experimental and documented profiles of cell cycle progression and checkpoint response, concentrating mainly in the regulation of Cdc25p. With this validated model we intend to reach the prediction stage, so that by means system manipulation and mathematical analyses we will be able to test, for instance, the contribution of the different species and reactions to the stability of periodic oscillation in the case of cell cycle progression or to the robustness of checkpoint response under stress

conditions. See DISCUSSION for an insight into the new model structure and some of the data we intend to achieve by means of the validated model.

DISCUSSION

In the present work we have explored by means of different approaches the consequences of mutating *S. pombe* Cdc14-like phosphatase Flp1p in checkpoint response to genotoxic stress.

In the course of an unperturbed cell cycle, Flp1p antagonizes mitotic CDK activity by promoting phosphorylation of the conserved tyrosine 15 residue of Cdc2p by dephosphorylating and, thus, down-regulating the Cdc2p Tyr15 phosphatase Cdc25p (Esteban *et al.*, 2004; Wolfe and Gould, 2004). Cdc25p is also a regulated target of the checkpoint cascade activated by genotoxic stress (Lopez-Girona *et al.*, 1999; Lopez-Girona *et al.*, 2001b). Thus, a role of Flp1p in regulating retardation of cell cycle progression in response to DNA-damage or replication stress seemed reasonable. However, according to our results, deletion of *flp1* does not significantly affect Cdc2p Tyr15 phosphorylation in response to genotoxic stress. Cdc2p becomes hyperphosphorylated on tyrosine 15 upon HU, MMS or UV light treatments (O'Connell *et al.*, 1997; Chu *et al.*, 2007 and this work). In this context, it is surprising that Flp1p, the phosphatase that reverts phosphorylation events on Cdc25p downregulating its activity as cells exit from mitosis, does not appear to exert a similar control under genotoxic stress.

The results of our study indicate that checkpoint-related events control Flp1p localization and levels upon genotoxic stress. Importantly, they clearly reveal a close interplay between Flp1p and the main effector of the checkpoint cascade response to replication stress, Cds1p. Interestingly, this interplay results in the full activation of the Cds1p checkpoint kinase. Flp1p has also been shown to interact physically or genetically with other proteins involved in checkpoint signalling upon different types of DNA-stress. In addition, alteration of Flp1p levels or localization results in deregulation of checkpoint response in different aspects including loss of efficiency in checkpoint block and appearance of unscheduled recombination events.

On the other hand, according to our preliminary gene expression studies, deletion of *flp1* results in a strong alteration of the checkpoint associated transcriptional response to genotoxic stress.

1. Flp1p LOCALIZATION DURING GENOTOXIC STRESS

During mitotic cell cycle, Flp1p localizes to the nucleolus and SPB during interphase and to the nucleus, spindle and medial ring during mitosis (Cueille *et al.*, 2001; Trautmann *et al.*, 2001).

Here we have shown that Flp1p is released to the nucleus to a higher or lower extent in cells undergoing genotoxic stress, even if checkpoint blocked cells remain at cell cycle stages at which Flp1p is normally located in the nucleus. This change of location does not occur in a Δ*rad3* strain, indicating that Flp1p changes its subcellular localization in a checkpoint dependent manner. Flp1p nuclear accumulation during genotoxic stress is also abolished in Δ*rad24* mutants, pointing to a role of the 14-3-3 protein in the transport of the phosphatase. However, it must be noted that deletion of *rad24* affects multiple cellular processes (Δ*rad24* cells present an *orb* morphology as well as mislocalization of proteins involved in cell cycle and checkpoint control) so the alteration of Flp1p localization in this strain could just be a consequence of an altered cellular environment.

Interestingly, whereas the cellular mechanism by which Flp1p is released to the nucleus at mitotic entry during an unperturbed cell cycle remains to be clarified (Chen *et al.*, 2006), our results show that under replication stress Cds1p triggers nuclear accumulation of the fission yeast Cdc14p phosphatase homologue: First, Flp1p does not localize to the nucleus during HU treatment in a Δ*cds1* strain and second, mutation of the *in vitro* phosphorylation sites for Cds1p on *flp1* abolishes the release of the phosphatase to nucleus specifically during checkpoint response. Further supporting the role of Cds1p in releasing Flp1p to the nucleus by direct phosphorylation, we could also detect Cds1p-Flp1p physical interaction during checkpoint response.

According to our results and since Cds1p seems to be present to a higher or lesser extent in the whole cell (Brondello *et al.*, 1999; Matsuyama *et al.*, 2006), the phosphorylation of Flp1p by the phosphatase may take place in the nucleolus. Alternatively, Cds1p phosphorylation could be required for the retention of Flp1p in the nucleus once released. The precise spatio-temporal determination of Cds1p action over Flp1p should be addressed in future studies.

During MMS and BL treatment the localization of Flp1p in *Δcds1* cells seems to be similar to that of *wt,* probably because the checkpoint response in these cases is mainly independent of Cds1p when Chk1p is active. However, Flp1p seems to be

strongly released to the nucleus in *chk1 flp1-GFP* both in MMS and BL resembling Flp1p localization during HU treatment in a *flp1-GFP* strain. Since Cds1p is also activated in response to MMS treatment, these results may further point to a relationship between Flp1p nuclear localization and the Cds1p branch of the checkpoint.

Flp1p in the nucleus during genotoxic stress

In *S. cerevisiae*, checkpoint response to DNA-damage involves activation of both response pathways, involving Chk1p and Rad53p respectively, which results in inhibition of both FEAR and MEN networks. This results in retention of ScCdc14p in the nucleolus during checkpoint activation (Liang and Wang, 2007). Our study proves that in *S. pombe* checkpoint response to DNA-damage leads to the release of Flp1p to the nucleus. Since both orthologous phosphatases are implicated in the regulation of mitotic CDK activity, the fact they seem to be regulated in opposite ways by checkpoint response is intriguing. However, the predominant nucleolar localization of Flp1p and its degradation during MMS treatment could indicate that checkpoint response in *S. pombe* acts to prevent Flp1p activity when DNA damage is detected just like the *S. cerevisiae* counterpart, but through a different mechanism.

Studies in *S. cerevisiae* have shown that ScCdc14p sequestration in the nucleolus during S-phase may be necessary to allow for the adequate kinase-associated events required for correct DNA replication. When artificially released to the nucleus ScCdc14p is able to dephosphorylate replication factors Sld2p and Dpb2p, which are phosphorylated by Clb5-CDK during S-phase to guarantee recruitment of polymerases to origins of replication. In this way unscheduled Cdc14p release from the nucleolus in S-phase in the absence of cyclin Clb5p prevents the completion of DNA replication (Bloom and Cross, 2007). In this study we have proven that the accumulation of Flp1p in the nucleus in S phase is a checkpoint specific event, and seems to be dependent not only on Cds1p presence but also on its activation. On the other hand we proved by synchronisation in G1 and release into cell cycle progression that the phosphatase is restricted to the nucleolus at these stages in an unperturbed environment. At sight of these results and the abovementioned observations in *S. cerevisiae* it is tempting to speculate that Flp1p could be released to the nucleus during replication stress to inhibit the replication machinery by counterbalancing CDK S-phase activities.

Our results show that *Δflp1* and *flp1-9A* present the same phenotypes of enhanced Rad22p foci appearance, modest checkpoint block defect and reduced Cds1p activation upon replication stress. This indicates that these defects are derived from the absence of the phosphatase in the nucleus. The fact that *flp1-9A* presents reduced Cds1p activation as *Δflp1* proves that Flp1p release from the nucleolus is a key event in the (auto-) control of checkpoint kinase activity during replication stress. The defectiveness of checkpoint block and Rad22p foci appearance in *flp1* mutants may well be consequences of reduced Cds1p activity. However, expression of genes involved in recombination and other aspects of checkpoint response is enhanced in a *Δflp1* strain, so a direct role of nuclear Flp1p in regulating transcriptional response to replication stress can not be ruled out.

2. INTERPLAY BETWEEN Cds1p AND Flp1p: A MECHANISM FOR FULL ACTIVATION OF CHECKPOINT RESPONSE TO REPLICATION STRESS

The results presented in this study relate Flp1p to the main effector of checkpoint response to replication stress, Cds1p. Interestingly our study evidences both an action of Cds1p over Flp1p and of Flp1p over Cds1p during checkpoint response to replication stress.

According to our observations Cds1p would act over Flp1p to regulate its localization, stability and phosphatase activity: (1) Flp1p is not released to the nucleus upon replication stress in a Δ*cds1* background. This change of localization is also abolished if the replication stress source does not trigger sufficient Cds1p activation, as observed upon conditional inactivation of *cdc17*. (2) Checkpoint activated Cds1p phosphorylates Flp1p *in vitro*. This phosphorylation does most likely also occur *in vivo* to trigger Flp1p release to the nucleus during replication stress, since mutation of all putative Cds1p phosphorylation sites on Flp1p (which disrupts Flp1p phosphorylation by the kinase *in vitro*) leads to specific abolishment of Flp1p change of localization upon checkpoint activation. (3) Phosphorylation of Flp1p by Cds1p *in vitro* leads to an enhancement of its phosphatase activity. Our preliminary *in vivo* studies show that Flp1p phosphatase activity increases after 2 hours of HU treatment, further pointing to a relationship between phosphorylation, localization and phosphatase activity enhancement. (4) Degradation of the phosphatase during MMS treatment is abolished

in Δ*cds1* background. This observation points to a dependence of Flp1p nuclear localization and degradation.

Flp1p in turn, would directly or indirectly regulate the levels and activity of the checkpoint kinase. (1) Δ*flp1* cells present lower protein levels of Cds1p than the *wt* upon replication stress. (2) In a Δ*flp1* background Cds1p presents lower kinase activity than in *wt* cells, both upon HU and MMS activation.

Regarding the timing of Flp1p-Cds1p interactions, the fact that disruption of Cds1p action over Flp1p in the *flp1-9A* mutant leads to the same checkpoint defects than deletion of *flp1* indicates that the influence of Flp1p on Cds1p activation and levels is dependent on a previous activator step of the kinase over the phosphatase.

We have shown that deletion of *flp1* leads to two different defects on checkpoint response. First, we could observe the appearance of recombination foci during replication stress in Δ*flp1* and second, a modest percentage of Δ*flp1* cells override checkpoint block and progress into mitosis presenting aberrant nuclei. These two kinds of defects could be explained by the reduced activity of Cds1p observed in

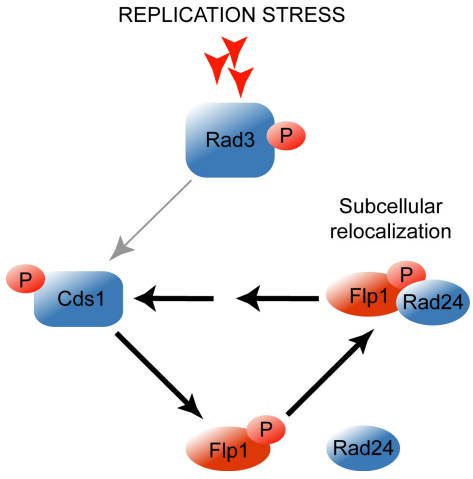

Figure D1. **A model for Flp1p function in the regulation of the replication stress response in fission yeast**

Upon replication stress Cds1p is activated through Rad3p phosphorylation. Active Cds1p phosphorylates Flp1p to regulate its release to the nucleus and its activity. According to our results, Rad24p may be involved in this shuttle mechanism. Nuclear Flp1p would in its turn directly or indirectly regulate full activation of Cds1p in response to replication stress.

Δ*flp1*.

Taken together, all these observations led us to propose the model for the involvement of Flp1p in checkpoint response to replication stress described in Figure D1.

A direct action of Flp1p on Cds1p?

Whether the control of Flp1p over Cds1p can be explained by a direct interaction is still unclear. A direct control is an interesting possibility since, according to our results dephosphorylation of the kinase should then act as an activating mechanism. If the phosphatase can enhance the activation of the kinase by playing a role in the dimerization and autophosphorylation steps of Cds1p activation will be addressed in future studies. Pointing to a direct action of the phosphatase over the kinase, physical interaction between Flp1p and Cds1p could be detected during genotoxic stress. The interaction is better detected in a *flp1*^{CS} background. This can be justified appealing to the transient nature of phosphatase- substrate interactions, indicating that the interaction in this case could certainly occur to dephosphorylate Cds1p. However, it should be kept in mind that this interaction was detected in conditions of over-expression of *flp1* and that Flp1p-Cds1p interaction is weak even in a *flp1*^{CS} background.

On the other hand, elements capable of regulating Cds1p protein levels and Cds1-associated kinase activity may be targets of Flp1p, leading to an indirect regulation of Cds1p by the phosphatase. Proteins implicated in replication and fork stabilization could thus be possible targets of Flp1p during replication stress, since as underscored in the introduction, many of them (Swi1p-Swi3p, Sap1p, Hsk1p, Cft18p, Orc1p Cdc45p, among others) are involved in Cds1p activation under stress conditions. Among the feasible targets for Flp1p indirect action over the checkpoint kinase it would be reasonable to include uncharacterized fission yeast Ssa1p and Ssa2p chaperone homologues (Wood *et al.*, 2002) that may eventually play a role in maintaining Cds1p levels. The study of a possible the role of these chaperones in Cds1p activation during genotoxic stress would be of particular interest in the framework of our investigation since we seem to co-immunoprecipitate Ssa2p with GST-Flp1p.

3. RECOMBINATION RELATED EVENTS IN *flp1* MUTANTS

Rad22p foci formation during an unperturbed cell cycle is indicative of ssDNA appearance and of post-replication repair. The observation that *flp1* mutants do not present more Rad22p foci than the *wt* during vegetative growth indicates that Flp1p is not required for replication or fork stabilization under these conditions. Whereas activation of the replication checkpoint in *wt* cells makes the appearance of Rad22p foci very rare, a considerable number of *Δflp1* and *flp1-9A* cells present multiple recombination foci upon HU treatment. If Rad22p foci appearance under these circumstances was associated to fork collapse, activation of Chk1p should be detected. Contrary to this hypothesis, we could not detect the checkpoint associated mobility shift of Chk1p in HU treated *Δflp1* cells (data not shown).

Appearance of Rad22p foci could also correlate with the checkpoint block defect we observe in a small percentage of *Δflp1* and *flp1-9A* cells. Rad22p and the recombination machinery are normally loaded into nuclear foci immediately as cells are released from replication arrest. In this way, Rad22p foci could appear in cells that override the checkpoint. However, this is not likely to be the explanation for the appearance of foci in *flp1* mutants, since, according to our experiments, the percentage of cells in these strains presenting multiple recombination foci is over two-fold that of cells that override the checkpoint.

The fact that the studied *flp1* mutant strains present an intermediate behaviour between *wt* and *Δcds1* in terms frequency of Rad22p foci appearance, rather correlates with the reduced activation of Cds1p that the phosphatase mutants present. Since we could not detect viability loss in *flp1* mutant strains as a consequence of the unscheduled appearance of recombination foci, an alternative mechanism is likely to override their potential deleterious effects. Identification of such mechanism would aid to further understanding the role of Flp1p in checkpoint response and the functioning of the checkpoint itself.

It should be kept in mind, however, that a delayed activation of Cds1p in *flp1* mutants to checkpoint proficient levels in terms of fork stabilization may be enough to make a putative loss of viability in the early stages of HU treatment undetectable.

4. Flp1p OVER-EXPRESSION AND SPB LOCALIZATION

According to our results moderate over-expression of *flp1* leads to defective checkpoint block and loss of viability in response to replication stress.

Since our previous results involved Flp1p in the timely full activation of Cds1p during replication stress, the fact that moderate over-expression of the protein leads to a partial override of the checkpoint response is intriguing.

In addition, over-expression of *flp1* under stronger promoters has been shown to induce a G2 delay. In this case overexpression of *flp1* leads to excessive Cdc25p down-regulation and cells can not reach the adequate CDK activity levels to induce entry into mitosis. Since checkpoints act to down-regulate CDK activity and prevent mitosis, a cell cycle alteration caused by moderate over-expression of Flp1p would therefore rather contribute to checkpoint arrest than produce further progression into mitosis.

Coherently with the role of Flp1p as an inducer of Cds1p activity, loss of viability in *opflp1* could be explained by an overactivation of the checkpoint. A too tight checkpoint control can lead to loss of viability during sustained exposures to stress, as observed in *Δdis2* cells. However, since we observed that a number of *opflp1* cells override checkpoint control during exposure to HU, the loss of viability in *opflp1* cells is most likely to be a consequence of the unscheduled progression of cells into mitosis with unreplicated DNA.

As underlined in RESULTS, this mutant presents enhanced Flp1p-EGFP signal in the SPB. The mechanisms regulating the different cellular localizations of Flp1p remain unknown. Ectopical expression of Flp1p in this case could be somehow responsible for Flp1p accumulation in the SPB. Many regulators of mitosis and cell division are located to the SPB, among them SIN components (Alfa *et al.*, 1990; Eng *et al.*, 1998; Sohrmann *et al.*, 1998; Cerutti and Simanis, 1999; Mulvihill *et al.*, 1999; Chang and Gould, 2000; Guertin *et al.*, 2000; Hou *et al.*, 2000, among others). It would be interesting to test if the selective accumulation of Flp1p in the SPB could cause an override of checkpoint response through deregulation of some of these components.

5. A POSSIBLE ROLE FOR Flp1p IN RECOVERY FROM CHECKPOINT ARREST?

After checkpoint activation, cells resume cell cycle progression when the source of stress is removed. It has been suggested that the type I phosphatase Dis2p downregulates Chk1p activity during this recovery stage to allow for cell cycle resumption (den Elzen and O'Connell, 2004). The mechanism responsible for Cds1p downregulation remains unclear, although interruption of Rad3p signalling seems to be enough to abolish replication checkpoint response (Martinho *et al.*, 1998). At sight of our first results relating Flp1p to the checkpoint effector Cds1p, we were interest in finding out if Flp1p could play a role in the inhibition of Cds1p activity. We found indeed genetical interaction between Flp1p and Dis2p in MMS. Deletion of *flp1* rescues to some extent the sensibility of *Δdis2* to this drug. Given our later discovery that Flp1p may enhance Cds1p activity rather than inhibit it, and since Cds1p is activated during MMS treatment, this result could reflect the advantage of a partial loss of Cds1p activity when Chk1p is overactivated in checkpoint response. However, the observed recovery of *Δdis2* by *Δflp1* could simply be a result of the own nature of the *Δflp1* strain. *Δflp1* presents high basal levels of Cdc2p activity during mitotic cell cycle. This could counterbalance the deleterious effects of checkpoint over-activation associated to the deletion of *dis2* in response to DNA damage.

According to our results Flp1p is required for the full activation of Cds1p during replication stress and can be phosphorylated by the kinase. This reciprocal interaction between Flp1p and Cds1p resembles that observed between some proteins implicated in checkpoint recovery like Hsk1p or Mcm4p and Cds1p. However, our preliminary work on the matter does not indicate the requirement of Flp1p for survival after replication stress.

In addition, two observations derived form our work speak against a role of Flp1p in recovery from checkpoint block. First, we have identified the functionality of the phosphorylation of Flp1p by Cds1p in triggering the release of the phosphatase from the nucleolus. Furthermore, although we have seen that this phosphorylation activates the phosphatase *in vitro*, the activation *in vivo* seems to be transient, pointing to a role of Flp1p in the early stages of checkpoint response. Second, Flp1p returns to its localization immediately after removal from the source of stress, further pointing to a role of the phosphatase during replication arrest rather than in cell cycle resumption.

6. SPECIFIC TRANSCRIPTIONAL RESPONSE OF Δ*flp1* CELLS TO REPLICATION STRESS

As specified in RESULTS and MATERIALS AND METHODS, we performed a gene expression analysis to uncover the specific transcriptional response of Δ*flp*1 cells to replication stress in terms of up or down regulation of specific genes when compared to the *wt* behavior. It should be noted that all the results here discussed were obtained in a single microarray analysis. We consider this experiment significative, since its outcome correlates with some important aspects of the biochemical and genetical analysis presented in this study. Further investigation of the potential role of Flp1p in regulating transcriptional-related events is being currently carried out in our group.

Analysis of the alteration of the global expression profile in response to HU in Δ*flp1*

Attending to the overall deregulation in gene expression of Δ*flp1* after 90 minutes of HU exposure, we found over 1100 genes whose expression was amplified or reduced at least twofold in this mutant with respect to *wt* behavior. This can be considered as an important deviation in the expression profile of the mutant, pointing to an important role of Flp1p in directly or indirectly controlling gene expression in checkpoint response to replication stress. However it must be kept in mind that, in this analysis, deviation in the gene expression derived of checkpoint response and deviations intrinsic to the mutant's nature are indistinguishable.

Expression of genes involved in stress response is specially altered in Δ*flp1* in our study. 25 genes presented reduced expression (*rad25, pap1, prr1, trr1, cdc48* and *cdc18* among others) and 24 enhanced expression (*chk1, wee1, csn2, top3, eme1, cid11, cid12* and *cid13* among others) with respect to *wt*. The clusters of genes involved in oxidative stress (11 repressed genes), osmotic stress (3 repressed, 4 induced genes) and spindle checkpoint (4 induced genes) responses seem to be highly deregulated in the mutant. Since Flp1p has been proposed to play a role in checkpoint response to oxidative stress, osmotic stress and unassembled spindle, the deregulation observed in genes involved in these responses, like the extensive induction of meiotic genes (77), may be due to the absence of the phosphatase in the

corresponding pathways rather than to a specific transcriptional regulation in checkpoint response to replication stress.

Although our studies of the implication of Flp1p in the response pathways to genotoxic stress have proven that the phosphatase is required to acquire adequate protein levels of Cds1p, no alteration in the expression of this checkpoint kinase was found in this analysis. This is indicative of a post-translational regulation of the protein levels, mechanism that could also account for the modified activity of Cds1p in checkpoint response. However, we did find enhanced expression of *chk1* and genes involved in its signaling pathway (such as *top3* and *dcr1*) and wee1, which can be seen as a compensatory mechanism to the loss of Cds1p in terms of checkpoint block proficiency. Enhancement of expression of genes like *cid13* (whose over-expression has been shown to compensate the hypersensitivity of S-M checkpoint mutants under DNA replication inhibition (Read *et al.*, 2002)) and *rpl1* could on their turn account for suppression of the loss of viability associated to replication checkpoint defectiveness.

19 genes implicated in DNA repair presented enhanced expression in Δ*flp1* (*eme1, rad22, rti1, pol4, rlp1, top3, rev1, nse1, rad16, slx1* and *slx4* among others). DNA damage and instability derived of defective Cds1p checkpoint response in cells deleted for *flp1* could account for this transcriptional effect, as well as for the induction of genes involved in the telomere protection machinery also observed in this assay.

Eme1p is required in mitosis for the processing of stalled or collapsed replication fork intermediates, and Rlp1p (known to work together with Rad22p and Rhp51p) is required for the full extent of DNA recombination and cell survival under condition of a replication fork collapse. Nse1p, Slx1p and Slx4p, are also involved in the processing of collapsed forks and stalled forks recovery. Top3p, which works in the Chk1p branch of checkpoint response, is essential for the processing of aberrant DNA structures that arise in S-phase (Win *et al.*, 2004). The induction of all these proteins could indicate an enhanced rate of fork instability in Δ*flp1*, which also correlates with Cds1p partial loss of function in this mutant. Accordingly, 10 genes involved in recombinational processes were also found to present increased expression. Among them both homologues of *S. cerevisiae rad52, rad22 and rti1/rad22B*, whose products have been shown to interact with each other and with Rhp51p (Rad51p in *S. cerevisiae*) and Rad11p/RPA (Kim *et al.*, 2000; Tsutsui *et al.*, 2001; van den Bosch *et al.*, 2002). Although the expression of *rph51* remained unaffected in our study, expression of *rlp1*, which codifies for a Rad51p like protein that works in the Rhp51p branch, also

resulted enhanced. Rad22p has been shown to appear in repair foci together with Rhp51p when the S-phase checkpoint is not active (Meister *et al.*, 2005). In *S. cerevisiae* RPA inhibits Rad51p binding to recombination sites, due to its high affinity to ssDNA, and Rad52p acts as a mediator protein to help Rad51p binding to ssDNA during homologous recombination. Interestingly RPA codifying gene in *S. pombe*, *rad11*, resulted to be repressed in Δ*flp1*. In this way induction of *rad22* and *rti1* and repression of *rad11* could account for a favoring of Rhp51p function during replication stress in cells deleted for *flp1*. On the other hand, the induction of genes implicated in recombinational processes in cells deleted for *flp1* may indicate that the phosphatase is directly (acting as a transcriptional repressor) or indirectly (through its action in Cds1p) involved in inhibiting recombination. This may explain the need for Flp1p degradation in the course of MMS treatment to allow for DNA repair and its stabilization during replication stress to inhibit detrimental recombinational processes during S-phase block.

Analysis of the modification on expression levels of CESR genes in Δ*flp1*

Global transcriptional response of *wt* cells to HU has been shown to partially overlap with the previously defined Core Environmental Stress Response (CESR) (Chu *et al.*, 2007). According to our results, the Core Environmental Stress Response is partially deregulated in a Δ*flp1* strain. Approximately 25% of the CESR genes regarded in our analysis presented an altered level of expression with respect to the *wt* transcriptional response (51 deregulated, 206 CESR, see RESULTS). This significant deregulation of genes included in the central mechanism of transcriptional response to stress, could point to a role of Flp1p in directly controlling gene expression in perturbed environmental conditions. This hypothesis is supported by observations from our laboratory that relate *flp1* to *atf1* (Canete & Bueno, unpublished results). A specially deregulated CESR group is that of antioxidants with three down-regulated genes in Δ*flp1* (*ctt1, gpx1* and *pmp20*) with respect to the stress triggered induction in *wt*. As stressed in the introduction, only two genes coding for proteins involved in DNA repair and two coding for heat shock proteins present an enhanced transcription in the environmental stress response. Correlating with the deregulation of CESR in Δ*flp1*, this strain presents up-regulation of one of the genes involved in DNA repair

(SPBC23G7.11) and down-regulation of the heat-shock protein encoding gene *hsp16*. The CESR stress response gene *rds1* is also down-regulated in Δ*flp1*.

Analysis of the deregulation of the specific checkpoint response to HU in Δ*flp1*

Genome wide micro-array analyses of the gene expression profiles during HU treatment revealed that two clusters of genes are specifically regulated as a result of checkpoint response to replication stress: the MCB (up-regulated during the S-phase arrest) and the FKH (down-regulated during the S-phase arrest) clusters of genes (Chu *et al.*, 2007). The S-phase peak of expression of MCB cluster during replication stress (which includes genes such as *cdc22*, *cdc18*, *cdt1*, *and cig2*, essential for DNA replication) is dependent on both Rad3p and Cds1p, and probably occurs to maintain forks in a replication competent state to allow for an adequate recovery from checkpoint block. According to our analysis Δ*flp1* presents reduced gene expression of the MCB components *cig2, cdc22, cdc18* and *SPAC644.05c* during HU treatment. Expression of MBF genes, responsible for MCB induction, did not appear to be modified in our analyses, although the gene *pas1*, whose product is known to be involved Res2p-Cdc10p activation, was repressed in Δ*flp1* with respect to *wt*. Repression of MCB induction in Δ*flp1*, correlates with our observations showing reduced Cds1p levels and activity during HU treatment in cells deleted for *flp1*, further supporting a role of the phosphatase in regulating adequate checkpoint response, in this case at the transcriptional level.

7. A MATHEMATICAL MODEL FOR CHECKPOINT RESPONSE TO REPLICATION STRESS IN *S. pombe*

In the framework of our investigation involving the role of Flp1p in checkpoint response to replication stress, we undertook the task of building a mathematical model for this signalling pathway in *S. pombe*. As emphasized previous sections, the model here presented is the result of an ongoing collaboration with the Computational Systems Biology Group of the Max Planck Institute for Molecular Genetics in Berlin, and should be regarded as preliminary. Including the sections involving our mathematical approach to checkpoint response we intend to give an insight into the

general process of developing mathematical models for biological networks, and show our achievements in building a novel model that accounts both for a simplified vision of cell cycle progression and for checkpoint response to replication stress. In this section, we will also discuss some of the improvements that will be made to the model and the future applications of the final, validated model.

Novel features of the presented model

As underscored in RESULTS, in order to develop an accurate model for checkpoint response, we first put our efforts in building a model for cell cycle progression adequate for our requirements. The currently available models for global cell cycle in *S. pombe* (that is, including progression through all cell cycle phases) (Novak, 1998 *et al.*; Sveiczer, 2000 *et al.*), force cell cycle progression by means of switches or programmed changes in the values of some parameters. These switches are activated if some species or reactions reach a certain threshold and are purely mathematical triggers inspired in biological observations. Since cell cycle and checkpoint regulation involve common species that are differently regulated, these external switches for cycle progression in unaltered conditions would interfere with the control of cell cycle progression during checkpoint activation. Therefore, in order to build a checkpoint module for replication stress conditions, we needed a cell cycle model entirely regulated by the species and reactions included in the model. We have thus presented here a self-regulated model, able to reproduce without mathematical switches the biological oscillations describing cell cycle progression. This model has been greatly simplified according to the assumptions listed in RESULTS and does not intend to account for a detailed mechanistic description of each cell cycle phase, but can still reproduce an adequate profile of Cdc2p activity during the entire cycle and includes the main players involved both in cell cycle and in checkpoint response to replication stress. The need to build the model in a reductionist way is linked to the lack of quantitative data for protein concentrations and reaction rates in *S. pombe*. This forced us to estimate all parameters and initial concentrations of the model, and made us keep the parameter set as reduced as possible.

On the other hand, a remarkable feature of our cell cycle model is that it has been fitted to experimental data points. That is, the parameter set has been selected in a

way that the system is not only able to reproduce the qualitative behaviour of the system but can also account for specific dynamic profiles represented by experimental time courses.

Regarding the checkpoint module, we present a model that is able to describe the observed down-regulation of Cdc2p activity as a result of detection of replication stress, as well as Cds1p activation and Cdc25p accumulation. In this model, we have included for validation a module for our proposed model for the role of Flp1p in checkpoint response to replication stress, discussed in previous sections. We have used once again experimental data to fit the parameters of the module, and we were able to validate the model using experimental data points for Δ*flp1*. Importantly, in addition to accounting for correct profiles for checkpoint response in *wt*, the model in its current state already accounts for a decrease in Cds1p activation in cells lacking Flp1p, as well as modified activation dynamics of the checkpoint kinase.

Outlook

As stated in RESULTS the presented model does not adequately account for regulation of Cdc25p protein levels during cell cycle progression or during checkpoint in Δ*flp1*. Due to this defect at the validation stage, we are currently developing an improved version based on a new scheme for Cdc25p regulation. On the other hand, some other changes are being included to improve the biological description of the system homogenize the kinetics of the involved reactions. The new scheme and an explanation of the planned improvements are found in Figure D2.

Once we obtain a fitted and validated model capable of satisfactorily reproducing the dynamic behaviour of all species involved, we will subject the system to different analyses. With them, we intend to better understand some issues arising from our investigation, like the differential role of Flp1p in maintaining cell cycle and checkpoint stability: a mathematical/mechanistic explanation for our observations of moderate defectiveness in checkpoint response for Δ*flp1* and *opflp1*; A mathematical description of the different thresholds of Cds1p activity linked to fork stability and checkpoint block, and the role of Flp1p in reaching them, etc. On the other hand, both built modules for cell cycle progression and checkpoint response can be used as basis for

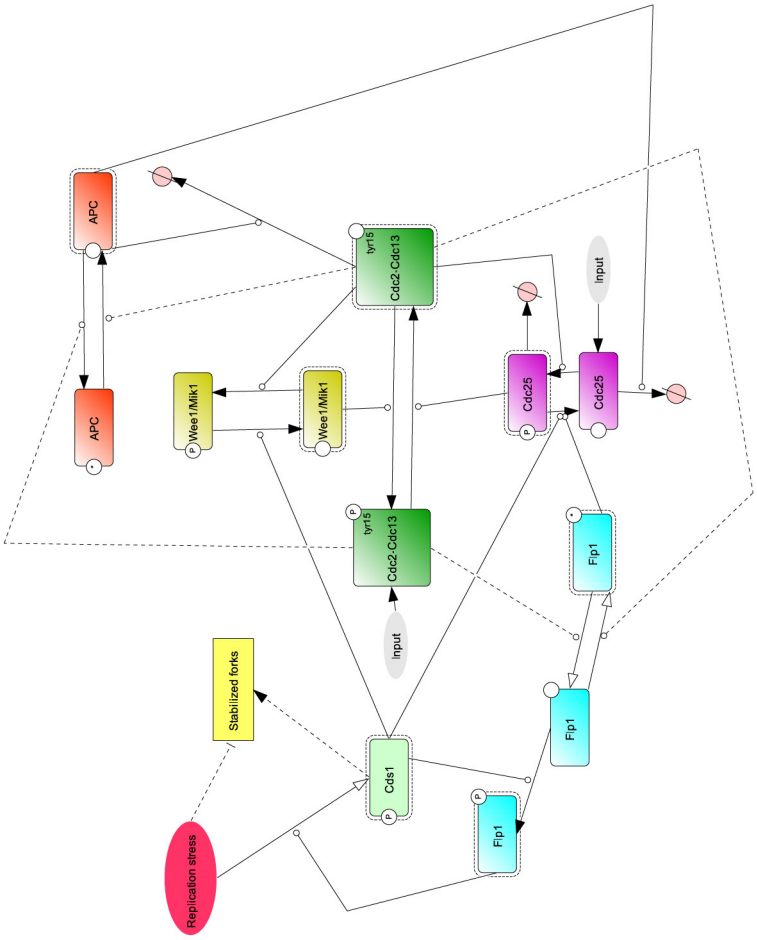

Figure D2. **A new working model for checkpoint response to replication stress in *S. pombe*.** As explained in the main text some changes in the working scheme are planned to obtain an improved version of the model. These include a refinement of Cdc25p regulation: inclusion of the dependence on APC of Cdc25p degradation, enforcement of Flp1p action over Cdc25p inactivation and inclusion of a secondary degradation system for Cdc25p. This new regulatory mechanism will allow us to include only one inactive form of Cdc25p both for cell cycle and checkpoint response. On the other hand, input to the degraded species will be written to their respective inactive forms, which better accounts for biological observations. Regarding checkpoint response, we plan to use the experimental activation profile of Cds1p as an input to reduce the uncertainty of the system.

more descriptive and comprehensive models. This will be of special interest once measured data for species concentrations and/or reactions rates will be available for *S. pombe*

.

CONCLUSIONS

1. The phosphatase Flp1p is involved in checkpoint response to genotoxic stress:
    a. Mutants of *flp1* present moderate defects in checkpoint response to replication stress.
    b. Flp1p changes its subcellular localization in cells exposed to genotoxic stress in a checkpoint dependent manner:
        i. Release of Flp1p to the nucleus during replication stress depends on Cds1p and most likely occurs through phosphorylation of the phosphatase.
        ii. Release of Flp1p to the nucleus is a determinant step for its activity in checkpoint response. Retention of Flp1p in the nucleolus during replications stress results phenotypes similar to that of the deletion of *flp1*.
    c. Flp1p performs a function in checkpoint response that is independent from its regulatory role during unperturbed cell cycle. Flp1p does not alter Cdc25p accumulation or Cdc2p Tyr15 phosphorylation profiles during checkpoint response to genotoxic stress, even if Cdc2p and Cdc25p are regulatory targets of this signalling cascade.
    d. Flp1p and Cds1p show a close interplay during checkpoint response to replication stress that results in the full activation of the kinase. The phenotypes associated to a partially deficient checkpoint in *flp1* mutants can be explained appealing to the reduced Cds1p activity they present.
    e. Flp1p might play an active role in the regulation of the transcriptional response to replication stress.
2. We have achieved a mathematical model that accounts for the simulation of both unperturbed cell cycle and checkpoint response to replication stress in *S. pombe*. An improved model is under development. By means of this future improved and validated model we intend to clarify some aspects of our investigation relating the mechanism of action of Flp1p in checkpoint response to unreplicated DNA.

APPENDIX 1

Ribosomal proteins and protein sintesis

REPRESSED					INDUCED				
Accesion Number	**Gene encoded**	**Protein type**	**Index**	**p value**	**Accesion Number**	**Gene encoded**	**Protein type**	**Index**	**p value**
S. pombe SPBC11G11.03		60S acidic ribosomal protein (predicted)	-4.20	0.999980	*S. pombe SPBC947.07*		Involved in ribosome biogenesis and assembly (predicted)	2.11	0.000492
S. pombe SPAC3A12.10	***rpl2001***	60S ribosomal protein L20a	-3.30	0.998514	*S. pombe SPCC1840.10*	***lsm8***	Ribonucleoprotein (RNP) complex	3.54	0.000030
S. pombe SPCC1322.15	***rpl3402***	60S ribosomal protein L34	-3.15	0.998168	*S. pombe SPMIT.08*	***rps3***	Ribosomal small subunit	5.57	0.000020
S. pombe SPBC11C11.09c	***rpl502***	60S ribosomal protein L5	-3.13	0.998799					
S. pombe SPAC3H5.07	***rpl701***	60S ribosomal protein L7	-3.25	0.999562					
S. pombe SPAC664.06	***rpl703***	60S ribosomal protein L7	-4.33	0.999980					
S. pombe SPBC839.04	***rpl803***	60S ribosomal protein L8	-3.26	0.999954					
S. pombe SPAC31G5.17c	***rps1001***	40S ribosomal protein S10	-2.58	0.998514					
S. pombe SPAC3H5.05c	***rps1401***	40S ribosomal protein S14	-3.68	0.999980					
S. pombe SPAC1805.11c	***rps2602***	40S ribosomal protein S26	-3.39	0.999034					

Ribosomal proteins and protein sintesis

REPRESSED					INDUCED				
Accesion Number	**Gene encoded**	**Protein type**	**Index**	**p value**	**Accesion Number**	**Gene encoded**	**Protein type**	**Index**	**p value**
S. pombe SPAC8C9.08	***rps5***	40S ribosomal protein S5	-4.14	0.999980					
S. pombe SPBC14F5.03c	***kap123***	Karyopherin	-3.71	0.999980					
S. pombe SPCC1840.03	***sal3***	Karyopherin	-3.80	0.999980					
S. pombe SPAC1B1.03c	***kap95***	Karyopherin (predicted)	-3.54	0.999965					
S. pombe SPAC30D11.04c	***nup124***	Nucleoporin	-3.56	0.999899					
S. pombe SPBC20F10.01	***gar1***	Ribonucleoprotein (RNP) complex (PMID 8502556)	-4.97	0.999980					
S. pombe SPBC646.10c		Ribonucleoprotein (RNP) complex (predicted) (PMID 12068309)	-3.39	0.999382					
S. pombe SPCP1E11.08		Ribosomal protein (S8E subunit) (predicted)	-3.62	0.999886					
S. pombe SPAC18G6.07c	***mra1***	Functions downstream of Ras1p	-3.53	0.999382					

Ribosomal proteins and protein sintesis

REPRESSED					INDUCED				
Accesion Number	**Gene encoded**	**Protein type**	**Index**	**p value**	**Accesion Number**	**Gene encoded**	**Protein type**	**Index**	**p value**
S. pombe SPAC140.02	***gar2***	GAR family	-5.18	0.999980					
S. pombe SPBC2D10.10c	***fib1***	Fibrillarin	-3.02	0.999899					
S. pombe SPAC12G12.06c		RNA 3-terminal phosphate cyclase (predicted)	-4.05	0.999965					

Putative transcription factors and general transcription

REPRESSED					INDUCED				
Accesion Number	**Gene encoded**	**Protein type**	**Index**	**p value**	**Accesion Number**	**Gene encoded**	**Protein type**	**Index**	**p value**
S. pombe SPAC17H9.04c		RNA-binding protein	-3.72	0.999034	*S. pombe SPCC338.16*	***pof3***	F-box protein	3.24	0.000020
S. pombe SPAC644.16		RNA-binding protein	-3.66	0.999308	*S. pombe SPCC1223.04c*		Histone lysine methyltransferase (predicted)	2.78	0.000020
S. pombe SPCC1183.07		RNA-binding protein	-3.36	0.999226	*S. pombe SPBC1718.02*	***hop1***	Horma domain protein (inferred from context)	2.75	0.000020
S. pombe SPCC550.14		RNA-binding protein	-4.12	0.999980	*S. pombe SPCC584.02*	***cuf2***	Involved in copper homeostasis	6.18	0.000020
S. pombe SPBP8B7.11	***nxt3***	RNA-binding protein	-2.79	0.999562	*S. pombe SPBC1778.02*	***rap1***	Involved in telomere maintenance	3.01	0.000020
S. pombe SPAC10F6.06	***vip1***	rrm RNA recognition motif	-3.40	0.999970	*S. pombe SPBC317.01*	***pvg4***	MADS-box transcription factor	3.05	0.000020
S. pombe SPAC1783.07c	***pap1/ caf3***	Transcription factor	-2.89	0.999135	*S. pombe SPAC31G5.10*	***eta2***	Myb family	2.32	0.000020
S. pombe SPAC8C9.14	***prr1***	Transcription factor	-4.21	0.999811	*S. pombe SPBC31F10.04c*	***srb4***	RNA polymerase II holoenzyme component (PMID 10625684)	2.68	0.000027
S. pombe SPAC25G10.03	***zip1***	Transcription factor	-3.48	0.999448	*S. pombe SPAC1002.15c*	***pmc5***	RNA polymerase II holoenzyme component (PMID 10625684)	2.64	0.000020

Putative transcription factors and general transcription

REPRESSED					INDUCED				
Accesion Number	**Gene encoded**	**Protein type**	**Index**	**p value**	**Accesion Number**	**Gene encoded**	**Protein type**	**Index**	**p value**
S. pombe SPAC23C4.19	***spt5***	Involved in transcriptional regulation	-3.59	0.998168	*S. pombe SPAC23H4.17c*	***srb10***	Serinethreonine protein kinase (predicted)	2.27	0.000020
S. pombe SPAC26H5.05		Involved in transcriptional regulation (predicted)	-3.05	0.999034	*S. pombe SPCC1739.05*		SET domain	1.98	0.000020
S. pombe SPBC11B10.10c	***pht1***	Histone H2A variant	-3.46	0.999833	*S. pombe SPBC215.04*	***git11***	Heterotrimeric G protein (gamma subunit) (PMID 11238401)	2.73	0.000040
S. pombe SPCC622.09	***htb1***	Histone H2B (alpha) (PMID 3018512)	-4.49	0.999980	*S. pombe SPBC1861.07*		SKP1 family	2.52	0.000147
S. pombe SPBC1105.11c	***h3.3***	Histone H3	-3.08	0.999811	*S. pombe SPBC2D10.06*	***rep1***	Transcription factor	2.83	0.000020
S. pombe SPBC8D2.04	***hht2***	Histone H3	-3.00	0.999948	*S. pombe SPAC22F3.09c*	***mcs1***	Transcription factor	2.65	0.000214
S. pombe SPBC1105.12	***h4.3***	Histone H4	-3.30	0.999980	*S. pombe SPAC22F3.02*	***atf31***	Transcription factor	3.32	0.000035
S. pombe SPAC1834.03c	***hhf1***	Histone H4	-3.03	0.999980	*S. pombe SPBC2F12.09c*	***atf21***	Transcription factor	5.92	0.000020
S. pombe SPBC8D2.03c	***hhf2***	Histone H4	-2.92	0.999811	*S. pombe SPAC11E3.06*	***map1***	Transcription factor	3.05	0.000020
S. pombe SPBC1289.07c	***rpc40***	DNA-directed RNA polymerase (I and III subunit) (predicted)	-3.92	0.999965	*S. pombe SPBC32H8.11*	***mei4***	Transcription factor (meiotic) (PMID 9528784)	3.64	0.000020

Putative transcription factors and general transcription

REPRESSED					INDUCED				
Accesion Number	**Gene encoded**	**Protein type**	**Index**	**p value**	**Accesion Number**	**Gene encoded**	**Protein type**	**Index**	**p value**
S. pombe SPAC1B3.12c	***rpb10***	DNA-directed RNA polymerase (I, II, and III subunit)	-2.63	0.999922	*S. pombe SPBP4H10.09*	***rsv1***	Transcription factor (predicted)	3.50	0.000020
S. pombe SPCC1020.04c	***rpb6***	DNA-directed RNA polymerase (I, II, and III subunit)	-3.35	0.999226	*S. pombe SPBC13E7.10c*	***brf1***	Transcription factor TFIIIB complex (PMID 12682361)	2.07	0.000046
S. pombe SPAC23C4.15	***rpb5***	DNA-directed RNA polymerase (I, II, and III subunit) (PMID 9077438)	-3.45	0.999932	*S. pombe SPCC1919.14c*	***bdp1***	Transcription factor TFIIIB complex (predicted)	2.01	0.000020
S. pombe SPAC23G3.01	***rpb2***	DNA-directed RNA polymerase (II subunit)	-3.98	0.999786	*S. pombe SPCC61.02*	***spt3***	Transcription initiation factor activity	2.94	0.000020
S. pombe SPAC3F10.03		Glycine tRNA-ligase	-3.83	0.999980	*S. pombe SPAC10F6.08c*		Transcriptional regulator	3.36	0.000020
S. pombe SPCC364.06	***nap1***		-4.02	0.999562	*S. pombe SPAC16A10.02*		TREX complex (predicted)	2.21	0.000035
S. pombe SPBC4C3.05c	***nuc1***	DNA-directed RNA polymerase I complex (large subunit) (PMID 2537310)	-3.92	0.999853	*S. pombe SPBPB8B6.04c*	***grt1***	zinc finger protein	2.35	0.001077
S. pombe SPAC29E6.08	***tbp1***	TATA-binding protein (TBP)	-4.07	0.999973	*S. pombe SPBP35G2.10*	***cfp1***	Zinc finger protein	2.75	0.000027
					S. pombe SPBC1685.08		Zinc finger protein	2.11	0.000020

Putative transcription factors and general transcription

REPRESSED					INDUCED				
Accesion Number	**Gene encoded**	**Protein type**	**Index**	**p value**	**Accesion Number**	**Gene encoded**	**Protein type**	**Index**	**p value**
					S. pombe SPCC576.13	***swc5***	Chromatin remodeling complex	2.41	0.000052
					S. pombe SPAC31G5.12c	***n150/ maf1***	Conserved eukaryotic protein	2.99	0.000020

Translation

REPRESSED					INDUCED				
Accesion Number	**Gene encoded**	**Protein type**	**Index**	**p value**	**Accesion Number**	**Gene encoded**	**Protein type**	**Index**	**p value**
S. pombe SPAC3C7.08c	***elf1***	AAA family ATPase	-4.26	0.999562	*S. pombe SPAC167.03c*	***snu66***	Involved in mRNA splicing	2.48	0.000020
S. pombe SPBC9B6.04c		Translation elongation factor (predicted)	-4.56	0.999980	*S. pombe SPBC3E7.13c*		Involved in mRNA splicing (predicted)	2.64	0.000046
S. pombe SPAC29A4.02c		Translation elongation factor 1 (gamma subunit) (PMID 9099890)	-3.10	0.999922	*S. pombe SPCC126.14*	***prp18***	Involved in mRNA splicing (predicted) (2nd step) (PMID 12212850)	5.89	0.000020
S. pombe SPCC417.08	***tef3***	Translation elongation factor activity (TAS) (PMID 9099890)	-3.68	0.999853	*S. pombe SPBC660.10*		Involved in translational elongation (factor g)	2.04	0.000020
S. pombe SPAC1006.07		Translation initiation factor	-4.06	0.999980	*S. pombe SPAC323.08*		Involved in tRNA processing (ISS)	3.01	0.000020
S. pombe SPAC25G10.08		Translation initiation factor	-5.26	0.999853	*S. pombe SPAC1805.09c*	***fmt1***	Methionyl-tRNA formyltransferase (predicted)	3.54	0.000020
S. pombe SPAC2F7.05c		Translation initiation factor	-3.80	0.999886	*S. pombe SPBC2F12.08c*	***ceg1***	mRNA guanylyl transferase	2.19	0.000020
S. pombe SPAC343.14c		Translation initiation factor	-3.20	0.999693	*S. pombe SPCC63.07*		tRNA guanylyltransferase activity (predicted)	2.11	0.000020

Translation

REPRESSED					INDUCED				
Accesion Number	**Gene encoded**	**Protein type**	**Index**	**p value**	**Accesion Number**	**Gene encoded**	**Protein type**	**Index**	**p value**
S. pombe SPAC821.05		Translation initiation factor	-3.40	0.999922	*S. pombe SPBC1289.02c*	***uap2***	U2 snRNA-associated protein	2.09	0.000020
S. pombe SPCC11E10.07c		Translation initiation factor	-3.52	0.999980	*S. pombe SPAC4A8.08c*		Valine-tRNA ligase (predicted)	2.98	0.000020
S. pombe SPAC637.07	***moe1***	Translation initiation factor	-3.82	0.999977	*S. pombe SPBC1685.06*	***cid11***	Cid1-related	4.42	0.000020
S. pombe SPBC18H10.04c	***sce3***	Translation initiation factor	-4.55	0.999980	*S. pombe SPCC663.12*	***cid12***	Cid1-related	2.36	0.000020
S. pombe SPAC4D7.05	***sum1***	Translation initiation factor	-3.30	0.999693	*S. pombe SPBC18H10.10c*	***cwc16***	Conserved eukaryotic protein	4.13	0.000020
S. pombe SPBC25H2.07	***tif11***	Translation initiation factor	-3.82	0.999973					
S. pombe SPAC3G9.09c	***tif211***	Translation initiation factor	-4.37	0.998799					
S. pombe SPAC32A11.04c	***tif212***	Translation initiation factor	-4.13	0.999980					
S. pombe SPAC8C9.15c	***tif225***	Translation initiation factor	-3.19	0.999226					
S. pombe SPBC17D11.05	***tif32***	Translation initiation factor	-4.96	0.999980					
S. pombe SPAC4A8.16c	***tif33***	Translation initiation factor	-3.43	0.999977					
S. pombe SPBC18H10.03	***tif35***	Translation initiation factor	-4.08	0.999970					

Translation

REPRESSED					INDUCED				
Accesion Number	**Gene encoded**	**Protein type**	**Index**	**p value**	**Accesion Number**	**Gene encoded**	**Protein type**	**Index**	**p value**
S. pombe SPAC16E8.15	***tif45***	Translation initiation factor	-3.48	0.999970					
S. pombe SPAC17C9.03	***tif471***	Translation initiation factor	-4.21	0.999980					
S. pombe SPAC26H5.10c	***tif51***	Translation initiation factor	-4.87	0.999960					
S. pombe SPCC1919.09	***tif6***	Translation initiation factor	-4.13	0.999886					
S. pombe SPBC646.09c	***yin6***	Translation initiation factor	-3.74	0.999833					
S. pombe SPBC17G9.09	***tif213***	Translation initiation factor 2 (gamma subunit)	-3.62	0.999980					
S. pombe SPAC56F8.03		Translation initiation factor if-2 (predicted)	-3.26	0.999759					
S. pombe SPAC1834.01	***sup45***	Translation release factor (PMID 9701287)	-3.04	0.999382					
S. pombe SPCC584.04	***sup35***	Translation release factor eRF3 (class II) (PMID 9701287)	-3.84	0.999980					
S. pombe SPCC830.07c	***psi1***	DNAJ domain protein	-3.90	0.999965					
S. pombe SPBC14F5.06		Iron-sulfur protein	-4.66	0.999980					

Translation

REPRESSED					INDUCED				
Accesion Number	**Gene encoded**	**Protein type**	**Index**	**p value**	**Accesion Number**	**Gene encoded**	**Protein type**	**Index**	**p value**
S. pombe SPBC8D2.06		Isoleucine-tRNA ligase (predicted)	-4.04	0.999980					
S. pombe SPAC26F1.13c		Leucine-tRNA ligase (predicted)	-3.86	0.999899					
S. pombe SPBC17G9.03c		Lysine-tRNA ligase	-4.13	0.999759					
S. pombe SPBC17A3.04c		Methionine-tRNA ligase (predicted)	-3.61	0.999922					
S. pombe SPBC25B2.09c		Arginine-tRNA ligase	-3.99	0.999980					
S. pombe SPBC28F2.02	***mep33***	mRNA export protein	-2.65	0.998923					
S. pombe SPAC29A4.15		Serine-tRNA ligase	-3.63	0.999980					
S. pombe SPBC25H2.02	***ths1***	Threonine-tRNA ligase (predicted)	-3.80	0.999980					
S. pombe SPBC19C7.06		Proline-tRNA ligase (predicted)	-4.54	0.999973					
S. pombe SPAC2F7.13c		Tryptophan-tRNA ligase (predicted)	-3.23	0.999980					
S. pombe SPCC1672.05c		Tyrosine-tRNA ligase (predicted)	-2.90	0.999833					
S. pombe SPBC1709.02c		Valine-tRNA ligase (predicted)	-3.28	0.999980					

Protein Folding and Degradation

REPRESSED					INDUCED				
Accesion Number	**Gene encoded**	**Protein type**	**Index**	**p value**	**Accesion Number**	**Gene encoded**	**Protein type**	**Index**	**p value**
S. pombe SPBC3E7.02c	***hsp16***	Heat shock protein	-3.57	0.999980	*S. pombe SPAC19G12.01c*	***cut20***	Anaphase-promoting complex (APC)	1.97	0.000020
S. pombe SPAC12G12.04	***mcp60***	Heat shock protein 60	-4.34	0.999980	*S. pombe SPBC83.04*	***apc15***	Anaphase-promoting complex (APC) (PMID 12477395)	1.99	0.000035
S. pombe SPAC57A7.12		Heat shock protein 70 family	-4.17	0.999980	*S. pombe SPBC28E12.01c*	***apc13***	Anaphase-promoting complex (APC) (PMID 12477395)	3.71	0.000068
S. pombe SPAC110.04c	***pss1***	Heat shock protein 70 family	-3.50	0.999980	*S. pombe SPBC1A4.01*	***apc10***	Anaphase-promoting complex (APC) (PMID 9736616)	2.14	0.000241
S. pombe SPAC13G7.02c	***ssa1***	Heat shock protein 70 family	-4.20	0.999980	*S. pombe SPAC21E11.05c*	***cyp8***	Cyclophilin	3.63	0.000020
S. pombe SPBC12D12.03	***cct1***	Chaperonin-containing T-complex	-4.82	0.999980	*S. pombe SPCC10H11.02*	***cwf23***	DNAJ domain protein	3.41	0.000020
S. pombe SPBC1A4.08c	***cct3***	Chaperonin-containing T-complex	-3.82	0.999932	*S. pombe SPBC1773.09c*	***mug184***	DNAJ domain protein	3.30	0.000020
S. pombe SPBC646.11	***cct6***	Chaperonin-containing T-complex	-3.00	0.999960	*S. pombe SPCC63.03*		DNAJ domain protein	3.91	0.000020

Protein Folding and Degradation

REPRESSED					INDUCED				
Accesion Number	**Gene encoded**	**Protein type**	**Index**	**p value**	**Accesion Number**	**Gene encoded**	**Protein type**	**Index**	**p value**
S. pombe SPBC25H2.12c	***cct7***	Chaperonin-containing T-complex	-4.85	0.999980	*S. pombe SPCC63.13*		DNAJ domain protein	3.41	0.000167
S. pombe SPBC337.05c	***cct8***	Chaperonin-containing T-complex	-3.72	0.999954	*S. pombe SPAC4G9.19*		DNAJ domain protein	2.48	0.000020
S. pombe SPBP19A11.03c	***mts4***	19S proteasome regulatory subunit	-4.18	0.999973	*S. pombe SPAC17G6.05c*		Endosome associated protein (predicted)	3.08	0.000023
S. pombe SPAC637.10c	***pus1***	19S proteasome regulatory subunit	-3.18	0.999448	*S. pombe SPBC3H7.06c*	***pof9***	F-box protein	2.61	0.000020
S. pombe SPBC16G5.01	***rpn12***	19S proteasome regulatory subunit	-3.72	0.999226	*S. pombe SPCC338.16*	***pof3***	F-box protein	3.24	0.000020
S. pombe SPBC17D11.07c	***rpn2***	19S proteasome regulatory subunit	-3.64	0.999833	*S. pombe SPAC16A10.03c*	***vps11***	Involved in intracellular protein transport (predicted)	2.29	0.000020
S. pombe SPAC23G3.11	***rpn6***	19S proteasome regulatory subunit	-4.39	0.999448	*S. pombe SPBC1734.05c*	***spf31***	Spliceosome associated protein (predicted)	2.12	0.000040
S. pombe SPBC582.07c	***rpn7***	19S proteasome regulatory subunit	-4.35	0.999980	*S. pombe SPCC777.10c*	***ubc12***	Ubiquitin conjugating enzyme	2.49	0.000618
S. pombe SPCC1682.10	***rpn8***	19S proteasome regulatory subunit	-3.36	0.999980	*S. pombe SPBP8B7.27*		Ubiquitin-protein ligase (E3)	2.77	0.000020
S. pombe SPBC16C6.07c	***rpt1***	19S proteasome regulatory subunit	-4.24	0.999980	*S. pombe SPBC32H8.02c*	***nep2***	Ulp1 protease family	2.47	0.000020

Protein Folding and Degradation

REPRESSED					INDUCED				
Accesion Number	**Gene encoded**	**Protein type**	**Index**	**p value**	**Accesion Number**	**Gene encoded**	**Protein type**	**Index**	**p value**
S. pombe SPCC1682.16	***rpt4***	19S proteasome regulatory subunit	-2.99	0.999899	*S. pombe SPCC4G3.03*		WD repeat protein	2.69	0.000020
S. pombe SPBC23G7.12c	***rpt6***	19S proteasome regulatory subunit	-3.89	0.999226	*S. pombe SPBC3D6.11c*	***slx8***	Zinc finger protein	2.37	0.000020
S. pombe SPAC1420.03	***rpn501***	19S proteasome regulatory subunit (PMID 12783882)	-3.40	0.999980	*S. pombe SPAC16E8.13*		Zinc finger protein	2.22	0.000020
S. pombe SPBC4.07c	***rpt2***	19S proteasome regulatory subunit (PMID 8247131)	-3.44	0.999654	*S. pombe SPBC1685.08*		Zinc finger protein	2.11	0.000020
S. pombe SPBC646.16		20S proteasome component (alpha 1)	-4.58	0.999980	*S. pombe SPAC6B12.08*		Zinc finger protein	4.55	0.000035
S. pombe SPCC1442.06		20S proteasome component (alpha 2)	-3.27	0.999886					
S. pombe SPAC323.02c		20S proteasome component (alpha 5)	-3.39	0.999899					
S. pombe SPAC6G10.04c		20S proteasome component (alpha 6)	-4.55	0.999980					
S. pombe SPCC1795.04c		20S proteasome component (alpha 7)	-3.82	0.999448					
S. pombe SPBC4C3.10c		20S proteasome component (beta 1)	-4.11	0.999980					
S. pombe SPAC23D3.07		20S proteasome component (beta 2)	-4.27	0.999980					
S. pombe SPCC63.12c		20S proteasome component (beta 3)	-4.19	0.999980					

Protein Folding and Degradation

REPRESSED					INDUCED				
Accesion Number	**Gene encoded**	**Protein type**	**Index**	**p value**	**Accesion Number**	**Gene encoded**	**Protein type**	**Index**	**p value**
S. pombe SPAC31A2.04c		20S proteasome component (beta 4)	-3.45	0.999226					
S. pombe SPAC4A8.13c	***pts1***	20S proteasome component (beta 5)	-3.97	0.999948					
S. pombe SPAC22F8.06	***pam1***	20S proteasome component (beta 6)	-4.08	0.999977					
S. pombe SPBC577.10		20S proteasome component (beta 7)	-3.64	0.998168					
S. pombe SPAC18B11.07c	***rhp6***	Ubiquitin conjugating enzyme	-3.27	0.999727					
S. pombe SPCC338.05c	***spm2***	Ubiquitin conjugating enzyme	-3.60	0.999948					
S. pombe SPBC1105.09	***ubc15***	Ubiquitin conjugating enzyme	-2.81	0.998664					
S. pombe SPBC713.02c	***ubp21***	Ubiquitin C-terminal hydrolase activity	-2.88	0.999382					
S. pombe SPAC26A3.16	***dph1***	Ubiquitin family protein	-4.23	0.999508					
S. pombe SPAC1805.12c	***uep1***	Ubiquitin family protein	-2.81	0.998799					
S. pombe SPAC15A10.11	***ubr11***	Ubiquitin-protein ligase (E3)	-3.18	0.999870					
S. pombe SPAC3C7.11c	***cnx1***	Calnexin (PMID 7876257)	-3.79	0.999973					

Protein Folding and Degradation

REPRESSED					INDUCED				
Accesion Number	**Gene encoded**	**Protein type**	**Index**	**p value**	**Accesion Number**	**Gene encoded**	**Protein type**	**Index**	**p value**
S. pombe SPBC3B9.19	***mge1***	Chaperone activity (predicted)	-3.83	0.999886					
S. pombe SPBC1734.11		Chaperone regulator activity (predicted)	-4.94	0.999980					
S. pombe SPAC2E1P5.03		DNAJ domain protein	-3.22	0.999940					
S. pombe SPCC830.07c	***psi1***	DNAJ domain protein	-3.90	0.999965					
S. pombe SPAC19D5.04	***ptr1***	HECT domain	-3.60	0.999973					
S. pombe SPCC14G10.03c		Proteasome maturation factor (predicted)	-3.18	0.999886					
S. pombe SPAC19G12.10c	***cpy1***	Serine carboxypeptidase (IDA) (PMID 9209031)	-4.00	0.999977					
S. pombe SPCC645.14c	***sti1***	TPR repeat protein	-4.99	0.999980					
S. pombe SPCC1795.11	***sum3***	DEADDEAH box helicase	-5.40	0.999980					
S. pombe SPAC17G6.14c	***uap56***	DEADDEAH box helicase	-4.07	0.999965					
S. pombe SPAC1F7.02c		DEADDEAH box helicase	-3.24	0.998514					

Protein Folding and Degradation

REPRESSED					INDUCED				
Accesion Number	**Gene encoded**	**Protein type**	**Index**	**p value**	**Accesion Number**	**Gene encoded**	**Protein type**	**Index**	**p value**
S. pombe SPAC694.02		DEADDEAH box helicase	-2.54	0.999811					
S. pombe SPBC17D1.06		DEADDEAH box helicase	-3.94	0.999980					
S. pombe SPCC285.03		DEADDEAH box helicase	-2.95	0.999135					
S. pombe SPAC16C9.06c	***upf1***	Involved in mRNA catabolism, nonsense-mediated	-3.19	0.999786					

Stress response

REPRESSED					INDUCED				
Accesion Number	**Gene encoded**	**Protein type**	**Index**	**p value**	**Accesion Number**	**Gene encoded**	**Protein type**	**Index**	**p value**
S. pombe SPAC17A2.13c	***rad25***	14-3-3 protein	-4.56	0.999811	*S. pombe SPBC16G5.12c*	***top3***	DNA topoisomerase III	3.61	0.000020
S. pombe SPAC1565.08	***cdc48***	AAA family ATPase	-5.00	0.999980	*S. pombe SPBC3D6.10*	***apn2***	DNA-(apurinic or apyrimidinic site) lyase activity (predicted)	2.72	0.000052
S. pombe SPAC1783.07c	***pap1/ caf3***	Transcription factor	-2.89	0.999135	*S. pombe SPAPB1E7.06c*	***eme1***	Endodeoxyribonuclease RUS activity (PMID 11741546)	3.27	0.000438
S. pombe SPBC3F6.03	***trr1/ caf4***	Thioredoxin reductase	-3.27	0.999562	*S. pombe SPCC191.09c*	***gst1***	Glutathione S-transferase (PMID 12063243)	4.69	0.000020
S. pombe SPAC8C9.14	***prr1***	Transcription factor	-4.21	0.999811	*S. pombe SPCC1281.07c*		Glutathione S-transferase (predicted)	2.38	0.000241
S. pombe SPCC757.07c	***ctt1/ cta1***	Catalase	-4.13	0.999980	*S. pombe SPBC20F10.06*	***mad2***	Horma domain protein	2.49	0.000020
S. pombe SPAC25G10.03	***zip1***	Transcription factor	-3.48	0.999448	*S. pombe SPCC417.02*	***dad5/ hos3***	Involved in osmotic stress response (required) (PMID 10879493)	3.40	0.000020
S. pombe SPBC14C8.07c	***cdc18***	Cell division control protein 18	-3.85	0.999886	*S. pombe SPAC27F1.04c*	***nuf2***	Localization spindle pole body	3.62	0.000020
S. pombe SPBC649.04	***uvi15***	Involved in stress response (required)	-3.40	0.999693	*S. pombe SPBC336.08*	***spc24***	Localization spindle pole body (predicted)	3.13	0.000078

Stress response

REPRESSED					INDUCED				
Accesion Number	**Gene encoded**	**Protein type**	**Index**	**p value**	**Accesion Number**	**Gene encoded**	**Protein type**	**Index**	**p value**
S. pombe SPBC3E7.02c	***hsp16***	Heat shock protein	-3.57	0.999980	*S. pombe SPAC31G5.10*	***eta2***	Myb family	2.32	0.000020
S. pombe SPAC12G12.04	***mcp60***	Heat shock protein 60	-4.34	0.999980	*S. pombe SPBC14C8.01c*	***cut2***	Securin	2.42	0.000241
S. pombe SPAC57A7.12		Heat shock protein 70 family	-4.17	0.999980	*S. pombe SPCC1259.13*	***chk1***	Serinethreonine protein kinase	4.52	0.000020
S. pombe SPAC110.04c	***pss1***	Heat shock protein 70 family	-3.50	0.999980	*S. pombe SPCC18B5.03*	***wee1***	Serinethreonine protein kinase	3.27	0.000020
S. pombe SPAC13G7.02c	***ssa1***	Heat shock protein 70 family	-4.20	0.999980	*S. pombe SPBC1685.06*	***cid11***	Cid1-related	4.42	0.000020
S. pombe SPBC409.13		6,7-dimethyl-8-ribityllumazine synthase (predicted)	-3.76	0.999970	*S. pombe SPCC663.12*	***cid12***	Cid1-related	2.36	0.000020
S. pombe SPBC2A9.02		Dyhydroflavanol-4-reductase (predicted)	-3.94	0.999980	*S. pombe SPAC821.04c*	***cid13***	Poly(A) polymerase (PMID 12062100)	2.65	0.000020
S. pombe SPBC32F12.03c	***gpx1***	Glutathione peroxidase (PMID 10455235)	-3.59	0.999980	*S. pombe SPAC1805.07c*	***dad2 /hos2***	DASH complex (predicted)	2.02	0.000020
S. pombe SPBC17A3.07	***pgr1***	Glutathione reductase (PMID 9287302)	-3.57	0.999448	*S. pombe SPAC589.08c*	***dam1***	DASH complex (predicted)	2.17	0.000346
S. pombe SPCC965.07c	***gst2***	Glutathione S-transferase (PMID 11997110)	-3.47	0.999833	*S. pombe SPCC188.13c*	***dcr1***	Dicer	2.00	0.000078

Stress response

REPRESSED					INDUCED				
Accesion Number	**Gene encoded**	**Protein type**	**Index**	**p value**	**Accesion Number**	**Gene encoded**	**Protein type**	**Index**	**p value**
S. pombe SPBC215.05	***gpd1***	Glycerol-3-phosphate dehydrogenase	-5.98	0.999980	*S. pombe SPAC4C5.02c*	***ryh1***	Small GTPase	3.36	0.000020
S. pombe SPAC343.12	***rds1***		-4.97	0.999977	*S. pombe SPBC725.02*	***mpr1/spy1***	Speedy.	2.22	0.000020
S. pombe SPBC16H5.11c	***skb1***	Methyltransferase (PMID 11278267)	-4.06	0.999948	*S. pombe SPAPB17E12.04c*	***csn2***	COP9signalosome complex (subunit 2) (PMID 11854407)	2.14	0.000040
S. pombe SPBC16D10.09	***pcn1***	PCNA (PMID 1361173)	-3.50	0.999693					
S. pombe SPAC2G11.07c	***ptc3***	Serinethreonine protein phosphatase	-4.93	0.999980					
S. pombe SPAC19G12.15c	***tpp1***	Trehalose-6-phosphate phosphatase (PMID 11004189)	-3.05	0.999727					

DNA repair

REPRESSED					INDUCED				
Accesion Number	**Gene encoded**	**Protein type**	**Index**	**p value**	**Accesion Number**	**Gene encoded**	**Protein type**	**Index**	**p value**
S. pombe SPCC622.08c	***hta1***	Histone H2A (alpha) (PMID 3018512)	-3.86	0.999980	*S. pombe SPBC119.14*	***rti1***	DNA binding	4.96	0.000618
S. pombe SPAC19G12.06c	***hta2***	Histone H2A (beta)	-3.88	0.999980	*S. pombe SPAC23C11.04c*	***pnk1***	DNA kinasephosphatase (PMID 11729194)	3.19	0.000020
S. pombe SPBC660.13c	***ssb1/ rpa1 /rad11***	DNA replication factor A complex (subunit 1) (PMID 9111307) (PMID 8702843)	-3.96	0.999811	*S. pombe SPAC2F7.06c*	***pol4***	DNA polymerase X family	7.96	0.000088
S. pombe SPBC16D10.09	***pcn1***	PCNA (PMID 1361173)	-3.50	0.999693	*S. pombe SPCC23B6.05c*	***ssb3***	DNA replication factor A complex (subunit 3)	3.11	0.000020
S. pombe SPBC3H7.15	***hhp1***	Serinethreonine protein kinase	-3.54	0.998799	*S. pombe SPBC3D6.10*	***apn2***	DNA-(apurinic or apyrimidinic site) lyase activity (predicted)	2.72	0.000052
					S. pombe SPBC23G7.11		DNA-3-methyladenine glycosidase	3.59	0.000023
					S. pombe SPAPB1E7.06c	***eme1***	Endodeoxy ribonuclease RUS activity (PMID 11741546)	3.27	0.000438

DNA repair

REPRESSED					INDUCED				
Accesion Number	**Gene encoded**	**Protein type**	**Index**	**p value**	**Accesion Number**	**Gene encoded**	**Protein type**	**Index**	**p value**
					S. pombe SPAC30D11.10	***rad22***	Involved in DNA repair (PMID 8290356)	4.19	0.000020
					S. pombe SPBC1685.11	***rlp1***	Involved in DNA repair (predicted)	2.03	0.000020
					S. pombe SPAC13A11.03	***mcp7***	Involved in homologous chromosome pairing at meiosis (predicted) (PMID 11940665)	4.19	0.000020
					S. pombe SPAC13F5.01c	***msh1***	MutS family	2.08	0.000020
					S. pombe SPAC25G10.02	***cce1***	Cruciform cutting endonuclease	4.26	0.000020
					S. pombe SPAC9.05	***mph1***	DEADDEAH box helicase	2.24	0.000020
					S. pombe SPAC22F3.03c	***rdh54***	DEADDEAH box helicase (PMID 14551247)	2.32	0.000020
					S. pombe SPBC1347.01c	***rev1***	Deoxycytidyl transferase (predicted)	2.93	0.000020
					S. pombe SPCC550.05	***nse1***	Smc5-6 complex (PMID 12966087)	2.02	0.000020

DNA repair

REPRESSED					INDUCED				
Accesion Number	**Gene encoded**	**Protein type**	**Index**	**p value**	**Accesion Number**	**Gene encoded**	**Protein type**	**Index**	**p value**
					S. pombe SPCC970.01	***rad16***	ssDNA endonuclease	2.13	0.000020
					S. pombe SPAP27G11.15	***slx1***	Stucture-specific endonuclease (catalytic subunit) (PMID 14528010)	2.45	0.000020
					S. pombe SPAC688.06c	***slx4***	Stucture-specific endonuclease (contributes_to) (PMID 14528010)	2.55	0.000020

DNA replication

REPRESSED					INDUCED				
Accesion Number	**Gene encoded**	**Protein type**	**Index**	**p value**	**Accesion Number**	**Gene encoded**	**Protein type**	**Index**	**p value**
S. pombe SPBC660.13c	***ssb1/ rpa1 /rad11***	DNA replication factor A complex (subunit 1) (PMID 9111307) (PMID 8702843)	-3.96	0.999811	*S. pombe SPAC2F7.06c*	***pol4***	DNA polymerase X family	7.96	0.000088
S. pombe SPBC14C8.07c	***cdc18***	Cell division control protein 18	-3.85	0.999886	*S. pombe SPCC23B6.05c*	***ssb3***	DNA replication factor A complex (subunit 3)	3.11	0.000020
S. pombe SPBC16D10.09	***pcn1***	PCNA (PMID 1361173)	-3.50	0.999693	*S. pombe SPBC16G5.12c*	***top3***	DNA topoisomerase III	3.61	0.000020
S. pombe SPAC1F7.05	***cdc22***	Ribonucleoside reductase	-5.24	0.999980	*S. pombe SPBC428.08c*	***clr4***	Histone H3 methyltransferase	4.06	0.000020
S. pombe SPBC25D12.04	***suc22***	Ribonucleotide reductase	-3.97	0.999973	*S. pombe SPAC8F11.07c*	***cdc24***	Involved in DNA replication (required)	2.05	0.000020
					S. pombe SPBC14C8.01c	***cut2***	Securin	2.42	0.000241
					S. pombe SPAC25G10.02	***cce1***	Cruciform cutting endonuclease	4.26	0.000020
					S. pombe SPBC3D6.11c	***slx8***	Zinc finger protein	2.37	0.000020

Cell cycle and cytoskeleton organization

REPRESSED					INDUCED				
Accesion Number	**Gene encoded**	**Protein type**	**Index**	**p value**	**Accesion Number**	**Gene encoded**	**Protein type**	**Index**	**p value**
S. pombe SPAP8A3.08	***cdc4***	Myosin II light chain. EF hand	-3.94	0.999932	*S. pombe SPBC20F10.10*		Cyclin	2.73	0.000020
S. pombe SPAC110.03	***cdc42***	GTPase	-4.33	0.999980	*S. pombe SPAC8F11.07c*	***cdc24***	Involved in DNA replication (required)	2.05	0.000020
S. pombe SPBC21B10.04c	***nrf1***	Chaperone activity (predicted)	-2.90	0.999980	*S. pombe SPBC1604.20c*	***tea2***	Kinesin-like protein	2.37	0.000020
S. pombe SPAC1F7.04	***rho1***	GTPase	-4.51	0.999980	*S. pombe SPAC3A11.14c*	***pkl1***	Kinesin-like protein	1.99	0.000020
S. pombe SPBC1289.03c	***spi1***	GTPase	-2.53	0.999135	*S. pombe SPAC29E6.04*	***nnf1***	Localization spindle pole body	2.39	0.000346
S. pombe SPAC18G6.03	***ypt3***	GTPase	-4.56	0.999980	*S. pombe SPAC27F1.04c*	***nuf2***	Localization spindle pole body	3.62	0.000020
S. pombe SPBC582.03	***cdc13***	Cyclin	-3.06	0.999973	*S. pombe SPBC12D12.01*	***sad1***	Localization spindle pole body (PMID 7744953)	2.12	0.000020
S. pombe SPAPB2B4.03	***cig2***	Cyclin	-4.09	0.999980	*S. pombe SPBC336.08*	***spc24***	Localization spindle pole body (predicted)	3.13	0.000078
S. pombe SPAC19E9.03	***pas1***	Cyclin (PMID 10982385)	-4.16	0.999886	*S. pombe SPCC970.04c*	***mob2***	Phosphoprotein (predicted)	2.22	0.000020
S. pombe SPCC1840.02c	***bgs4***	1,3-beta-glucan synthase (subunit) (predicted)	-3.89	0.999980	*S. pombe SPCC18B5.03*	***wee1***	Serinethreonine protein kinase	3.27	0.000020

Cell cycle and cytoskeleton organization

REPRESSED					INDUCED				
Accesion Number	**Gene encoded**	**Protein type**	**Index**	**p value**	**Accesion Number**	**Gene encoded**	**Protein type**	**Index**	**p value**
S. pombe SPAC6F6.10c	***arc2***	ARP23 actin-organizing complex	-3.90	0.999980	*S. pombe SPAC9G1.09*	***sid1***	Serinethreonine protein kinase	2.35	0.000020
S. pombe SPBC1778.08c	***arc2***	ARP23 actin-organizing complex	-3.42	0.999034	*S. pombe SPAC1805.07c*	***dad2 /hos2***	DASH complex (predicted)	2.02	0.000020
S. pombe SPAC17G8.04c	***arc5***	ARP23 actin-organizing complex	-2.71	0.999980	*S. pombe SPBC32F12.08c*	***duo1***	DASH complex (predicted)	4.83	0.000046
S. pombe SPAC630.03	***arp3***	ARP23 actin-organizing complex	-3.38	0.999886	*S. pombe SPAC589.08c*	***dam1***	DASH complex (predicted)	2.17	0.000346
S. pombe SPAC1002.13c	***psu1***	Beta-glucosidase (predicted)	-4.17	0.999980	*S. pombe SPCC188.13c*	***dcr1***	Dicer	2.00	0.000078
S. pombe SPAC3A12.14	***cam1***	Calmodulin (PMID 3035538)	-3.26	0.999970	*S. pombe SPAC4C5.02c*	***ryh1***	Small GTPase	3.36	0.000020
S. pombe SPBC646.13	***sds23/ psp1/ moc1***	CBS domain protein	-3.63	0.999980	*S. pombe SPBC725.02*	***mpr1/ spy1***	Speedy	2.22	0.000020
S. pombe SPAC3H8.10	***spo20***	CRALTRIO domain	-3.72	0.999980	*S. pombe SPBC2D10.06*	***rep1***	Transcription factor	2.83	0.000020
S. pombe SPBC1778.06c	***fim1***	Fimbrin	-4.60	0.999980	*S. pombe SPAC22F3.09c*	***mcs1***	Transcription factor	2.65	0.000214
S. pombe SPAC12B10.07	***acp1***	F-actin capping protein (alpha subunit)	-3.47	0.999508	*S. pombe SPAC6F6.08c*	***cdc16/bub2***	Two-component GAP for GTPase spg1	2.45	0.000020
S. pombe SPCC364.06	***nap1***	Involved in nucleosome assembly (predicted)	-4.02	0.999562	*S. pombe SPCC613.04c*	***rng3***	UCS-domain protein (PMID 1085282)	2.68	0.000020

Cell cycle and cytoskeleton organization

REPRESSED					INDUCED				
Accesion Number	**Gene encoded**	**Protein type**	**Index**	**p value**	**Accesion Number**	**Gene encoded**	**Protein type**	**Index**	**p value**
S. pombe SPBC146.13c	***myo1***	Myosin (type I)	-4.12	0.999727	*S. pombe SPBPB8B6.04c*	***grt1***	Zinc finger protein	2.35	0.001077
S. pombe SPAC9E9.13	***wos2***	P23 homolog (PMID 10581266)	-3.64	0.999382	*S. pombe SPCC1672.06c*	***asp1***	Acid phosphatase activity (predicted)	2.08	0.000020
S. pombe SPAPYUG7.03c	***mid2***	Pleckstrin homology domain	-3.97	0.999980	*S. pombe SPAC22F3.05c*	***alp41***	ADP-ribosylation factor	2.30	0.000020
S. pombe SPACUNK4.07c	***cta4***	P-type ATPase (PMID 12707717)	-3.73	0.999954	*S. pombe SPAC890.02c*	***alp7***	Coiled-coil (predicted)	3.13	0.000046
S. pombe SPAC1F7.05	***cdc22***	Ribonucleoside reductase	-5.24	0.999980					
S. pombe SPBC25D12.04	***suc22***	Ribonucleotide reductase	-3.97	0.999973					
S. pombe SPAC821.06	***spn2***	Septin (predicted)	-3.03	0.998168					
S. pombe SPBC16H5.07c	***ppa2***	Serinethreonine protein phosphatase (catalytic subunit)	-2.78	0.998799					
S. pombe SPAC823.15	***ppa1***	Serinethreonine protein phosphatase (minor) (catalytic subunit)	-3.89	0.999870					
S. pombe SPBC1D7.04	***mlo3***	TREX complex (predicted)	-4.03	0.999973					
S. pombe SPAC27F1.02c	***cdc8***	Tropomyosin	-4.62	0.999911					

Cell cycle and cytoskeleton organization

REPRESSED					INDUCED				
Accesion Number	**Gene encoded**	**Protein type**	**Index**	**p value**	**Accesion Number**	**Gene encoded**	**Protein type**	**Index**	**p value**
S. pombe SPBC16A3.15c	***nda2***	Tubulin (alpha 1)	-4.28	0.999980					
S. pombe SPBC800.05c	***tub1***	Tubulin (alpha 2)	-4.94	0.999980					
S. pombe SPBC26H8.07c	***nda3***	Tubulin (beta) (PMID 6094012)	-5.27	0.999654					

Meiosis

REPRESSED					INDUCED				
Accesion Number	**Gene encoded**	**Protein type**	**Index**	**p value**	**Accesion Number**	**Gene encoded**	**Protein type**	**Index**	**p value**
S. pombe SPAC31G5.11	***pac2***	cAMP-independent regulatory protein (PMID 8536311)	-3.52	0.999940	*S. pombe SPBC16E9.17c*	***rem1***	Cyclin	4.98	0.000020
S. pombe SPBC646.13	***sds23/ psp1/ moc1***	CBS domain protein	-3.63	0.999980	*S. pombe SPBC2G2.09c*	***crs1***	Cyclin (predicted)	3.03	0.000060
S. pombe SPAC3H8.10	***spo20***	CRALTRIO domain	-3.72	0.999980	*S. pombe SPAC21E11.05c*	***cyp8***	Cyclophilin	3.63	0.000020
S. pombe SPAC1805.08	***dlc1***	Dynein light chain	-3.10	0.998168	*S. pombe SPBC1773.09c*	***mug184***	DNAJ domain protein	3.30	0.000020
S. pombe SPAC18G6.07c	***mra1***	Functions downstream of Ras1p	-3.53	0.999382	*S. pombe SPAC27D7.13c*	***ssm4***	Dynactin complex (predicted)	6.87	0.000020
S. pombe SPBC1778.06c	***fim1***	Fimbrin	-4.60	0.999980	*S. pombe SPAC20G4.02c*	***fus1***	Formin	3.05	0.000020
S. pombe SPBC146.13c	***myo1***	Myosin (type I)	-4.12	0.999727	*S. pombe SPBC14C8.05c*	***meu17***	Glucoamylase	4.84	0.000030
S. pombe SPAC1F7.05	***cdc22***	Ribonucleoside reductase	-5.24	0.999980	*S. pombe SPBC428.08c*	***clr4***	Histone H3 methyltransferase	4.06	0.000020
					S. pombe SPCC1223.12c	***meu10***	Involved in cell wall biosynthesis (predicted)	4.69	0.000020

Meiosis

REPRESSED					INDUCED				
Accesion Number	**Gene encoded**	**Protein type**	**Index**	**p value**	**Accesion Number**	**Gene encoded**	**Protein type**	**Index**	**p value**
					S. pombe SPAC1565.04c	***ste4***	Involved in conjugation	3.76	0.000020
					S. pombe SPAC30D11.10	***rad22***	Involved in DNA repair (PMID 8290356)	4.19	0.000020
					S. pombe SPBC1685.11	***rlp1***	Involved in DNA repair (predicted)	2.03	0.000020
					S. pombe SPAC13A11.03	***mcp7***	Involved in homologous chromosome pairing at meiosis (predicted) (PMID 11940665)	4.19	0.000020
					S. pombe SPBC31F10.08	***mde2***	Involved in meiosis (implicated)	4.35	0.000020
					S. pombe SPBC119.04	***mei3***	Involved in meiosis (induction) (PMID 3034608)	9.17	0.000020
					S. pombe SPBC1347.03	***meu14***	Involved in meiosis (PMID 12759375)	4.51	0.000020
					S. pombe SPBC29A10.14	***rec8***	Involved in meiotic recombination (required)	3.72	0.000692
					S. pombe SPCC1753.03c	***rec7***	Involved in meiotic recombination (required) (PMID 1339382)	5.98	0.000060

Meiosis

REPRESSED					INDUCED				
Accesion Number	**Gene encoded**	**Protein type**	**Index**	**p value**	**Accesion Number**	**Gene encoded**	**Protein type**	**Index**	**p value**
					S. pombe SPAC25G10.04c	***rec10***	Involved in meiotic recombination (required) (PMID 7586030)	3.09	0.000167
					S. pombe SPBC21B10.12	***rec6***	Involved in meiotic recombination (required) (PMID 8005432)	3.07	0.000020
					S. pombe SPBC1711.14	***rec15***	Involved in meiotic recombination (required) (PMID 8559063)	2.99	0.000020
					S. pombe SPAC1F8.05	***isp3***	Involved in sexual differentiation	3.58	0.000035
					S. pombe SPAC1039.09	***isp5***	Involved in sexual differentiation (PMID 7954893)	3.47	0.000020
					S. pombe SPBC428.07	***meu6***	Lysine-rich protein	2.54	0.000020
					S. pombe SPAC222.15	***meu13***	Meiosis specific transcript (PMID 11447128)	2.38	0.000167
					S. pombe SPAC1A6.06c	***meu31***	Meiotic expression upregulated	3.74	0.000273
					S. pombe SPBC19F8.06c	***meu22***	Meiotic expression upregulated	3.94	0.000101

Meiosis

REPRESSED					INDUCED				
Accesion Number	**Gene encoded**	**Protein type**	**Index**	**p value**	**Accesion Number**	**Gene encoded**	**Protein type**	**Index**	**p value**
					S. pombe SPBC27.03	***meu25***	Meiotic expression upregulated	2.83	0.000020
					S. pombe SPCPJ732.03	***meu15***	Meiotic expression upregulated	4.60	0.000020
					S. pombe SPCC1235.13	***ght6***	Meiotic expression upregulated	5.55	0.000068
					S. pombe SPAC1556.06	***meu1***	Meiotic expression upregulated (PMID 11376151)	3.86	0.000020
					S. pombe SPAC1556.06b	***meu2***	Meiotic expression upregulated (PMID 11376151)	2.56	0.000020
					S. pombe SPBC1711.01c	***matmi***	Mating-type m-specific polypeptide mi	10.10	0.000020
					S. pombe SPAPB8E5.05	***mfm1***	M-factor precursor (PMID 8196631)	6.91	0.000346
					S. pombe SPCC1795.06	***map2***	P-factor (PMID 8314086)	5.45	0.000020
					S. pombe SPAC11H11.04	***mam2***	Pheromone p-factor receptor (PMID 1657593)	2.74	0.000035
					S. pombe SPAC8E11.03c	***dmc1***	RecA family	3.38	0.000346

Meiosis

REPRESSED					INDUCED				
Accesion Number	**Gene encoded**	**Protein type**	**Index**	**p value**	**Accesion Number**	**Gene encoded**	**Protein type**	**Index**	**p value**
					S. pombe SPCC4E9.01c	***rec11***	Region specific activator of recombination	3.78	0.000020
					S. pombe SPAC27D7.03c	***mei2***	RNA-binding protein	2.49	0.000241
					S. pombe SPCC320.07c	***mde7***	RNA-binding protein	7.59	0.001832
					S. pombe SPAC1610.03c	***crp79***	RNA-binding protein	6.94	0.000020
					S. pombe SPBC19F8.01c	***spn7***	Septin	1.99	0.000023
					S. pombe SPCC188.12	***spn6***	Septin	5.62	0.000035
					S. pombe SPAC24C9.15c	***spn5***	Septin (predicted)	3.07	0.000492
					S. pombe SPAC16E8.05c	***mde1***	Sequence orphan	3.67	0.000020
					S. pombe SPAC1296.03c	***sxa2***	Serine carboxypeptidase	2.30	0.000035
					S. pombe SPBC8D2.19	***mde3***	Serinethreonine protein kinase	3.72	0.000060
					S. pombe SPBC21C3.18	***spo4***	Serinethreonine protein kinase	5.92	0.000020
					S. pombe SPAC14C4.03	***mek1***	Serinethreonine protein kinase (predicted)	3.79	0.000346

Meiosis

REPRESSED					INDUCED				
Accesion Number	**Gene encoded**	**Protein type**	**Index**	**p value**	**Accesion Number**	**Gene encoded**	**Protein type**	**Index**	**p value**
					S. pombe SPCC417.06c	***ppk35***	Serinethreonine protein kinase (predicted)	6.87	0.000030
					S. pombe SPBP35G2.03c	***sgo1***	Shugoshin	2.74	0.000020
					S. pombe SPAC22F3.03c	***rdh54***	DEADDEAH box helicase (PMID 14551247)	2.32	0.000020
					S. pombe SPCC188.13c	***dcr1***	Dicer	2.00	0.000078
					S. pombe SPBC29A10.02	***spo5***	Single-strand polynucleotide binding protein (predicted)	3.49	0.000346
					S. pombe SPBC18H10.07		Small nuclear ribonucleoprotein (snRNP) (predicted) (pers. comm. J.A. Potashkin)	4.23	0.000027
					S. pombe SPCC550.05	***nse1***	Smc5-6 complex (PMID 12966087)	2.02	0.000020
					S. pombe SPAC17A5.11	***rec12***	Spo11Top6A topoisomerase family (PMID 12437782)	3.07	0.000346
					S. pombe SPBC1778.04	***spo6***	Spo4p regulatory subunit	2.18	0.000020

Meiosis

REPRESSED					INDUCED				
Accesion Number	**Gene encoded**	**Protein type**	**Index**	**p value**	**Accesion Number**	**Gene encoded**	**Protein type**	**Index**	**p value**
					S. pombe SPCC1919.11		Src (SH3) homology domain	8.61	0.000035
					S. pombe SPCC970.01	***rad16***	ssDNA endonuclease	2.13	0.000020
					S. pombe SPBC32H8.06		TPR repeat protein	6.83	0.000020
					S. pombe SPBC2D10.06	***rep1***	Transcription factor	2.83	0.000020
					S. pombe SPAC22F3.09c	***mcs1***	Transcription factor	2.65	0.000214
					S. pombe SPAC22F3.02	***atf31***	Transcription factor	3.32	0.000035
					S. pombe SPBC2F12.09c	***atf21***	Transcription factor	5.92	0.000020
					S. pombe SPAC11E3.06	***map1***	Transcription factor	3.05	0.000020
					S. pombe SPBC32H8.11	***mei4***	Transcription factor (meiotic) (PMID 9528784)	3.64	0.000020
					S. pombe SPBC1198.12	***mfr1***	WD repeat protein	3.60	0.000020
					S. pombe SPBC646.17c	***dic1***	WD repeat protein	3.64	0.000020
					S. pombe SPAC25H1.09	***mde5***	Alpha-amylase	3.77	0.000020

Meiosis

REPRESSED					INDUCED				
Accesion Number	**Gene encoded**	**Protein type**	**Index**	**p value**	**Accesion Number**	**Gene encoded**	**Protein type**	**Index**	**p value**
					S. pombe SPCC550.10	***meu8***	Betaine aldehyde dehydrogenase (predicted)	2.31	0.000020
					S. pombe SPAC6G9.12		BRCT domain	2.97	0.000020
					S. pombe SPAC2G11.05c		BRO1-like domain	2.43	0.000027
					S. pombe SPBC947.12	***kms2***	Coiled-coil (predicted)	3.33	0.000020
					S. pombe SPBC216.02	***mcp5***	Coiled-coil (predicted)	4.93	0.000020
					S. pombe SPCC11E10.03	***mug1***	Coiled-coil (predicted)	3.23	0.000020
					S. pombe SPAC6B12.16	***meu26***	Conserved fungal protein	4.74	0.000020

APPENDIX 2

$$\frac{d([Cdc25\_off]\cdot V_{compartment})}{dt} = -V_{compartment}\cdot\left(\frac{Kcdc25\_on\cdot[Cdc25\_off]\cdot[Cdc2\_on]}{Jcdc25\_on+[Cdc25\_off]}\right) + V_{compartment}\cdot\left(\frac{Kcdc25\_off\cdot[Cdc25\_on]\cdot(1+[Flp1\_on])}{Jcdc25\_off+[Cdc25\_on]}\right) - V_{compartment}\cdot(Kcdc25\_deg\cdot[Cdc25\_off]) + V_{compartment}\cdot\left(Kinput\cdot\left(1-\frac{Cdc25\_tot}{Kconc\_max}\right)\right)$$

$$\frac{d([Cdc25\_on]\cdot V_{compartment})}{dt} = +V_{compartment}\cdot\left(\frac{Kcdc25\_on\cdot[Cdc25\_off]\cdot[Cdc2\_on]}{Jcdc25\_on+[Cdc25\_off]}\right) - V_{compartment}\cdot\left(\frac{Kcdc25\_off\cdot[Cdc25\_on]\cdot(1+[Flp1\_on])}{Jcdc25\_off+[Cdc25\_on]}\right) - V_{compartment}\cdot\left(\frac{Kcds1\_cdc25\cdot[Cdc25\_on]\cdot[Cds1\_on]}{Jcdc25\_off+[Cdc25\_on]}\right)$$

$$\frac{d([Cdc2\_on]\cdot V_{compartment})}{dt} = -V_{compartment}\cdot(Kcdc2\_off\cdot[Cdc2\_on]\cdot[Wee1\_on]) + V_{compartment}\cdot\left(Kinput\cdot\left(1-\frac{Cdc2\_tot}{Kconc\_max}\right)\right) - V_{compartment}\cdot(Kcdc2\_deg\cdot[Cdc2\_on]\cdot[APC\_on]) + V_{compartment}\cdot(Kcdc2\_on\cdot[Cdc2\_off]\cdot[Cdc25\_on])$$

$$\frac{d([Cdc2\_off]\cdot V_{compartment})}{dt} = +V_{compartment}\cdot(Kcdc2\_off\cdot[Cdc2\_on]\cdot[Wee1\_on]) - V_{compartment}\cdot(Kcdc2\_on\cdot[Cdc2\_off]\cdot[Cdc25\_on])$$

$$\frac{d([Wee1\_on]\cdot V_{compartment})}{dt} = +V_{compartment}\cdot\left(\frac{(Kwee\_on+Kcds1\_wee1\cdot[Cds1\_on])\cdot[Wee1\_off]}{Jwee\_on+[Wee1\_off]}\right) - V_{compartment}\cdot\left(\frac{Kwee\_off\cdot[Wee1\_on]\cdot[Cdc2\_on]}{Jwee\_off+[Wee1\_on]}\right)$$

$$\frac{d([Wee1\_off]\cdot V_{compartment})}{dt} = -V_{compartment}\cdot\left(\frac{(Kwee\_on+Kcds1\_wee1\cdot[Cds1\_on])\cdot[Wee1\_off]}{Jwee\_on+[Wee1\_off]}\right) + V_{compartment}\cdot\left(\frac{Kwee\_off\cdot[Wee1\_on]\cdot[Cdc2\_on]}{Jwee\_off+[Wee1\_on]}\right)$$

$$\frac{d([APC\_on]\cdot V_{compartment})}{dt} = -V_{compartment}\cdot(Kapc\cdot[APC\_on]\cdot[Cdc2\_off]) + V_{compartment}\cdot(Kapc\cdot[APC\_off]\cdot[Cdc2\_on])$$

$$\frac{d([APC\_off]\cdot V_{compartment})}{dt} = +V_{compartment}\cdot(Kapc\cdot[APC\_on]\cdot[Cdc2\_off]) - V_{compartment}\cdot(Kapc\cdot[APC\_off]\cdot[Cdc2\_on])$$

$$\frac{d([Cds1\_off]\cdot V_{compartment})}{dt} = -V_{compartment}\cdot(Krs\cdot[Replication\_stress]\cdot[Cds1\_off]\cdot(1+Kflp1\_Cds1\cdot[Flp1\_checkpoint]))$$

$$\frac{d([Cds1\_on]\cdot V_{compartment})}{dt} = +V_{compartment}\cdot(Krs\cdot[Replication\_stress]\cdot[Cds1\_off]\cdot(1+Kflp1\_Cds1\cdot[Flp1\_checkpoint]))$$

$$\frac{d([Flp1\_off]\cdot V_{compartment})}{dt} = -V_{compartment}\cdot(Kflp1\cdot[Flp1\_off]\cdot[Cdc2\_on]\cdot(1+[Flp1\_on])) + V_{compartment}\cdot(Kflp1\cdot[Flp1\_on]\cdot[Cdc2\_off]) - V_{compartment}\cdot(Kcds1\_flp1\cdot[Flp1\_off]\cdot[Cds1\_on])$$

$$\frac{d([Flp1\_on]\cdot V_{compartment})}{dt} = +V_{compartment}\cdot(Kflp1\cdot[Flp1\_off]\cdot[Cdc2\_on]\cdot(1+[Flp1\_on])) - V_{compartment}\cdot(Kflp1\cdot[Flp1\_on]\cdot[Cdc2\_off])$$

$$\frac{d([Flp1\_checkpoint]\cdot V_{compartment})}{dt} = +V_{compartment}\cdot(Kcds1\_flp1\cdot[Flp1\_off]\cdot[Cds1\_on])$$

$$\frac{d([Cdc25\_checkpoint]\cdot V_{compartment})}{dt} = +V_{compartment}\cdot\left(\frac{Kcds1\_cdc25\cdot[Cdc25\_on]\cdot[Cds1\_on]}{Jcdc25\_off+[Cdc25\_on]}\right)$$

$$Cdc2\_tot = [Cdc2\_on]+[Cdc2\_off]$$

$$Cdc25\_tot = [Cdc25\_on]+[Cdc25\_off]+[Cdc25\_checkpoint]$$

APPENDIX 2. Set of differential equations for the presented model

APPENDIX 3. RESUMEN EN ESPAÑOL

SOBRE ESTA TESIS

El estudio presentado en esta Tesis Doctoral se centra en la investigación de la función de la fosfatasa Flp1p (también conocida como Clp1p) de la familia Cdc14 en los mecanismos de vigilancia celular, especialmente en la cascada de señalización en respuesta al estrés replicativo y al daño en el DNA. Para ello se llevaron a cabo análisis genéticos y bioquímicos comparados de las mencionadas respuestas en cepas silvestres y mutadas para *flp1*, así como estudios de la expresión génica en respuesta a estrés. En el marco de esta tesis se está desarrollando así mismo un modelo matemático del *checkpoint* de replicación en colaboración con el grupo de Biología Computacional de Sistemas del Instituto Max Planck de Genética Molecular de Berlín, Alemania.

Este apéndice corresponde a un resumen en Español de la Tesis Doctoral "ANÁLISIS DE LA FUNCIÓN DE CDC14/FLP1 EN LA RESPUESTA A ESTRÉS GENOTÓXICO EN *Schizosaccharomyces pombe*" cuya memoria ha sido escrita en Inglés. Dado que nuestros resultados apuntan claramente a una implicación de la fosfatasa Flp1p en la ruta de señalización en respuesta a estrés replicativo, en este resumen nos centraremos en los análisis bioquímicos y genéticos realizados a este respecto. Los datos correspondientes a la respuesta a daño en el DNA, así como los estudios realizados utilizando otro tipo de aproximaciones teóricas y experimentales se pueden encontrar en la versión íntegra de la Tesis, referenciada como texto principal.

INTRODUCCIÓN

1. LOS MECANISMOS DE VIGILANCIA CELULARES ANTE ESTRÉS REPLICATIVO Y DAÑO AL DNA

En cada ciclo celular la replicación del material genético y su segregación entre las células hijas se ven afectados por una serie de factores intra- y extra-celulares que amenazan la estabilidad del genoma. Por ello en organismos eucariotas existen mecanismos moleculares conservados que preservan la integridad genética, denominados *checkpoints* (del inglés, puntos de control). Los *checkpoints* de respuesta a alteraciones en el DNA son cascadas de señalización por medio de las cuales se detecta la presencia de DNA no replicado o DNA dañado mediante proteínas sensoras que inducen una serie de respuestas encaminadas a garantizar la estabilidad del genoma. Estas respuestas incluyen el retraso o parada del ciclo celular, la estabilización de horquillas de replicación, procesos de reparación del DNA, la alteración del programa transcripcional, la alteración del patrón de la cromatina y mecanismos de muerte celular o apoptosis. A su vez existen mecanismos que permiten la reanudación de los procesos celulares y ciclo celular cuando la fuente de estrés desaparece o cuando el estrés persiste indefinidamente. Estos mecanismos se conocen como recuperación y adaptación respectivamente.

Los defectos en originar y transmitir las señales de vigilancia adecuadas pueden resultar en aneuploidía, acumulación de mutaciones y reordenamientos cromosómicos, procesos que se asocian a la muerte celular y el cáncer.

Schizosaccharomyces pombe es un organismo modelo de gran utilidad para el estudio de los *checkpoints*, debido a su relativa simplicidad y paralelismo con las células humanas. Los mecanismos de vigilancia del DNA en la levadura de fisión incluyen el *checkpoint* en respuesta al DNA no replicado durante fase S y el *checkpoint* en respuesta a lesiones en el DNA durante G2. Además, existe un *checkpoint* de intra-fase S, responsable de la ralentización de la progresión a través de dicha fase en respuesta a daño en el DNA detectado durante la replicación.

En *S. pombe* la proteína sensora principal de los *checkpoints* de DNA dañado o no adecuadamente replicado es Rad3p, una quinasa emparentada con ATM y ATR, las quinasas sensoras en mamíferos. El estrés replicativo y el daño al DNA producido en

fase S conlleva la activación mediante fosforilación por Rad3p de la quinasa efectora del *checkpoint* Cds1p (Murakami and Okayama, 1995; Lindsay *et al.*, 1998; Brondello *et al.*, 1999; Xu *et al.*, 2006), mientras que el daño al DNA activa la quinasa efectora Chk1p durante G2, también a través de Rad3p (Walworth *et al.*, 1993; Brondello *et al.*, 1999).

La activación de Cds1p y/o Chk1p resulta en una parada en el ciclo celular que impide la entrada en mitosis si el DNA está dañado o no está replicado completamente. Esta parada se produce mediante inhibición de la fosfatasa Cdc25p y potenciación de la actividad de la quinasa Mik1p (Furnari *et al.*, 1997; Rhind *et al.*, 1997; Furnari *et al.*, 1999; Rhind and Russell, 2001). Estos procesos resultan a su vez en la potenciación de la fosforilación en tirosina 15 de Cdc2p y en la correspondiente inhibición su actividad, de modo que se asegura que no se alcancen niveles de actividad quinasa suficientes para la entrada en mitosis.

Además de su función en ralentizar el ciclo celular en respuesta a alteraciones en el DNA, Cds1p desempeña un papel esencial en la protección y estabilización de horquillas de replicación conservando el ensamblaje del replisoma y manteniendo la estructura del DNA en un estado adecuado para la reanudación de la replicación (Lopes *et al.*, 2001; Tercero and Diffley, 2001; Sogo *et al.*, 2002; Noguchi *et al.*, 2003; Tercero *et al.*, 2003; Noguchi *et al.*, 2004; Meister *et al.*, 2005; Ansbach *et al.*, 2007). Las células delecionadas para *cds1* son capaces de frenar la progresión a través del ciclo celular gracias a la activación de Chk1p, pero rápidamente pierden viabilidad tras el estrés replicativo (Boddy *et al.*, 1998; Lindsay *et al.*, 1998), hecho que pone de manifiesto la importancia de la función estabilizadora específica de Cds1p.

2. LA FOSFATASA Flp1p

Flp1p y sus ortólogos

La familia de fosfatasas Cdc14 desempeña una importante función en la regulación negativa de las quinasas dependientes de ciclina mitóticas, CDKs mitóticas (del inglés, Cyclin Dependent Kinases), mediante la desfosforilación específica de residuos fosforilados por dichas quinasas (Visintin *et al.*, 1998; Kaiser *et al.*, 2002; Gray *et al.*, 2003). En *Saccharomyces cerevisiae* el gen *CDC14* es esencial para la viabilidad celular y los mutantes termosensibles paran su progresión celular en

telofase con niveles altos de actividad quinasa asociada al complejo Cdc28p-Clb (Wan *et al.*, 1992; Taylor *et al.*, 1997; Visintin *et al.*, 1998). Atendiendo a la similitud en la secuencia, se han encontrado miembros de la familia Cdc14 en varios organismos eucariotas, incluyendo *S. pombe* (Flp1p o Clp1p, del inglés cdc-fourteen-like-protein)*, Caenorhabditis elegans* (CeCDC-14)*, Xenopus laevis* (XCdc14A and XCdc14B) y *Homo sapiens* (hCdc14A and hCdc14B) (Li *et al.*, 1997; Cueille *et al.*, 2001; Trautmann *et al.*, 2001; Gruneberg *et al.*, 2002; Kaiser *et al.*, 2002; Krasinska *et al.*, 2007).

Las Cdc14 son fosfatasas de doble especificidad que comparten un núcleo de aproximadamente 300 aminoácidos en la zona amino terminal que incluye un dominio proteína-fosfatasa bien conservado entre los miembros de la familia (Gray *et al.*, 2003).

Las fosfatasas Cdc14 y el control de la salida de mitosis

En *S. cerevisiae* Cdc14p regula la salida de mitosis mediante desfosforilación y activación de sustratos de la CDK mitótica como la proteína Hct1p/Cdh1p, un componente del complejo promotor de anafase/ciclosoma APC/C (del inglés *anaphase promoting complex/cyclosome*) responsable de la ubiquitinación de las ciclinas mitóticas, o el inhibidor de CDK Sic1p, en ambos casos para conseguir una bajada de la actividad quinasa (Walworth *et al.*, 1993; Brondello *et al.*, 1999; Jaspersen *et al.*, 1999; Shou *et al.*, 1999; Visintin *et al.*, 1999).

En *S. pombe* Flp1p también regula la salida de mitosis, pero lo hace a través de un mecanismo diferente. Flp1p no desfosforila a Rum1p ni Ste9p (los homólogos de Sic1p y Hct1p), si no que antagoniza la actividad CDK desfosforilando y marcando para degradación a la fosfatasa Cdc25p, lo que indirectamente conlleva un aumento en la fosforilación en tirosina 15 de Cdc2p bajando su actividad quinasa (Cueille *et al.*, 2001; Trautmann *et al.*, 2001; Esteban *et al.*, 2004; Wolfe and Gould, 2004).

Los residuos fosforilados por CDK1 en la fosfatasa humana Cdc25A son sustratos *in vitro* de hCdc14A, y esta fosfatasa puede rescatar una deleción de *flp1* en *S. pombe* desfosforilando Cdc25p, sugiriendo un paralelismo en el mecanismo de salida de mitosis entre la levadura de fisión y los humanos (Vazquez-Novelle *et al.*, 2005; Esteban *et al.*, 2006). Sin embargo Hct1p también ha sido identificado como un sustrato de hCdc14A (Bembenek and Yu, 2001; Kaiser *et al.*, 2002).

La regulación de la actividad de las proteínas Cdc14

La actividad de las proteínas Cdc14 está regulada al menos en parte por su secuestro en el nucleolo y posterior liberación (Shou *et al.*, 1999; Visintin *et al.*, 1999; Bembenek and Yu, 2001; Cueille *et al.*, 2001; Trautmann *et al.*, 2001; Kaiser *et al.*, 2002).

En *S. cerevisiae* Cdc14p se encuentra secuestrada en el nucleolo en forma inactiva desde G1 hasta metafase mediante su unión con el inhibidor nucleolar Net1p/Cfi1p, miembro del complejo RENT (del inglés *regulator of nucleolar silencing and telophase*) (Shou *et al.*, 1999; Straight *et al.*, 1999; Visintin *et al.*, 1999; Traverso *et al.*, 2001). En anafase temprana, ScCdc14p es liberado del nucleolo mediante la acción coordinada de una serie de proteínas englobadas en la red de señalización FEAR (del inglés *cdc-fourteen early anaphase release*) (Stegmeier *et al.*, 2002; Azzam *et al.*, 2004). La red FEAR induce la fosforilación de Net1p/Cfi1p por CDK (Azzam *et al.*, 2004) y su disociación de Cdc14p (Queralt *et al.*, 2006). La red MEN (del inglés *mitotic exit network*) mantiene a la fosfatasa fuera del nucleolo durante la progresión a través de anaphase (Jaspersen *et al.*, 1998; Bardin *et al.*, 2000). Recientemente se ha descubierto que la propia Cdc14p es responsable de su inactivación al final de mitosis, ya que promueve la degradación de la polo quinasa Cdc5p (componente de la red FEAR y regulador clave de la red MEN) mediante la activación de APC/C-Cdh1p. La degradación de Cdc5p mediada por Cdc14p provoca el silenciamiento de las redes FEAR y MEN y promueve el retorno de la fosfatasa al nucleolo (Visintin *et al.*, 2008).

Mientras que ScCdc14p está secuestrada en el nucleolo hasta anafase, otros miembros de la familia Cdc14 no están regulados de la misma manera. Los ortólogos de *S. pombe* Flp1p, las isoformas humanas Cdc14A y B y Cdc14A de *Xenopus* sufren un cambio en su localización celular ya en la entrada a mitosis (Cueille *et al.*, 2001; Trautmann *et al.*, 2001; Kaiser *et al.*, 2002; Mailand *et al.*, 2002; Kaiser *et al.*, 2004).

La localización y las funciones de Flp1p

La serina/treonina fosfatasa Flp1p, al contrario que su ortóloga ScCdc14p, no es esencial y las células delecionadas para *flp1* sobreviven con un fenotipo avanzado en mitosis (Cueille *et al.*, 2001).

Flp1p controla la rápida degradación de Cdc25p al final de mitosis (Esteban *et al.*, 2004; Wolfe and Gould, 2004), lo que resulta en la potenciación de fosforilación inhibidora en tirosina 15 de Cdc2p y en la consiguiente bajada de actividad quinasa necesaria para la salida de mitosis. La acción de Flp1p es necesaria para la ubiquitinación de Cdc25p por APC/C en este punto del ciclo, de modo que las células delecionadas para *flp1* presentan niveles basales altos de Cdc25p. Como se ha mencionado anteriormente esta función podría estar conservada en eucariotas multicelulares.

En la levadura de fisión las células delecionadas para *flp1* entran en mitosis con un tamaño reducido, es decir presentan un fenotipo *wee (*Cueille *et al.,* 2001*;* Trautmann *et al.,* 2001*)*. La sobrexpresión de *flp1* provoca una parada de las células en G2 con Cdc25p desfosforilado, en un proceso dependiente de la actividad de Wee1p (Cueille *et al.*, 2001; Esteban *et al.*, 2004).

Además de su función durante la progresión celular, Flp1p es necesario para la efectividad del *checkpoint* de citoquinesis (Cueille *et al.*, 2001; Trautmann *et al.*, 2001; Trautmann and McCollum, 2005) y para una adecuada segregación cromosómica (Trautmann *et al.*, 2004).

Para desempeñar sus distintas funciones, Flp1p debe estar adecuadamente localizado en la célula. Durante un ciclo celular normal, Flp1p se localiza en el nucleolo y en el cuerpo polar del huso durante interfase, y en el núcleo, en el huso mitótico y en el anillo medial durante mitosis (Cueille *et al.*, 2001; Trautmann *et al.*, 2001).

Se desconocen los mecanismos por los cuales Flp1p permanece retenido en el nucleolo en interfase y es liberado a sus posiciones mitóticas en profase. Recientemente se ha identificado una proteína nucleolar, Dnt1p, que presenta homología de secuencia con ScNet1/Cfi1p, pero se ha demostrado que no es responsable del secuestro o inhibición de Flp1p (Jin *et al.*, 2007). Por otra parte, aunque los componentes de la red FEAR (separasa Esp1p, polo quinasa Cdc5p, Slk19p y Spo12p) están conservados en *S. pombe*, éstos no median la salida de Flp1p del nucleolo (Chen *et al.*, 2006). Una red de iniciación de septación, SIN (del inglés *septation initiation network*) se encarga de mantener a Flp1p en sus posiciones mitóticas hasta que se completa la citoquinesis. Esto es de especial importancia en caso de activación del *checkpoint* de citoquinesis (Cueille *et al.*, 2001; Mishra *et al.*, 2005). Se ha demostrado que Flp1p permanece en el citoplasma unido a la proteína

14-3-3 Rad24p en respuesta a defectos en citoquinesis (Mishra *et al* 2005.; Trautmann et al., 2005). La atenuación del SIN es necesaria para la correcta relocalización de Flp1p en el nucleolo al final de mitosis (Cueille *et al.*, 2001).

Ya en el núcleo Flp1p es inhibido mediante hiperfosforilación por CDK en los estadios tempranos de la mitosis. hCdc14A y XCdc14A también se encuentran hiperfosforiladas en mitosis temprana (Kaiser *et al.*, 2002; Kaiser *et al.*, 2004). Durante anafase Flp1p revierte la hiperfosforilación inhibidora mediante su autodesfosforilación. En esta fase alcanza la actividad catalítica necesaria para actuar sobre Cdc25p marcándola para degradación, de modo que se interrumpe el proceso de autoactivación de Cdc2p y se potencia la señalización de la red SIN (Esteban *et al.*, 2004; Wolfe and Gould, 2004).

OBJETIVOS

1. Dilucidar si la fosfatasa Flp1p de Schizosaccharomyces pombe está implicada en los mecanismos de respuesta a estrés genotóxico en dicho organismo.
2. Estudiar la función de la fosfatasa en la respuesta a estrés genotóxico: análisis de los fenotipos asociados a la mutación de *flp1* en el marco de la respuesta celular a alteraciones en el DNA.
3. Estudiar el mecanismo de acción de la fosfatasa Flp1p dentro de la respuesta a estrés genotóxico: análisis de la relación funcional de la fosfatasa con diferentes proteínas implicadas en los checkpoints de respuesta a estrés genotóxico.

RESULTADOS

En el ciclo celular vegetativo Flp1p regula la salida de mitosis provocando la inactivación de Cdc25p y su degradación rápida, promoviendo indirectamente la reducción de actividad quinasa necesaria en este punto del ciclo.

Una de las respuestas activadas por los mecanismos de vigilancia ante estrés replicativo es precisamente la reducción de la actividad de Cdc2p, en este caso para impedir la entrada en mitosis si la replicación del DNA no ha sido completa. Esta reducción de actividad quinasa se consigue en parte debido a la acción inhibidora de las proteínas efectoras del *checkpoint* sobre Cdc25p.

De este modo, las dianas de la cascada de señalización en respuesta a alteraciones en el DNA y las de la red que garantiza la salida de mitosis son similares. Este hecho nos llevó a investigar una posible implicación de Flp1p en la obtención de una respuesta celular adecuada en respuesta a estrés replicativo.

1. ESTUDIO DE LA LOCALIZACIÓN DE Flp1p DURANTE ESTRÉS REPLICATIVO

Flp1p se libera al núcleo en células que sufren estrés replicativo

Durante un ciclo celular normal Flp1p cambia de localización subcelular para llevar a cabo sus diferentes funciones. Flp1p está en el nucleolo y en el cuerpo polar de uso en interfase. En profase es liberado del nucleolo mediante un mecanismo desconocido para ocupar sus posiciones mitóticas, en el núcleo, huso mitótico y anillo medial (Cueille *et al.*, 2001; Trautmann *et al.*, 2001). Como se ha resaltado en la introducción, la presencia de Flp1p en sus posiciones mitóticas es importante para la regulación de la salida de mitosis y para una correcta segregación cromosómica. Por otra parte la retención de Flp1p en el citoplasma asegura una respuesta celular adecuada a defectos en citoquinesis.

Como primera aproximación a nuestro estudio, asumimos que si la fosfatasa estaba implicada en la respuesta a estrés replicativo probablemente se pudiera observar una salida de Flp1p del nucleolo en células sometidas a este tipo de estrés.

Con el fin de probar esta hipótesis, tratamos cultivos asíncronos en crecimiento exponencial de una cepa *flp1-GFP* con hidroxiurea (HU), sustancia inhibidora de la ribonucleótido reductasa que provoca estrés replicativo por depleción de nucleótidos. Después de dos horas de tratamiento con una concentración 12mM de la droga, la mayoría de las células de la población carecían de septo, tenían un solo núcleo y se habían alargado como consecuencia de la parada en fase S producida por el *checkpoint* ante el estrés replicativo. Para estudiar en detalle la localización de Flp1p-GFP durante el estrés, utilizamos Gar2p-RFP como marcador nucleolar y tinción con Hoechst para distinguir la parte no nucleolar del núcleo. Como se puede observar en la Figura 2 del texto principal Flp1p es nuclear en células tratadas con HU. Observando la localización de la proteína nucleolar Gar2p-RFP podemos además concluir que el cambio de localización observado en Flp1p no es general para las proteínas nucleolares, y que la concentración de HU utilizada no produce una reestructuración del nucleolo.

Mediante un estudio más detallado a los realizados anteriormente (Cueille *et al.*, 2001; Trautmann *et al.*, 2001) probamos que Flp1p permanece localizado en el nucleolo y en el cuerpo polar del uso durante toda la fase S cuando el *checkpoint* de replicación no está activo (Figura 3). De este modo, el cambio de localización de Flp1p observado tras el tratamiento con HU se debe específicamente a la acción de la droga y no es inherente al punto del ciclo celular en el cual las células están bloqueadas.

El mismo cambio de localización se observó en cultivos sincronizados de la cepa *cdc10-129 flp1-GFP* y tratados con HU en fase S (Figura 4).

La acumulación nuclear de Flp1p durante estrés replicativo depende de un checkpoint activo y de Cds1p

Por otra parte quisimos probar que el cambio de localización de Flp1p estaba asociado a la activación del *checkpoint* y no era un efecto colateral del tratamiento con HU. Para ello comprobamos la localización de Flp1p-GFP en un mutante *rad3*, incapaz de producir un bloqueo en la progresión celular durante el tratamiento con HU al carecer de la principal proteína detectora del estrés replicativo. Tras dos horas de tratamiento la localización de Flp1p-GFP era indistinguible de la observada en células

sin tratar, probando que la liberación al núcleo de la fosfatasa tras el tratamiento con drogas dependía de un mecanismo de vigilancia activo (Figura 5).

A la vista de este resultado, era de esperar que se produjera una relocalización de Flp1p a sus posiciones típicas de ciclo celular una vez que se retirara la fuente de estrés replicativo. En efecto, tratando las células durante tres horas con HU 12mM y liberando a las células del bloqueo mediante lavados y trasferencia a medio libre de droga, observamos Flp1p de vuelta en el nucleolo en un intervalo tan corto como 5 minutos después de la liberación y más tarde, cuando las células entran en fase M, en sus localizaciones mitóticas (Figura 6).

Como las dos ramas de respuesta ante alteraciones del DNA están íntimamente relacionadas y el cambio de localización de Flp1p se podía observar tanto en respuesta a estrés replicativo como a daño en el DNA (véase texto principal), quisimos comprobar si la liberación de Flp1p al nucleolo dependía específicamente de alguna de las dos proteínas efectoras del *checkpoint*, Cds1p y Chk1p. Para ello estudiamos la localización de Flp1p en cepas delecionadas para *cds1* o *chk1* respectivamente. En cultivos sin tratar de Δ*cds1 flp1-GFP* o Δ*chk1 flp1-GFP* la localización de la fosfatasa era igual a la observada en un tipo silvestre (Figuras 7 y 8). Sin embargo en cultivos tratados con HU 12mM durante 2 horas, Flp1p seguía localizado en el nucleolo y en el cuerpo polar del huso en el mutante *cds1* (localización correspondiente a fase S sin perturbar), mientras que en el mutante *chk1* si se observaba liberación al núcleo. Este resultado indica que la localización de Flp1p durante estrés replicativo dependía directa o indirectamente de Cds1p.

2. Flp1p interacciona funcionalmente con la proteína 14-3-3 Rad24p en respuesta a estrés replicativo

Rad24p y Flp1p interaccionan en respuesta a defectos durante la citoquinesis (Mishra *et al.*, 2005; Trautmann and McCollum, 2005). Rad24p y Rad25p están además implicados en la correcta localización y función de proteínas implicadas en la respuesta a alteraciones en el DNA. Daño en el DNA estimula la asociación de Chk1p con las proteínas 14-3-3 y esta interacción afecta tanto la localización como la función de Chk1p como efector del *checkpoint* (Chen *et al.*, 1999a; Dunaway *et al.*, 2005). Además Rad24p media la exclusión nuclear de Cdc25p asociada a la respuesta celular a alteraciones en el DNA (Lopez-Girona *et al.*, 1999; Lopez-Girona *et al.*, 2001a).

Estas funciones descritas de las proteínas 14-3-3 asociadas al *checkpoint* nos impulsaron a estudiar si Rad24p estaba implicado en la acumulación nuclear de Flp1p en respuesta a estrés replicativo. La acumulación de Flp1p en el núcleo depende en efecto de un alelo funcional de *rad24+*, sugiriendo que Rad24p es necesario para la liberación de la fosfatasa del nucleolo asociada a la activación del *checkpoint* (Figura 24A).

Por otra parte, por medio de un ensayo de purificación por afinidad de la etiqueta GST, en el cual purificamos GST-Rad24p e inmunodetectamos Flp1p-Ha, probamos que Flp1p y Rad24p interaccionan físicamente en respuesta al *checkpoint* (Figura 24B).

Por otra parte también probamos que el doble mutante ∆*rad24* ∆*flp1* es más sensible a HU que el mutante simple ∆*rad*24 (Figura 24C). Esta interacción genética indica que la deleción de *flp1* agrava el defecto de la deleción de *rad24* en respuesta a estrés replicativo, sugiriendo que Flp1p y Rad24 tendrían alguna función relacionada con vías del *checkpoint* independientes.

3. ANÁLISIS DE LA RELACIÓN ENTRE Flp1p Y Cds1p EN LA RESPUESTA A ESTRÉS REPLICATIVO

Flp1p y Cds1p interaccionan físicamente

Como hemos mostrado anteriormente el cambio de localización de Flp1p durante la respuesta a estrés replicativo depende de Cds1p. Una posibilidad interesante era que la mediación de este cambio de localización se debiera a una interacción *in vivo* entre la quinasa y la fosfatasa. Para ello purificamos GST-Flp1p en una cepa *cds1p-Ha* en cultivos sin droga y tras el tratamiento con HU e inmunodetectamos Cds1p-Ha. También realizamos el ensayo purificando la forma catalíticamente inactiva de Flp1p ($Flp1p^{CS}$), ya que habíamos demostrado anteriormente en nuestro grupo que GST-$Flp1p^{CS}$ interacciona más eficientemente con Cdc25p *in vivo* que GST-Flp1p (Esteban et al., 2004; Vazquez-Novelle et al., 2005).

Mientras que en células no tratadas no se detecta interacción, pudimos observar interacción entre Cds1p y Flp1p en células tratadas con agentes genotóxicos (Figura 12A). Tal y como esperábamos el resultado es más evidente en cepas que expresan

la forma catalíticamente inactiva de Flp1p, en las cuales la interacción se puede detectar incluso en células sin tratar.

Estos resultados indican que Cds1p y Flp1p pueden formar un complejo *in vivo*, sugiriendo la existencia de una interacción enzima/sustrato.

Δflp1 presenta bajos niveles proteicos de Cds1p y actividad reducida de la quinasa en respuesta a estrés replicativo

Flp1p como fosfatasa podría tener una función en la atenuación de la respuesta celular a estrés replicativo revertiendo fosforilaciones activadores sobre algún efector de la cascada de señalización correspondiente. Dadas nuestras observaciones que relacionan Flp1p y Cds1p, quisimos comprobar si Flp1p ejercía alguna acción sobre Cds1p en respuesta a estrés replicativo.

Como primera aproximación, analizamos los niveles de Cds1p durante estrés replicativo en una cepa delecionada para *flp1* mediante *western blot*. Mientras en una cepa silvestre los niveles de Cds1p aumentan significativamente en las primeras 2 horas de tratamiento con HU, en Δ*flp1* este aumento en los niveles de la quinasa es mucho más moderado (Figura 12B).

A continuación analizamos si la actividad de Cds1p en respuesta al *checkpoint* se veía afectada en una deleción de *flp1*. Para ello inmunoprecipitamos Cds1p-Ha de células sin tratar y de cultivos tratados con HU cada media hora durante 4 horas de exposición a la droga. La actividad de Cds1p-Ha se ensayó usando MBP (del inglés *myelin basic protein*) como sustrato. La actividad medida se normalizó teniendo en cuenta la cantidad de Cds1p-Ha presente en cada muestra. La actividad de la fosfatasa en un fondo Δ*flp1* resultó ser más baja que la detectada en la cepa silvestre durante el tratamiento completo (Figura 12C). La diferencia más significativa en activación de la quinasa entre las dos cepas se detectó a los 90 minutos de tratamiento, tiempo de máxima activación, momento en el cual Δ*flp1* presenta una actividad reducida en un 30% con respecto al tipo silvestre.

Tomados en conjunto estos resultados desmienten nuestra hipótesis de partida, ya que al presentar Δ*flp1* niveles y actividad reducidos de la quinasa, la función de Flp1p en la respuesta a estrés replicativo parecería ser la de activar a Cds1p bien

directamente, bien a través de la regulación de algún inhibidor o activador de la quinasa.

Cds1p fosforila a Flp1p *in vitro* y esta fosforilación potencia su actividad fosfatasa

Anteriormente demostramos que el cambio de localización de Flp1p-GFP durante estrés replicativo depende de la presencia de Cds1p. Esto parecía indicar que la quinasa ejerce una acción sobre Flp1p en el marco de la respuesta celular a este tipo de estrés. Por ello decidimos estudiar si Flp1p podía ser fosforilado por Cds1p activo.

Para ello inmunoprecipitamos Cds1p-Ha de cultivos en los que habíamos inducido estrés replicativo mediante la adición de HU 12mM o MMS 0.033% y ensayamos su actividad sobre MBP. Con ello comprobamos que la quinasa estaba activa en ambas condiciones, alcanzando un máximo de activación tras 2 horas de tratamiento. A continuación realizamos ensayos quinasa de Cds1p inmunoprecipitado en el punto de máxima activación sobre GST-Flp1p purificado por afinidad de células Δ*cds1*. Como referencia también utilizamos GST como sustrato. El ensayo resultó en la fosforilación específica de Flp1p por Cds1p activado por la acción de ambas drogas (Figura 13A). También detectamos una banda inferior de fosforilación específica que corresponde a una proteína que inmunoprecipita con la quinasa.

Este resultado tomado en conjunto con nuestras observaciones anteriores sugeriría que Flp1p es un sustrato de Cds1p en el marco de la respuesta celular a estrés replicativo o daño al DNA asociado a la replicación.

A continuación probamos si la fosforilación de Flp1p por Cds1p alteraba su actividad fosfatasa *in vitro*. Para ello realizamos ensayos de fosforilación análogos a los descritos anteriormente (utilizando ATP no hidrolizable para evitar el posible efecto de la autofosforilación de Flp1p durante el posterior ensayo fosfatasa). Posteriormente la actividad de este GST-Flp1p fosforilado fue comparada con la de GST-Flp1p sometido al mismo proceso pero sin adición de la quinasa. Mediante ensayos fosfatasa sobre DiFMUP probamos que la fosforilación de Flp1p por Cds1p estimula su actividad fosfatasa (Figura 13B).

El mutante *flp1-9A*: obtención de una forma de Flp1p no fosforilable por Cds1p

A continuación procedimos a la identificación de los residuos en los cuales ocurría la reacción de fosforilación de Flp1p por Cds1p con el objetivo de construir una forma de Flp1p no fosforilable por la quinasa. De este modo, la cepa modificada resultante sería una herramienta de gran utilidad para estudiar las consecuencias de abolir la propuesta modificación *in vivo* de Flp1p por Cds1p en condiciones de estrés replicativo.

Mediante espectrometría de masas se identificó la fosforilación del residuo Serina 468 en GST-Flp1p fosforilado por Cds1p activado tanto en HU como en MMS. Este residuo se encuentra en un sitio RXXS consenso para la fosforilación por la quinasa humana homóloga Chk2p en Cdc25A (O'Neill *et al.*, 2002).

Mutación de esta Serina al residuo no fosforilable Alanina no fue suficiente para abolir al fosforilación por Cds1p de la correspondiente proteína mutada (GST-Flp1p^{S468A}).

Existen otros 8 sitios RXXS en Flp1p situados respectivamente en las Serinas 160, 396, 408, 467, 493, 499, 513 and 537. Mediante mutación de los 9 sitios RXXS a RXXA en el plásmido pREP-KZ-*flp1+* nos permitió expresar una forma de la proteína (GST-Flp1p^{9A}) no fosforilable por Cds1p *in vitro* (Figura 14).

A la vista de nuestros resultados anteriores que relacionaban Cds1p con el cambio de localización de Flp1p y mostraban la capacidad de la quinasa de fosforilar a Flp1p *in vitro*, una posibilidad interesante era que la mutación de los sitios de fosforilación por Cds1p conllevase una anulación *in vivo* de la salida de Flp1p al núcleo en condiciones de estrés replicativo.

Para probar esta hipótesis, construimos una versión integrada de la proteína mutada marcada con EGFP (en adelante *flp1-9A*), tal y como se describe en la sección MATERIALES Y MÉTODOS del texto principal.

La proteína Flp1p-9A-EGFP presentaba localización silvestre de Flp1p durante el ciclo mitótico normal. Sin embargo mientras el tratamiento con HU 12mM causa una liberación de Flp1p en la cepa silvestre, la proteína mutante Flp1p-9A-EGFP permanece en sus localizaciones interfásicas en condiciones de estrés replicativo (Figura 15).

Este resultado es especialmente interesante ya que apunta la existencia de una modificación por fosforilación *in vivo* de Flp1p por Cds1p en respuesta a estrés replicativo que sería responsable del cambio de localización de la fosfatasa observado en estas condiciones.

4. ANÁLISIS DE LA INFLUENCIA DE Flp1p EN LA RESPUESTA CELULAR EFICIENTE ANTE ESTRÉS REPLICATIVO

Comportamiento de los mutantes de *flp1* en respuesta a tratamientos prolongados con HU

Para estudiar el efecto de Flp1p en respuesta al *checkpoint* estudiamos como primera aproximación si la deleción de *flp1* producía sensibilidad a la exposición prolongada a HU o agravaba el fenotipo asociado a la deleción de *cds1*. Como se muestra en la figura 16, *Δflp1* se comporta de manera silvestre en cuanto a supervivencia en HU y no añade ningún defecto observable al crecimiento impedido de los mutantes del *checkpoint* a las concentraciones estudiadas. El mutante *flp1-9A* presenta un comportamiento similar a *Δflp1* en estas condiciones. Sin embargo, observamos que las células carentes de *flp1* son sensibles a la exposición prolongada a estrés replicativo tras sincronización en G1.

Comportamiento de los mutantes de *flp1* la respuesta celular a corto plazo inducida por estrés replicativo

Como acabamos de señalar, el mutante *flp1-9A* no presenta defectos observables en cuanto a supervivencia en tratamientos prolongados con HU. Sin embargo después de dos horas de tratamiento con esta droga en medio líquido, pudimos detectar que mientras que una cepa silvestre sólo presentaba un 9% de células en mitosis, en el mutante el porcentaje de células que no estaban respondiendo adecuadamente al bloqueo ascendía al 24%. Mediante análisis del índice de septación en el tipo silvestre, *flp1-9A* y *Δflp1* durante tratamiento con HU probamos que este defecto en el bloqueo se producía de forma similar para ambos mutantes de *flp1* (Figura 17).

A continuación quisimos estudiar si este defecto en bloqueo en respuesta a estrés replicativo se traducía en una segregación aberrante del DNA durante mitosis. Para ello monitorizamos la presencia de células binucleadas (tanto normales como aberrantes o *cut*) durante el tratamiento con HU en cultivos control de *cdc10-129* y *cdc10-129 ⊿rad3* así como de *cdc10-129 ⊿flp1* sincronizados en G1 y liberados en presencia de la droga. También analizamos el contenido en DNA y el tamaño de las células mediante citometría de flujo. El estudio se realizó en cultivos sincronizados para descartar que los defectos observados pudieran ser consecuencia de una dinámica de progresión celular alterada en el mutante. En la Figura 18 se puede observar que efectivamente existe un defecto asociado a la deleción de *flp1* presentando más de un 15% de mitosis aberrantes a partir de las dos horas de tratamiento con HU. Esto se refleja en el análisis de citometría de flujo en el que se observan contenidos en DNA inferiores a 1C para el mutante. Este defecto es moderado en comparación con el observado para el mutante *⊿rad3*.

La acumulación de Cdc25p y el aumento de fosforilación en Tirosina 15 de Cdc2p no se ven afectadas por la deleción de *⊿flp1*

La respuesta celular a alteraciones en el DNA incluye la exclusión de Cdc25p del núcleo (Lopez-Girona *et al.*, 1999; Lopez-Girona *et al.*, 2001b). Dada la implicación de Flp1p durante el ciclo mitótico en la degradación de Cdc25p para garantizar la bajada en la actividad quinasa de Cdc2p necesaria para la salida de mitosis (Esteban *et al.*, 2004; Wolfe and Gould, 2004), decidimos analizar si la deleción de *flp1* alteraba la cinética de acumulación de Cdc25p o el patrón de fosforilación en Tirosina 15p de Cdc2p durante estrés replicativo.

Mediante detección de Cdc25p y Tyr15 de Cdc2p a diferentes tiempos del tratamiento observamos que no existía diferencia apreciable entre las correspondientes cinéticas para la cepa silvestre y *Δflp1* (Figura 20).

Estos resultados indican que Flp1p no desempeña un papel relevante en el control de los niveles de Cdc25p o en la regulación de la actividad de Cdc2p durante la acción del *checkpoint*.

Los mutantes de *flp1* presentan focos de recombinación en respuesta a estrés replicativo

Además de regular la actividad de Cdc2p en respuesta a estrés replicativo, Cds1p desempeña funciones en la protección del DNA que Chk1p no puede realizar. Como se ha detallado en la introducción, Cds1p juega un papel central en la estabilización de horquillas de replicación en situaciones de estrés y en la coordinación de los procesos de recuperación, garantizando el ensamblaje del replisoma durante el bloqueo y regulando los procesos de recombinación. Cds1p está implicada en la inhibición de la recombinación en las horquillas paradas mediante estabilización de sus componentes y a través de la regulación de la endonucleasa Mus81p, de la helicasa Rqh1p y de Rad60p. Así las cepas delecionadas para *cds1* presentan múltiples focos de recombinación durante tratamiento con HU (Meister *et al.*, 2005), no observados en una cepa silvestre. La concentración de Rad22p (homólogo a ScRad52p) en focos nucleares es indicativo de la inducción de recombinación homóloga (Lisby *et al.*, 2001; Du *et al.*, 2003; Meister *et al.*, 2003; Noguchi *et al.*, 2003).

Dadas las evidencias que relacionan Flp1p con Cds1p durante estrés replicativo y a la vista de que la ausencia de Flp1p no parece alterar significativamente el patrón de fosforilación en Tirosina 15 de Cdc2p, decidimos estudiar si la interacción de Flp1p y Cds1p podía estar relacionada con las funciones de la quinasa en la inhibición de recombinación en horquillas pausadas.

Para ello analizamos la presencia de focos de recombinación en cultivos sin tratar y sometidos a estrés replicativo del tipo silvestre, Δ*cds1,* Δ*flp1* y *flp1-9A* detectando Rad22p-YFP (Figura 21). Mediante clasificación de los núcleos dependiendo del número de focos observados en ellos (sin focos, un foco, múltiples focos), observamos que mientras que la cepa silvestre presentaba un número similar de focos en células tratadas y sin tratar, los mutantes de *flp1* sufrían una acumulación considerable de focos múltiples como consecuencia del tratamiento con HU. El número de focos observado en los mutantes de *flp1* es moderado en comparación con la acumulación detectada en Δ*cds1*. Estos resultados apuntan una vez más a una pérdida de función de la repuesta celular a alteraciones en el DNA en mutantes de *flp1* y son coherentes con nuestra anterior observación correlacionando la presencia de Flp1p con una activación completa de Cds1p.

DISCUSIÓN

El mantenimiento de la estabilidad del genoma a través de generaciones de células hijas asegura una transmisión fiel de la información genética que la célula contiene. Toda célula asegura dicha estabilidad durante la replicación del genoma en fase S y también tiene que hacerlo cuando eventualmente se expone a daños en el DNA o a paradas o pausas circunstanciales en la replicación. Para ello las células eucariotas tienen mecanismos de control que protegen activamente la integridad del genoma. Estos mecanismos están conservados en todos los sistemas modelo estudiados hasta el momento.

El trabajo presentado se centra en el estudio de la fosfatasa Flp1p (cdc fourteen-like phosphatase, también llamada Clp1p) en el organismo modelo *S. pombe* y en papel que desempeña en los *checkpoints* frente a alteraciones en el DNA.

La serina/treonina fosfatasa Flp1p de *S. pombe* desempeña funciones descritas en ciclo celular, controlando la degradación rápida de la proteína Cdc25p al final de mitosis (Esteban et al., 2004; Wolfe and Gould, 2004), necesaria para la bajada de actividad quinasa de Cdc2p correspondiente a este punto del ciclo.

En la levadura de fisión al igual que en eucariotas superiores, la entrada a mitosis se retrasa en células que tienen su integridad genómica comprometida, bien por daño al DNA o por estrés replicativo. Este retraso se regula por medio de cascadas de señalización o *checkpoint*s que inhiben de Cdc25p y estimulan la actividad de Mik1p mediante las quinasas Cds1p y Chk1p (Furnari et al., 1999), que se traduce en inhibición de Cdc2p (Rhind et al., 1997).

Nuestra hipótesis inicial de trabajo para investigar la implicación de la fosfatasa Flp1 en las cascadas de respuesta a daño genotóxico se basó en la similitud existente entre las dianas reguladoras de la salida mitosis, proceso en el cual Flp1p participa activamente, y las que en última instancia son responsables de la ralentización del ciclo celular en caso de amenaza a la integridad genómica.

Nuestra investigación nos ha llevado a plantear, en efecto, una función para Flp1p dentro de la respuesta a estrés replicativo. Sorprendentemente, esta función es independiente de la que la fosfatasa desempeña durante el ciclo vegetativo, ya que la deleción de *flp1* no conlleva una alteración significativa de la dinámica de

acumulación de Cdc25p ni de la inhibición por fosforilación de Cdc2p características de la respuesta celular a estrés genotóxico.

Los resultados de nuestro estudio indican que la respuesta celular a estrés replicativo produce una alteración en la situación sub-celular de Flp1p y claramente relacionan a Flp1p con la principal quinasa efectora del *checkpoint*, Cds1p. Hemos probado que la interacción entre Flp1p y Cds1p es importante para la consecución de una completa activación de la quinasa durante la respuesta a estrés replicativo. También hemos demostrado que Flp1p interacciona físicamente y/o genéticamente con otras proteínas implicadas en la correcta señalización celular en condiciones de estrés, como Rad24p (véase texto principal). Además la alteración de los niveles proteicos de Flp1p o su localización resulta en la desregulación de la respuesta a estrés, produciéndose efectos como pérdida de eficiencia en el bloqueo de la progresión celular o la aparición de focos de recombinación.

1. LA LOCALIZACIÓN DE Flp1p EN RESPUESTA A ESTRÉS GENOTÓXICO

Durante un ciclo normal Flp1p se localiza en el nucleolo y en el cuerpo polar del huso durante la replicación del DNA en fase S (Cueille *et al.*, 2001; Trautmann *et al.*, 2001) y este trabajo). Sin embargo cuando se activa la respuesta celular por la detección de estrés replicativo, Flp1p se libera del nucleolo para ocupar todo el núcleo. Este cambio de localización no ocurre en una cepa delecionada para *rad3* indicando que es un efecto específico de la activación del *checkpoint.* Flp1p permanece también en su localización nucleolar durante estrés replicativo en un mutante ∆*rad24*, indicando que la proteína 14-3-3 estaría implicada en el transporte de la fosfatasa. Sin embargo, se debe tener en cuenta que la deleción de *rad24* afecta a numerosos procesos celulares (las células ∆*rad24* presentan una morfología tipo *orb* además de localización alterada de proteínas implicadas en el ciclo celular y los mecanismos de vigilancia), así que la deslocalización de Flp1p en este mutante podría ser la consecuencia de un entorno celular alterado.

Mientras que se desconoce el mecanismo por el cual durante el ciclo mitótico Flp1p se libera al núcleo en mitosis temprana, los datos que presentamos en este trabajo demuestran que es la acción de Cds1p, la que libera a Flp1p al núcleo en condiciones de estrés replicativo: Flp1p no sale del nucleolo durante el tratamiento con HU en una cepa ∆*cds1* y por otra parte, la mutación de los sitios de fosforilación *in vitro* de Cds1p

en Flp1p anula la liberación de la fosfatasa al núcleo específicamente durante situaciones de estrés. En concordancia con este argumento también pudimos detectar interacción física entre Flp1p y Cds1p en respuesta a estrés replicativo.

De acuerdo con nuestros resultados y ya que Cds1p parece estar localizada en mayor o menor medida en toda la célula (Brondello *et al.*, 1999; Matsuyama *et al.*, 2006), la fosforilación de Flp1p por la fosfatasa podría tener lugar en el nucleolo. En futuros estudios se analizará detalladamente la regulación espacio-temporal de la acción de Cds1p sobre Flp1p.

Flp1p en el núcleo en situaciones de estrés replicativo

En *S. cerevisiae*, la respuesta a daño al DNA conlleva la activación de las dos rutas de respuesta, asociadas a Chk1p y Rad53 respectivamente, lo que resulta en la inhibición de las redes FEAR y MEN. Esto produce la retención de ScCdc14p en el nucleolo durante la activación del *checkpoint (*Liang and Wang*, 2007)*.

En nuestro estudio hemos probado que en *S. pombe* la respuesta celular a alteraciones en el DNA provoca la liberación de Flp1p al núcleo (véase también texto principal). Dado que ambas fosfatasas ortólogas están implicadas en la regulación de la actividad mitótica de CDK durante la progresión celular, el hecho de que la activación del *checkpoint* provoque reacciones opuestas en el control de la localización de Flp1p y ScCdc14p es en principio desconcertante. Por otra parte, la predominante localización nucleolar de Flp1p durante tratamiento con MMS, así como la degradación de la fosfatasa en estas condiciones (véase texto principal), podría indicar que la respuesta celular en *S. pombe* provoca la inhibición de la actividad de Flp1p específicamente ante daño en el DNA, de forma similar a lo que ocurre en *S. cerevisiae*, pero a través de otro mecanismo.

Estudios en *S. cerevisiae* han planteado, por otra parte, que el secuestro de ScCdc14p en el nucleolo durante la fase S podría ser necesario para que se produzcan adecuadamente las modificaciones mediadas por CDK necesarias para la replicación del DNA. Si se fuerza una localización de ScCdc14p al núcleo, ésta es capaz de desfosforilar los factores de replicación Sld2p y Dpb2p, que se fosforilan por Clb5-CDK durante fase S para garantizar la asociación de polimerasas a los orígenes de replicación. De este modo la presencia forzada de Cdc14p en el núcleo en ausencia de ciclina Clb5p dificulta la compleción de la replicación del DNA (Bloom

and Cross, 2007). En este estudio hemos probado que la respuesta del *checkpoint* a DNA no replicado causa una acumulación de Flp1p en el núcleo. En vista de las observaciones mencionadas para *S. cerevisiae*, se podría especular que la liberación de Flp1p al núcleo durante estrés replicativo puede producirse para inhibir de alguna manera la maquinaria de replicación revirtiendo los efectos de los complejos mitóticos de fase S.

Nuestros resultados relativos a la mutación de *flp1* durante estrés replicativo muestran que *Δflp1* y *flp1-9A* presentan fenotipos similares de recombinación, defecto en el bloqueo asociado al *checkpoint* y activación reducida de Cds1p. Esto indicaría que estos defectos se derivan de la ausencia de Flp1p en el núcleo en respuesta al *checkpoint*. El hecho de que *flp1-9A* presente actividad reducida de Cds1p como *Δflp1* prueba que la salida de Flp1p al núcleo es un suceso clave en el control de la actividad de la quinasa efectora del *checkpoint* durante estrés replicativo. Los defectos en el bloqueo mediado por el *checkpoint* y la aparición de focos de recombinación en los mutantes de *flp1* se pueden justificar apelando a la reducción en la actividad de Cds1p. Sin embargo, hemos probado por otra parte que la expresión de genes implicados en recombinación y en otros aspectos de la respuesta a estrés replicativo se ve alterada en una deleción de *flp1* (véase texto principal), por lo que no se puede descartar una función directa de la forma nuclear de Flp1p en la regulación transcripcional asociada al *checkpoint.*

2. La relación funcional entre Cds1p y Flp1p: un mecanismo para la adecuada activación de la respuesta celular a estrés replicativo

Los resultados presentados en este estudio relacionan a Flp1p con el principal efector de la cascada de señalización en respuesta a estrés replicativo, Cds1p. Sorprendentemente, nuestras evidencias experimentales indican que existe tanto una acción de Cds1p sobre Flp1p como de la fosfatasa sobre la quinasa en el marco de la respuesta celular a estrés replicativo.

De acuerdo con nuestras observaciones Cds1p tendría una acción sobre Flp1p para regular su localización, su estabilidad y su actividad ya que: (1) Flp1p no se libera al núcleo en un fondo *Δcds1*. (2) La quinasa activada por el *checkpoint* es capaz de fosforilar Flp1p *in vitro*. Esta fosforilación tendría lugar muy probablemente también *in vivo* con el fin de liberar Flp1p al núcleo en respuesta a estrés replicativo, ya que la

mutación de todos los sitios putativos de fosforilación por Cds1p en Flp1p (lo que anula la fosforilación de la fosfatasa por la quinasa *in vitro*) conlleva una abolición específica del cambio de localización de Flp1p en respuesta al *checkpoint*. (3) La fosforilación de Flp1p por Cds1p *in vitro* produce una potenciación de su actividad fosfatasa. Nuestros resultados preliminares *in vivo* muestran que la actividad de la fosfatasa aumenta tras dos horas de tratamiento, observación que refuerza la relación propuesta entre fosforilación, localización y aumento de la actividad fosfatasa.

Por otra parte Flp1p regula directa o indirectamente los niveles y la actividad de Cds1p: (1) Δ*flp1* presenta niveles reducidos de Cds1p en respuesta a estrés replicativo en comparación con el tipo silvestre. (2) En un fondo Δ*flp1* Cds1p es menos activa que en células silvestres en respuesta a HU y MMS.

En lo que respecta a la sucesión temporal de las distintas interacciones funcionales entre Cds1p y Flp1p, el hecho de que la disrupción de la acción de Cds1p sobre Flp1p en el mutante *flp1-9A* produzca el mismo tipo de defectos en respuesta al *checkpoint* que la deleción de *flp1* parece indicar que la acción de Flp1p sobre Cds1p (regulando su actividad y niveles) sería dependiente de un paso previo en el cual la quinasa activa la fosfatasa.

Hemos probado que la deleción de *flp1* causa dos defectos diferentes en la respuesta celular a estrés replicativo. Por una parte pudimos observar la aparición de focos de recombinación durante la activación del *checkpoint* en Δ*flp1* y además observamos que un porcentaje moderado de células de esta cepa escapa al bloqueo producido por el *checkpoint* en estas condiciones, y progresan en el ciclo dando lugar a mitosis aberrantes. Estos dos defectos se pueden explicar por la bajada en la actividad quinasa de Cds1p observada en Δ*flp1.*

Todas estas observaciones nos llevan a plantear un modelo para el mecanismo de la implicación de Flp1p en la respuesta celular a estrés replicativo (Figura D1): en respuesta a estrés replicativo Cds1p es activada mediante fosforilación por Rad3p. Una vez activado Cds1p fosforilaría a Flp1p para regular su salida del nucleolo y su actividad. Rad24p podría estar implicado en este mecanismo de localización. Finalmente la forma nuclear de Flp1p activaría directa o indirectamente la activación completa de Cds1p.

¿Una acción directa de Flp1p sobre Cds1p?

Una importante pregunta abierta en nuestro trabajo es si el control de Flp1p sobre Cds1p se debe a una acción directa. Un control directo sería una posibilidad interesante, ya que, de acuerdo con nuestros resultados esto implicaría que la desfosforilación de la quinasa produciría su activación. En futuros estudios se analizará si la fosfatasa puede potenciar la activación de Cds1p favoreciendo la dimerización o autofosforilación de la quinasa, pasos descritos de su activación. Apuntando a una acción directa de la fosfatasa sobre la quinasa, pudimos detectar interacción física entre Cds1p y Flp1p durante estrés genotóxico. La interacción se detecta mejor cuando utilizamos una forma catalíticamente inactiva de Flp1p, lo que indicaría que la interacción podría ocurrir para desfosforilar Cds1p. Sin embargo, estos datos no deberían considerarse concluyentes ya que hay que tener en cuenta que la interacción se ha detectado en condiciones de sobre-expresión de Flp1p y que la señal que observamos es débil incluso cuando utilizamos la forma catalíticamente inactiva de la fosfatasa.

Por otra parte, considerando una regulación indirecta de Cds1p por la fosfatasa, Flp1p podría estar actuando sobre proteínas implicadas en la regulación de los niveles y actividad de Cds1p. Así, posibles dianas de Flp1p serían las proteínas implicadas en replicación y estabilización de horquillas, ya que muchas de ellas median la activación de Cds1p en condiciones de estrés replicativo. Entre las posibles dianas sería interesante considerar las chaperonas Ssa1p y Ssa2p, no caracterizadas en *S. pombe*, que podrían tener una función en la estabilización de Cds1p. El estudio de la posible función de estas chaperonas en la activación de Cds1p durante estrés genotóxico nos parece de especial interés en el marco de nuestra investigación ya que hemos comprobado que Ssa2p co-purifica con GST-Flp1p.

3. CONSTRUCCIÓN DE UN MODELO MATEMÁTICO PARA LA RESPUESTA CELULAR A ESTRÉS REPLICATIVO EN *S. pombe*

Como se ha indicado anteriormente, en el marco de esta Tesis se está desarrollando un modelo matemático del *checkpoint* de replicación en colaboración con el grupo de Biología Computacional de Sistemas del Instituto Max Planck de Genética Molecular de Berlín, Alemania. Los detalles de la construcción de este modelo así como los

resultados obtenidos y nuestros planes para mejora del mismo se pueden encontrar en el texto principal.

Nuestro modelo está formado por dos módulos: uno mediante el cual reproducimos el ciclo celular mitótico y un submódulo para la acción del *checkpoint* en condiciones de estrés replicativo. Una de las principales novedades que aporta nuestro modelo, es que el módulo para el ciclo celular es autónomo y autoregulado, es decir, es capaz de reproducir la naturaleza oscilatoria de la progresión celular sin la necesidad de introducir ninguna orden matemática ajena al esquema biológico empleado.

Otra característica destacable de nuestro modelo global es que ha sido ajustado a datos experimentales, es decir, el conjunto de parámetros del sistema ha sido seleccionado de manera que no sólo se reproduce el comportamiento biológico cuantitativo, si no que responde a perfiles dinámicos específicos representados por cinéticas experimentales.

También se han empleado cinéticas experimentales en el estadio de validación del modelo.

Como se detalla en el texto principal, se está trabajando en la construcción de un modelo mejorado principalmente en lo que respecta a la regulación de Cdc25p.

Una vez que obtengamos un modelo ajustado y validado capaz de reproducir, de acuerdo con nuestras exigencias, el comportamiento dinámico de todas las especies implicadas, someteremos al sistema a diferentes análisis. Con ellos pretendemos obtener información que nos ayude a comprender algunos aspectos de nuestra investigación (el mecanismo que subyace al defecto observado en repuesta al *checkpoint* tanto de Δ*flp1* como de *opflp1;* una descripción matemática de los umbrales de actividad de Cds1p asociados a estabilidad de horquillas y al bloqueo de la progresión celular, y de la función de Flp1p en alcanzarlos, etc).

Por otra parte, tanto el módulo para el ciclo celular como el submódulo para la respuesta celular a estrés replicativo, pueden ser usados como base para modelos más descriptivos y/o exhaustivos. Esto será de especial interés cuando se disponga de un mayor número de datos experimentales de concentraciones proteicas y velocidades de reacción en *S. pombe*.

CONCLUSIONES

1. La fosfatasa Flp1p está implicada en la respuesta celular a estrés genotóxico:
    a. Los mutantes estudiados de *flp1* presentan defectos moderados en la respuesta celular a estrés replicativo.
    b. La fosfatasa cambia de localización en respuesta a estrés genotóxico de manera dependiente de la activación del checkpoint.
        i. La liberación de Flp1p al núcleo en condiciones de estrés replicativo ocurre dependientemente de Cds1p y ocurre con gran probabilidad por fosforilación de la fosfatasa.
        ii. La liberación de Flp1p al núcleo es decisiva para sus funciones ya que la retención de Flp1p en el nucleolo en condiciones de estrés provoca fenotipos análogos a la deleción de *flp1*.
    c. En respuesta a estrés genotóxico Flp1p no actúa sobre Cdc25p ni afecta indirectamente de forma significativa los niveles de fosforilación en Tirosina 15 de Cdc2p, en contraste con su función durante ciclo celular y a pesar de que la respuesta celular a estrés replicativo conlleva la regulación de Cdc25p y Cdc2p.
    d. Existe una estrecha relación funcional entre Flp1p y Cds1p, que resulta en la correcta activación de la quinasa en respuesta a estrés replicativo. Los fenotipos asociados a una respuesta celular parcialmente deficiente en respuesta a estrés replicativo en los mutantes de *flp1* se pueden explicar en su mayoría por la actividad atenuada de Cds1p que presentan.
    e. No podemos descartar que Flp1p desempeñe un papel activo en la regulación transcripcional en respuesta al *checkpoint*.
2. Se ha construido un modelo matemático capaz de simular el ciclo celular mitótico y la respuesta celular a estrés replicativo en *S. pombe*. Un modelo mejorado está en proceso, el cual una vez validado, pretendemos emplear como herramienta para esclarecer algunos aspectos de nuestra investigación relativos al mecanismo de acción de Flp1p en la respuesta a estrés replicativo.

BIBLIOGRAPHY

Aguda, B.D. (1999a). Instabilities in phosphorylation-dephosphorylation cascades and cell cycle checkpoints. Oncogene *18*, 2846-2851.

Aguda, B.D. (1999b). A quantitative analysis of the kinetics of the G(2) DNA damage checkpoint system. Proceedings of the National Academy of Sciences of the United States of America *96*, 11352-11357.

Aguda, B.D., and Algar, C.K. (2003). A structural analysis of the qualitative networks regulating the cell cycle and apoptosis. Cell Cycle *2*, 538-544.

Ahn, J., and Prives, C. (2002). Checkpoint kinase 2 (Chk2) monomers or dimers phosphorylate Cdc25C after DNA damage regardless of threonine 68 phosphorylation. The Journal of Biological Chemistry *277*, 48418-48426.

Ahn, J.Y., Li, X., Davis, H.L., and Canman, C.E. (2002). Phosphorylation of threonine 68 promotes oligomerization and autophosphorylation of the Chk2 protein kinase via the forkhead-associated domain. The Journal of Biological Chemistry *277*, 19389-19395.

Akamatsu, Y., Dziadkowiec, D., Ikeguchi, M., Shinagawa, H., and Iwasaki, H. (2003). Two different Swi5-containing protein complexes are involved in mating-type switching and recombination repair in fission yeast. Proceedings of the National Academy of Sciences of the United States of America *100*, 15770-15775.

al-Khodairy, F., and Carr, A.M. (1992). DNA repair mutants defining G2 checkpoint pathways in Schizosaccharomyces pombe. EMBO Journal *11*, 1343-1350.

al-Khodairy, F., Fotou, E., Sheldrick, K.S., Griffiths, D.J., Lehmann, A.R., and Carr, A.M. (1994). Identification and characterization of new elements involved in checkpoint and feedback controls in fission yeast. Molecular Biology of the Cell *5*, 147-160.

Alarcon, T., and Tindall, M.J. (2007). Modelling cell growth and its modulation of the G1/S transition. Bulletin of Mathematical Biology *69*, 197-214.

Alfa, C.E., Booher, R., Beach, D., and Hyams, J.S. (1989). Fission yeast cyclin: subcellular localisation and cell cycle regulation. Journal of Cell Science Supplement *12*, 9-19.

Alfa, C.E., Ducommun, B., Beach, D., and Hyams, J.S. (1990). Distinct nuclear and spindle pole body population of cyclin-cdc2 in fission yeast. Nature *347*, 680-682.

Alfieri, R., Merelli, I., Mosca, E., and Milanesi, L. (2007). A data integration approach for cell cycle analysis oriented to model simulation in systems biology. BMC Systems Biology *1*, 35.

Alfieri, R., Merelli, I., Mosca, E., and Milanesi, L. (2008). The cell cycle DB: a systems biology approach to cell cycle analysis. Nucleic Acids Research *36*, D641-645.

Ansbach, A.B., Noguchi, C., Klansek, I.W., Heidlebaugh, M., Nakamura, T.M., and Noguchi, E. (2007). RFCCtf18 and the Swi1-Swi3 Complex Function in Separate and Redundant Pathways Required for the Stabilization of Replication Forks to Facilitate Sister Chromatid Cohesion in *Schizosaccharomyces pombe*. Molecular Biology of the Cell *19*, 595-607.

Arcangioli, B., Copeland, T.D., and Klar, A.J. (1994). Sap1, a protein that binds to sequences required for mating-type switching, is essential for viability in Schizosaccharomyces pombe. Molecular and Cellular Biology *14*, 2058-2065.

Azzam, R., Chen, S.L., Shou, W., Mah, A.S., Alexandru, G., Nasmyth, K., Annan, R.S., Carr, S.A., and Deshaies, R.J. (2004). Phosphorylation by cyclin B-Cdk underlies release of mitotic exit activator Cdc14 from the nucleolus. Science *305*, 516-519.

Bailis, J.M., Luche, D.D., Hunter, T., and Forsburg, S.L. (2008). MCM proteins interact with checkpoint and recombination proteins to promote S phase genome stability. Molecular and Cellular Biology. *28*, 1724-38.

Barberis, M., Klipp, E., Vanoni, M., and Alberghina, L. (2007). Cell size at S phase initiation: an emergent property of the G1/S network. PLoS Computational Biology *3*, e64.

Bardin, A.J., Visintin, R., and Amon, A. (2000). A mechanism for coupling exit from mitosis to partitioning of the nucleus. Cell *102*, 21-31.

Barker, D.G., White, J.H., and Johnston, L.H. (1987). Molecular characterisation of the DNA ligase gene, CDC17, from the fission yeast *Schizosaccharomyces pombe*. European Journal of Biochemistry / FEBS *162*, 659-667.

Bembenek, J., and Yu, H. (2001). Regulation of the anaphase-promoting complex by the dual specificity phosphatase human Cdc14a. The Journal of Biological Chemistry *276*, 48237-48242.

Benito, J., Martin-Castellanos, C., and Moreno, S. (1998). Regulation of the G1 phase of the cell cycle by periodic stabilization and degradation of the p25rum1 CDK inhibitor. EMBO Journal *17*, 482-497.

Bloom, J., and Cross, F.R. (2007). Novel role for Cdc14 sequestration: Cdc14 dephosphorylates factors that promote DNA replication. Molecular and Cellular Biology *27*, 842-853.

Boddy, M.N., Furnari, B., Mondesert, O., and Russell, P. (1998). Replication checkpoint enforced by kinases Cds1 and Chk1. Science *280*, 909-912.

Boddy, M.N., Lopez-Girona, A., Shanahan, P., Interthal, H., Heyer, W.D., and Russell, P. (2000). Damage tolerance protein Mus81 associates with the FHA1 domain of checkpoint kinase Cds1. Molecular and Cellular Biology *20*, 8758-8766.

Boddy, M.N., Shanahan, P., McDonald, W.H., Lopez-Girona, A., Noguchi, E., Yates, I.J., and Russell, P. (2003). Replication checkpoint kinase Cds1 regulates recombinational repair protein Rad60. Molecular and Cellular Biology *23*, 5939-5946.

Booher, R.N., Alfa, C.E., Hyams, J.S., and Beach, D.H. (1989). The fission yeast cdc2/cdc13/suc1 protein kinase: regulation of catalytic activity and nuclear localization. Cell *58*, 485-497.

Breeding, C.S., Hudson, J., Balasubramanian, M.K., Hemmingsen, S.M., Young, P.G., and Gould, K.L. (1998). The cdr2(+) gene encodes a regulator of G2/M progression and cytokinesis in Schizosaccharomyces pombe. Molecular Biology of the Cell *9*, 3399-3415.

Brondello, J.M., Boddy, M.N., Furnari, B., and Russell, P. (1999). Basis for the checkpoint signal specificity that regulates Chk1 and Cds1 protein kinases. Molecular and Cellular Biology *19*, 4262-4269.

Buck, V., Ng, S.S., Ruiz-Garcia, A.B., Papadopoulou, K., Bhatti, S., Samuel, J.M., Anderson, M., Millar, J.B., and McInerny, C.J. (2004). Fkh2p and Sep1p regulate mitotic gene transcription in fission yeast. Journal of Cell Science *117*, 5623-5632.

Bueno, A., Richardson, H., Reed, S.I., and Russell, P. (1991). A fission yeast B-type cyclin functioning early in the cell cycle. Cell *66*, 149-159.

Byun, T.S., Pacek, M., Yee, M.C., Walter, J.C., and Cimprich, K.A. (2005). Functional uncoupling of MCM helicase and DNA polymerase activities activates the ATR-dependent checkpoint. Genes & Development *19*, 1040-1052.

Caligiuri, M., Connolly, T., and Beach, D. (1997). Ran1 functions to control the Cdc10/Sct1 complex through Puc1. Molecular Biology of the Cell *8*, 1117-1128.

Canman, C.E. (2003). Checkpoint mediators: relaying signals from DNA strand breaks. Current Biology *13*, R488-490.

Capasso, H., Palermo, C., Wan, S., Rao, H., John, U.P., O'Connell, M.J., and Walworth, N.C. (2002). Phosphorylation activates Chk1 and is required for checkpoint-mediated cell cycle arrest. Journal of Cell Science *115*, 4555-4564.

Caspari, T., Murray, J.M., and Carr, A.M. (2002). Cdc2-cyclin B kinase activity links Crb2 and Rqh1-topoisomerase III. Genes & Development *16*, 1195-1208.

Cerutti, L., and Simanis, V. (1999). Asymmetry of the spindle pole bodies and spg1p GAP segregation during mitosis in fission yeast. Journal of Cell Science *112*, 2313-2321.

Ciliberto, A., Lukacs, A., Toth, A., Tyson, J.J., and Novak, B. (2005). Rewiring the exit from mitosis. Cell Cycle *4*, 1107-1112.

Ciliberto, A., Petrus, M.J., Tyson, J.J., and Sible, J.C. (2003). A kinetic model of the cyclin E/Cdk2 developmental timer in Xenopus laevis embryos. Biophysical Chemistry *104*, 573-589.

Cokus, S., Rose, S., Haynor, D., Gronbech-Jensen, N., and Pellegrini, M. (2006). Modelling the network of cell cycle transcription factors in the yeast Saccharomyces cerevisiae. BMC Bioinformatics *7*, 381.

Coleman, T.R., Tang, Z., and Dunphy, W.G. (1993). Negative regulation of the wee1 protein kinase by direct action of the nim1/cdr1 mitotic inducer. Cell *72*, 919-929.

Collura, A., Blaisonneau, J., Baldacci, G., and Francesconi, S. (2005). The fission yeast Crb2/Chk1 pathway coordinates the DNA damage and spindle checkpoint in response to replication stress induced by topoisomerase I inhibitor. Molecular and Cellular Biology *25*, 7889-7899.

Correa-Bordes, J., Gulli, M.P., and Nurse, P. (1997). p25rum1 promotes proteolysis of the mitotic B-cyclin p56cdc13 during G1 of the fission yeast cell cycle. EMBO Journal *16*, 4657-4664.

Coulon, S., Noguchi, E., Noguchi, C., Du, L.L., Nakamura, T.M., and Russell, P. (2006). Rad22Rad52-dependent repair of ribosomal DNA repeats cleaved by Slx1-Slx4 endonuclease. Molecular Biology of the Cell *17*, 2081-2090.

Cox, M.M. (2001). Historical overview: searching for replication help in all of the rec places. Proceedings of the National Academy of Sciences of the United States of America *98*, 8173-8180.

Creanor, J., and Mitchison, J.M. (1996). The kinetics of the B cyclin p56cdc13 and the phosphatase p80cdc25 during the cell cycle of the fission yeast Schizosaccharomyces pombe. Journal of Cell Science *109*, 1647-1653.

Csikasz-Nagy, A., Gyorffy, B., Alt, W., Tyson, J.J., and Novak, B. (2008). Spatial controls for growth zone formation during the fission yeast cell cycle. Yeast *25*, 59-69.

Csikasz-Nagy, A., Kapuy, O., Gyorffy, B., Tyson, J.J., and Novak, B. (2007). Modeling the septation initiation network (SIN) in fission yeast cells. Current Genetics *51*, 245-255.

Cueille, N., Salimova, E., Esteban, V., Blanco, M., Moreno, S., Bueno, A., and Simanis, V. (2001). Flp1, a fission yeast orthologue of the s. cerevisiae CDC14 gene, is not required for cyclin degradation or rum1p stabilisation at the end of mitosis. Journal of Cell Science *114*, 2649-2664.

Chang, D.Y., and Lu, A.L. (2005). Interaction of checkpoint proteins Hus1/Rad1/Rad9 with DNA base excision repair enzyme MutY homolog in fission yeast, Schizosaccharomyces pombe. The Journal of Biological Chemistry *280*, 408-417.

Chang, L., and Gould, K.L. (2000). Sid4p is required to localize components of the septation initiation pathway to the spindle pole body in fission yeast. Proceedings of the National Academy of Sciences of the United States of America *97*, 5249-5254.

Chen, C.T., Peli-Gulli, M.P., Simanis, V., and McCollum, D. (2006). *S. pombe* FEAR protein orthologs are not required for release of Clp1/Flp1 phosphatase from the nucleolus during mitosis. Journal of Cell Science *119*, 4462-4466.

Chen, D., Toone, W.M., Mata, J., Lyne, R., Burns, G., Kivinen, K., Brazma, A., Jones, N., and Bahler, J. (2003). Global transcriptional responses of fission yeast to environmental stress. Molecular Biology of the Cell *14*, 214-229.

Chen, K.C., Calzone, L., Csikasz-Nagy, A., Cross, F.R., Novak, B., and Tyson, J.J. (2004). Integrative analysis of cell cycle control in budding yeast. Molecular Biology of the Cell *15*, 3841-3862.

Chen, K.C., Csikasz-Nagy, A., Gyorffy, B., Val, J., Novak, B., and Tyson, J.J. (2000). Kinetic analysis of a molecular model of the budding yeast cell cycle. Molecular Biology of the Cell *11*, 369-391.

Chen, L., Liu, T.H., and Walworth, N.C. (1999a). Association of Chk1 with 14-3-3 proteins is stimulated by DNA damage. Genes & Development *13*, 675-685.

Chen, P., Gatei, M., O'Connell, M.J., Khanna, K.K., Bugg, S.J., Hogg, A., Scott, S.P., Hobson, K., and Lavin, M.F. (1999b). Chk1 complements the G2/M checkpoint defect and radiosensitivity of ataxia-telangiectasia cells. Oncogene *18*, 249-256.

Cho, H.P., Liu, Y., Gomez, M., Dunlap, J., Tyers, M., and Wang, Y. (2005). The dual-specificity phosphatase CDC14B bundles and stabilizes microtubules. Molecular and Cellular Biology *25*, 4541-4551.

Chu, Z., Li, J., Eshaghi, M., Peng, X., Karuturi, R.K., and Liu, J. (2007). Modulation of cell cycle-specific gene expressions at the onset of S phase arrest contributes to the robust DNA replication checkpoint response in fission yeast. Molecular Biology of the Cell *18*, 1756-1767.

Daga, R.R., and Jimenez, J. (1999). Translational control of the cdc25 cell cycle phosphatase: a molecular mechanism coupling mitosis to cell growth. Journal of Cell Science *112 Pt 18*, 3137-3146.

Dalgaard, J.Z., and Klar, A.J. (2000). swi1 and swi3 perform imprinting, pausing, and termination of DNA replication in *S. pombe*. Cell *102*, 745-751.

de Vries, F.A., Zonneveld, J.B., de Groot, A.J., Koning, R.I., van Zeeland, A.A., and Pastink, A. (2007). Schizosaccharomyces pombe Rad22A and Rad22B have similar biochemical properties and form multimeric structures. Mutation Research *615*, 143-152.

den Elzen, N.R., and O'Connell, M.J. (2004). Recovery from DNA damage checkpoint arrest by PP1-mediated inhibition of Chk1. EMBO Journal *23*, 908-918.

Doe, C.L., Ahn, J.S., Dixon, J., and Whitby, M.C. (2002). Mus81-Eme1 and Rqh1 involvement in processing stalled and collapsed replication forks. The Journal of Biological Chemistry *277*, 32753-32759.

Doe, C.L., Osman, F., Dixon, J., and Whitby, M.C. (2004). DNA repair by a Rad22-Mus81-dependent pathway that is independent of Rhp51. Nucleic Acids Research *32*, 5570-5581.

Du, L.L., Moser, B.A., and Russell, P. (2004). Homo-oligomerization is the essential function of the tandem BRCT domains in the checkpoint protein Crb2. The Journal of Biological Chemistry *279*, 38409-38414.

Du, L.L., Nakamura, T.M., Moser, B.A., and Russell, P. (2003). Retention but not recruitment of Crb2 at double-strand breaks requires Rad1 and Rad3 complexes. Molecular and Cellular Biology *23*, 6150-6158.

Ducommun, B., Draetta, G., Young, P., and Beach, D. (1990). Fission yeast cdc25 is a cell-cycle regulated protein. Biochemical and Biophysical Research Communications *167*, 301-309.

Dunaway, S., Liu, H.Y., and Walworth, N.C. (2005). Interaction of 14-3-3 protein with Chk1 affects localization and checkpoint function. Journal of Cell Science *118*, 39-50.

Durocher, D., Henckel, J., Fersht, A.R., and Jackson, S.P. (1999). The FHA domain is a modular phosphopeptide recognition motif. Molecular Cell *4*, 387-394.

Durocher, D., Taylor, I.A., Sarbassova, D., Haire, L.F., Westcott, S.L., Jackson, S.P., Smerdon, S.J., and Yaffe, M.B. (2000). The molecular basis of FHA domain:phosphopeptide binding specificity and implications for phospho-dependent signaling mechanisms. Molecular Cell *6*, 1169-1182.

Edwards, R.J., Bentley, N.J., and Carr, A.M. (1999). A Rad3-Rad26 complex responds to DNA damage independently of other checkpoint proteins. Nature Cell Biology *1*, 393-398.

Eng, K., Naqvi, N.I., Wong, K.C., and Balasubramanian, M.K. (1998). Rng2p, a protein required for cytokinesis in fission yeast, is a component of the actomyosin ring and the spindle pole body. Current Biology *8*, 611-621.

Enoch, T., Carr, A.M., and Nurse, P. (1992). Fission yeast genes involved in coupling mitosis to completion of DNA replication. Genes & Development *6*, 2035-2046.

Espinoza, F.H., Farrell, A., Erdjument-Bromage, H., Tempst, P., and Morgan, D.O. (1996). A cyclin-dependent kinase-activating kinase (CAK) in budding yeast unrelated to vertebrate CAK. Science *273*, 1714-1717.

Esteban, V., Blanco, M., Cueille, N., Simanis, V., Moreno, S., and Bueno, A. (2004). A role for the Cdc14-family phosphatase Flp1p at the end of the cell cycle in controlling the rapid degradation of the mitotic inducer Cdc25p in fission yeast. Journal of Cell Science *117*, 2461-2468.

Esteban, V., Vazquez-Novelle, M.D., Calvo, E., Bueno, A., and Sacristan, M.P. (2006). Human Cdc14A reverses CDK1 phosphorylation of Cdc25A on serines 115 and 320. Cell Cycle, 2894-2898.

Faure, A., Naldi, A., Chaouiya, C., and Thieffry, D. (2006). Dynamical analysis of a generic Boolean model for the control of the mammalian cell cycle. Bioinformatics *22*, e124-131.

Featherstone, C., and Russell, P. (1991). Fission yeast p107wee1 mitotic inhibitor is a tyrosine/serine kinase. Nature *349*, 808-811.

Feng, W., Collingwood, D., Boeck, M.E., Fox, L.A., Alvino, G.M., Fangman, W.L., Raghuraman, M.K., and Brewer, B.J. (2006). Genomic mapping of single-stranded DNA in hydroxyurea-challenged yeasts identifies origins of replication. Nature Cell Biology *8*, 148-155.

Ferreira, M.G., and Cooper, J.P. (2001). The fission yeast Taz1 protein protects chromosomes from Ku-dependent end-to-end fusions. Molecular Cell *7*, 55-63.

Fisher, D.L., and Nurse, P. (1996). A single fission yeast mitotic cyclin B p34cdc2 kinase promotes both S-phase and mitosis in the absence of G1 cyclins. EMBO Journal *15*, 850-860.

Fisher, R.P., and Morgan, D.O. (1994). A novel cyclin associates with MO15/CDK7 to form the CDK-activating kinase. Cell *78*, 713-724.

Forbes, K.C., Humphrey, T., and Enoch, T. (1998). Suppressors of cdc25p overexpression identify two pathways that influence the G2/M checkpoint in fission yeast. Genetics *150*, 1361-1375.

Ford, J.C., al-Khodairy, F., Fotou, E., Sheldrick, K.S., Griffiths, D.J., and Carr, A.M. (1994). 14-3-3 protein homologs required for the DNA damage checkpoint in fission yeast. Science *265*, 533-535.

Forsburg, S.L. (2008). The MCM helicase: linking checkpoints to the replication fork. Biochemical Society Transactions *36*, 114-119.

Foss, E.J. (2001). Tof1p regulates DNA damage responses during S phase in Saccharomyces cerevisiae. Genetics *157*, 567-577.

Froget, B., Blaisonneau, J., Lambert, S., and Baldacci, G. (2007). Cleavage of Stalled Forks by Fission Yeast Mus81/Eme1 in Absence of DNA Replication Checkpoint. Molecular Biology of the Cell.

Furnari, B., Blasina, A., Boddy, M.N., McGowan, C.H., and Russell, P. (1999). Cdc25 inhibited in vivo and in vitro by checkpoint kinases Cds1 and Chk1. Molecular Biology of the Cell *10*, 833-845.

Furnari, B., Rhind, N., and Russell, P. (1997). Cdc25 mitotic inducer targeted by chk1 DNA damage checkpoint kinase. Science *277*, 1495-1497.

Furuya, K., Poitelea, M., Guo, L., Caspari, T., and Carr, A.M. (2004). Chk1 activation requires Rad9 S/TQ-site phosphorylation to promote association with C-terminal BRCT domains of Rad4TOPBP1. Genes & Development *18*, 1154-1164.

Garcia, V., Furuya, K., and Carr, A.M. (2005). Identification and functional analysis of TopBP1 and its homologs. DNA Repair *4*, 1227-1239.

Gatti, L., Chen, D., Beretta, G.L., Rustici, G., Carenini, N., Corna, E., Colangelo, D., Zunino, F., Bahler, J., and Perego, P. (2004). Global gene expression of fission yeast in response to cisplatin. Cellular and Molecular Life Sciences *61*, 2253-2263.

Goldbeter, A. (1991). A minimal cascade model for the mitotic oscillator involving cyclin and cdc2 kinase. Proceedings of the National Academy of Sciences of the United States of America *88*, 9107-9111.

Golub, E.I. (1988). 'One minute' transformation of competent E. coli by plasmid DNA. Nucleic Acids Research *16*, 1641.

Gordon, C., McGurk, G., Dillon, P., Rosen, C., and Hastie, N.D. (1993). Defective mitosis due to a mutation in the gene for a fission yeast 26S protease subunit. Nature *366*, 355-357.

Gordon, C., McGurk, G., Wallace, M., and Hastie, N.D. (1996). A conditional lethal mutant in the fission yeast 26 S protease subunit mts3+ is defective in metaphase to anaphase transition. The Journal of Biological Chemistry *271*, 5704-5711.

Gotter, A.L. (2003). Tipin, a novel timeless-interacting protein, is developmentally co-expressed with timeless and disrupts its self-association. Journal of Molecular Biology *331*, 167-176.

Gray, C.H., Good, V.M., Tonks, N.K., and Barford, D. (2003). The structure of the cell cycle protein Cdc14 reveals a proline-directed protein phosphatase. EMBO Journal *22*, 3524-3535.

Gruneberg, U., Glotzer, M., Gartner, A., and Nigg, E.A. (2002). The CeCDC-14 phosphatase is required for cytokinesis in the Caenorhabditis elegans embryo. The Journal of Cell Biology *158*, 901-914.

Guertin, D.A., Chang, L., Irshad, F., Gould, K.L., and McCollum, D. (2000). The role of the sid1p kinase and cdc14p in regulating the onset of cytokinesis in fission yeast. EMBO Journal *19*, 1803-1815.

Haber, J.E. (1999). DNA recombination: the replication connection. Trends in Biochemical Sciences *24*, 271-275.

Harris, S., Kemplen, C., Caspari, T., Chan, C., Lindsay, H.D., Poitelea, M., Carr, A.M., and Price, C. (2003). Delineating the position of rad4+/cut5+ within the DNA-structure checkpoint pathways in Schizosaccharomyces pombe. Journal of Cell Science *116*, 3519-3529.

Hayles, J., Fisher, D., Woollard, A., and Nurse, P. (1994). Temporal order of S phase and mitosis in fission yeast is determined by the state of the p34cdc2-mitotic B cyclin complex. Cell *78*, 813-822.

Hermand, D., and Nurse, P. (2007). Cdc18 enforces long-term maintenance of the S phase checkpoint by anchoring the Rad3-Rad26 complex to chromatin. Molecular Cell *26*, 553-563.

Hoops, S., Sahle, S., Gauges, R., Lee, C., Pahle, J., Simus, N., Singhal, M., Xu, L., Mendes, P., and Kummer, U. (2006). COPASI--a COmplex PAthway SImulator. Bioinformatics *22*, 3067-3074.

Hope, J.C., Cruzata, L.D., Duvshani, A., Mitsumoto, J., Maftahi, M., and Freyer, G.A. (2007). Mus81-Eme1-dependent and -independent crossovers form in mitotic cells during double-strand break repair in Schizosaccharomyces pombe. Molecular and Cellular Biology *27*, 3828-3838.

Hou, M.C., Salek, J., and McCollum, D. (2000). Mob1p interacts with the Sid2p kinase and is required for cytokinesis in fission yeast. Current Biology *10*, 619-622.

Jaspersen, S.L., Charles, J.F., and Morgan, D.O. (1999). Inhibitory phosphorylation of the APC regulator Hct1 is controlled by the kinase Cdc28 and the phosphatase Cdc14. Current Biology *9*, 227-236.

Jaspersen, S.L., Charles, J.F., Tinker-Kulberg, R.L., and Morgan, D.O. (1998). A late mitotic regulatory network controlling cyclin destruction in Saccharomyces cerevisiae. Molecular Biology of the Cell *9*, 2803-2817.

Jin, Q.W., Ray, S., Choi, S.H., and McCollum, D. (2007). The nucleolar Net1/Cfi1-related protein Dnt1 antagonizes the septation initiation network in fission yeast. Molecular Biology of the Cell *18*, 2924-2934.

Kai, M., Boddy, M.N., Russell, P., and Wang, T.S. (2005). Replication checkpoint kinase Cds1 regulates Mus81 to preserve genome integrity during replication stress. Genes & Development *19*, 919-932.

Kai, M., Furuya, K., Paderi, F., Carr, A.M., and Wang, T.S. (2007). Rad3-dependent phosphorylation of the checkpoint clamp regulates repair-pathway choice. Nature Cell Biology *9*, 691-697.

Kaiser, B.K., Nachury, M.V., Gardner, B.E., and Jackson, P.K. (2004). Xenopus Cdc14 alpha/beta are localized to the nucleolus and centrosome and are required for embryonic cell division. BMC Cell Biology *5*, 27.

Kaiser, B.K., Zimmerman, Z.A., Charbonneau, H., and Jackson, P.K. (2002). Disruption of centrosome structure, chromosome segregation, and cytokinesis by misexpression of human Cdc14A phosphatase. Molecular Biology of the Cell *13*, 2289-2300.

Kaldis, P., Sutton, A., and Solomon, M.J. (1996). The Cdk-activating kinase (CAK) from budding yeast. Cell *86*, 553-564.

Kanoh, J., and Russell, P. (1998). The protein kinase Cdr2, related to Nim1/Cdr1 mitotic inducer, regulates the onset of mitosis in fission yeast. Molecular Biology of the Cell *9*, 3321-3334.

Katou, Y., Kanoh, Y., Bando, M., Noguchi, H., Tanaka, H., Ashikari, T., Sugimoto, K., and Shirahige, K. (2003). S-phase checkpoint proteins Tof1 and Mrc1 form a stable replication-pausing complex. Nature *424*, 1078-1083.

Keeney JB, Boeke JD. (1994) Efficient Targeted Integration at Leu1-32 and Ura4-294 in Schizosaccharomyces pombe. Genetics. 136(3):849–856

Khasanov, F.K., Salakhova, A.F., Chepurnaja, O.V., Korolev, V.G., and Bashkirov, V.I. (2004). Identification and characterization of the rlp1+, the novel Rad51 paralog in the fission yeast Schizosaccharomyces pombe. DNA Repair *3*, 1363-1374.

Kim, S.M., and Huberman, J.A. (2001). Regulation of replication timing in fission yeast. EMBO Journal *20*, 6115-6126.

Kim, W.J., Lee, S., Park, M.S., Jang, Y.K., Kim, J.B., and Park, S.D. (2000). Rad22 protein, a rad52 homologue in Schizosaccharomyces pombe, binds to DNA double-strand breaks. The Journal of Biological Chemistry *275*, 35607-35611.

Kolpakov, F., Poroikov, V., Sharipov, R., Kondrakhin, Y., Zakharov, A., Lagunin, A., Milanesi, L., and Kel, A. (2007). CYCLONET--an integrated database on cell cycle regulation and carcinogenesis. Nucleic Acids Research *35*, D550-556.

Kondo, T., Wakayama, T., Naiki, T., Matsumoto, K., and Sugimoto, K. (2001). Recruitment of Mec1 and Ddc1 checkpoint proteins to double-strand breaks through distinct mechanisms. Science *294*, 867-870.

Kovelman, R., and Russell, P. (1996). Stockpiling of Cdc25 during a DNA replication checkpoint arrest in Schizosaccharomyces pombe. Molecular and Cellular Biology *16*, 86-93.

Krasinska, L., de Bettignies, G., Fisher, D., Abrieu, A., Fesquet, D., and Morin, N. (2007). Regulation of multiple cell cycle events by Cdc14 homologues in vertebrates. Experimental Cell Research *313*, 1225-1239.

Kushner, S. (1978). An improved method for transformation of Escherichia coli with colE1 derived plasmids. Elsevier.

Lee, C.H., and Chung, J.H. (2001). The hCds1 (Chk2)-FHA domain is essential for a chain of phosphorylation events on hCds1 that is induced by ionizing radiation. The Journal of Biological Chemistry *276*, 30537-30541.

Lee, J.K., Seo, Y.S., and Hurwitz, J. (2003). The Cdc23 (Mcm10) protein is required for the phosphorylation of minichromosome maintenance complex by the Dfp1-Hsk1 kinase. Proceedings of the National Academy of Sciences of the United States of America *100*, 2334-2339.

Lee, M.S., Enoch, T., and Piwnica-Worms, H. (1994). mik1+ encodes a tyrosine kinase that phosphorylates p34cdc2 on tyrosine 15. The Journal of Biological Chemistry *269*, 30530-30537.

Li, L., Ernsting, B.R., Wishart, M.J., Lohse, D.L., and Dixon, J.E. (1997). A family of putative tumor suppressors is structurally and functionally conserved in humans and yeast. The Journal of Biological Chemistry *272*, 29403-29406.

Liang, F., and Wang, Y. (2007). DNA damage checkpoints inhibit mitotic exit by two different mechanisms. Molecular and Cellular Biology *27*, 5067-5078.

Lindsay, H.D., Griffiths, D.J., Edwards, R.J., Christensen, P.U., Murray, J.M., Osman, F., Walworth, N., and Carr, A.M. (1998). S-phase-specific activation of Cds1 kinase defines a subpathway of the checkpoint response in Schizosaccharomyces pombe. Genes & Development *12*, 382-395.

Lisby, M., Rothstein, R., and Mortensen, U.H. (2001). Rad52 forms DNA Repair and recombination centers during S phase. Proceedings of the National Academy of Sciences of the United States of America *98*, 8276-8282.

Liu, C., Powell, K.A., Mundt, K., Wu, L., Carr, A.M., and Caspari, T. (2003). Cop9/signalosome subunits and Pcu4 regulate ribonucleotide reductase by both checkpoint-dependent and -independent mechanisms. Genes & Development *17*, 1130-1140.

Liu, Q., Guntuku, S., Cui, X.S., Matsuoka, S., Cortez, D., Tamai, K., Luo, G., Carattini-Rivera, S., DeMayo, F., Bradley, A., Donehower, L.A., and Elledge, S.J. (2000). Chk1 is an essential kinase that is regulated by Atr and required for the G(2)/M DNA damage checkpoint. Genes & Development *14*, 1448-1459.

Lopes, M., Cotta-Ramusino, C., Pellicioli, A., Liberi, G., Plevani, P., Muzi-Falconi, M., Newlon, C.S., and Foiani, M. (2001). The DNA replication checkpoint response stabilizes stalled replication forks. Nature *412*, 557-561.

Lopez-Girona, A., Furnari, B., Mondesert, O., and Russell, P. (1999). Nuclear localization of Cdc25 is regulated by DNA damage and a 14-3-3 protein. Nature *397*, 172-175.

Lopez-Girona, A., Kanoh, J., and Russell, P. (2001a). Nuclear exclusion of Cdc25 is not required for the DNA damage checkpoint in fission yeast. Current Biology *11*, 50-54.

Lopez-Girona, A., Tanaka, K., Chen, X.B., Baber, B.A., McGowan, C.H., and Russell, P. (2001b). Serine-345 is required for Rad3-dependent phosphorylation and function of checkpoint kinase Chk1 in fission yeast. Proceedings of the National Academy of Sciences of the United States of America *98*, 11289-11294.

Lundgren, K., Walworth, N., Booher, R., Dembski, M., Kirschner, M., and Beach, D. (1991). mik1 and wee1 cooperate in the inhibitory tyrosine phosphorylation of cdc2. Cell *64*, 1111-1122.

Mailand, N., Lukas, C., Kaiser, B.K., Jackson, P.K., Bartek, J., and Lukas, J. (2002). Deregulated human Cdc14A phosphatase disrupts centrosome separation and chromosome segregation. Nature Cell Biology *4*, 317-322.

Marlovits, G., Tyson, C.J., Novak, B., and Tyson, J.J. (1998). Modeling M-phase control in Xenopus oocyte extracts: the surveillance mechanism for unreplicated DNA. Biophysical Chemistry *72*, 169-184.

Martin-Castellanos, C., Blanco, M.A., de Prada, J.M., and Moreno, S. (2000). The puc1 cyclin regulates the G1 phase of the fission yeast cell cycle in response to cell size. Molecular Biology of the Cell *11*, 543-554.

Martin-Castellanos, C., Labib, K., and Moreno, S. (1996). B-type cyclins regulate G1 progression in fission yeast in opposition to the p25rum1 cdk inhibitor. EMBO Journal *15*, 839-849.

Martin-Cuadrado, A.B., Duenas, E., Sipiczki, M., Vazquez de Aldana, C.R., and del Rey, F. (2003). The endo-beta-1,3-glucanase eng1p is required for dissolution of the primary septum during cell separation in Schizosaccharomyces pombe. Journal of Cell Science *116*, 1689-1698.

Martinho, R.G., Lindsay, H.D., Flaggs, G., DeMaggio, A.J., Hoekstra, M.F., Carr, A.M., and Bentley, N.J. (1998). Analysis of Rad3 and Chk1 protein kinases defines different checkpoint responses. EMBO Journal *17*, 7239-7249.

Matsuyama, A., Arai, R., Yashiroda, Y., Shirai, A., Kamata, A., Sekido, S., Kobayashi, Y., Hashimoto, A., Hamamoto, M., Hiraoka, Y., Horinouchi, S., and Yoshida, M.

(2006). ORFeome cloning and global analysis of protein localization in the fission yeast Schizosaccharomyces pombe. Nature Biotechnology *24*, 841-847.

Mayer, M.L., Pot, I., Chang, M., Xu, H., Aneliunas, V., Kwok, T., Newitt, R., Aebersold, R., Boone, C., Brown, G.W., and Hieter, P. (2004). Identification of protein complexes required for efficient sister chromatid cohesion. Molecular Biology of the Cell *15*, 1736-1745.

McGlynn, P., and Lloyd, R.G. (2002a). Genome stability and the processing of damaged replication forks by RecG. Trends in Genetics *18*, 413-419.

McGlynn, P., and Lloyd, R.G. (2002b). Recombinational repair and restart of damaged replication forks. Nature Reviews Molecular Cell Biology *3*, 859-870.

McGlynn, P., and Lloyd, R.G. (2002c). Replicating past lesions in DNA. Molecular Cell *10*, 700-701.

Meister, P., Poidevin, M., Francesconi, S., Tratner, I., Zarzov, P., and Baldacci, G. (2003). Nuclear factories for signalling and repairing DNA double strand breaks in living fission yeast. Nucleic Acids Research *31*, 5064-5073.

Meister, P., Taddei, A., Vernis, L., Poidevin, M., Gasser, S.M., and Baldacci, G. (2005). Temporal separation of replication and recombination requires the intra-S checkpoint. The Journal of Cell Biology *168*, 537-544.

Mejia-Ramirez, E., Sanchez-Gorostiaga, A., Krimer, D.B., Schvartzman, J.B., and Hernandez, P. (2005). The mating type switch-activating protein Sap1 Is required for replication fork arrest at the rRNA genes of fission yeast. Molecular and Cellular Biology *25*, 8755-8761.

Melo, J., and Toczyski, D. (2002). A unified view of the DNA-damage checkpoint. Current Opinion in Cell Biology *14*, 237-245.

Melo, J.A., Cohen, J., and Toczyski, D.P. (2001). Two checkpoint complexes are independently recruited to sites of DNA damage in vivo. Genes & Development *15*, 2809-2821.

Mishra, M., Karagiannis, J., Sevugan, M., Singh, P., and Balasubramanian, M.K. (2005). The 14-3-3 protein rad24p modulates function of the cdc14p family phosphatase clp1p/flp1p in fission yeast. Current Biology *15*, 1376-1383.

Miyabe, I., Morishita, T., Hishida, T., Yonei, S., and Shinagawa, H. (2006). Rhp51-dependent recombination intermediates that do not generate checkpoint signal are accumulated in Schizosaccharomyces pombe rad60 and smc5/6 mutants after release from replication arrest. Molecular and Cellular Biology *26*, 343-353.

Mondesert, O., McGowan, C.H., and Russell, P. (1996). Cig2, a B-type cyclin, promotes the onset of S in *Schizosaccharomyces pombe*. Molecular and Cellular Biology *16*, 1527-1533.

Moreno, S., Hayles, J., and Nurse, P. (1989). Regulation of p34cdc2 protein kinase during mitosis. Cell *58*, 361-372.

Moreno, S., Klar, A., and Nurse, P. (1991). Molecular genetic analysis of fission yeast Schizosaccharomyces pombe. Methods in Enzymology *194*, 795-823.

Moreno, S., Nurse, P., and Russell, P. (1990). Regulation of mitosis by cyclic accumulation of p80cdc25 mitotic inducer in fission yeast. Nature *344*, 549-552.

Morishita, T., Tsutsui, Y., Iwasaki, H., and Shinagawa, H. (2002). The Schizosaccharomyces pombe rad60 gene is essential for repairing double-strand DNA breaks spontaneously occurring during replication and induced by DNA-damaging agents. Molecular and Cellular Biology *22*, 3537-3548.

Mulvihill, D.P., Petersen, J., Ohkura, H., Glover, D.M., and Hagan, I.M. (1999). Plo1 kinase recruitment to the spindle pole body and its role in cell division in Schizosaccharomyces pombe. Molecular Biology of the Cell *10*, 2771-2785.

Murakami, H., and Okayama, H. (1995). A kinase from fission yeast responsible for blocking mitosis in S phase. Nature *374*, 817-819.

Murakami, H., Yanow, S.K., Griffiths, D., Nakanishi, M., and Nurse, P. (2002). Maintenance of replication forks and the S-phase checkpoint by Cdc18p and Orp1p. Nature Cell Biology *4*, 384-388.

Muris, D.F., Vreeken, K., Schmidt, H., Ostermann, K., Clever, B., Lohman, P.H., and Pastink, A. (1997). Homologous recombination in the fission yeast Schizosaccharomyces pombe: different requirements for the rhp51+, rhp54+ and rad22+ genes. Current Genetics *31*, 248-254.

Nakamura, T.M., Du, L.L., Redon, C., and Russell, P. (2004). Histone H2A phosphorylation controls Crb2 recruitment at DNA breaks, maintains checkpoint arrest, and influences DNA Repair in fission yeast. Molecular and Cellular Biology *24*, 6215-6230.

Nedelcheva, M.N., Roguev, A., Dolapchiev, L.B., Shevchenko, A., Taskov, H.B., Shevchenko, A., Stewart, A.F., and Stoynov, S.S. (2005). Uncoupling of unwinding from DNA synthesis implies regulation of MCM helicase by Tof1/Mrc1/Csm3 checkpoint complex. Journal of Molecular Biology *347*, 509-521.

Nitani, N., Nakamura, K., Nakagawa, C., Masukata, H., and Nakagawa, T. (2006). Regulation of DNA replication machinery by Mrc1 in fission yeast. Genetics *174*, 155-165.

Noguchi, C., and Noguchi, E. (2007). Sap1 promotes the association of the replication fork protection complex with chromatin and is involved in the replication checkpoint in Schizosaccharomyces pombe. Genetics *175*, 553-566.

Noguchi, E., Noguchi, C., Du, L.L., and Russell, P. (2003). Swi1 prevents replication fork collapse and controls checkpoint kinase Cds1. Molecular and Cellular Biology *23*, 7861-7874.

Noguchi, E., Noguchi, C., McDonald, W.H., Yates, J.R., 3rd, and Russell, P. (2004). Swi1 and Swi3 are components of a replication fork protection complex in fission yeast. Molecular and Cellular Biology *24*, 8342-8355.

Norbury, C., and Moreno, S. (1997). Cloning cell cycle regulatory genes by transcomplementation in yeast. Methods in Enzymology *283*, 44-59.

Novak, B., Csikasz-Nagy, A., Gyorffy, B., Chen, K., and Tyson, J.J. (1998). Mathematical model of the fission yeast cell cycle with checkpoint controls at the G1/S, G2/M and metaphase/anaphase transitions. Biophysical Chemistry *72*, 185-200.

Novak, B., Pataki, Z., Ciliberto, A., and Tyson, J.J. (2001). Mathematical model of the cell division cycle of fission yeast. Chaos 277-286.

Novak, B., and Tyson, J.J. (1993). Numerical analysis of a comprehensive model of M-phase control in Xenopus oocyte extracts and intact embryos. Journal of Cell Science *106*, 1153-1168.

Novak, B., and Tyson, J.J. (1997). Modeling the control of DNA replication in fission yeast. Proceedings of the National Academy of Sciences of the United States of America *94*, 9147-9152.

Novak, B., and Tyson, J.J. (2003). Modelling the controls of the eukaryotic cell cycle. Biochemical Society Transactions *31*, 1526-1529.

Novak, B., and Tyson, J.J. (2004). A model for restriction point control of the mammalian cell cycle. Journal of Theoretical Biology *230*, 563-579.

Nyberg, K.A., Michelson, R.J., Putnam, C.W., and Weinert, T.A. (2002). Toward maintaining the genome: DNA damage and replication checkpoints. Annual Review of Genetics *36*, 617-656.

O'Connell, M.J., Raleigh, J.M., Verkade, H.M., and Nurse, P. (1997). Chk1 is a wee1 kinase in the G2 DNA damage checkpoint inhibiting cdc2 by Y15 phosphorylation. EMBO Journal *16*, 545-554.

O'Neill, T., Giarratani, L., Chen, P., Iyer, L., Lee, C.H., Bobiak, M., Kanai, F., Zhou, B.B., Chung, J.H., and Rathbun, G.A. (2002). Determination of substrate motifs for human Chk1 and hCds1/Chk2 by the oriented peptide library approach. The Journal of Biological Chemistry *277*, 16102-16115.

Oliva, A., Rosebrock, A., Ferrezuelo, F., Pyne, S., Chen, H., Skiena, S., Futcher, B., and Leatherwood, J. (2005). The cell cycle-regulated genes of Schizosaccharomyces pombe. PLoS Biology *3*, e225.

Osborn, A.J., Elledge, S.J., and Zou, L. (2002). Checking on the fork: the DNA-replication stress-response pathway. Trends in Cell Biology *12*, 509-516.

Palermo, C., Hope, J.C., Freyer, G.A., Rao, H., and Walworth, N.C. (2008). Importance of a C-terminal conserved region of chk1 for checkpoint function. PLoS ONE *3*, e1427.

Parker, L.L., Atherton-Fessler, S., and Piwnica-Worms, H. (1992). p107wee1 is a dual-specificity kinase that phosphorylates p34cdc2 on tyrosine 15. Proceedings of the National Academy of Sciences of the United States of America *89*, 2917-2921.

Parker, L.L., Walter, S.A., Young, P.G., and Piwnica-Worms, H. (1993). Phosphorylation and inactivation of the mitotic inhibitor Wee1 by the nim1/cdr1 kinase. Nature *363*, 736-738.

Paulovich, A.G., and Hartwell, L.H. (1995). A checkpoint regulates the rate of progression through S phase in S. cerevisiae in response to DNA damage. Cell *82*, 841-847.

Peng, X., Karuturi, R.K., Miller, L.D., Lin, K., Jia, Y., Kondu, P., Wang, L., Wong, L.S., Liu, E.T., Balasubramanian, M.K., and Liu, J. (2005). Identification of cell cycle-regulated genes in fission yeast. Molecular Biology of the Cell *16*, 1026-1042.

Qu, Z., MacLellan, W.R., and Weiss, J.N. (2003a). Dynamics of the cell cycle: checkpoints, sizers, and timers. Biophysical Journal *85*, 3600-3611.

Qu, Z., Weiss, J.N., and MacLellan, W.R. (2003b). Regulation of the mammalian cell cycle: a model of the G1-to-S transition. American Journal of Physiology *284*, C349-364.

Queralt, E., Lehane, C., Novak, B., and Uhlmann, F. (2006). Downregulation of PP2A(Cdc55) phosphatase by separase initiates mitotic exit in budding yeast. Cell *125*, 719-732.

Read, R.L., Martinho, R.G., Wang, S.W., Carr, A.M., and Norbury, C.J. (2002). Cytoplasmic poly(A) polymerases mediate cellular responses to S phase arrest. Proceedings of the National Academy of Sciences of the United States of America *99*, 12079-12084.

Rhind, N., Furnari, B., and Russell, P. (1997). Cdc2 tyrosine phosphorylation is required for the DNA damage checkpoint in fission yeast. Genes & Development *11*, 504-511.

Rhind, N., and Russell, P. (2001). Roles of the mitotic inhibitors Wee1 and Mik1 in the G(2) DNA damage and replication checkpoints. Molecular and Cellular Biology *21*, 1499-1508.

Russell, P., and Nurse, P. (1987). Negative regulation of mitosis by wee1+, a gene encoding a protein kinase homolog. Cell *49*, 559-567.

Rustici, G., Mata, J., Kivinen, K., Lio, P., Penkett, C.J., Burns, G., Hayles, J., Brazma, A., Nurse, P., and Bahler, J. (2004). Periodic gene expression program of the fission yeast cell cycle. Nature Genetics *36*, 809-817.

Sambrook, J., Fritsch, E.F. y Maniatis, T (1989). Molecular cloning: a laboratory manual. Cold Spring Harbor Laboratory Press.

Saka, Y., Esashi, F., Matsusaka, T., Mochida, S., and Yanagida, M. (1997). Damage and replication checkpoint control in fission yeast is ensured by interactions of Crb2, a protein with BRCT motif, with Cut5 and Chk1. Genes & Development *11*, 3387-3400.

Sanders, S.L., Portoso, M., Mata, J., Bahler, J., Allshire, R.C., and Kouzarides, T. (2004). Methylation of histone H4 lysine 20 controls recruitment of Crb2 to sites of DNA damage. Cell *119*, 603-614.

Santocanale, C., and Diffley, J.F. (1998). A Mec1- and Rad53-dependent checkpoint controls late-firing origins of DNA replication. Nature *395*, 615-618.

Sauvageau, S., Stasiak, A.Z., Banville, I., Ploquin, M., Stasiak, A., and Masson, J.Y. (2005). Fission yeast rad51 and dmc1, two efficient DNA recombinases forming helical nucleoprotein filaments. Molecular and Cellular Biology *25*, 4377-4387.

Sazer, S., and Sherwood, S.W. (1990). Mitochondrial growth and DNA synthesis occur in the absence of nuclear DNA replication in fission yeast. Journal of Cell Science *97*, 509-516.

Seeger, M., Gordon, C., Ferrell, K., and Dubiel, W. (1996). Characteristics of 26 S proteases from fission yeast mutants, which arrest in mitosis. Journal of Molecular Biology *263*, 423-431.

Segurado, M., Gomez, M., and Antequera, F. (2002). Increased recombination intermediates and homologous integration hot spots at DNA replication origins. Molecular Cell *10*, 907-916.

Shikata, M., Ishikawa, F., and Kanoh, J. (2007). Tel2 is required for activation of the Mrc1-mediated replication checkpoint. The Journal of Biological Chemistry *282*, 5346-5355.

Shou, W., Seol, J.H., Shevchenko, A., Baskerville, C., Moazed, D., Chen, Z.W., Jang, J., Shevchenko, A., Charbonneau, H., and Deshaies, R.J. (1999). Exit from mitosis is

triggered by Tem1-dependent release of the protein phosphatase Cdc14 from nucleolar RENT complex. Cell *97*, 233-244.

Simanis, V. (2003). Events at the end of mitosis in the budding and fission yeasts. Journal of Cell Science *116*, 4263-4275.

Snaith, H.A., Brown, G.W., and Forsburg, S.L. (2000). Schizosaccharomyces pombe Hsk1p is a potential cds1p target required for genome integrity. Molecular and Cellular Biology *20*, 7922-7932.

Sogo, J.M., Lopes, M., and Foiani, M. (2002). Fork reversal and ssDNA accumulation at stalled replication forks owing to checkpoint defects.Science *297*, 599-602.

Sohrmann, M., Schmidt, S., Hagan, I., and Simanis, V. (1998). Asymmetric segregation on spindle poles of the Schizosaccharomyces pombe septum-inducing protein kinase Cdc7p. Genes & Development *12*, 84-94.

Sommariva, E., Pellny, T.K., Karahan, N., Kumar, S., Huberman, J.A., and Dalgaard, J.Z. (2005). Schizosaccharomyces pombe Swi1, Swi3, and Hsk1 are components of a novel S-phase response pathway to alkylation damage. Molecular and Cellular Biology *25*, 2770-2784.

Srividhya, J., and Gopinathan, M.S. (2006). A simple time delay model for eukaryotic cell cycle. Journal of Theoretical Biology *241*, 617-627.

Stegmeier, F., Visintin, R., and Amon, A. (2002). Separase, polo kinase, the kinetochore protein Slk19, and Spo12 function in a network that controls Cdc14 localization during early anaphase. Cell *108*, 207-220.

Stewart, E., Chapman, C.R., Al-Khodairy, F., Carr, A.M., and Enoch, T. (1997). rqh1+, a fission yeast gene related to the Bloom's and Werner's syndrome genes, is required for reversible S phase arrest. EMBO Journal *16*, 2682-2692.

Straight, A.F., Shou, W., Dowd, G.J., Turck, C.W., Deshaies, R.J., Johnson, A.D., and Moazed, D. (1999). Net1, a Sir2-associated nucleolar protein required for rDNA silencing and nucleolar integrity. Cell *97*, 245-256.

Sugimoto, I., Murakami, H., Tonami, Y., Moriyama, A., and Nakanishi, M. (2004). DNA replication checkpoint control mediated by the spindle checkpoint protein Mad2p in fission yeast. The Journal of Biological Chemistry *279*, 47372-47378.

Sun, Z., Hsiao, J., Fay, D.S., and Stern, D.F. (1998). Rad53 FHA domain associated with phosphorylated Rad9 in the DNA damage checkpoint. Science *281*, 272-274.

Sveiczer, A., Csikasz-Nagy, A., Gyorffy, B., Tyson, J.J., and Novak, B. (2000). Modeling the fission yeast cell cycle: quantized cycle times in wee1- cdc25Delta mutant cells. Proceedings of the National Academy of Sciences of the United States of America *97*, 7865-7870.

Sveiczer, A., Tyson, J.J., and Novak, B. (2001). A stochastic, molecular model of the fission yeast cell cycle: role of the nucleocytoplasmic ratio in cycle time regulation. Biophysical Chemistry *92*, 1-15.

Sveiczer, A., Tyson, J.J., and Novak, B. (2004). Modelling the fission yeast cell cycle. Briefings in Functional Genomics & Proteomics *2*, 298-307.

Takeda, T., Ogino, K., Tatebayashi, K., Ikeda, H., Arai, K., and Masai, H. (2001). Regulation of initiation of S phase, replication checkpoint signaling, and maintenance of mitotic chromosome structures during S phase by Hsk1 kinase in the fission yeast. Molecular Biology of the Cell *12*, 1257-1274.

Tanaka, K., Boddy, M.N., Chen, X.B., McGowan, C.H., and Russell, P. (2001). Threonine-11, phosphorylated by Rad3 and atm in vitro, is required for activation of fission yeast checkpoint kinase Cds1. Molecular and Cellular Biology *21*, 3398-3404.

Tanaka, K., and Russell, P. (2001). Mrc1 channels the DNA replication arrest signal to checkpoint kinase Cds1. Nature Cell Biology *3*, 966-972.

Tanaka, K., and Russell, P. (2004). Cds1 phosphorylation by Rad3-Rad26 kinase is mediated by forkhead-associated domain interaction with Mrc1. The Journal of Biological Chemistry *279*, 32079-32086.

Taricani, L., and Wang, T.S. (2006). Rad4TopBP1, a scaffold protein, plays separate roles in DNA damage and replication checkpoints and DNA replication. Molecular Biology of the Cell *17*, 3456-3468.

Taylor, G.S., Liu, Y., Baskerville, C., and Charbonneau, H. (1997). The activity of Cdc14p, an oligomeric dual specificity protein phosphatase from Saccharomyces cerevisiae, is required for cell cycle progression. The Journal of Biological Chemistry *272*, 24054-24063.

Tercero, J.A., and Diffley, J.F. (2001). Regulation of DNA replication fork progression through damaged DNA by the Mec1/Rad53 checkpoint. Nature *412*, 553-557.

Tercero, J.A., Longhese, M.P., and Diffley, J.F. (2003). A central role for DNA replication forks in checkpoint activation and response. Molecular Cell *11*, 1323-1336.

Tindall, M.J., and Please, C.P. (2007). Modelling the cell cycle and cell movement in multicellular tumour spheroids. Bulletin of Mathematical Biology *69*, 1147-1165.

Toth, A., Queralt, E., Uhlmann, F., and Novak, B. (2007). Mitotic exit in two dimensions. Journal of Theoretical Biology *248*, 560-573.

Trautmann, S., and McCollum, D. (2005). Distinct nuclear and cytoplasmic functions of the *S. pombe* Cdc14-like phosphatase Clp1p/Flp1p and a role for nuclear shuttling in its regulation. Current Biology *15*, 1384-1389.

Trautmann, S., Rajagopalan, S., and McCollum, D. (2004). The *S. pombe* Cdc14-like phosphatase Clp1p regulates chromosome biorientation and interacts with Aurora kinase. Developmental Cell *7*, 755-762.

Trautmann, S., Wolfe, B.A., Jorgensen, P., Tyers, M., Gould, K.L., and McCollum, D. (2001). Fission yeast Clp1p phosphatase regulates G2/M transition and coordination of cytokinesis with cell cycle progression. Current Biology *11*, 931-940.

Traverso, E.E., Baskerville, C., Liu, Y., Shou, W., James, P., Deshaies, R.J., and Charbonneau, H. (2001). Characterization of the Net1 cell cycle-dependent regulator of the Cdc14 phosphatase from budding yeast. The Journal of Biological Chemistry *276*, 21924-21931.

Tsutsui, Y., Khasanov, F.K., Shinagawa, H., Iwasaki, H., and Bashkirov, V.I. (2001). Multiple interactions among the components of the recombinational DNA Repair system in Schizosaccharomyces pombe. Genetics *159*, 91-105.

Tyson, J.J. (1979). Periodic enzyme synthesis: reconsideration of the theory of oscillatory repression. Journal of Theoretical Biology *80*, 27-38.

Unsal-Kacmaz, K., Mullen, T.E., Kaufmann, W.K., and Sancar, A. (2005). Coupling of human circadian and cell cycles by the timeless protein. Molecular and Cellular Biology *25*, 3109-3116.

van den Bosch, M., Vreeken, K., Zonneveld, J.B., Brandsma, J.A., Lombaerts, M., Murray, J.M., Lohman, P.H., and Pastink, A. (2001). Characterization of RAD52 homologs in the fission yeast Schizosaccharomyces pombe. Mutation Research *461*, 311-323.

van den Bosch, M., Zonneveld, J.B., Vreeken, K., de Vries, F.A., Lohman, P.H., and Pastink, A. (2002). Differential expression and requirements for Schizosaccharomyces pombe RAD52 homologs in DNA Repair and recombination. Nucleic Acids Research *30*, 1316-1324.

van Hemert, M.J., van Heusden, G.P., and Steensma, H.Y. (2001). Yeast 14-3-3 proteins. Yeast *18*, 889-895.

Vazquez-Novelle, M.D., Esteban, V., Bueno, A., and Sacristan, M.P. (2005). Functional homology among human and fission yeast Cdc14 phosphatases. Journal of Biological Chemistry *280*, 29144-29150.

Venclovas, C., and Thelen, M.P. (2000). Structure-based predictions of Rad1, Rad9, Hus1 and Rad17 participation in sliding clamp and clamp-loading complexes. Nucleic Acids Research *28*, 2481-2493.

Visintin, C., Tomson, B.N., Rahal, R., Paulson, J., Cohen, M., Taunton, J., Amon, A., and Visintin, R. (2008). APC/C-Cdh1-mediated degradation of the Polo kinase Cdc5 promotes the return of Cdc14 into the nucleolus. Genes & Development *22*, 79-90.

Visintin, R., Craig, K., Hwang, E.S., Prinz, S., Tyers, M., and Amon, A. (1998). The phosphatase Cdc14 triggers mitotic exit by reversal of Cdk-dependent phosphorylation. Molecular Cell *2*, 709-718.

Visintin, R., Hwang, E.S., and Amon, A. (1999). Cfi1 prevents premature exit from mitosis by anchoring Cdc14 phosphatase in the nucleolus. Nature *398*, 818-823.

Walworth, N., Davey, S., and Beach, D. (1993). Fission yeast chk1 protein kinase links the rad checkpoint pathway to cdc2. Nature *363*, 368-371.

Walworth, N.C., and Bernards, R. (1996). rad-dependent response of the chk1-encoded protein kinase at the DNA damage checkpoint. Science *271*, 353-356.

Wan, J., Xu, H., and Grunstein, M. (1992). CDC14 of Saccharomyces cerevisiae. Cloning, sequence analysis, and transcription during the cell cycle. The Journal of Biological Chemistry *267*, 11274-11280.

Wan, S., Capasso, H., and Walworth, N.C. (1999). The topoisomerase I poison camptothecin generates a Chk1-dependent DNA damage checkpoint signal in fission yeast. Yeast *15*, 821-828.

Wang, H., and Elledge, S.J. (2002). Genetic and physical interactions between DPB11 and DDC1 in the yeast DNA damage response pathway. Genetics *160*, 1295-1304.

Watson, A., Mata, J., Bahler, J., Carr, A., and Humphrey, T. (2004). Global gene expression responses of fission yeast to ionizing radiation. Molecular Biology of the Cell *15*, 851-860.

Wilkinson, C.R., Wallace, M., Morphew, M., Perry, P., Allshire, R., Javerzat, J.P., McIntosh, J.R., and Gordon, C. (1998). Localization of the 26S proteasome during mitosis and meiosis in fission yeast. EMBO Journal *17*, 6465-6476.

Win, T.Z., Goodwin, A., Hickson, I.D., Norbury, C.J., and Wang, S.W. (2004). Requirement for Schizosaccharomyces pombe Top3 in the maintenance of chromosome integrity. Journal of Cell Science *117*, 4769-4778.

Wolfe, B.A., and Gould, K.L. (2004). Fission yeast Clp1p phosphatase affects G2/M transition and mitotic exit through Cdc25p inactivation. EMBO Journal *23*, 919-929.

Wolkow, T.D., and Enoch, T. (2002). Fission yeast Rad26 is a regulatory subunit of the Rad3 checkpoint kinase. Molecular Biology of the Cell *13*, 480-492.

Wood, V., Gwilliam, R., Rajandream, M.A., Lyne, M., Lyne, R., Stewart, A., Sgouros, J., Peat, N., Hayles, J., Baker, S., Basham, D., Bowman, S., Brooks, K., Brown, D., Brown, S., Chillingworth, T., Churcher, C., Collins, M., Connor, R., Cronin, A., Davis, P., Feltwell, T., Fraser, A., Gentles, S., Goble, A., Hamlin, N., Harris, D., Hidalgo, J., Hodgson, G., Holroyd, S., Hornsby, T., Howarth, S., Huckle, E.J., Hunt, S., Jagels, K., James, K., Jones, L., Jones, M., Leather, S., McDonald, S., McLean, J., Mooney, P.,

Moule, S., Mungall, K., Murphy, L., Niblett, D., Odell, C., Oliver, K., O'Neil, S., Pearson, D., Quail, M.A., Rabbinowitsch, E., Rutherford, K., Rutter, S., Saunders, D., Seeger, K., Sharp, S., Skelton, J., Simmonds, M., Squares, R., Squares, S., Stevens, K., Taylor, K., Taylor, R.G., Tivey, A., Walsh, S., Warren, T., Whitehead, S., Woodward, J., Volckaert, G., Aert, R., Robben, J., Grymonprez, B., Weltjens, I., Vanstreels, E., Rieger, M., Schafer, M., Muller-Auer, S., Gabel, C., Fuchs, M., Dusterhoft, A., Fritzc, C., Holzer, E., Moestl, D., Hilbert, H., Borzym, K., Langer, I., Beck, A., Lehrach, H., Reinhardt, R., Pohl, T.M., Eger, P., Zimmermann, W., Wedler, H., Wambutt, R., Purnelle, B., Goffeau, A., Cadieu, E., Dreano, S., Gloux, S., Lelaure, V., Mottier, S., Galibert, F., Aves, S.J., Xiang, Z., Hunt, C., Moore, K., Hurst, S.M., Lucas, M., Rochet, M., Gaillardin, C., Tallada, V.A., Garzon, A., Thode, G., Daga, R.R., Cruzado, L., Jimenez, J., Sanchez, M., del Rey, F., Benito, J., Dominguez, A., Revuelta, J.L., Moreno, S., Armstrong, J., Forsburg, S.L., Cerutti, L., Lowe, T., McCombie, W.R., Paulsen, I., Potashkin, J., Shpakovski, G.V., Ussery, D., Barrell, B.G., and Nurse, P. (2002). The genome sequence of Schizosaccharomyces pombe. Nature *415*, 871-880.

Wu, L., and Russell, P. (1993). Nim1 kinase promotes mitosis by inactivating Wee1 tyrosine kinase. Nature *363*, 738-741.

Wu, X., Shell, S.M., and Zou, Y. (2005). Interaction and colocalization of Rad9/Rad1/Hus1 checkpoint complex with replication protein A in human cells. Oncogene *24*, 4728-4735.

Xu, X., Tsvetkov, L.M., and Stern, D.F. (2002). Chk2 activation and phosphorylation-dependent oligomerization. Molecular and Cellular Biology *22*, 4419-4432.

Xu, Y.J., Davenport, M., and Kelly, T.J. (2006). Two-stage mechanism for activation of the DNA replication checkpoint kinase Cds1 in fission yeast. Genes & Development *20*, 990-1003.

You, Z., Chahwan, C., Bailis, J., Hunter, T., and Russell, P. (2005). ATM activation and its recruitment to damaged DNA require binding to the C terminus of Nbs1. Molecular and Cellular Biology *25*, 5363-5379.

You, Z., Kong, L., and Newport, J. (2002). The role of single-stranded DNA and polymerase alpha in establishing the ATR, Hus1 DNA replication checkpoint. The Journal of Biological Chemistry *277*, 27088-27093.

Zeng, Y., and Piwnica-Worms, H. (1999). DNA damage and replication checkpoints in fission yeast require nuclear exclusion of the Cdc25 phosphatase via 14-3-3 binding. Molecular and Cellular Biology *19*, 7410-7419.

Zhao, H., and Piwnica-Worms, H. (2001). ATR-mediated checkpoint pathways regulate phosphorylation and activation of human Chk1. Molecular and Cellular Biology *21*, 4129-4139.

Zhao, H., and Russell, P. (2004). DNA binding domain in the replication checkpoint protein Mrc1 of Schizosaccharomyces pombe. The Journal of Biological Chemistry *279*, 53023-53027.

Zhao, H., Tanaka, K., Nogochi, E., Nogochi, C., and Russell, P. (2003). Replication checkpoint protein Mrc1 is regulated by Rad3 and Tel1 in fission yeast. Molecular and Cellular Biology *23*, 8395-8403.

Zi, Z., and Klipp, E. (2006). SBML-PET: a Systems Biology Markup Language-based parameter estimation tool. Bioinformatics *22*, 2704-2705.

Zilahi, E., Salimova, E., Simanis, V., and Sipiczki, M. (2000). The *S. pombe* sep1 gene encodes a nuclear protein that is required for periodic expression of the cdc15 gene. FEBS Letters *481*, 105-108.

Zou, L., and Elledge, S.J. (2003). Sensing DNA damage through ATRIP recognition of RPA-ssDNA complexes. Science 300, 1542-1548.